

DEVELOPMENT OF A LC-MS/MS METHOD FOR THE DETECTION OF SNAKE VENOM TOXINS IN HUMAN PLASMA

Anné Lermer

*Thesis presented in fulfilment of the requirements for the degree of Master of
Science (Pharmacology) in the Faculty of Medicine and Health at Stellenbosch*



Supervisors:

Dr T A Kellermann (Primary)

Division of Clinical Pharmacology (Stellenbosch University)

Dr N M Vlok

Central Analytical Facilities: Proteomics (Stellenbosch University)

Ms. C J Marks

Division of Clinical Pharmacology (Stellenbosch University)

Declaration

By submitting this thesis electronically, I declare that the entirety of the work contained therein is my own, original work, that I am the sole author thereof, that reproduction and publication thereof by Stellenbosch University will not infringe any third party rights and that I have not previously in its entirety or in part submitted it for obtaining any qualification.

Signature:

Date:.....

Abstract

Background: Snakebite envenomation in sub-Saharan Africa significantly threatens human health. Species that was responsible for the envenomation are rarely positively identified. There are no rapid methods/diagnostics available for conclusive identification of the organism/species responsible. Venomous species can be categorised based on the composition and primary effect caused by their venom components as neurotoxic, cytotoxic and/or hemotoxic.

Aim: To develop an LC-MS/MS method for the species-specific detection of snake venom toxins from human plasma.

Methods: An epidemiological study on the incidence of snakebite in South Africa as reported to Poisons Information Helpline of Western Cape (PIHWC) was performed to provide rationale for the analytical study. Analytical methodology includes identification of species-specific venom toxins by high resolution (HR) LC-MS/MS, fractionation of *Naja nivea* venom by size exclusion chromatography and compositional analysis of the fractions by HR-LC-MS/MS. Venom fractions were screened for toxicity using a zebrafish model, utilising DanioVision for phenotypic screening and behavioural tracking of the larvae. Thereafter, a triple quadrupole LC-MS/MS method was developed containing species-specific toxins.

Results: Analysis of PIHWC call data revealed that in 43.73% of the recorded snakebite cases the causative snake species were unidentified. The snake species *Naja nivea*, *Bitis arietans* and *Bitis atropos* species were identified as most medically significant in South Africa and consequently included in the study. Venom from *N. nivea* was chosen as the species for fractionation after common peptides from inter-region venom were identified as unique to the species. Behavioural changes in larvae were observed after exposure to sub-lethal concentrations of *N. nivea* venom fractions. Significant ($p < 0.0001$) changes in larval behaviour were observed in two treatment groups compared to the control. Using transitions that was generated during HR-LC-MS/MS analysis, FASTA files were generated and converted into MRM's onto the triple quadrupole LC-MS. Toxins were positively identified from human plasma by LC-MS/MS.

Discussion: This study identified the species predominantly responsible for snakebites from PIHWC call data, and highlighted a need for a diagnostic to identify the species responsible for envenomation. Analysis of the venom proteomes by HR-LC-MS/MS revealed similarities

and differences in the venom profiles of *Naja nivea*, *Bitis arietans* and *Bitis atropos* species. In-solution, HILIC assisted tryptic digestion produced the identification of more proteins from the *N. nivea* crude venom compared to in-gel digestion and while fractionation by size exclusion chromatography prior to MS analysis increased the detection of low molecular weight toxins. It was also shown that using a combination of conventional HR-MS (with database/library searches) and triple quadrupole MS, a method could be created that identified species specific venom peptides from human plasma to aid diagnosis.

Conclusion: This is a proof of concept for future work that will include the development of a lateral flow assay to detect venom from envenomed plasma that is cost-effective to produce, aids in defining diagnosis and importantly serves victims of snakebite envenomation in rural communities.

Keywords: snake venom, snakebite, toxin, pharmacology, LC-MS/MS, zebrafish, proteomics, diagnostics

Opsomming

Agtergrond: Slangbytvergiftiging in Afrika suid van die Sahara hou 'n beduidende bedreiging vir menslike gesondheid in. Die spesie wat vir die vergiftiging verantwoordelik is, word selde positief uitgeken. Daar is geen vinnige metodes/diagnostiek beskikbaar vir voldoende uitkenning van die verantwoordelike organisme/spesie nie. Giftige spesies kan op grond van die samestelling en primêre effek van hulle gif as neurotoksies, sitotoksies en/of hemotoksies gekategoriseer word.

Doel: Om 'n vloeistofchromatografie-massaspektografie- (LC-MS/MS) metode van spesie-spesifieke opsporing van slanggiftoksiene uit menslike plasma te ontwikkel.

Metodes: 'n Epidemiologiese studie oor die voorkoms van slangbyt in Suid-Afrika, soos by die Wes-Kaapse Gifinligtingshulplyn (PIHWC) aangemeld, is gedoen om die beweegrede vir die analitiese studie te bied. Analitiese metodologie sluit in die identifisering van spesie-spesifieke giftoksiene deur hoëresolusie- (HR-) LC-MS/MS, fraksionering van die gif van *Naja nivea* deur grootte-uitsluitingschromatografie en samestellingsontleding van die fraksies deur HR-LC-MS/MS. Giffraksies is vir giftigheid getoets deur van 'n sebravismodel gebruik te maak, met behulp van DanioVision vir fenotipiese sifting en gedragstredhou van die larwes. Daarna is 'n drievoudige vierpool-LC-MS/MS-metode ontwikkel, wat spesie-spesifieke toksiene bevat.

Uitslae: Ontleding van die oproepdata van die PIHWC getoon dat in 43.73% van die aangemelde slangbytgevalle die spesie van die betrokke slang nie uitgeken is nie. Die slangspesies *Naja nivea*, *Bitis arietans* en *Bitis atropos* is uitgeken as die medies mees beduidende in Suid-Afrika en is gevolglik by die studie ingesluit. Gif uit *N. nivea* is gekies as die spesie vir fraksionering, nadat gedeelde peptiede uit tussenstreekse gif as uniek tot die spesies geïdentifiseer is. Gedragsverandering is in larwes waargeneem ná blootstelling aan subdodelike konsentrasies van giffraksies van *N. nivea*. Beduidende ($p < 0.0001$) veranderinge in larwegedrag is waargeneem in die twee behandelingsgroepe, vergeleke met die kontrolegroep. Met behulp van die m/z-oorgange wat tydens die HR-LC-MS/MS-ontleding gegenereer is, is FASTA-lêers gegenereer en omgeskakel na meervoudige reaksie-monitoring (MRM) op die drievoudige vierpool-LC-MS. Toksiene is positief met behulp van LC-MS/MS uit menslike plasma geïdentifiseer.

Bespreking: Die studie identifiseer die drie medies-beduidende spesies wat hoofsaaklik vir slangbyte verantwoordelik is en hoe dikwels die oorsaakorganismes volgens die PIHWS-data

onbekend is. Dit lig die behoefte aan diagnostiek vir die uitkenning van die spesie wat vir die vergiftiging verantwoordelik is, uit. Ontleding van die gifproteome deur HR-LC-MS/MS onthul ooreenkomste en verskille in die gifprofiel van *Naja nivea*, *Bitis arietans* en *Bitis atropos*. In-oplossing, HILIC-gesteunde (hidrofiliese interaksie vloeistofchromatografie) triptiese vertering identifiseer nog proteïene uit onverwerkte *N.nivea*-gif vergeleke met in-jel-vertering. Daar word ook getoon dat, met die gebruik van 'n kombinasie van konvensionele HR-MS (met databasis-/biblioteeksoektogte) en drievoudige vierpool-MS, 'n metode geskep kan word wat spesie-spesifieke gifpeptiede uit menslike plasma kan identifiseer om met diagnose te help.

Gevolgtrekking: Dit is 'n bewys van die konsep vir toekomstige werk, insluitend die ontwikkeling van 'n laterale vloei-toets vir die opspoor van gif uit vergiftigde plasma, wat kostedoeltreffend is om te vervaardig, help met die definiëring van diagnose en die slagoffers van slangbytvergiftiging in landelike gemeenskappe kan dien.

Sleutelwoorde: slanggif, slangbyt, toksien, farmakologie, LC-MS/MS, sebravis, proteomika, diagnostiek

Dedication

To my late sister Chloë Leah Lermer

Acknowledgements

Most importantly I would like to thank my supervisors Dr Tracy Kellermann, Dr Maré Vlok and Ms Carine Marks for all their support and guidance during this journey. Without you this project would not have been possible and I am eternally grateful for this opportunity.

I would like to acknowledge The Poison Information Centre of the Western Cape and in particular Mr Gonwayne Voigt and Ms Arina du Plessis for welcoming me into the Poison Information Centre and their assistance in understanding the AfriTox Telelog system and epidemiological data. To Prof Carine Smith and Dr Kelly Petersen-Ross, thank you for sharing your expertise and teaching me the required skills pertaining to the use of zebrafish larvae in the toxicological assays conducted during this study. I would like to express gratitude towards Prof Kenyon and Mr Lutho Mbabala and the Division of Human Genomics and TB at Stellenbosch University for insightful discussions and assistance with reagents, electrophoresis laboratory equipment and training. A massive thank you to Prof Johann van Zyl for allowing me to use his laboratory equipment, consumables, reagents and training me on the use, troubleshooting and care of the ÄKTA explorer system. Thank you for all the great conversations and your passion for science, I am inspired. Thank you to all my experimental pharmacology colleagues from the Division of Clinical Pharmacology for great discussions, attending presentations on my work and the immense support during this time.

I would like to acknowledge and express gratitude towards my funders, the Harry Crossley Foundation for the provision of project funding and Stellenbosch University for the Postgraduate scholarship that they awarded me.

Special thanks to Johan Marais from the African Snakebite Institute for the hands on training in venomous snake handling and for providing photos of *Naja nivea*, *Bitis arietans* and *Bitis atropos*.

Lastly, but definitely not the least, I would like to thank my family, David, Susan and Jonathan. None of my incredible academic journey would've been possible without your love and support.

List of Tables

Table 1.1 Medically significant venomous species in South Africa and their overall toxic effect	20
Table 1.2 Enzymatic snake venom proteins and peptides and general characteristics.....	28
Table 1.3 Non-enzymatic snake venom proteins and peptides and general characteristics .	30
Table 1.4 Overlap of the major signs and symptoms of neurotoxic snakebite, scorpionism and latrodectism (Muller et al., 2012a; Rossiter et al., 2020)	38
Table 2.1 The population and land surface area of each province in South Africa.....	44
Table 2.2 Field and filter parameters set for data extraction from the AfriTox Telelog database	45
Table 2.3 Poison severity score allocated to snakebites inflicted by unknown species causing no defined toxidrome	50
Table 2.4 Sex of all snakebite victims over five year period	50
Table 2.5 Snakebite calls received by the PIHWC broken down according to age and sex of subjects	51
Table 2.6 Category of caller medical vs public.....	52
Table 2.7 Geographical distribution of snakebite calls received by the PIHWC from each of the nine provinces that make up South Africa.....	53
Table 2.8 Type of toxicity caused by snakebites that occurred in the Western Cape over 5 years from 1 June 2015 - 31 May 2020.....	54
Table 4.1 List of proteins positively identified in the two regionally different <i>N. nivea</i> WC (n=3) and <i>N. nivea</i> NC (n=3) venoms by in-solution tryptic digestion and HR-LC-MS/MS.	85
Table 4.2 List of venom proteins and peptides identified by HR-LC-MS/MS in supernatants (undigested) from human plasma spiked with crude venom from <i>B. atropos</i> , <i>B. arietans</i> and <i>N. nivea</i> and precipitated with acetonitrile.....	94
Table 4.3 Major peaks detected during fractionation of <i>N. nivea</i> venom by size exclusion chromatography on an AKTA explorer	97
Table 4.4 Proteins identified in <i>N. nivea</i> venom fractions 5, 6, 7, 8 and C with protein identification probability and percentage of total spectra	100
Table 4.5 Summary of the iRT standard multiple reaction monitoring transitions.....	107
Table 4.6 Multiple reaction monitoring transitions for a shot gun approach of cytotoxin 1, cytotoxin 3 and cytotoxin 10 from human plasma spiked with <i>N. nivea</i> venom (V) and unspiked human plasma (B), prepared by three different tryptic digestion protocols (18 h, 50 mm ABC, 100 mm ABC).....	108

Table 0.1 List of proteins that were identified in the venom from <i>Bitis atropos</i> after in-gel trypsin digestion and HR-LC-MS/MS analysis.....	145
Table 0.2 List of proteins that were identified in <i>N. nivea</i> venom by in-gel tryptic digestion and HR-LC-MS/MS analysis.....	164
Table 0.3 List of proteins that were identified in <i>B. arietans</i> venom by in-gel tryptic digestion and HR-LC-MS/MS analysis.....	170

List of Figures

Figure 1.1 The Elapidae family include cobras, mambas and sea snakes for example the cobra species <i>Naja nivea</i> (left) and the Viperidae family include vipers and pit vipers for example <i>Bitis arietans</i> (right). Credit to the African Snakebite Institute (Johan Marais) for the photos of <i>Naja nivea</i> , <i>Bitis arietans</i> and <i>Bitis atropos</i>	20
Figure 1.2 Overview of the process of electrospray ionisation of an analyte. The ESI process involves three steps: the generation of charged droplets under a high voltage (HV) electric field from a liquid sample, desolvation of the charged droplets that causes their surface charge to increase and force the droplets to fission and form smaller multiple charged droplets. These decrease in size and turn into gas phase analyte ions.	34
Figure 1.3 Overview of the triple quadrupole mass spectrometer (QQQ MS). Analyte ions produced by electrospray ionisation are introduced into the mass spectrometer vacuum. In quadrupole 1, the analyte precursor mass to charge is selected, collision induced dissociation cause fragmentation of the precursor ion in quadrupole 2 and in quadrupole 3, co-eluting interferences are removed and the mass to charge for product ions are selected, detected and monitored over the elution time on a chromatogram.	35
Figure 1.4 Overview of the orbitrap high resolution mass analyser in tandem quadrupole system. Analyte ions produced by nano-electrospray ionisation are introduced into the mass spectrometer vacuum. In quadrupole 1, intense precursor mass to charge is selected for mass spectrometry MS/MS analysis, higher energy collisional dissociation (HCD) cause fragmentation of the precursor ions in quadrupole 2 coupled to a high resolution orbitrap mass analyser, where ions are separated based on their mass to charge (m/z) and peptides identified by matching of fragment ion mass spectra to protein database.	35
Figure 2.1 Poison centres in South Africa and location of the PIHWC.....	42
Figure 2.2 Overall categorisation of all human related calls received by the PIHWC over the 5-year study period	48

Figure 2.3 Snakebite calls recorded at the PIHWC over 5 years, according to toxidrome and causative species.....	49
Figure 2.4 Pie chart showing the breakdown of female (left) and male (right) subjects bitten by a snake the over 5-year period according to age.....	51
Figure 2.5 Snakebite related calls that occurred in South Africa over a 5-year period. The amount of calls received are indicated per year.....	52
Figure 2.6 Seasonal distribution of snakebite calls received from 1 June 2015- 31 May 2020. Over the duration of the study period the most snake bite calls were received from December to February each year and the least during June to August.	53
Figure 2.7 Incidence of snakebite per 100 000 population by province	54
Figure 2.8 Categorisation of snakebites reported from the Western Cape to the PIHWC over 5 years according to type of envenomation and causative species	56
Figure 2.9 Sex and age of snakebite subjects from the Western Cape over the 5-year period.	57
Figure 2.10 Caller categorisation of the snakebite call made to the PIHWC.....	57
Figure 2.11 Snakebite calls made to the PIHWC and the facilities located in the Western Cape, from which the calls were received.....	58
Figure 3.1 Overview of the experimental workflow for the investigation of snake venom proteins/peptides. Diagram created with BioRender.com.....	62
Figure 3.2 Workflow overview of proteomic sample preparation for mass spectrometry.....	67
Figure 3.3 In-gel protein digestion for analysis by HR-LC-MS/MS	67
Figure 3.4 <i>N. nivea</i> was injected onto a FPLC system and fractionated by size exclusion chromatography. Diagram generated in BioRender.com	73
Figure 3.5 Trypsin digestion sample preparation protocols. Aliquots of supernatant containing low molecular weight plasma and venom proteins, obtained following protein precipitation with acetonitrile (ACN) were subjected to three different tryptic digestion protocols prior to peptide analysis by LC-MS/MS. Protocol one followed a traditional in-solution, HILIC assisted tryptic digestion, 20 µg/mL trypsin was added at a 1:50 enzyme to substrate ratio and incubated overnight in a 37°C oven. Protocol two involves resuspension of supernatant in ammonium bicarbonate (AMBIC), samples were then placed on a 99°C heating block for 10 min, 20 µg/mL trypsin was added at a 1:50 enzyme to substrate ratio and samples were incubated for 30 min in a 37°C preheated water bath, the digestion process was stopped by the addition of formic acid (FA). The third protocol involves resuspension of the supernatant in ammonium bicarbonate (AMBIC), addition 20 µg/mL trypsin at a 1:7.4 enzyme to substrate ratio, samples were thoroughly mixed by vortex and 50% methanol was added, thereafter samples were incubated for 30 min in a 37°C in a preheated water bath. The digestion process was stopped by the addition of acetic acid (AA).....	75

Figure 4.1 Native PAGE protein profiles of crude venom from <i>B. atropos</i> (A), <i>N. nivea</i> (WC) (B), <i>N. nivea</i> (NC) (C) and <i>B. arietans</i> (D) (M – molecular weight marker)	80
Figure 4.2 A summary of the dominant protein families that were identified in the venom proteomes of the species <i>B. atropos</i> (A), <i>N. nivea</i> (B) and <i>B. arietans</i> venoms (C)	82
Figure 4.3 Venn diagram showing the qualitative relationship of identified proteins in the venom from <i>B. atropos</i> , <i>N. nivea</i> and <i>B. arietans</i> based on the presence/absence in each venom.....	82
Figure 4.4 Abundant protein families identified in <i>N. nivea</i> venom proteome	83
Figure 4.5 Abundant protein families identified from <i>N. nivea</i> -WC (A) and <i>N. nivea</i> -NC (B) venoms.....	83
Figure 4.6 RP-HPLC chromatograms of Blank 0.1% formic acid in water (A), <i>B. atropos</i> (B), <i>N. nivea</i> (WC) (C), <i>N. nivea</i> (NC) (D) and <i>B. arietans</i> venoms in water with 0.1% formic acid (D) precipitated with two volumes acetonitrile.....	89
Figure 4.7 RP-HPLC chromatograms obtained from blank blood plasma precipitated with two volumes acetonitrile (A). Crude <i>B. atropos</i> (B), <i>N. nivea</i> (WC) (C) and <i>N. nivea</i> (NC) (D) and <i>B. arietans</i> venoms (E) spiked into plasma and precipitated with two volumes acetonitrile. .	90
Figure 4.8 Crude venoms from <i>B. Atropos</i> (A), <i>N. nivea</i> (WC) (B), <i>N. nivea</i> (NC) (C) and <i>B. arietans</i> (D) in 0.1% formic acid in water precipitated with three volumes acetonitrile	90
Figure 4.9 RP-HPLC chromatograms of plasma (A) and plasma spiked with crude venom from <i>B. atropos</i> (B), <i>N. nivea</i> (WC) (C), <i>N. nivea</i> (NC) (D) and <i>B. arietans</i> (E) precipitated with three volumes acetonitrile	91
Figure 4.10 RP-HPLC chromatograms of venom from the species <i>B. atropos</i> (A), <i>N. nivea</i> (WC) (B), <i>N. nivea</i> (NC) (C) and <i>B. arietans</i> (D) in 0.1% formic acid in water, precipitated with four volumes acetonitrile.....	91
Figure 4.11 RP-HPLC chromatograms of blood plasma precipitated with four volumes acetonitrile (A) and <i>B. atropos</i> (B), <i>N. nivea</i> (WC) (C), <i>N. nivea</i> (NC) (D), <i>B. arietans</i> (E) venoms spiked in plasma and precipitated with four volumes acetonitrile	92
Figure 4.12 Mass spectrometry of crude venom from <i>B. arietans</i> (A) and <i>N. nivea</i> -NC (B) spiked into plasma with two volumes of acetonitrile and injected onto the HR-LC-MS/MS. TIC generated in Excalibur, Thermo Scientific™	92
Figure 4.13 Chromatogram obtained during fractionation of <i>N. nivea</i> venom on AKTA Explorer, read at 280 nm.....	96
Figure 4.14 Native page protein profile of <i>N. nivea</i> venom fractions obtained by size exclusion chromatography	97
Figure 4.15 Zebrafish larvae after treatment with 0.5 µg/µL <i>Naja nivea</i> venom fractions 5, 6, 7, 8 and C.....	103

Figure 4.16 Zebrafish larvae after treatment with 0.25 µg/µL *Naja nivea* venom fractions 5, 6, 7, 8 and C..... 103

Figure 4.17 Zebrafish larvae after treatment with 0.125 µg/µL *Naja nivea* venom fractions 5, 6, 7, 8 and C..... 103

Figure 4.18 Significant toxic effects of *N. nivea* venom fractions observed in zebrafish larva include oedematous enlarged eyes (A), flaking of the skin body (B) and flared gills (C)..... 104

Figure 4.19 Distance moved (mm/min) by zebrafish larvae over a 10-minute observation period, acute after treatment (A) and 24-hours after treatment (B) tracked by Daniovision. Accumulative distance moved per treatment group acute (C) and 24-hours (D) post-treatment. Stacked locomotor track visualisation pattern for each treatment group, acute (E) and 24-hours after treatment (F)..... 105

Figure 4.20 Zebrafish larvae 1-hour and 24-hours after treatment with *Naja nivea* venom fractions 6 and 8 105

List of abbreviations and symbols

3FTX	3-finger toxin
5'-NUC	5'nucleotidase
ACE	Acetylcholinesterase
BPP	Bradykinin potentiating peptide
BUP	Bottom-up proteomics
CID	Collision induced dissociation
CP	Complement protein
CPS	Count per second
CRISP	Cysteine-rich secretory protein
CTL	C-type lectin
CVF	Cobra venom factor
CYS	Cystatin
DIS	Disintegrin
ELISA	Enzyme Linked Immunosorbent Assay
ESI	Electrospray ionisation
FDR	False discovery rate
HIC	Hydrophobic interaction chromatography
HR-LC-MS/MS	High resolution liquid chromatography tandem mass spectrometry
HYA	Hyaluronidase
ICP-QQQ	Inductively coupled plasma and triple quadrupole mass analyser
KTI	Kunitz-type serine protease inhibitor
LAO	L-amino acid oxidase
LC-MS/MS	Liquid chromatography with tandem mass spectrometry
MALDI	Matrix assisted laser desorption/ionisation
MS	Mass spectrometry
MS/MS	Tandem mass spectrometry
nano-ESI-LC-MS/MS	nano electrospray ionisation tandem mass spectrometry
NP	Natriuretic peptide
PAGE	Polyacrylamide gel electrophoresis
PANAF	Premium Serums Pan Africa polyvalent antivenom
PDE	Phosphodiesterase
PLA2	Phospholipase A2
PLI	Phospholipase A2 Inhibitor
PLB	Phospholipase B
PTM	Post translational modification
Q-Tof	Quadrupole and time of flight mass analyser
RP	Reverse phase
RP-HPLC	Reverse-Phase high performance liquid chromatography
SBE	snakebite envenomation

SDS-PAGE	sodium dodecyl sulfate-polyacrylamide gel electrophoresis
SEC	Size exclusion chromatography
SVMP	Snake venom metalloprotease
SVSP	Snake venom serine protease
TDP	Top down proteomics
TOF	Time of flight
VAVPAV	VINS African polyvalent antivenom
VES	Vespryn
VF	Venom factor
VNGF	Venom nerve growth factor
WAP	Waprin

Table of Contents

Declaration	ii
Abstract	iii
Opsomming	v
Dedication	vii
Acknowledgements	vii
List of Tables	viii
List of Figures	ix
List of abbreviations and symbols	xiii
CHAPTER 1 Introduction and Literature Review	19
1.1 Venomous snake species in South Africa	19
1.2 Envenomation: Clinical signs, symptoms and therapeutic approach	20
1.2.1 Syndromic management approach to envenomation	21
1.2.2 Clinical and laboratory monitoring	23
1.3 Detection of venom proteins	24
1.4 Antivenom	24
1.4.1 Production.....	25
1.4.2 Adverse effects of antivenom therapy	25
1.5 Proteomic composition of snake venom	26
1.5.1 Structural and functional classes of venom toxins	26
1.5.2 Enzymatic venom components	27
1.5.3 Non-enzymatic	29
1.6 Research techniques used in the analysis of venom	31
1.6.1 Proteomic profiling of snake venom	31
1.6.1.1 Separation methods	32
1.6.1.2 Mass spectrometric approaches	33
1.7 Toxicity and physiological effects of snake venom toxins in an <i>In vivo</i> model	36
1.8 Medical interests of venom toxins in diagnostics and therapeutics	37
1.9 Problem statement: positive identification of species responsible for envenomation ..	37
1.10 Research question	39
1.11 Hypothesis	39
1.12 Aims and objectives	40
1.13 Ethical considerations	40
CHAPTER 2 Incidence of Snakebite in South Africa	41
2.1 Introduction	41

2.1.1	Tygerberg Poisons Information Centre (TPIC)	41
2.1.2	Case Reports.....	42
2.1.2.1	Case one	42
2.1.2.2	Case two	43
2.1.2.3	Case three.....	44
2.2	Materials and Methods	44
2.2.1	Study area	44
2.2.2	Study design	45
2.2.3	Data Source	45
2.2.4	Data exposure and outcome definitions.....	46
2.2.5	Ethics	46
2.2.6	Statistical analysis	46
2.3	Results.....	47
2.3.1	Overall breakdown	47
2.3.2	Poison Severity Score of Unknown bites	50
2.3.3	Sex and age of snakebite envenoming sufferers	50
2.3.4	Category of caller for snakebite consultation with the PIHWC	52
2.3.5	Annual, quarterly (seasonal), and geographical distribution of snakebites over 5-years	52
2.3.6	Incidence of snakebite by geographical location	54
2.3.7	Snakebite related calls received from the Western Cape, South Africa	54
2.4	Discussion and Conclusion.....	59
CHAPTER 3	Materials and Methods	61
3.1	Materials	63
3.1.1	Reagents and consumables.....	63
3.1.2	General Instrumentation	64
3.1.3	Instrumentation	65
3.1.3.1	HR-LC-MS/MS	65
3.1.3.2	HPLC.....	65
3.1.3.3	SEC	65
3.1.3.4	LC-MS/MS	65
3.1.3.5	<i>In vivo</i> study.....	66
3.2	Methods.....	66
3.2.1	Gel electrophoresis of venom proteins	66
3.3	Trypsin digestion protocols	66
3.3.1	In gel tryptic digestion of proteins	67
3.3.2	On-bead (HILIC) tryptic digestion of proteins	68
3.4	Liquid chromatography	69

3.5	Mass spectrometry	69
3.5.1	Scaffold.....	70
3.5.1.1	Database searching	70
3.5.1.2	Criteria for protein identification	70
3.6	Reversed-phase high performance liquid chromatography (RP-HPLC).....	71
3.6.1	Acetonitrile precipitation of high molecular mass venom proteins	71
3.6.1.1	HR-LC-MS/MS of undigested samples and protein identification	72
3.7	Size-exclusion chromatography of <i>N. nivea</i> venom	73
3.8	Triple quadrupole LC-MS/MS	73
3.8.1	Sample preparation.....	73
3.8.1.1	iRT peptides	73
3.8.1.2	Venom fractions	74
3.8.2	Trypsin digestion protocols of <i>N. nivea</i> venom	74
3.8.2.1	Protocol 1: Traditional trypsin digestion on HILIC beads	74
3.8.2.2	Protocol 2: Accelerated tryptic digestion protocol	74
3.8.2.3	Protocol 3: Accelerated tryptic digestion protocol	75
3.8.3	Triple quadrupole LC-MS method development	76
3.8.3.1	Building multiple reaction monitoring peptide transition lists using Skyline	76
3.8.3.2	Liquid chromatography NexeraXR System	77
3.8.3.3	Triple quadrupole mass spectrometry	77
3.9	<i>In vivo</i> zebrafish larval toxicity assay	77
3.9.1	Zebrafish husbandry and breeding	78
3.9.2	Survival/dose response test.....	78
3.9.3	Behavioral Assay – measurement of zebrafish larval locomotion after exposure to venom fractions	78
CHAPTER 4	Results	80
4.1	Overall venom composition.....	80
4.1.1	Native PAGE	80
4.1.2	HR-LC-MS/MS analysis of <i>Naja nivea</i> , <i>Bitis arietans</i> and <i>Bitis atropos</i> crude venom	81
4.2	<i>Naja nivea</i> venom from the Western Cape and the Northern Cape.....	82
4.3	Depletion of highly abundant proteins from venom and plasma.....	89
4.3.1	Reversed phase HPLC.....	89
4.3.2	HR-LC-MS/MS analysis plasma spiked with venom of acetonitrile high molecular weight protein depleted venom.....	92
4.4	Size exclusion chromatography	96
4.4.1	PAGE <i>Naja nivea</i> venom fractions	97
4.4.2	HR-LC-MS/MS of <i>Naja nivea</i> venom fractions	98

4.5	Toxicity assay	103
4.5.1	Establish treatment concentration	103
4.5.2	Sub-lethal venom treatment acute - 24 hour response	104
4.6	LC-MS/MS	106
4.6.1	iRT Standard	106
4.6.2	<i>N. nivea</i> venom spiked in human plasma	106
CHAPTER 5	Discussion	121
5.1	Incidence of snakebite in South Africa	121
5.2	Venom analysis by gel electrophoresis	121
5.3	Qualitative proteomic analysis of <i>B. atropos</i>, <i>N. nivea</i> and <i>B. arietans</i> venoms	122
5.4	Quantitative proteomic analysis of regionally different <i>N. nivea</i> venoms	123
5.5	HPLC of <i>B. atropos</i>, <i>B. arietans</i> and <i>N. nivea</i> crude venom	124
5.6	Size exclusion chromatography	126
5.7	Development of an LC-MS/MS method to detect <i>N. nivea</i> venom toxins when spiked into plasma	127
5.8	<i>In vivo</i> toxicity assay	127
CHAPTER 6	Conclusion, Limitations and Future work	130
6.1	Conclusion	130
6.2	Limitations	130
6.3	Future work	131
CHAPTER 7	References	132
Appendix		145

CHAPTER 1 Introduction and Literature Review

Snakebite envenoming is a serious public health threat especially in developing countries of sub-Saharan African countries where the high prevalence of snakebite is high (Chippaux, 2017, 2008; Gutiérrez et al., 2017; WHO, 2019). The World Health Organisation (WHO) formally classified snakebite envenomation as a category A priority neglected tropical disease. According to the WHO 5.4 million snakebites occur each year with 1.8 to 2.7 million of these cases of envenomation. Up to 5% of snakebites result in death and approximately 15% of the victims are left with amputations and lifelong disabilities including post-traumatic stress disorder (PTSD). The most vulnerable populations are agricultural workers, hunters, working children, fishers and those living in rural impoverished areas with limited access to education and healthcare (Gomes et al., 2019; WHO, 2019). The mainstay treatment for envenomation is the administration of high quality antivenom, however significant challenges are associated with antivenom therapy and therapy is not always indicated. When an envenomed patient reaches medical care, the species responsible for the envenomation is rarely positively identified and management is based on patient symptomatology (Blaylock, 2005).

1.1 Venomous snake species in South Africa

Globally there are about 1300 species of venomous snakes, which can be classified according to five families. South Africa is home to 170 snake species of which 80 species are venomous and 16 of these species capable of causing debilitating or fatal envenomation syndromes. Species have evolved venom to fulfil the purpose of prey immobilization and as defence against predators by utilising a chemical means of inducing a pathophysiological effect in the recipient (Fry et al., 2012; Gutiérrez et al., 2017; Mtewa, 2019). Venom is usually injected by specialised appendices such as stings, fangs, claws and spines. The most medically significant venomous snakes belong to the Elapidae (cobras, mambas, kraits and sea snake), Viperidae (adders), Atractaspidae (stiletto snakes) and some species of the Colubridae (boomslang and vine/twig snake) snake families. The elapid and viperid families are responsible for the most severe effects following envenomation (Gutiérrez et al., 2006). In general, even though variations and exceptions exist, elapid venoms are typically primarily neurotoxic, whereas viperid venoms are cytotoxic, hemotoxic or myotoxic (Gutiérrez et al., 2006). Figure 1.1 shows an example of an elapid species, the neurotoxic *Naja nivea* (Cape cobra) (A), an example of a viperid species, the cytotoxic *Bitis arietans* (puff adder) (B) and *Bitis atropos* (berg adder) (C), a viperid species that cause both cytotoxic and neurotoxic effects. In South Africa, significant neurotoxicity is caused by envenoming from the elapid species *Naja melanoleuca*, *Naja nivea*, *Naja haje*, *Dendroaspis polylepis*, *Dendroaspis*

angusticeps and *Dendroaspis jamesoni* and cytotoxicity by the venom from the viper species *Bitis arietans* and *Bitis gabonica* and minor adders like *Bitis caudalis*. Spitting cobras such as *Naja mossambica*, *Naja nigricollis*, *Naja nigricincta* and although not a true cobra (*Naja sp.*), the closely related, the *Hemachatus haemachatus* species mostly cause severe cytotoxicity, however varying degrees of neurotoxicity is caused when their venom is delivered via a bite (Petras et al., 2011). In Table 1.1 the snake species of medical significance categorised according to the toxicity caused by their venom.

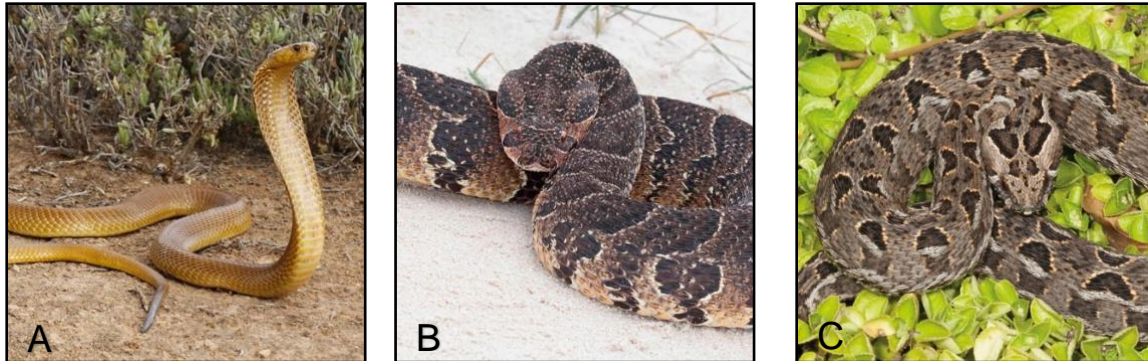


Figure 1.1 The Elapidae family include cobras, mambas and sea snakes for example the cobra species *Naja nivea* (left) and the Viperidae family include vipers and pit vipers for example *Bitis arietans* (right). Credit to the African Snakebite Institute (Johan Marais) for the photos of *Naja nivea*, *Bitis arietans* and *Bitis atropos*.

Table 1.1 Medically significant venomous species in South Africa and their overall toxic effect

Neurotoxic	Cytotoxic	Hemotoxic
<i>Dendroaspis polylepis</i> <i>Dendroaspis angusticeps</i> <i>Dendroaspis jamesoni</i> <i>Naja melanoleuca</i> <i>Naja nivea</i> <i>Naja haje</i>	<i>Naja mossambica</i> <i>Naja nigricollis</i> <i>Naja nigricincta</i> <i>Hemachatus haemachatus</i> <i>Bitis arietans</i> <i>Bitis gabonica</i> <i>Causus rhombeatus</i> <i>Atractaspis bibronii</i> <i>Macrelaps microlepidotus</i>	<i>Dispholidus typus</i> <i>Thelotornis sp.</i>
<i>Bitis atropos</i>		

1.2 Envenomation: Clinical signs, symptoms and therapeutic approach

Venom toxins are very successful at disrupting homeostatic mechanisms due to their specificity, causing pathophysiological changes to different components of the organism. Consequently the clinical manifestations in snakebite envenomation are numerous (Meier and Stocker, 1991). Some of these features may include paralysis, respiratory depression,

incoagulable blood, severe pain, tissue damage, blistering, necrosis, haemorrhage, vomiting, muscle spasms, imbalances in various haematological factors, kidney injury and many more (Gutiérrez et al., 2017; Warrell, 2010).

The initial features of neurotoxicity are vomiting, transient paraesthesia of the tongue and lips, blurred and double vision, ptosis and paralysis of the eye- and facial muscles including other muscles innervated by the cranial nerves. The most important symptoms of neurotoxicity is the progressive, descending flaccid paralysis and development of respiratory weakness. Victims bitten by *Dendroaspis species* may present with muscle fasciculations and in some cases cardiac dysrhythmias in addition to other neurotoxic effects (Muller et al., 2012b). The extent of neurotoxicity depend on the snake genus, species, subspecies, local geographical variation which highlight the vast diversity of snake toxins (Ranawaka et al., 2013).

Cytotoxicity following snake envenomation is characterized by severe local pain, extensive swelling, blistering, necrosis, compartmental syndrome, hypovolaemia and shock. In neglected cases thrombocytopenia (decrease in number of platelets in the blood) and other haemostatic abnormalities may be prominent which is characteristic of viperid envenoming (Reid and Theakston, 1983). The clinical features following a *Bitis atropos* envenoming include local cytotoxicity and systemic neurotoxic effects such as prominent vomiting, loss of taste and smell, paralysis of the muscles within or around the eye, hyponatraemia and respiratory paralysis (van der Walt and Muller, 2019).

In South Africa, the species *Dispholidus typus* and *Thelotornis* species are hemotoxic. Following envenomation, some of clinical manifestations include local pain with insignificant or mild swelling around the bite site. The venom is a procoagulant that activates clotting factor II (prothrombin) and factor X that causes persistent bleeding and diffuse intravascular clotting. The victim may present with bleeding from the gums and nose, blood in the urine and or faeces, vomiting blood, skin discoloration due to haemorrhage from small blood vessels and subarachnoid or intracerebral haemorrhage in severe cases. Multiple organ failure may develop later on due to disseminated coagulopathy (DIC).

1.2.1 Syndromic management approach to envenomation

In South Africa treatment for snakebite follows a syndromic approach based on patient symptomatology. Blaylock (2005) identified three primary syndromes of envenomation and with a recently added fourth syndrome for the management of snake envenomation (Blaylock,

2005). The clinical syndromes explained here are based on the five clinical syndromes identified by Muller et al. (2012b). It is possible for an envenomed victim to present with an overlap of syndromes.

Syndrome 1: Painful progressive swelling

This syndrome is associated with prominent cytotoxic skin changes and coagulable blood. Snake species responsible for this syndrome include *Bitis arietans* (puff adder), *Bitis gabonica* (gaboon adder), spitting cobras, e.g. *Naja mossambica* (Mozambique spitting cobra, M'fesi), *Naja nigricollis* (black-necked spitting cobra), *Naja nigricincta* (barred, zebra spitting cobra) and *Naja nigricincta woodii* (black spitting cobra), and *Hemachatus haemachatus* (rinkhals).

Syndrome 2: Progressive paralysis (neurotoxicity) with negligible or minor local swelling

Snake species that cause this syndrome are the neurotoxic cobra species, *Naja nivea* (Cape cobra), *Naja annulifera* (banded or snouted cobra), *Naja melanoleuca* (forest, black and white-lipped cobra) and mamba species, *Dendroaspis polylepis* (black mamba) and *Dendroaspis angusticeps* (green mamba). Due to variation in venom composition there have been cases reported where envenomation by *Dendroaspis angusticeps* caused insignificant neurotoxicity and extensive cytotoxicity (Muller et al., 2012b). Life threatening paralysis and death can be inflicted by neurotoxic venom within 1 – 8 hours post envenomation. A polyvalent antivenom, produced by South African Vaccine Producers (SAVP) is available for syndrome 1 and 2, if indicated.

Syndrome 3: Coagulopathy with bleeding

This syndrome is caused by the snake species *Dispholidus typus* and *Thelotornis capensis* (South eastern Savanna vine / bird / twig snake) and is classified by incoagulable blood, with negligible to mild local swelling. A SAVP monovalent antivenom is available for *Dispholidus typus* bite but not for envenomation by *Thelotornis species*.

Syndrome 4: Marked local swelling associated with neurotoxicity

Snakes responsible are berg adder (*Bitis atropos*) and other small / dwarf adders (e.g. side-winding adder – *B. peringueyi* and desert mountain adder – *B. xeropaga*).

Within 2 -3 hours of the bite local swelling, paraesthesia of the tongue and lips, blurring of vision and the loss of the sense of smell (anosmia) and taste, and dysphagia develops. A frequent complication involves muscle weakness and respiratory failure that occurs 6 – 36 hours post bite. Hyponatraemia caused by natriuretic toxins is another complication that may cause unexpected convulsions if left untreated. Locally blistering and necrosis may develop

in the region of the bite site, but not to the same extent as cytotoxicity caused by the major adder species (syndrome 1). No antivenom is available for *Bitis atropos* bites.

Syndrome 5: Mild to moderate swelling with negligible or absent systemic symptoms

This syndrome is caused by envenomation from *Causus rhombeatus*, *Atractaspis bibronii*, *Macrelaps microlepidotus* and some dwarf adders, for example *Bitis caudalis*. It has been reported that envenomation by *Macrelaps microlepidotus* (Natal black snake) caused collapse and loss of consciousness (Visser and Chapman, 1978). No antivenom is available to treat envenomation by these species.

1.2.2 Clinical and laboratory monitoring

Laboratory tests can be used to determine systemic envenomation and assist in making decisions about patient management. Recommended tests involve a full blood count, coagulation tests such as the prothrombin time (PT) and partial thromboplastin time as well as quantifying thrombin and fibrinogen levels, fibrinogen degradation products and D-dimer concentrations, urine analysis, urea and electrolytes and serum creatine concentrations (Muller et al., 2012b; Warrell, 2010). Tests used to determine the activity of serum enzymes such as creatine phosphokinase (CK) and lactate dehydrogenase (LDH) could be useful in suspected cytotoxic bites, where an elevated activity would be indicative of tissue damage (Sant'Ana Malaque and Gutiérrez, 2015).

These tests are not available in all health facilities and as an alternative to establish coagulopathy, a 20 minute whole blood clotting profile test is used (Otero et al., 1999; Warrell, 1999). This is a simple, rapid test which can be performed at the bedside and correlates well with the fibrinogen concentration. A few millilitres of venous blood is placed in a new, clean, dry glass vessel and left undisturbed at room temperature for 20 minutes, then tilted once to see if the blood has clotted or not (Sano-Martins et al., 1994; Warrell et al., 1977). This procedure has been shown to lack sensitivity in clinical settings and is time consuming as it may take up to 24 hours to confirm results (Isbister et al., 2013). A phospholipase A₂ bedside assay has been suggested as a useful test to identify whether a patient has systemic envenomation (Maduwage et al., 2015). However these tests do not solve the issue of identifying the species responsible for envenomation. Due to the rapid onset of effects following envenomation, immediate detection and quantification of venom would be beneficial to patient management and subsequent outcome (Dias-Lopes et al., 2018).

1.3 Detection of venom proteins

Conventional detection methods for snake envenomation rely primarily on *in vitro* immunological based bio-assays and over the years numerous assays have been developed. Enzyme-linked immunosorbent assays (ELISA) are the most widely used immunological assay (Minton, 1987; Theakston and Laing, 2014), however more recently detection kits relying on Polymerase Chain Reaction (PCR), Optical Immuno-assays (OIA) electrophysiology, absorbance/fluorescence based and radioligand binding assays. Newer technologies include label-free technologies such as bioluminescence, polarization, fluorescence and fluorescence-resonance energy transfer (FRET), scintillation proximity and bioluminescence resonance energy transfer assays (Duracova et al., 2018; Prashanth et al., 2017; Wilson and Daly, 2018). These assays are used in the discovery of venom peptides for screening of expansive compound libraries and to successfully detect interactions of venom peptides with their biological targets such as G-protein coupled receptors, ion-channels, enzymes and transporters. Immune-affinity chromatography has formed the basis for research into methods for detection of venom compounds in blood/serum and tissues as this is also the basis for the production of antivenom (Dong et al., 2003).

Identification of the snake specie responsible for envenomation could assist in deciding on antivenom use and management of the victim. Currently there is only one commercially available diagnostic test to decide the appropriate antivenom if required, the snake venom detection kit (SVDK) which was developed by Commonwealth Serum Laboratories (CSL) in Australia (Cox et al., 1992). The drawbacks of the SVDK are cross-reactivity with other snake species and false-positive or false-negative conclusions due to saturation of antibodies at higher concentrations of snake venom toxins (Nimorakiotakis and Winkel, 2016; Steuten et al., 2007). Unfortunately, this kit is only available in Australia. More recently an immunochromatographic test for cobra (ICT-Cobra) was developed by Lin et al. (2020) in Taiwan. The test that relies on Western blotting and sandwich enzyme-linked immunosorbent assay (ELISA) was successful in the detection of the venom from *Naja atra* and other Asian cobra species. Even though the test was not successful in the detection of venom from African cobras, the study did show that due to a close immunological relationship in the genus *Naja species*, a transregional venom detection kit could potentially be developed (Lin et al., 2020).

1.4 Antivenom

Since the 1890s when antivenom serotherapy was developed, antivenoms continue to be the mainstay treatment for snakebite envenoming and play an invaluable role in saving thousands

of lives. However, many disadvantages relating to safety, efficacy and availability are associated with antivenoms (Knudsen et al., 2019). Variability of snake venom within and between species, due to toxin isoforms that cause distinct pathologies in snakebite victims cause serious consequences for the management of snakebite victims due to these toxins affecting the efficacy of antivenoms (Casewell et al., 2020).

1.4.1 Production

The South African Vaccine Producers (SAVP) produces four different antivenoms that are used in South Africa. The first is a polyvalent snake antivenom that is effective against envenomation by ten different snake species. These species include mambas (*Dendroaspis spp.*), spitting and non-spitting cobras (*Naja spp.*) and major adders (*B. arietans*, *B. gabonica*). The second is a monovalent snake antivenom that is effective against boomslang (*Dispholidus typus*) bite. The remaining two SAVP antivenoms include a spider antivenom effective against bites inflicted by *Latrodectus* species and a scorpion antivenom, effective against envenomation by *Parabuthus species*. Anti-venom is produced by the immunization of other mammals such as horses and sheep with venom. A hyperimmunized animal will be created within 9 months. Manufactures produce antivenom by the fractionation of hyperimmunized plasma. In Sub-Saharan Africa, only one country, namely South Africa, produces antivenom (Habib et al., 2020). According to Johan Marais, herpetologist, and C.E.O. of the African Snakebite institute, the SAVP dispatch antivenom to a central provincial depot, and from there it is distributed to the various hospitals and medical facilities in that province. Antivenom is expensive, has a short shelf life and therefore often not available in smaller hospitals (African Snakebite Institute, 2021). It is quite possible for a snakebite victim to arrive at a smaller hospital with no antivenom available. This can lead to high morbidity and cost, as patients are often transferred to bigger hospitals who stock the antivenom. Complexity of the production of antivenoms that are efficient in reversing the effects of envenomation is an issue already highlighted by the WHO in 1964 (Wachel and Cole, 1964), who also reported on the cycle of antivenom market decline and unfortunately this is still case (Kularatne and Senanayake, 2014; Puzari and Mukherjee, 2020; Silva and Isbister, 2020; Slagboom et al., 2022)..

1.4.2 Adverse effects of antivenom therapy

Horses or rabbits that are used to produce venom antibodies are of different genetic make-up and have different proteins to humans, and hence the human body may perceive it as foreign and reject it resulting in anaphylaxis. Other serious adverse effects from antivenom include delayed reactions such serum sickness (de Silva et al., 2016). Accurate dosing and effective use of antivenom is important as, in addition to potential anaphylaxis, the production of

antivenom is costly and the supply is limited (Sanhajariya et al., 2018; Williams et al., 2019a). Knowing exactly which antivenom needs to be procured will drastically lessen costs. Antivenom will not reverse respiratory depression caused by neurotoxic bites and ventilatory support will still be required in these cases. The same holds for tissue damage caused by cytotoxic bites, where it may limit the effects of envenomation, but cannot reverse necrosis. (Rossiter et al., 2020) Thus antivenom should ideally be administered only when the animal species responsible for envenomation is positively identified. The complications caused by antivenom indicate the need for high quality monovalent antivenoms, which can be cost effectively produced and widely distributed (de Silva et al., 2016; Williams et al., 2019a).

1.5 Proteomic composition of snake venom

Snake venoms are complex mixtures of proteins, peptides, organic and inorganic molecules, and metal ion salts that are produced in specialised glands and delivered to the recipient by specialised delivery systems i.e. stings or fangs. These compounds have undergone extensive evolutionary alterations to successfully incapacitate and kill prey or predator to increase survival of the venom-producing species. The observed complex symptomatology of snakebite envenomation is due to the combination of these various venom components (Kang et al, 2011). Even though a high degree of variability in the composition of snake venoms exist, venom mixtures are homologous and contain only a small number of protein families (Fox, 2013; Fry, 2005; Torres et al., 2003).

In the case of snakes which contains cytotoxic venom, for example *Bitis arietans*, the toxins in the venom include mainly proteolytic enzymes and peptides and phospholipases with molecular weights in the range of 13-50 kDa (Hider et al., 1991; Paixão-Cavalcante et al., 2015). These components are responsible for the destruction of tissues. The venom from snakes such as the *Naja nivea* that cause neurotoxicity, includes polypeptide toxins, such as α – neurotoxins, belonging to the three-finger toxin protein family with molecular weight of 6-9 kDa. These toxins competes with acetylcholine at post synaptic nicotinic receptors and causes paralysis. Snakes such as the African boomslang (*Dispholidus typus*) that cause hemotoxic effects in their victims and severe consumptive coagulopathy are due to their potent procoagulant toxins (Debono et al., 2017).

1.5.1 Structural and functional classes of venom toxins

Venomous snakes from different taxonomic families differ in the composition of their venoms. Proteins and peptides in venom can be generally categorised into two groups, those that have

enzymatic activity and those that are non-enzymatic. Extensive variability in venom composition exists across different families of snakes. In general, the venom of elapid snakes are dominated by non-enzymatic toxins such as neurotoxins, cytotoxins and to a lesser extent enzymatic toxins such as phospholipase A2s, whereas the viperid venoms are dominated by enzymatic toxins such as serine- and metalloproteases and to a lesser extent non-enzymatic toxins (Ferraz et al., 2019; Kularatne and Senanayake, 2014).

1.5.2 Enzymatic venom components

Enzymatic toxin families include phospholipase A2 (PLA2), phospholipase B, snake venom metalloproteinases (SVMP), snake venom serine proteases (SVSP) phosphodiesterase (PDE) and L-amino-acid oxidases (LAAO) (Kang et al., 2011). Various studies into the structure, activity and underlying mechanisms of action of these toxins have been done in an attempt to understand the pathophysiological effects caused by envenomation by viperid species (Kang et al., 2011; Kini, 2003; Williams et al., 2019b). Some of the enzymatic proteins and peptides of snake venoms and key characteristics are listed in Table 1.2.

Viperid venoms are abundant in snake venom metalloproteinases and serine proteases. Snake venom serine proteases catalyse various reactions in the coagulation cascade, fibrinolytic systems, complement systems, kallikrein-kinin system, blood platelets and endothelial cells and thereby promote the effects of envenomation (Serrano, 2013). Snake venom metalloproteinases catalyse the hydrolysis of structural molecules including basal lamina and fibrinogen and are primarily responsible for causing haemorrhage, myonecrosis and disruption of hemostasis as a result of envenomation (Bjarnason and Fox, 1994; Fox and Serrano, 2005; Kamiguti et al., 1998; Williams et al., 2019b).

Phospholipases A2 (PLA2) is a super family of enzymes are found in almost all snake venoms. Currently more than 600 snake venom secreted PLA2 enzymes have been isolated from snake venoms (Lomonte and Križaj, 2021). They are potent toxins capable of causing a variety of toxic activities. These enzymes catalyse the hydrolysis of the ester bond at the sn-2-position of membrane glycerophospholipids (Murakami and Kudo, 2002). This reaction produce lipid mediators the free fatty acids including arachidonic acid (AA) and another class of lipid mediators called lysophospholipids (Burke and Dennis, 2009; Lambeau and Gelb, 2008; Murakami and Kudo, 2002). Some biological activities of PLA2 enzymes include pre-and post-synaptic neurotoxicity, myotoxicity, inflammatory action and hemostatic disruption (Lambeau and Gelb, 2008; Sajevic et al., 2014) Enzymatic catalytic efficiency was measured by Wang

et al., (2020) using an MS-based PLA2 enzyme assay. The author found that the monomeric PLA2 had less bioactivity than the dimeric PLA2 (dimeric greater bioactivity than monomeric).

Phosphodiesterase enzymes have multiple roles in regulation of nucleotide-based intracellular signalling as well as metabolism of extracellular nucleotides (Uzair et al., 2018). Mechanism of action involve hydrolyses of phosphodiester bonds from the 3' terminus of polynucleotides to produce 5-mononucleotides. The enzymatic mechanisms of PDE have been extensively studied (Mitra and Bhattacharyya, 2014; Uzair et al., 2018). Activity of PDE has been found in almost all snake venoms, however PDE in viperid venoms appear to have greater activity (Uzawa, 1932). Less research has been performed in studying the venom enzymes L-amino acid oxidases (LAO), hyaluronidases (HYA) and phosphodiesterase (PDE) as these apparently contribute to a lesser extent to snake venom pathophysiology (Kularatne and Senanayake, 2014). However, there have been reports on the biological functions of these enzymes that could have relevance to the envenomation syndrome. There may be benefits to learning more about the role of these enzymes in the pathophysiology observed in snake envenomation.

Table 1.2 Enzymatic snake venom proteins and peptides and general characteristics

Protein/peptide	Approximate mass	Function	Biological activity	References
Phospholipase A2 (PLA2)	3 - 15	Hydrolysis of ester bond at sn-2 position glycerophospholipids	Myotoxicity, myonecrosis, lipid membrane damage	(Kini, 2003; Murakami and Kudo, 2002)
Snake venom serine proteases Kallikrein-like Thrombin-like	27-34 31-36	Act on plasma kininogen to release bradykinin; hydrolysis of angiotensin; catalysis of fibrinogen hydrolysis;	Degradation of fibrinogen; rapid fall of blood pressure; immobilise prey; rapid depletion of fibrinogen and disruption of hemostasis	(Komori and Nikai, 1998; Markland, 1998; Swenson and Markland, 2005)
Snake venom metalloproteinases M12 reprotolysins, P-I, P-II, P-III	20 – 85	Hydrolysis of many structural proteins, including fibrinogen and basal lamina	Induce haemorrhage, proteolytic degradation, myonecrosis, lipid membrane damage	(Fox and Serrano, 2005)
Hyaluronidase	73	Hydrolysis of interstitial hyaluronan	Decrease the interstitial viscosity - diffusion of venom components	(Fox, 2013; Kudo and Tu, 2001)
Phosphodiesterase	94 – 140	Hydrolysis of nucleotides and nucleic acids	Depletes cyclic, di- and tri- nucleotides Hypotension initiating enzyme (speculation)	(Fox, 2013; Mitra and Bhattacharyya, 2014; Uzair et al., 2018)
L-amino acid oxidase	85 - 150	Oxidative deamination of L-amino acids	Induce apoptosis and cellular damage	(Fox, 2013; Wiezel et al., 2015)

Acetylcholinesterase	55 - 60	Hydrolysis of acetylcholine in the synaptic cleft	Cessation of neuromuscular stimulation	(Bourne et al., 1995; Frobert et al., 1997)
5'-nucleotidase	53 - 82	Hydrolysis of 5'-nucleotides	Generation and liberation of purines (mainly adenosine); assist in prey immobilisation	(Dhananjaya and D'Souza, 2010)
Pro-thrombin activators Group C Group D Group A	>250 45-58 ~45	Activate factor VII or X Activate factor X Activate factor X	Highly toxic, induce disseminated intravascular coagulation (DIC)	(Fry et al., 2008; Rosing and Tans, 1992; Tans and Rosing, 2001)
Natriuretic peptide	3	Induce hypotension, vasoactive	Potentiates hypotension	(Epstein et al., 1998)
Bradykinin potentiating peptide	1.0 – 1.5	Increase potency of bradykinin	Hypotension, pain; prey immobilisation	(Soares et al., 2005)

1.5.3 Non-enzymatic

Non-enzymatic toxins include: three-finger toxins (3FTXs), C-type lectins (CTLs), proteinase inhibitors (PIs), nerve growth factors, bradykinin potentiating peptides (BPPs), cysteine rich secretory proteins (CRiSPs) vascular endothelial growth factors (VEGFs) and disintegrins (DIS). All non-enzymatic toxins interfere directly with the cardiovascular and neuromuscular systems and are believed to be the major role players in prey immobilisation (McCleary and Kini, 2013). One of the most abundant and potentially toxic non-enzymatic venom components found within the venom of elapid snakes are three-finger toxins. This is one of the largest protein families with about 300 different isoforms identified. A structural characteristic of these toxins are the three fingers created by the beta loop. The major toxic effects from envenomation by elapid species are caused by α -neurotoxins. These toxins can be long- and short chain neurotoxins capable of exerting various toxic effects on the cardio and nervous systems. These toxins bind with high affinity, non-covalently to muscular and neuronal nicotinic acetylcholine receptors (nAChR), thereby blocking the action of acetylcholine (antagonist) at the post synaptic membrane which consequently impairs both neuromuscular and neuronal transmission. Having the ability to act at different sites of the nervous system and being complementary to produce cumulative effects that result in lethality or debilitation, makes three-finger toxins highly efficient at immobilizing prey (Dyba et al., 2021; Osipov and Utkin, 2015).

Non-enzymatic proteins and peptides that are commonly found in the venom of many elapid and viperid species and general characteristics are listed in Table 1.3. below.

Table 1.3 Non-enzymatic snake venom proteins and peptides and general characteristics

Protein/peptide	Approximate mass	Function	Biological activity	References
Non-Enzymatic				
Cysteine-rich secretory proteins (CRiSPs)	20-30	Possibly block carbon nanotube pore (cNTP)-gated channels	Inhibit ion channels and growth of new vessels (angiogenesis), increase vascular permeability, promote inflammatory response, induced hyperthermia	(Tadokoro et al., 2020; Yamazaki and Morita, 2004)
Nerve growth factors	14-32.5	Neurotrophic factor (neuronal maintenance)	Unknown; potential role in apoptosis	(Kostiza and Meier, 1996; Yamazaki et al., 2009)
Phospholipase A ₂ - based neurotoxins	13-16	Pre-synaptic neurotoxin - block release of acetylcholine from axon terminus; blood coagulation inhibitor	Potent neurotoxicity: immobilise prey	(Fathi H et al., 2001; Ferraz et al., 2019; Rigoni et al., 2008)
Disintegrins	4 – 15	Antagonist of integrin receptors	Inhibits platelet aggregation, promote hemorrhage	(Calvete et al., 2005; Rivas-Mercado and Garza-Ocañas, 2017)
C-type lectins	27 – 29	Binds to platelet and collagen receptors	Anticoagulant- and platelet modulating activities	(Lu et al., 2005; Morita, 2005)
Non-PLA ₂ myotoxins	4 – 5.3	Voltage-gated potassium channel inhibitor, acts as cell penetrating peptide	Severe muscle necrosis (myonecrosis), antimicrobial activities	(Baker et al., 1992)
Three-finger toxins α - neurotoxins cytotoxins cardiotoxins fasciculins	6 – 8	Inhibition of neuromuscular transmission, cardiac function, acetylcholinesterase	Rapidly immobilise prey, paralysis, death	(Kini, 2002; Kini and Doley, 2010; Nirthanan and Gwee, 2004; Utkin, 2019)
Phospholipase A ₂ Inhibitor	75 – 100	Neutralises PLA ₂ myotoxic activity through different mechanisms including denaturation, modification of specific amino acids and others	PLA ₂ enzyme inhibitor	(Marcussi et al., 2007)
Kunitz-type serine protease inhibitor	9	Inhibition of serine proteases and potassium, sodium and calcium channel blocker	Disruption of blood coagulation by targeting factors Xa and XIIa, activated protein C, plasmin and thrombin	(Harvey, 2001; Inagaki, 2017)
Cystatin	~16	Cysteine-type protease inhibitor	Speculated as housekeeping or regulatory protein	(Boldrini-França et al., 2017)
Vespryn/Ohanin	21-24	Neurotoxin	Hypolocomotion and hyperalgesia	(Pung et al., 2006)

Waprin	8 - 13	Peptidase inhibitor	Selective anti-microbial properties	(Fry, 2005)
Ficolin lectin	17 - 38	Initiate complement activation and/or blood coagulation and/or interferes in platelet aggregation	Impairs hemostasis	(OmPraba et al., 2010)

1.6 Research techniques used in the analysis of venom

In general up to up 90 - 95% of dry weight of venom is composed of proteins and peptides (Hider et al., 1991; Liu et al., 2011; Tu, 1988), hence research methods involved in the study of venoms (“venomics”) rely primarily on the application of proteomics techniques. Proteomics have enabled an understanding into snake venom protein diversity, characterization of venom proteins and peptides, can aid an understanding of the underlying molecular mechanisms of venom components resulting in physiological after-effects of envenomation (Casewell et al., 2020). Due to the complexity and often limited quantity of venom that is available, the successful separation and quantification of venom components requires multidimensional high-throughput proteomic strategies. Protein toxins have been detected by various conventional methods that involve bioassays including nucleic acid-based assays, such as enzyme-linked immunosorbent assays (ELISA), Polymerase Chain Reaction (PCR) or western blotting (Dorner et al., 2016).

1.6.1 Proteomic profiling of snake venom

Over the last decade, advances in technology and the resolving power and sensitivity of mass spectrometry has enabled a rapid increase in the characterisation of snake venom proteomes from numerous species (El-Aziz et al., 2020). This has generated great possibilities for the use of venom components in diagnostics, anti-venom research, biotechnology and drug discovery. A major complication of the characterisation of venom toxins is the complexity of venom to be analysed, therefore no single proteomics method is capable of providing a complete analysis of the venom proteome and analysis relies on various proteomic based techniques performed in series (Fox and Serrano, 2008; Serrano et al., 2005).

Decomplexation strategies and sample preparation are important aspects to enable successful investigation of the venom components. The focus of this study is not on the characterisation of the complete venom proteome of each species, but on venom proteins and peptides that fall within the low molecular weight range, namely lower than 30 kDa. Protein toxins share commonalities with biological components and since human blood contains abundant proteins in the range from 40 – 245 kDa, to increase the probability of venom toxin

detection, venom toxins outside of this range are the primary focus. Attempts to reduce complexity of the venom samples, such as protein depletion, protein enrichment and enzymatic degradation of proteins by proteolytic cleavage are used in preparation for mass spectrometry analysis. This involves precipitation of proteins with an organic solvent or another technique that typically used to precipitate large biomolecules involves the utilisation of very high ionic strength that cause a decrease in protein solubility and thereby 'salting-out' the proteins with an inorganic solvent like ammonium sulfate (Duong-Ly and Gabelli, 2014). Organic solvents commonly used include acetone, methanol and acetonitrile (Luque-Garcia and Neubert, 2007).

There are two mainstream proteomic approaches that are followed to identify and quantify the proteins and peptides in venom these are top-down and bottom-up. A bottom-up proteomics (BUP) is the preferred approach as it is both experientially and computationally more feasible (Wilson and Daly, 2018), although there has been an increase in the use of top-down proteomic approach (TDP) in snake venoms (Ghezellou et al., 2019). Methods that are used for the separation of toxins include gel-filtration chromatography, ion-exchange chromatography and reversed-phase high pressure liquid chromatography (RP-HPLC). In this study venom is investigated in a plasma matrix. Methods that are used for the depletion of highly abundant plasma proteins include centrifugal ultrafiltration, solid phase extraction, organic solvent extraction, gel- and capillary electrophoresis, fractional precipitation methods (use of organic solvents) and immune electrophoresis (Kay et al., 2008; Luque-Garcia and Neubert, 2007).

1.6.1.1 Separation methods

Reversed-phase high pressure liquid chromatography (RP-HPLC) is a venom decomplexation strategy often used as the initial step prior to analysis by mass spectrometry (MS) (Calvete, 2014). In this study, size exclusion or gel-filtration chromatography (SEC) was the first technique used for the fractionation of venom proteins based on their size prior to the identification of the venom toxins by mass spectrometry. Here separation is not based on the interaction between the analyte and the column surface, but rather on the degree of inclusion or exclusion of the analyte onto the pores within the stationary phase. The hydrodynamic volume of the pores of the stationary phase has different accessibility for molecules. Larger molecules are generally poorly retained, eluting first whereas smaller molecules, as size dependent, can diffuse to a greater extent into the pores and are retained for longer, and thus elute later. The smallest molecules will elute last. In addition to decomplexation of the venom proteome, both techniques offer a means to quantify the relative abundance of the different

venom components in each fraction, by monitoring the column eluate at a wavelength of 215-220 nm (RP-HPLC) and 280 nm (SEC) and applying the Lambert-Beer Law ($A = \epsilon cl$; where ϵ is the molar extinction coefficient [$M^{-1}cm^{-1}$] of the absorbing species, c is the concentration of the absorbing species [M] and l is the light path length [cm]. SEC chromatograms are usually viewed at 280 nm UV absorption, as tryptophan and tyrosine possess strong absorption in this range and most of the eluant buffers are transparent (Hider et al., 1991).

1.6.1.2 Mass spectrometric approaches

Mass spectrometry (MS) is an analytical technique that offers fast, sensitive and specific detection of an analyte. It is a powerful tool in proteomic analysis that involves relative/absolute and targeted/untargeted proteomics. The continuous development of MS instruments offering high resolution accurate mass (HRAM) instruments and hybrid configurations enable analysis of a wide range of analytes, from small organic molecules to large biomolecules (Duracova et al., 2018). MS based methods are utilised in this study to identify unique and abundant species specific venom proteins and peptides and then to detect these toxins from human plasma. The basic principle of mass spectrometry is to identify molecules based on the molecular weight by generating ions from either inorganic or organic molecules, fragmentation of the charged molecules and then to measure the mass-to-charge ratio (m/z) of the fragments.

Electrospray ionisation (ESI) is a technique that uses electrical energy to transform the protein samples from solution to gaseous phase before they are introduced into the mass spectrometer. This process involves three steps: first a charge is applied and a fine mist of highly charged droplets is generated. The second step involves desolvation. The solvent is evaporated by applying a nebulising gas, heating and drying gas that cause the size of droplets to decrease, and the surface charge density of the droplet to increase, until the Rayleigh limit is reached and the electric field strength within the droplet is overcome by Coulombic repulsive forces between the charges on the droplet surface and the droplet fissions. During the third step, the analyte ions are released from the charged droplets and are sampled by the sampling skimmer cone and accelerated into the mass analyser (Ho et al., 2003). The high temperatures, organic solvents and acids typically used to assist desolvation could be limiting factors when analysing native proteins. Nano-electrospray ionisation (nano-ESI) allows for a smaller sample volume and at a reduced flow rate which increases sensitivity (El-Faramawy et al., 2005).

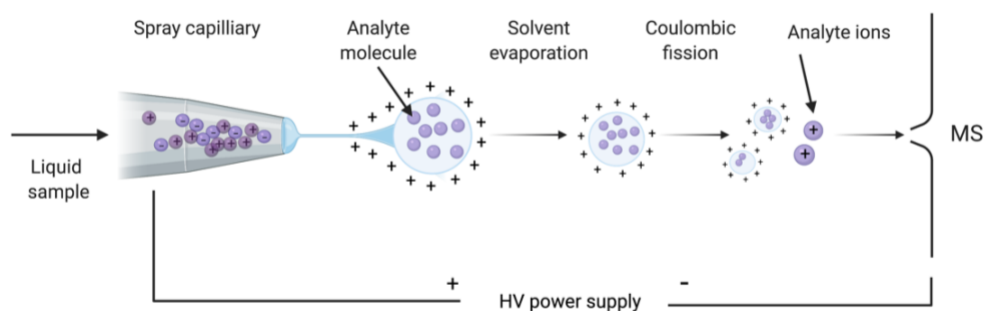


Figure 1.2 Overview of the process of electrospray ionisation of an analyte. The ESI process involves three steps: the generation of charged droplets under a high voltage (HV) electric field from a liquid sample, desolvation of the charged droplets that causes their surface charge to increase and force the droplets to fission and form smaller multiple charged droplets. These decrease in size and turn into gas phase analyte ions.

Different mass analysers are coupled to ESI to obtain structural information on the analyte. The precursor ion mass can be selected and further fragmented in the collision cell and the product ions further analysed. Mass analysers that are often used in clinical laboratories include quadrupole mass analysers, the tandem quadrupole systems and the ion trap mass analysers.

In a quadrupole mass analysers, the system is made up of four parallel rods distributed at an equal distance from each other. Opposite rods are electrically connected to each other, and an opposite but equal DC voltage that is superimposed with radio frequency (RF) AF electric current is applied. The electrical field causes the ions to move in an oscillatory pattern from the source to reach the detector. The DC and RF voltages can be optimised to the m/z ratios to ensure a stable flight (Ho et al., 2003). In tandem quadrupole, three quadrupole mass analysers are linked in series. In the first quadrupole (Q1), the precursor mass is selected, in a second collision cell (Q2), collision between the precursor ion and collision gas (usually argon or nitrogen gas) causes fragmentation of the ion, known as collision-induced dissociation (CID). The resulting daughter ions can then be monitored by the third quadrupole mass analyser (Q3) to reveal information on the molecular structure of the ions. Figure 1.3. shows a schematic diagram of a triple quadrupole mass spectrometer. The target analytes are analysed by multiple reaction monitoring in positive ion mode.

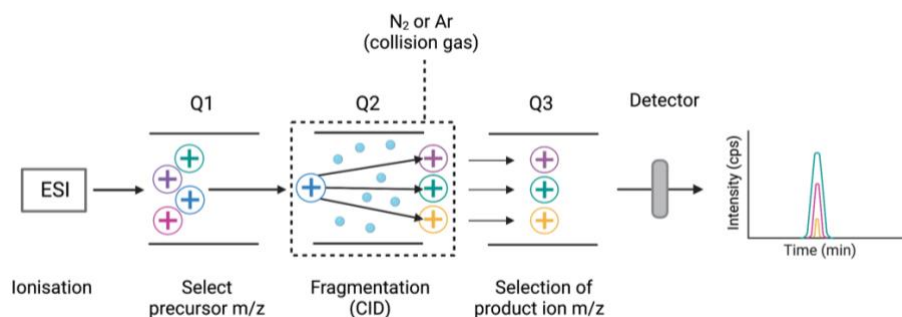


Figure 1.3 Overview of the triple quadrupole mass spectrometer (QQQ MS). Analyte ions produced by electrospray ionisation are introduced into the mass spectrometer vacuum. In quadrupole 1, the analyte precursor mass to charge is selected, collision induced dissociation cause fragmentation of the precursor ion in quadrupole 2 and in quadrupole 3, co-eluting interferences are removed and the mass to charge for product ions are selected, detected and monitored over the elution time on a chromatogram.

The ion trap mass analyser consists of two end cap electrodes and ring electrodes. Ions are introduced from the source, often nano-electrospray ionisation, into the trap through the quadrupole, collision cell and entrance end cap electrode. Various voltages are applied to the electrodes which trap the ions according to their m/z ratios in a stable oscillating trajectory. During detection, instabilities in the ion trajectories are produced and ions are ejected in order of increasing m/z ratio. Figure 1.4 shows an example of a high resolution orbitrap mass analyser in a tandem mass spectrometry system. The sensitivity of ion trap analysers are 10 times less than that of the tandem triple quadrupole system (Ho et al., 2003). Peptides are identified by search engines such as mascot, MsAmanda etc. and protein data base searches.

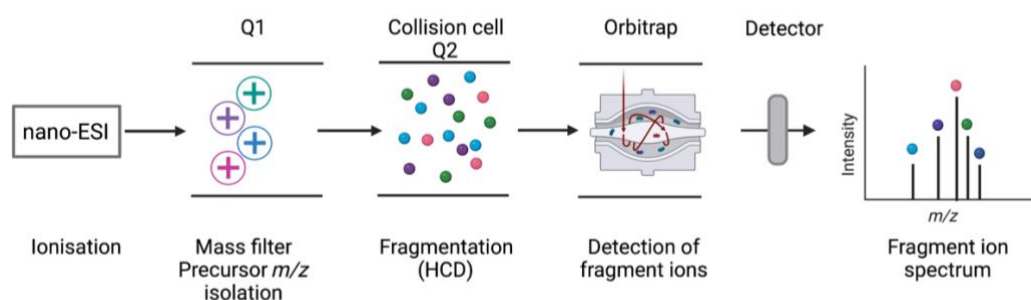


Figure 1.4 Overview of the orbitrap high resolution mass analyser in tandem quadrupole system. Analyte ions produced by nano-electrospray ionisation are introduced into the mass spectrometer vacuum. In quadrupole 1, intense precursor mass to charge is selected for mass spectrometry MS/MS analysis, higher energy collisional dissociation (HCD) cause fragmentation of the precursor ions in quadrupole 2 coupled to a high resolution orbitrap mass analyser, where ions are separated based on their mass to charge (m/z) and peptides identified by matching of fragment ion mass spectra to protein database.

A look into the future for the absolute quantification of proteins, the developed molecular mass spectrometry-based methods usually require analogous stable-isotope labelled standards that

were certified using natural standards for each target protein or peptide being investigated. Calderón-Celis *et al.* (2016) circumvented this issue by developing a methodology that involves separation of venom by RP- μ HPLC capillary liquid chromatography inductively coupled plasma triple quadrupole which is based in the elemental content of the sample. Calderón-Celis *et al.* (2016) developed a reversed-phase micro high performance liquid chromatography inductively coupled plasma triple quadrupole tandem mass spectrometry- (RP- μ HPLC-ICP-QQQ) and online S34 isotope dilution method for the absolute quantitative analysis of the major toxins found in the proteome of the Mozambique spitting cobra, *Naja mossambica* (Calderón-Celis *et al.*, 2016). No work in recent years has been published on the use of triple quadrupole LC-MS/MS method for investigation of venom toxins in human plasma.

1.7 Toxicity and physiological effects of snake venom toxins in an *In vivo* model

In vivo models that are used in the assessment of activity and toxicity of venom proteins and peptides include various animal models, such as rats, mice, rabbits and zebrafish models. Zebrafish (*Danio rerio*) are small fresh-water fish from South Asia that have unique genomic and morphological characteristics advantageous for experimental research in various fields including pharmacology, biochemistry and physiology. Their unique features, such as homology to the human genome, the ease at which they are genetically manipulated, accessibility, high fecundity and transparency of larval to juvenile bodies make them ideal for toxicological studies as substances capable of causing acute toxicity which interfere with an organisms development can be easily evaluated (Hill *et al.*, 2005). Additional benefits of using zebrafish as a model for toxicity testing is the sensitivity of the zebrafish to the presence of various toxins, even at very low concentrations. This can be assessed according to the phenotypic changes, such as deformities in terms of normal development, behavioural assays tracking movement and histopathology of various physiological systems e.g. neurological and cardiovascular systems (Chahardehi *et al.*, 2020; Chan *et al.*, 2017; Garcia *et al.*, 2016; Rubinstein, 2006). Acute toxicity can be evaluated by assessing the lethal toxic concentration, which will effectively kill zebrafish larvae in minutes. At non-lethal concentrations, toxicity could be evaluated based on the malformation of zebrafish embryos, delayed or completely halted hatching, adversely affected embryonic development and attenuation of swimming distance (Chan *et al.*, 2017). In a study by Chan *et al.* (2017) where the toxicity of rhodamine B-conjugated crotamine (toxic peptide from rattle snake venom) was evaluated in a zebrafish model, translocation across the vitelline membrane and accumulation of the toxic peptide in zebrafish yolk sac was reported.

1.8 Medical interests of venom toxins in diagnostics and therapeutics

Snake venoms are cocktails of complex pharmacologically active proteins and peptides that cause augmentation of biological activity with an intent to incapacitate or kill the predator or prey (Kerckamp et al., 2015). Investigation into the proteomic composition and variability of snake venoms provide important insights into the specificity and potency of the venom toxins and offers an opportunity for therapeutic applications (Wang, 2019). Some of the key properties that make snake venom toxins good candidates for drug discovery are that the toxins target molecules that regulate and control homeostasis such receptors, ion channels and components of enzymatic processes with high affinity, the mechanism of action of the toxin (agonist, antagonist, modulator) is often desirable for therapeutic application. Currently the field of drug development and discovery from venom toxins is largely based on research involving the characterisation of the molecular structure and function of toxins. The relationship between toxin structure and activity provide directionality in the search for novel therapeutics (El-Aziz et al., 2019). The first FDA approved drug from snake venom toxins were Captopril, an angiotensin converting enzyme inhibitor used for the treatment of hypertension and cardiac failure from the species *Bothrops jararaca* (Ferguson and Vlasses, 1981). Another drug that originated from snake venom toxins are Tirofiban, an antagonist of fibrinogen binding to glycoprotein IIb/IIIa receptor that inhibits platelet aggregation and prolong bleeding times in patients with acute coronary syndrome (McClellan and Goa, 1998) .

1.9 Problem statement: positive identification of species responsible for envenomation

The positive identification of the species responsible for envenomation is very difficult and in many cases identification is based on what the envenomed patient or bystanders present during the incident might have witnessed, when the species responsible for the bite or sting is brought into the hospital (Muller et al., 2012) or a clear picture of the species was captured and health care professionals or SPIs (specialist in poison information) were able to send it to an expert for identification. Diagnosis of envenomation is based on patient symptomatology and the five clinical syndromes of snake envenoming (Muller et al., 2012b). It is also possible for several types of envenomation to produce similar symptoms and this can lead to incorrect patient management. For example, the mechanism of action of neurotoxic venom from the Cape cobra (*Naja nivea*), *Parabuthus granulatus* scorpion and Black widow spider (*Latrodectus sp.*) all act on the peripheral nervous system, each acting on their respective neurotransmitter, ion channel or receptor. This leads to blocking, stimulation or inhibition at

the pre- and postsynaptic neurons causing neurotoxic symptoms (Muller et al., 2012a). The symptoms of envenomation by either of these species overlap, as shown in **Error! Reference source not found.**

Table 1.4 Overlap of the major signs and symptoms of neurotoxic snakebite, scorpionism and latrodectism (Muller et al., 2012a; Rossiter et al., 2020)

Signs and symptoms of envenomation	Scorpionism	Latrodectism	Neurotoxic bite by <i>Naja spp.</i>
Local symptoms and signs			
Degree of local physical signs (bite or sting site)	(+)	+	++
Local pain	++++	+	++
Regional lymph nodes, pain and swelling	+	+++	+
Systemic symptoms and signs			
Generalised muscular pain	++(+)	++++	–
Increase in muscle tone: extremities, abdomen and chest	+(+)	+++	–
Paraesthesia, hyperaesthesia	++++	+	–
Dysphagia, dysarthria	++++	–	+++
Involuntary movements, tremor, fasciculations	++++	++	+
Hyperactivity, restlessness	++++*	++	–
Increase in stretch reflexes	+++	++	–
Flaccid paralysis	–	–	++++
Difficulty in breathing, requiring ventilatory support	+++*	–	++++
Ophthalmoplegia	(+)	–	++++
Ptosis	++	–	++++
Autonomic dysfunction:			
- pulse rate: fast or slow, ↑ blood pressure	++++**	+++	(+)
- ↑ sweating	++	+++(+)	+
- ↑ temperature	++	+	(+)
- salivation ↑ upper respiratory secretions*	++++	–	++
* Especially in children			
** Inter species variation, for example <i>P. granulatus</i> : ↑ pulse rate; <i>P. transvaalicus</i> : ↓ pulse rate			

A further complication of diagnosis and antivenom efficacy is caused by variations in regional interspecies venom composition (Andrejčáková et al., 2015; Cochran et al., 2019; Wong et al., 2018). Anecdotal evidence suggests a difference in the toxicity in the venom of the same species from different geographical areas in South Africa, particularly in the case of envenomation by the species *Naja nivea*, although no studies have reported such findings. In one such case documented by the Poisons Information Helpline of the Western Cape (PIHWC), the toxicity of the venom from the *Naja nivea*, which is neurotoxic and usually does not show cytotoxic symptoms, caused severe cytotoxic damage in a patient in the Northern

Cape Province of South Africa. The development of a rapid, robust LC-MS/MS method to determine the major toxin present in envenomed plasma can potentially lead to the development of novel diagnostic tools and therapeutics for snake envenomation to provide snakebite victims with a rapid and inexpensive test to determine the species responsible for envenomation and ensure that the best care is provided. This can lead to more species specific treatment in terms of the anti-venom administered and the response time to administration of effective treatment. In many cases the unknown identity of the species responsible for the bite or sting is one of the main factors leading to increased morbidity and mortality of patients. The development of this LC-MS/MS protocol would focus on envenomed humans. However, this method could also be used to test for the species responsible for an envenomation in other mammals (i.e. horses) or in forensics in cases of accidental or deliberate (murder or suicide) deaths.

1.10 Research question

Could unique species specific venom toxins be targeted to develop an analytical diagnostic tool to determine cause of envenomation in South Africa?

1.11 Hypothesis

The investigators hypothesize that unique species specific venom proteins responsible for envenomation could remain intact *in vivo* following envenomation, allowing for their use in the development of diagnostic tools for envenomation in South Africa.

1.12 Aims and objectives

Aim

To develop an LC-MS/MS method for the rapid detection of species-specific venom toxins from patient plasma.

Objectives

1. To report on the incidence of envenomation by snakes in South Africa using the Poisons Information Helpline of the Western Cape (PIHWC) AfriTox Telelog database to provide a rationale for how often the cause of envenomation is unknown, leading to a delay in diagnosis and to identify medically important venomous species in South Africa responsible for envenomation.
2. To fractionate venom components by fast protein liquid chromatography (FPLC), size exclusion chromatography.
3. Toxicity screening of venom fractions using zebrafish (*Danio rerio*) larvae. The larvae will also be used to determine whether the toxic components are subjected to metabolism or remain intact within the vertebrate model.
4. To partially identify toxic components unique to each snake species by HR-LC-MS/MS.
5. To use the information from all of the species to determine the species specific peptides/proteins that could be useful as a diagnostic tool and develop a triple quadrupole LC-MS/MS method containing the toxic components specific to a single species.

1.13 Ethical considerations

Ethical clearance for the research study was obtained from the Human Research Ethics Committee (HREC) of Stellenbosch University (South Africa) (reference: S21/03/034, project ID: 21752). Approval for the use of AfriTox Telelog data for the epidemiological component of the research study was obtained from the Poison Information Helpline of the Western Cape. AfriTox Telelog database is registered at HREC University of Cape Town (South Africa) (reference number: R014/2014). Ethical approval for the use of zebrafish larvae up to 5 days post fertilization (dpf) for drug and toxicological screening was obtained from Research Ethics Committee: Animal Care and Use (REC: ACU) (reference number: ACU-2021-21995).

CHAPTER 2 Incidence of Snakebite in South Africa

2.1 Introduction

Snakebites in South Africa are common and envenomations present a significant public health care problem. To establish the severity of this problem from a South African context and to rationalise the importance and need for an analytical method to diagnose snakebite envenomation we collaborated with the Poison Information Helpline of the Western Cape (PIHWC) to obtain their Telelog call records related to the sub-category of biological toxins (Stephen et al., 2016). The study timeline stretches over a five year period, from 1st of June 2015 – 31st May 2020. This will be the first report of its kind for this period in South Africa. The aim, in addition to providing a rationale for the project, was to reveal valuable insights into the origin and incidence of snakebite and more importantly, report on trends observed in snakebites caused by venomous snake species that may add predictive value in diagnosis and management of victims. By applying herpetological knowledge regarding physiology, morphology and demography of venomous snake species occurring in South Africa, an investigation into how often species responsible for envenomation were correctly identified and appropriate treatment initiated, as well as which venomous species caused the most frequent and problematic envenomation symptomatology. This will help to direct efforts to address the problems encountered by venomous snake species responsible for problematic clinical presentations and show the contribution of this research towards a solution in mitigating this neglected tropical disease.

Limitations to the epidemiological study is that calls received by the PIHWC do not include all the snakebites that have occurred in the country or the outcomes of every snakebite call that was received by the centre as this is not their only function. No regulated protocol/database exists for all bites to be logged to monitor bite to treatment and final outcome. However, this provides a general overview of the extent of snake bites in South Africa .

2.1.1 Tygerberg Poisons Information Centre (TPIC)

The TPIC is a specialized service that is provided by the Tygerberg Academic Hospital, a tertiary hospital of the Western Cape Province of South Africa, and the Division of Clinical Pharmacology in the Faculty of Medicine and Health Science (FMHS), Stellenbosch University. Until the end of June 2015, the TPIC operated independently. On 1 June 2015, the Red Cross Children's Hospital Poisons Information Centre and the Tygerberg Poisons Information Centre combined their poisons telephonic services, and a single combined

helpline service was created, namely the Poisons Information Helpline of the Western Cape (PIHWC) (Figure 2.1). This was done due to important telephonic and computing technological advancements.



Figure 2.1 Poison centres in South Africa and location of the PIHWC

The PIHWC has a dedicated telephone line with a single share call telephone number (0861 555 777). The Helpline provides a free 24/7 poison information service to health care professionals and members of the public throughout South Africa. The data from the calls are recorded in real-time, i.e., it is recorded while the call is in progress on AfriTox Telelog which is a live server-based data system. The Telelog system uses a File Maker application, that is licensed through Apple inc., and set up for use by multiple users, which enables the simultaneous recording of data on the system (Stephen et al., 2016).

Following are three cases that were reported to the PIHWC showing complications caused by snakebite envenomation. If there was a test to show cause of envenomation, complication could have been circumvented to the patients' benefit. Together with the analysis of call center records, this chapter highlights the importance of this research study.

2.1.2 Case Reports

2.1.2.1 Case one

On 29 January 2012, a comatose adult male was admitted to the trauma ward (F1) at Tygerberg Hospital. The history surrounding the incident was vague, but the paramedics reported that a reptile or arachnid bit the patient. The patient had to be intubated and ventilated and the TPIC was contacted for advice. Due to the poisoning severity, it was assumed that the bite was inflicted by a Cape cobra (*Naja nivea*) and the treatment advise was to administer 80mL of polyvalent antivenom. After no improvement after 48 hours in ICU (A5), the TPIC was contacted again. A specialist in Poisons Information (SPI) from the TPIC visited the patient in

ICU. She noticed that the patient presented with hyper-salivation and involuntary movements. These symptoms are far more common in scorpionism as compared to neurotoxic snakebite envenomation (Rossiter et al., 2020). Treatment with 10 mL of scorpion antivenom was advised and 3-6 hours later the patient was stable, awake, and extubated. Unfortunately, the exact recovery time after administration of antivenom was not available for this case. Upon gaining consciousness, the patient admitted that he was stung by a scorpion when crossing the railway line. The availability of a simple and rapid diagnostic test could have reduced the cost of treatment and trauma caused by the incident could have been avoided.

2.1.2.2 Case two

On 26 February 2013, a 39-year-old man from a nearby wine farm was taken to Stellenbosch Hospital after accidentally stepping on a snake, resulting in a bite to the right foot. He could not identify the snake and described it as dark green and greater than 1 m in length. The patient's foot was very swollen and the TPIC advised treatment with polyvalent antivenom. The patient was sent to Paarl Hospital and on arrival the treating physician suspected a *Dispholidus typus* (boomslang) bite as the wound was bleeding profusely and the patient experienced three episodes of hematemesis (vomiting of blood). Vitamin K, fresh frozen plasma (FFP) and two units of blood were administered as a coagulation factor replacement to manage and prevent further bleeding. The TPIC then suggested that the patient be transferred to Tygerberg Hospital, a tertiary level hospital. The toxicologist on call recommended that several tests should be conducted. These tests included prothrombin time (INR), thrombin and fibrinogen levels, activated partial thromboplastin times, measurement of fibrinogen degradation products, D-dimer concentrations, and full blood count. At this stage, the patient presented with petechiae (pinpoint sized red, brown, or purple dots on the skin formed when capillaries break open and blood leaks into the skin), conjunctival hemorrhages and it was believed to be a *Dispholidus typus* bite. Monovalent Antivenom from the South African Vaccine producers (SAVP), which is situated in Sandringham, Johannesburg was needed. Due to the expense of the antivenom, the TPIC had to request special permission from the senior medical superintendent at Tygerberg Hospital to place the order. The blood results were delayed and arrived after the antivenom was couriered. The results were in normal ranges and did not concur with the typical results of *Dispholidus typus* envenomation. It was agreed that the patient presented with an atypical *Bitis arietans* (puff adder) bite, and the patient was sent back to Paarl hospital where he received symptomatic and supportive treatment. The final outcome of the patient was not documented by the PIHWC.

2.1.2.3 Case three

The third case is that of a complicated *Bitis atropos* (Berg adder) bite as was published in 2017 (Wium et al., 2017). A 5-year-old boy was admitted to a medical facility in Johannesburg upon arrival after flying from Cape Town. He presented with severe neurotoxic symptoms and mild cytotoxic symptoms. The neurotoxic symptoms included respiratory failure, flaccid paralysis, ptosis (drooping of the eyelids), and fixed dilated pupils. He also had mild hyponatremia (low concentration of sodium in the blood). He was resuscitated, intubated, and ventilated. While being ventilated standard routine laboratory blood tests and serum and urine toxicology tests were done. Various unsuccessful treatments were attempted including administration of polyvalent antivenom. Only after a consulting with a SPI 24 hours after the incident was a diagnosis made of a *Bitis atropos* bite and symptomatic and supportive care was recommended. Since bites by *Bitis atropos* species are uncommon it was not initially considered as a differential diagnosis in this patient. The unexplained clinical presentation of *Bitis atropos* envenomation due to the venom producing both neurotoxic and cytotoxic signs and symptoms made this envenomation challenging to diagnose.

2.2 Materials and Methods

2.2.1 Study area

The study was conducted in South Africa which covers an area of 1,22 million km² divided into nine provinces with a total population of 59622351 (South African Government, 2021). (Table 2.1)

Table 2.1 The population and land surface area of each province in South Africa

Province	Population	Area (km ²)
Eastern Cape	6734001	168966
Free State	2928903	129825
Gauteng	15488137	18178
KwaZulu-Natal	11531628	94361
Limpopo	5852553	125755
Mpumalanga	4679786	76495
Northern Cape	1292786	372889
Northwest	4108816	104882
Western Cape	7005741	129462

2.2.2 Study design

A retrospective cross-sectional study of AfriTox Telelog data consisting of calls received by the PIHWC for the five-year period from 1 June 2015 – 31 May 2020 was conducted. This period was chosen since the call centre started to digitally log calls from the 1st of June 2015.

2.2.3 Data Source

The criteria that were set as parameters for the PIHWC data search can be seen in Table 2.2. These include total number of calls, total number of animal calls, category of call (patient related only), patient type (human or animal), calls from both public and medical personnel, the province where the calls came from, sex and age of human patients and amount of human and animal patients. The requested categories include snakes, scorpions and spiders. Further specified categories include route: bite, stings and ocular envenomation, interval since exposure (hours) and poison severity score (PSS) reference. This report includes all human related calls and all repeated calls (unless otherwise specified).

Table 2.2 Field and filter parameters set for data extraction from the AfriTox Telelog database

Fields	Filters
Total number of calls	Human
Total number of calls	Animal
Call category	Patient related
Category of caller	Medical personnel and public
Country of origin	SA and Outside SA
Districts	All districts in SA
Facility type	Clinic, Community Health Centre, District Hospital, EMRS, Medical Centre, Military Hospital, National Central Hospital, Pharmacy, Private Clinic, Private Hospital, Private Practice, Provincial Tertiary Hospital, Regional Hospital, Specialised Psychiatric Hospital, Specialised TB Hospital, Unknown
Interval since exposure	Hours
Patient type	Human and animal
Patient age	Years old
Poison severity score	0 = No symptoms or signs related to poisoning 1=Mild, transient, and spontaneously resolving symptoms or signs 2 = Pronounced or prolonged symptoms or signs 3= Severe or life-threatening symptoms or signs 4 = Death
Province	Eastern Cape, Free State, Gauteng, KwaZulu-Natal, Limpopo, Mpumalanga, North West, Northern Cape, Western Cape, Unknown
Sex	Female and Male

Substances: AfriTox name	All species
Substances: Use Category	Animals, Bites, Stings
Substances: Route of exposure	Bite, Sting, Ocular, Oral, Skin

2.2.4 Data exposure and outcome definitions

Snakebites were reported by medical personnel, the victim, family members or bystanders. The data were then recorded by a SPI in the PIHWC and logged in real-time onto the AfriTox Telelog database. The final outcomes of all the calls have not been recorded and follow up call updates are not included in the data system. The caller received a clinical severity rating, termed a poisoning severity score (PSS). The PSS score is a standardised universal grading system that allows the qualitative evaluation of morbidity in acute poisoning and enable comparability of data. The PSS grade severity as (0) no symptoms or signs related to poisoning, (1) mild with transient, and spontaneously resolving symptoms or signs, (2) pronounced or prolonged symptoms or signs, (3) severe or life-threatening symptoms or signs and (4) fatal poisoning. (Persson et al., 1998)

2.2.5 Ethics

Approval from the PIHWC to do this study and obtain this data for the above listed criteria has been obtained. The database is registered at the Human Research Ethics Committee (HREC), University of Cape Town reference number R014/2014. Internal ethical clearance by HREC Stellenbosch University has been obtained, ethics reference number S21/03/034.

2.2.6 Statistical analysis

Stellenbosch University Center for Biostatistics and Epidemiology has been consulted from the proposal phase of this research and provided guidance on the approach of analysing the specific set of data. Descriptive statistics were used to quantitatively describe the variables in study dataset. The program that was used to analyse the data was Microsoft Excel.

2.3 Results

2.3.1 Overall breakdown

Figure 2.2 shows the overall break-down of calls received by the PIHWC over the five-year period from June 2015 to May 2020. There was a total of 51704 human related calls received. Calls are logged according to the type of calls as unknown, other, biological toxins, pharmaceuticals, and non-drug chemicals. There were 5239 calls received that involved biological toxins. The biological toxins category comprises calls from 1411 (27%) snakebites, 858 (16%) scorpion stings, 774 (15%) spider bites and 2196 (42%) from unknown, plants and marine-related calls. Snake species are categorized according to the toxidrome caused by envenomation. In 521 (37%) cases the bite was inflicted by snake species having predominantly cytotoxic venom, 138 (10%) from snake species with neurotoxic venom and 51 (4%) from snake species with hemotoxic venom. The snake species *Bitis atropos* with neuro- and cytotoxic venom were responsible for 15 (1%) bites that occurred during this period. The group 'other' includes 69 (5%) snake species that are either non-venomous, have low-toxicity, non-venomous constrictors or species with poorly defined toxicity. In 617 (44%) calls the snakebite was inflicted by an unidentified species.

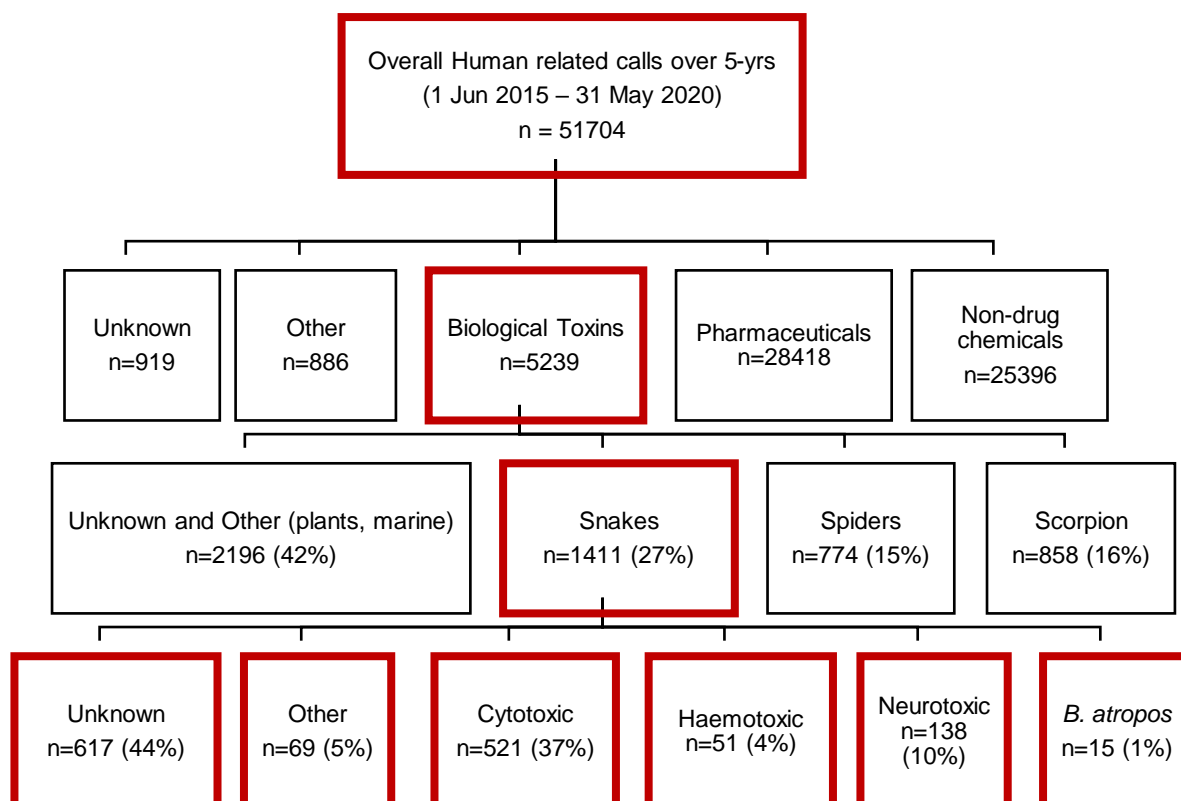


Figure 2.2 Overall categorisation of all human related calls received by the PIHWC over the 5-year study period

After categorisation of snakebite calls according to toxidrome, the calls were delineated according to causative species, as depicted in Figure 2.3. This was done to identify the snake species responsible for the most bites and to determine in how many of the snakebite cases the snake species responsible for the bite was unknown.

The cytotoxic bites were caused by *Bitis arietans* (puff adder) (n=80), *Hemachatus haemachatus* (rinkhals snake) (n=53), *Atractaspis species* (stiletto snake) (n=45), *Naja mossambica* (Mozambique spitting cobra) (n=44) and *Causus species* (night adder) (n=27). There were 36 (7%) calls reported as venom in the eye and 236 (45%) as bites from unknown and other snake species causing cytotoxic signs and symptoms. Snake envenomation causing a neurotoxic toxidrome was inflicted by *Naja nivea* (Cape cobra) (n=36), *Dendroaspis species* (mamba) (n=30) and non-spitting *Naja species* (including forest cobra, Egyptian cobra, snouted cobra, black necked cobra and zebra cobra) (n=9). There were 63 (46%) unknown neurotoxic snake bites. A hemotoxic toxidrome was caused by *Dispholidus typus* (boomslang) (n=25) and other hemotoxic snake species (including vine snake) (n=4). In 22 (43%) cases bites causing hemotoxic symptoms were from unknown species. Envenomation by *Bitis atropos* bite caused a neuro- and cytotoxic symptomatology in 15 cases.

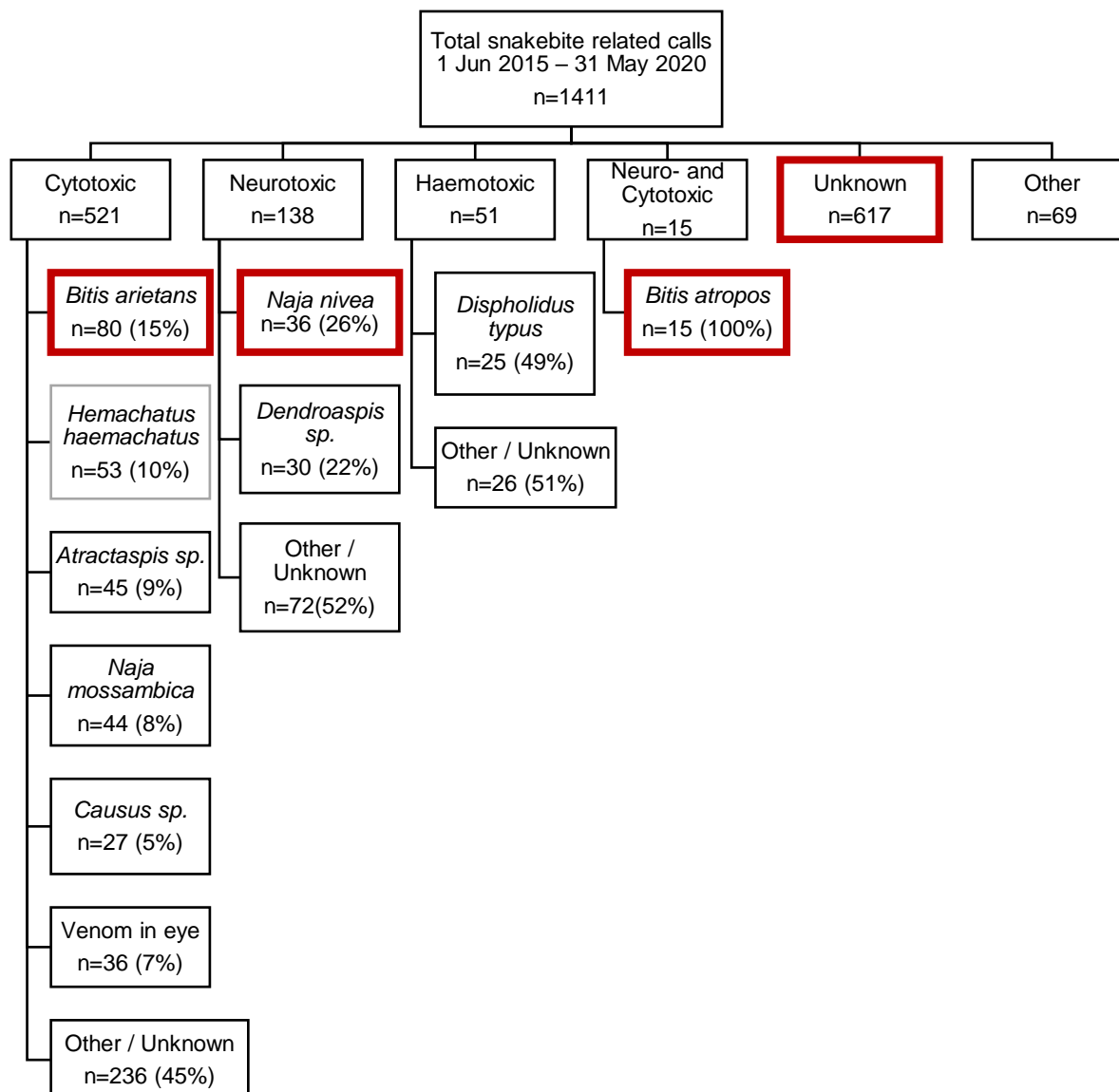


Figure 2.3 Snakebite calls recorded at the PIHWC over 5 years, according to toxidrome and causative species.

The cytotoxic toxidrome was caused by *Bitis arietans* (Puff adder), *Hemachatus haemachatus* (rinkhals snake), *Atractaspis sp.* (Stiletto snake), *Naja mossambica* (Mozambique spitting cobra), *Causus sp.* (night adder) and *Bitis caudalis* (horned adder). Cytotoxic snake venom in the eye was reported separately, and many of the cytotoxic bites were identified by the signs and symptoms with which the patient was presenting with, and not due to identification of the snake species. Neurotoxic toxidrome was inflicted by *Naja nivea* (Cape cobra), *Dendroaspis sp.* (mamba) and non-spitting *Naja sp.* (including forest cobra, Egyptian cobra, snouted cobra, black necked cobra and zebra cobra). Most neurotoxic snakebites were from unknown species and identified due to patient's presenting signs and symptoms. Haemotoxic toxidrome was caused by *Dispholidus typus* (boomslang) and other hemotoxic snake species including

Thelotornis capensis sp. (vine snake) and unknown species, identified by patient's signs and symptoms. *Bitis atropos* is categorised separately as a patient can present with both neuro- and cytotoxic symptoms. The red rectangular text boxes (Figure 2.3) indicate the primary species and area of interest for this research study.

2.3.2 Poison Severity Score of Unknown bites

The poisoning severity scores (PSS) that were allocated to patients bitten by unknown snake species presenting with no defined toxidrome can be seen in Table 2.3. In 65% a PSS score of 1 was given, with 10% receiving a score of 2 and 2% a score of 3. In 4% of the calls, no PSS score was assigned.

Table 2.3 Poison severity score allocated to snakebites inflicted by unknown species causing no defined toxidrome

PSS	n (%)
0 = No symptoms or signs related to poisoning	120 (19)
1 = Mild, transient and spontaneously resolving symptoms or signs	398 (65)
2 = Pronounced or prolonged symptoms or signs	62 (10)
3 = Severe or life-threatening symptoms or signs	10 (2)
Unknown	27 (4)
Grand Total	617

2.3.3 Sex and age of snakebite envenoming sufferers

The sex of the snakebite study cohort (n=1411) during the five-year period, was 67% (n=944) male and 32.5% (n=459) female. In 0.5% of the cases the sex of the individuals was unknown (Table 2.4).

Table 2.4 Sex of all snakebite victims over five year period

Sex	n (%)
Male	944 (67%)
Female	459 (32.5%)
Unknown	8 (0.5%)

Snakebite calls were analyzed according to age and sex of the subjects affected by the snakebite, as can be seen in Table 2.5. Overall, across all age groups more male subjects

were bitten than female subjects. Most of the snakebite subjects were aged 20 – 39 years, comprising 35% (n=502) of the total reported snakebites. In 356 of these snakebite incidences the subject bitten was male and in 146 snakebite incidences the subject was female. This group is indicated on Table 2.5 with a red border.

In 17% (n=235) of the calls, the bitten subjects were in the age category 40 – 59 and in 12% (n=170) of the calls, 6 - 12 years. In 10% (n=142) of the snakebite calls the bitten subject was recorded as adult with no specified age.

Table 2.5 Snakebite calls received by the PIHWC broken down according to age and sex of subjects

Age	Sex			Total (%)
	Female	Male	Unknown	
0 - 5	53	63	2	118 (8)
6 - 12	68	102		170 (12)
13 - 19	54	94		148 (11)
20 - 39	146	356		502 (36)
40 - 59	72	163		235 (17)
≥ 60 yrs.	37	52		89 (6)
Adult	29	110	3	142 (10)
Unknown		4	3	7 (0.5)

A graphical presentation of the age and sex of the subjects that were bitten by snakes over the 5-year study period can be seen in Figure 2.4. In both male and females, the yellow and light blue slices are the largest and represent the age groups 20 – 39 and 40 – 59, respectively.

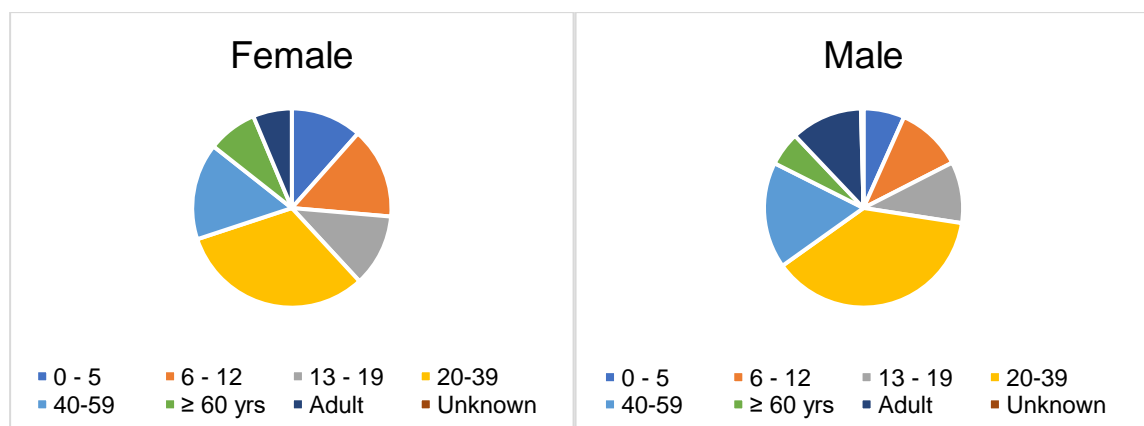


Figure 2.4 Pie chart showing the breakdown of female (left) and male (right) subjects bitten by a snake the over 5-year period according to age.

2.3.4 Category of caller for snakebite consultation with the PIHWC

The snakebite related calls made to the PIHWC came from either medical personnel or the public. In 91% of the snakebite calls, the caller was medical personnel, with 9% of the calls received from a public caller (Table 2.6).

Table 2.6 Category of caller medical vs public

Category of caller	n (%)
Medical Personnel	1283 (91)
Public	128 (9)

2.3.5 Annual, quarterly (seasonal), and geographical distribution of snakebites over 5-years

Over the five-year study timeline from 1st of June 2015 – 31st of May 2020 the highest number of snakebite related calls were received in 2019, 21% (n=297) and in 2018 (21%, n= 294). In 2016, 18% (n= 251) of the total calls received were for snakebite and in 2017, 17% (n=245). In 2015 and 2020 the least calls were received, with 9% (n=122) received in 2015 and 14% (n=202) in 2020. The annual amount of snakebite calls received by the PIHWC are shown in Figure 2.5

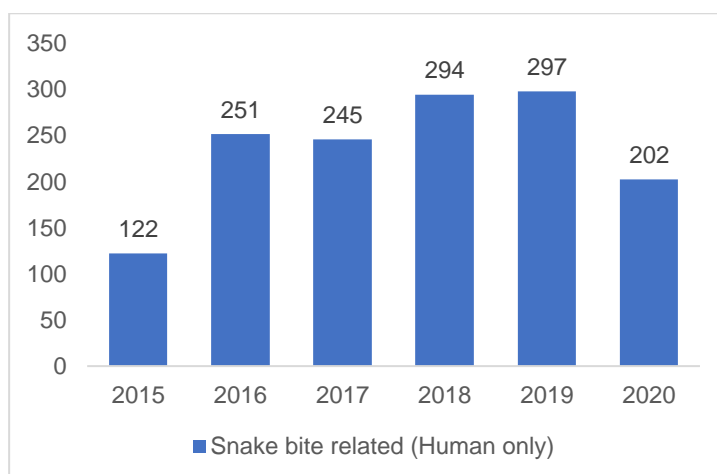


Figure 2.5 Snakebite related calls that occurred in South Africa over a 5-year period. The amount of calls received are indicated per year

Figure 2.6 shows the distribution of snakebite calls received on a seasonal level. In the years 2016 - 2020 the most snakebites were recorded in the months December to February (summer). In 2015 the most snakebite calls were recorded from September to November

(spring). Over the 5-year period the months June – August had the lowest number of snakebite related calls were received by the PIHWC. This data set does not include snakebite data from 1 January to 31 May 2015 and 1 June – 31 December 2020.

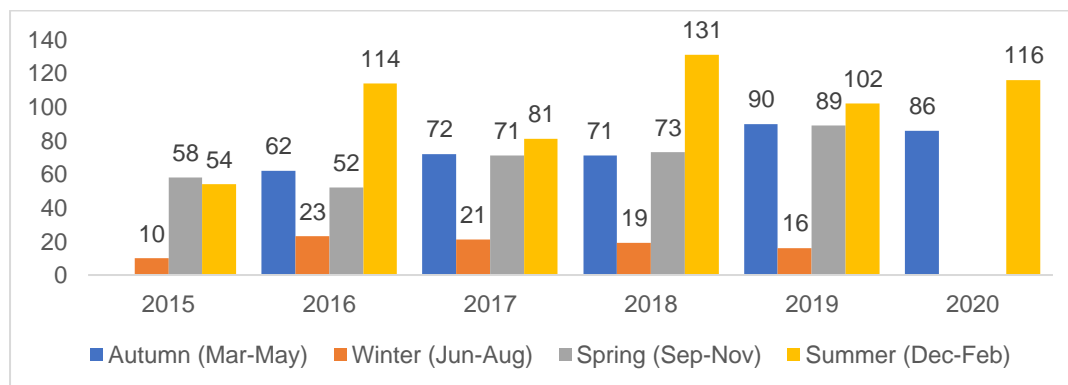


Figure 2.6 Seasonal distribution of snakebite calls received from 1 June 2015- 31 May 2020. Over the duration of the study period the most snake bite calls were received from December to February each year and the least during June to August.

Geographically the most snakebite calls were received from Kwazulu-Natal, with 305 calls, followed by 247 calls from the Western Cape and 202 from Gauteng. There were 178 calls received from the North West province and 175 received from Mpumalanga. A total of 134 calls were received from Limpopo and 100 calls from the Eastern Cape. The least calls, each with a count of 31 calls, were received from the Free State and Northern Cape. (Table 2.7)

Table 2.7 Geographical distribution of snakebite calls received by the PIHWC from each of the nine provinces that make up South Africa.

Province	n (%)
KwaZulu-Natal	305 (22)
Western Cape	247 (18)
Gauteng	202 (14)
North West	178 (13)
Mpumalanga	175 (12)
Limpopo	134 (9)
Eastern Cape	100 (7)
Free State	31 (2))
Northern Cape	31 (2)
Unknown	1 (0.07)
Grand Total	1404
Note that calls received from other African countries (Zambia, Malawi, and Mozambique) and the United Kingdom were excluded from this table	

2.3.6 Incidence of snakebite by geographical location

The incidence of snakebite in each province of South Africa based on the AfriTox Telelog record was calculated using the estimated population counts released by the South African government ((Department of Statistics South Africa, 2019). The incidence of snakebite in South Africa over 5 years was 2.39 per 100 000. The highest incidence of snakebite was in the North-West province with 4.42 snakebites per 100 000 population. Mpumalanga had the second highest incidence of snakebite with 3.81, followed by the Western Cape with an incidence of 3.61. The incidence of snakebites was the lowest in the Free State (1.07) and in Gauteng (1.33) provinces. Figure 2.7 shows the complete breakdown of incidence of snakebite per 100 000 population in each province of South Africa.

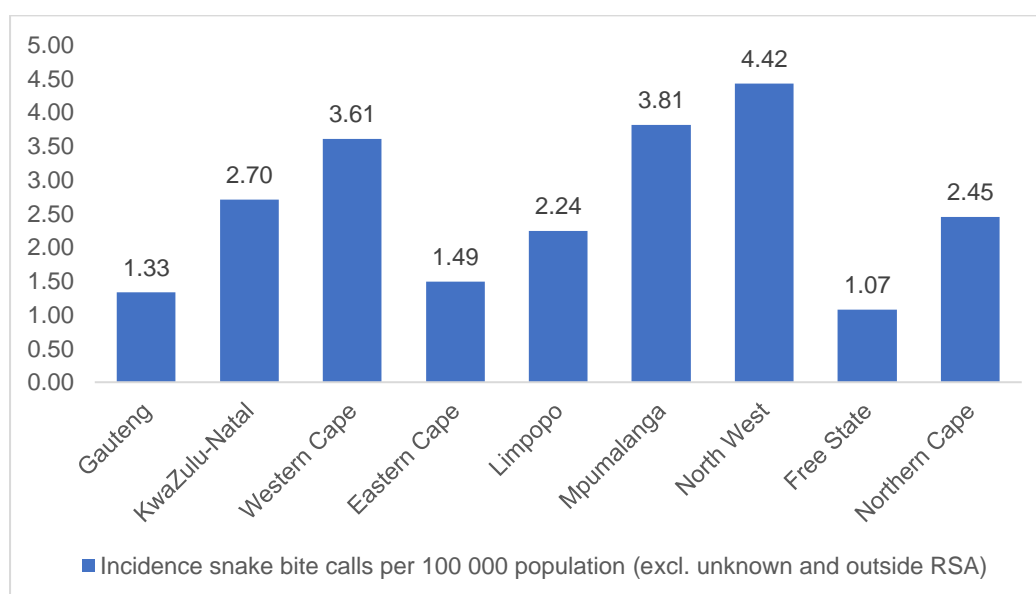


Figure 2.7 Incidence of snakebite per 100 000 population by province

2.3.7 Snakebite related calls received from the Western Cape, South Africa

Over the 5-year period from June 2015 – May 2020 there were a total of 1411 snakebite related calls received by the PIHWC, which included 247 (18%) calls from the Western Cape (Table 2.7). The calls received from the Western Cape, counted by year and toxidrome caused by envenomation, can be seen in Table 2.8.

Table 2.8 Type of toxicity caused by snakebites that occurred in the Western Cape over 5 years from 1 June 2015 - 31 May 2020

	No. of snakebites	Proportion (%)
Snakes unidentified	90	36%
Neurotoxic venom	51	21%
Cytotoxic venom	56	23%

Haemotoxic venom	18	7%
<i>Bitis atropos</i> (berg adder)	14	6%
Low toxicity	6	2%
Non-venomous	12	5%
Grand total	247	

Categorisation of snakebite calls from the Western Cape according to type of venom and species responsible for envenomation is shown in Table 2.8. The most prevalent envenomation toxidrome that occurred was cytotoxic (n=56) and by the *Bitis arietans* snake species (n=21). A neurotoxic toxidrome was caused in 51 cases of snakebite, where most bites were by *Naja nivea* species (n=27). Eighteen cases of hemotoxic envenomation toxidrome were reported and *Bitis atropos* species inflicted 14 bites. In 90 (36%) of the recorded cases the species responsible for the bite could not be identified.

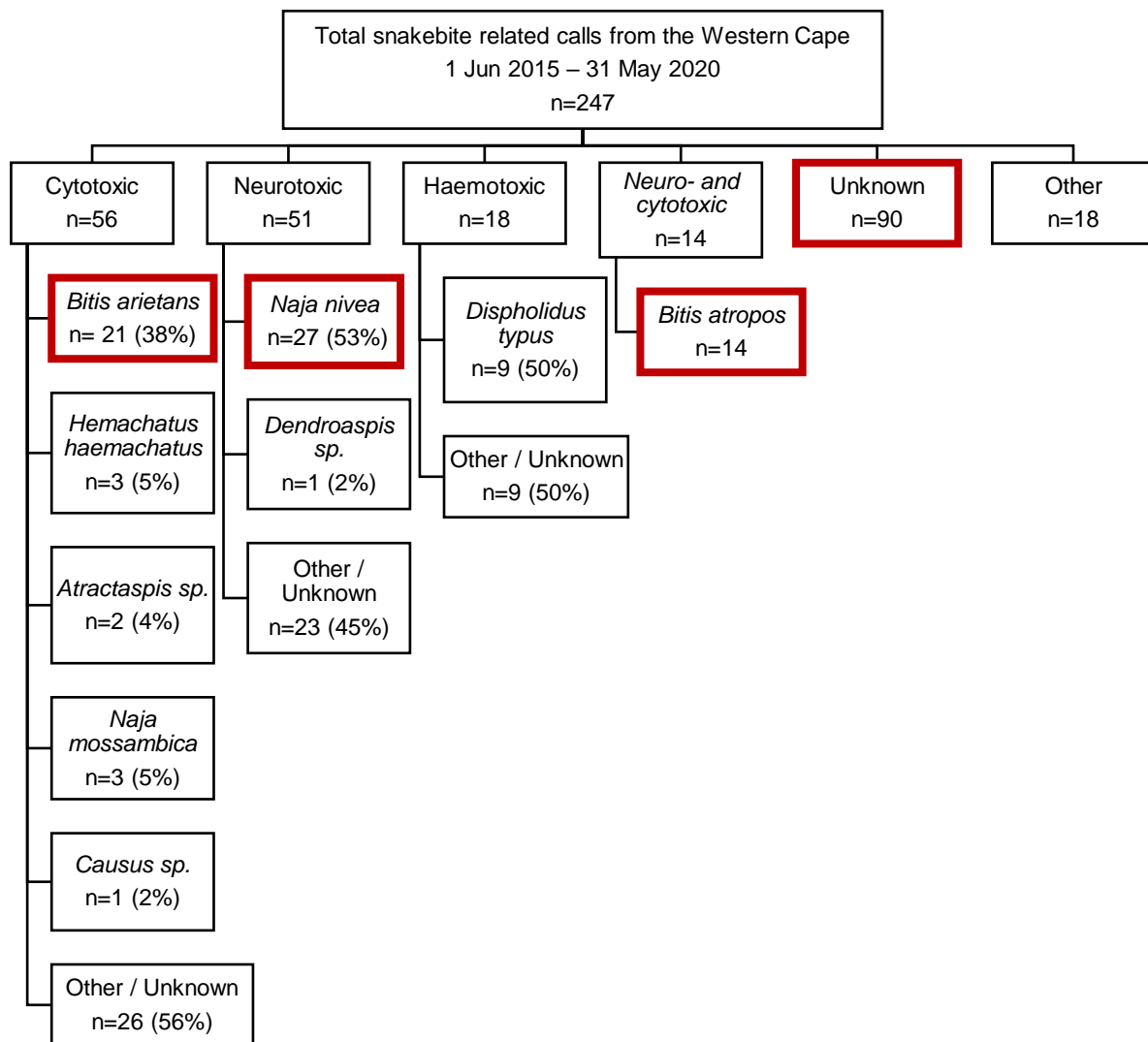


Figure 2.8 Categorisation of snakebites reported from the Western Cape to the PIHWC over 5 years according to type of envenomation and causative species

In terms of sex and age of subjects affected by snakebite in the Western Cape over the 5-year period, more male (n=169) than female (n=77) individuals were bitten. This correlates with overall snakebite data found in Table 2.4 showing more male than female individuals were bitten over the 5 years in South Africa. Most bites occurred in the age range 20 – 39 years in both males (n=49) and females (n=22). In age group 40 – 59 years, the largest difference in the number of snakebite subjects occurred, in males there were 38 bites reported, and 7 for females. In children aged 6 – 12, there were 22 males and 20 females subjected to snakebite (Figure 2.9).

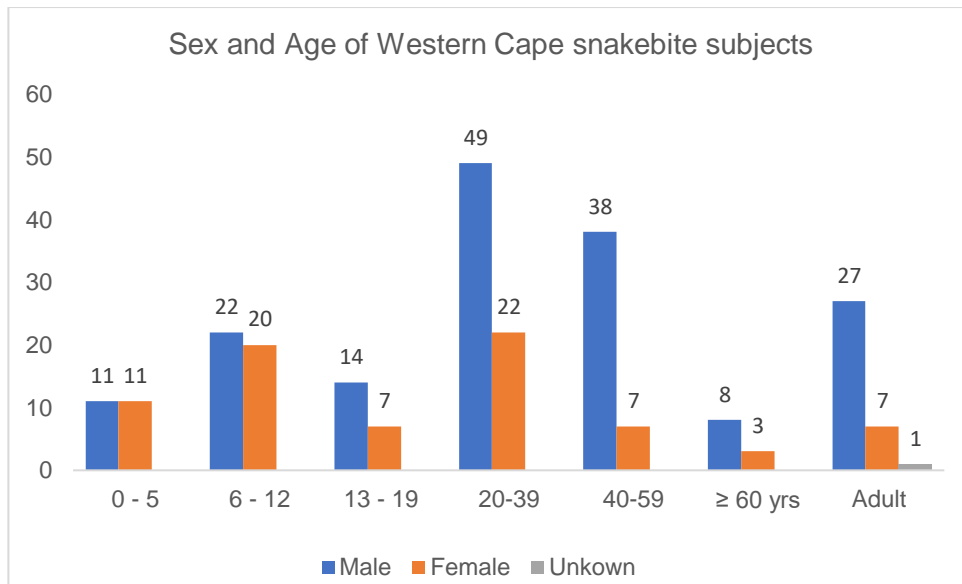


Figure 2.9 Sex and age of snakebite subjects from the Western Cape over the 5-year period.

In 84% of the snakebite incidences that occurred in the Western Cape, the calls came from medical personnel and 16% from members of the public (Figure 2.10).

Category of caller for snakebite incidences reported over 5-years originating from the Western Cape

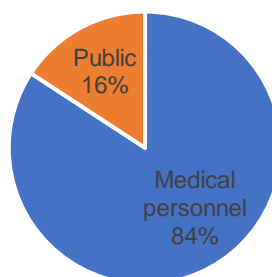


Figure 2.10 Caller categorisation of the snakebite call made to the PIHWC

The districts and facilities the snakebite calls were received from can be used as guides for the availability of antivenom. Facilities that the majority of snakebite calls were received from included 83 district hospitals (34%), 141 private hospitals (17%), 27 National central hospitals (11%) and 26 regional hospitals (11%). Calls were also received to a lesser extent from private practices (4%), clinics (3%) and provincial hospitals (2%)(Figure 2.11).

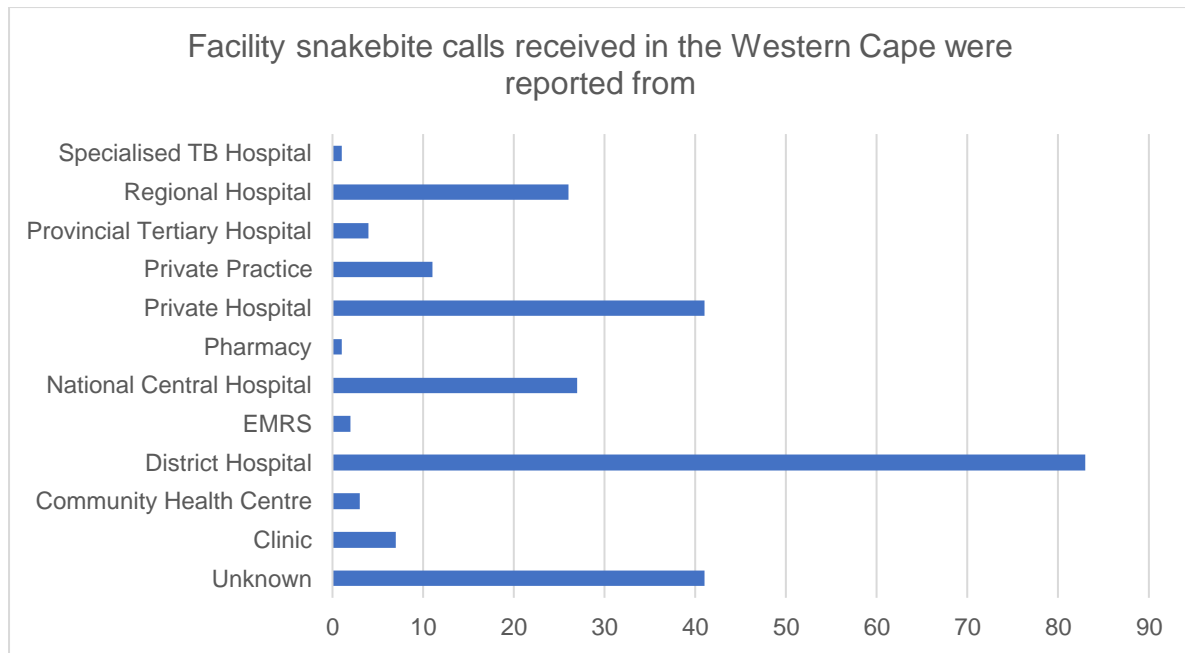


Figure 2.11 Snakebite calls made to the PIHWC and the facilities located in the Western Cape, from which the calls were received

2.4 Discussion and Conclusion

This retrospective analysis describes previously unknown epidemiological data regarding snakebite reported calls made to a South African poison information helpline. Over the five-year period from 1 June 2015 to 31 May 2020, 1411, snakebite related calls were received by the PIHWC. The total snakebite related calls were delineated according to the toxidrome caused by the venom as neurotoxic, cytotoxic, and hemotoxic. The species *B. atropos* was classified separately due to envenomation causing both neurotoxic and cytotoxic signs and symptoms. In 44% of all snakebite calls the bite were inflicted by an unidentified snake species.

The symptomatology of envenomation by cytotoxic snakebite includes local pain and progressive swelling as well as skin changes with coagulable blood, whereas neurotoxicity is characterised by progressive, descending flaccid paralysis. Haemotoxicity is characterized by persistent oozing of blood from fang punctures, as well as manifestations of other bleeding that includes gingival bleeding, epistaxis, hematemesis, melaena, purpura, hematuria, extensive ecchymoses and intracranial hemorrhage. The clinical syndrome of envenomation by *B. atropos* can cause cytotoxic symptoms which include blistering and local swelling around the bite site, as well as neurotoxic symptoms such as paresthesia (tingling or prickling sensation) of the tongue and lips, ptosis, fixed dilated pupils and loss of sense of smell (anosmia) and taste, as well as dysphagia that can develop (Muller et al., 2012b). Most frequent snakebite envenomation causing cytotoxic toxidrome were by *Bitis arietans* (puff adder) species (Lobetti and Joubert, 2004), neurotoxic toxidrome by *Naja nivea* (Cape cobra) species and hemotoxic toxidrome by *Dispholidus typus* (boomslang) species.

The most snakebites occurred during the warm summer months from December – March (Figure 2.6). This is consistent with what was found in literature reporting on seasonal snakebite trends observed in South Africa as well as other countries (Da and Salomão, 1994; Mhaskar et al., 2014; Wood et al., 2016a). According to South African herpetologist Johan Marais, this is due to more people being out in nature during summer months, which increases the likelihood of people encountering a venomous snake species. The most bites occurred in males (20 - 60 years). This is in accordance with what other researchers found in rural Sri Lanka and Kenya (Jayawardana et al., 2021; Ochola et al., 2018). The incidence of snakebite in South Africa was 2.39 per 100 000 population, with the highest incidence of snakebite in North-West province of South Africa (Figure 2.7). This is comparable to the extrapolated incidence of 2.34-3.3 per 100 000 population for sub-Saharan Africa as a whole (Kasturiratne et al., 2008). However, this differs from a study conducted in Kwazulu-Natal, where the

incidence of snakebite was determined by extrapolation of antivenom usage and accounted for an incidence of 16 per 100 000 population (Wood et al., 2016b). In another study the incidence of snakebite in Kwazulu-Natal, South Africa was reported as 32 per 100 000 (Wood et al., 2016c). In this study, incidence was determined based on admissions to an emergency department of the district's hospital. This shows that the number can vary considerably by region and quality of data records (Chippaux, 2017, 2011). In sub-Saharan Africa there is a major underestimation of the incidence of snakebite. This is due to under reporting and absence of physical attendance to health care facilities. A snakebite is commonly only taken care of 24 hours post bite. This phenomenon is due to popular belief in African populations that traditional medicine rather than health care facilities is the best able to treat snakebite envenomation (Chuat et al., 2021; Newman et al., 1997).

The PIHWC provides an invaluable service in assisting and informing medical personnel and the public on the management of snakebites. Data collected by centers provides a great source of information on the prevalence of snakebites and medically important species that research should be aimed towards. This was shown by Kasturiratne et al. 2008, who used data from National Poison Centers in combination with the WHO mortality database, Ministries of Health, and unpublished literature from snakebite experts to build a model to establish the global burden of snakebite (Kasturiratne et al., 2008).

CHAPTER 3 Materials and Methods

The methodology described in this chapter is for the quantitative research of venom components from medicinally important species endemic to South Africa. The species' venom that were investigated include *Naja nivea*, *Bitis atropos* and *Bitis arietans*. These were chosen based on the retrospective study of snakebite in South Africa and the regional relevance of these species to the Western Cape of South Africa, as described in Chapter 2.

The analytical methodologies that were developed serve as proof of concept for the development of novel diagnostics for envenomation in South Africa. Analytical methods were chosen based on suitability to the proteinaceous nature of the sample components and the objectives set out for the research study. Plasma proteins fall within a molecular weight range of between 21 kDa – 350 kDa. Classes of plasma proteins include albumins, globulins (α , β , γ), fibrinogen and other transport proteins. Albumin makes up about 60% of plasma with a molecular weight of 66 kDa and globulins 35% of total plasma with a molecular weight range of 90-150 kDa. Hence, the target venom proteins were selected based on the composition of human plasma and quantity of venom that will be present within envenomed plasma. Venom proteins and peptides in the molecular mass range below 20 kDa were targeted as those fall outside of the molecular weight range of abundant plasma proteins. This will also decrease the probability of false positives.

The graphic below in Figure 3.1 provides an overview of the experimental workflow. An initial screen of crude venom was performed using native polyacrylamide gel electrophoresis (PAGE) to determine the overall size distribution of venom proteins from the different snake species. The protein bands were excised and an in-gel digestion with trypsin was performed in preparation for analysis by mass spectrometry (MS) to identify the proteins and peptides contained within these bands. The mass spectra were matched to the UniProt Serpentes peptide library. Due to detrimental effects that are caused by the presence of inorganic ions, surfactants and possible contaminants in samples on MS analysis and proteome data, crude venom was also digested on MagReSyn HILIC magnetic particles to produce a cleaner sample. Crude *N. nivea* venom was fractionated and partially purified by fast protein liquid chromatography (FPLC) size exclusion chromatography (SEC). The fractions were collected according to the major chromatographic peaks. All the fractions were run on native polyacrylamide gel electrophoresis (PAGE) and analysed on an Orbitrap high resolution mass spectrometer (HR-MS) for the identification of the venom peptides within each fraction. Fractions containing proteins and peptides with a molecular weight below 20 kDa were used

for liquid chromatography tandem mass spectrometry (LC-MS/MS) method development to identify specie-specific toxins from human plasma and for toxicity screening in an *in vivo* zebrafish model.

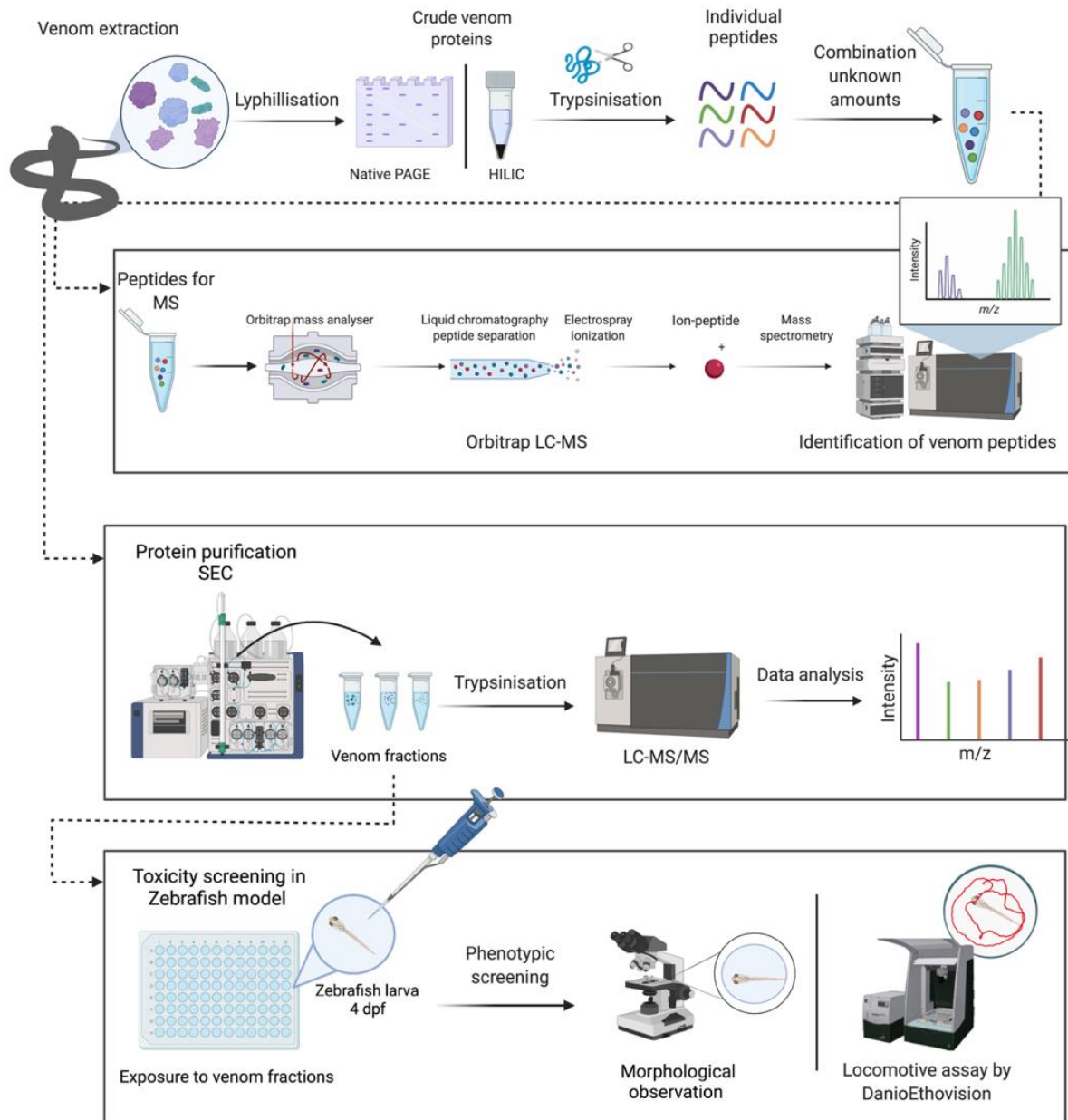


Figure 3.1 Overview of the experimental workflow for the investigation of snake venom proteins/peptides. Diagram created with BioRender.com

3.1 Materials

3.1.1 Reagents and consumables

Lyophilised venoms from the snake species *N. nivea*, *B. arietans*, *B. atropos* were obtained from SA Venom Suppliers CC (Louis Trichardt, South Africa).

Bio-Rad 4 – 20% Mini-PROTEAN® TGX™ pre-cast gradient gels were used for the analysis of crude venom samples and a 15 % separating gel with a 4% stacking gel for venom fractions. All the reagents for the stacking- and separating gels, sample buffer, staining- and de-staining solutions were sourced from Sigma-Aldrich (Schnelldorf, Germany). The separating gel consisted of 30% acrylamide/bis-acrylamide, Trizma base, tetramethyl ethylenediamine (TEMED) at a pH of 8.0 and water. The stacking gel consisted of Trizma base, TEMED at a pH of 6.9, ammonium peroxy-disulphate and water. Native PAGE sample buffer consisted of 60 mM Tris hydrochloric acid at pH 6.8 with 40% glycerol. Gels were stained with 0.05% Coomassie brilliant blue R250, 50 % methanol and 10% acetic acid and de-stained in 10% acetic acid and 10% methanol solution. The Bio-Rad Precision Plus Protein Dual Xtra, containing a 12 band extended-range recombinant ladder with bands from 2 kDa – 250 kDa, was used as molecular weight marker. Gels were run in a Bio-Rad XT MOPS (3-(N-Morpholino)-Propane sulfonic acid) running buffer in a Bio-Rad Mini-PROTEIN Electrophoresis cell. A Bio-Rad ChemiDoc imaging system was used for gel imaging and viewing and analysis of the gels on the Bio-Rad Image lab software. All Bio-Rad reagents and instrumentation sourced from Bio-Rad, California, USA and software available from <https://www.bio-rad.com/en-za/product/image-lab-software?ID=KRE6P5E8Z>.

Gel slice de-staining solution consisted of 200 mM ammonium bicarbonate (NH_5CO_3) (Sigma-Aldrich, Schnelldorf, Germany) in 50 % acetonitrile (Romil, Cambridge, England). TCEP (Tris(2-carboxyethyl)phosphine hydrochloride solution) was used as reducing agent and S-Methyl methanethiosulfonate (MMTS) as alkylating agent, both purchased from Sigma-Aldrich (Schnelldorf, Germany). MagReSyn® HILIC magnetic microparticles used for in-solution 18-hour tryptic digestion protocols were purchased from Separations (Cape Town, South Africa). Mass spectrometry grade trypsin was used for the proteolytic cleavage of venom proteins (New England Biosystems, Massachusetts, United States). Mobile phases consisted of 2% acetonitrile with 0.1% formic acid (Fisher Chemicals, Czech Republic) at pH 3 in water (A) and acetonitrile with 0.1% formic acid (B). Samples were cleaned-up after digestion with inhouse manufactured solid phase extraction columns. The columns were prepared by packing P200 pipette tips with disks of 3M Empore® C18 47 mm solid phase extraction disks, sufficient to bind 30 µg of peptide, from 3M Bioanalytical technologies (Minnesota, United States). Methanol was sourced from Romil (Cambridge, England). The low molecular weight protein

standard kit was purchased from GE Healthcare Amersham Pharmacia (Uppsala, Sweden). An iRT Kit was purchased from Biognosys (Schlieren, Switzerland).

Ammonium acetate, ammonium bicarbonate, TCEP, trifluoroacetic acid (TFA) were purchased from Sigma-Aldrich (Schnelldorf, Germany). LC-MS mobile phases consisted of water with 0.1% formic acid at a pH of 3 (A) and acetonitrile with 0.1% formic acid (B). Buffers for the preparation of HILIC magnetic particles included an equilibration buffer, 100 mM ammonium acetate, pH 4.5, 15% acetonitrile, binding buffer consisting of 200 mM ammonium acetate, pH 4.5, 30% acetonitrile and wash buffer consisting of 95% acetonitrile. Acetonitrile and methanol were purchased from Romil (Cambridge, England) and HPLC grade formic acid and LC-MS grade formic acid and acetic acid was purchased from Fisher Chemical (Madrid, Spain and Norcross, United States).

Human blood was obtained from volunteers and collected in K2EDTA tubes. Consent for the collection of blood from healthy individuals was obtained as well as ethical clearance from Stellenbosch University for the use of human plasma during method development.

For the *in vivo* experimental procedure longfin zebrafish (*Danio rerio*) larvae were used. Larvae were bred from D1 breeding group (batch number: D1 15/07). The venom fractions were prepared by size exclusion chromatography as described in Section 3.7. Embryo medium E3 salts (13.7 mM NaCl, 540 mM KCl, pH 7.4, 25 mM Na₂HPO₄, 44 mM KH₂PO₄, 300 mM CaCl₂, 100 mM MgSO₄, 420 mM NaHCO₃, pH 7.4) was purchased from Sigma Aldrich (Schnelldorf, Germany). Petri dishes, Pasteur pipettes and 96-well plates were obtained from WhiteHead Scientific (Cape Town, South Africa).

3.1.2 General Instrumentation

BOECO Balances BXX (Axiology Lab, South Africa) was used for the accurate weighing of venoms and reagents used during sample preparations. Polished distilled water from a Milli-Q® water purification system coupled to a Synergy® UV system (Millipore, Milford, USA) was used for the preparation of samples, buffers and mobile phases. Samples were vortexed on an Eins-Sci E-VM-A analogue vortex mixer and centrifuged in an Eins-Sci E-C15-24.2PR refrigerated centrifuge (Johannesburg, South Africa). An ultrasonic cleaner (United Scientific, Cape Town, South Africa) was used for resuspension of venom samples and to degas mobile phases. An Orion Star A111 Benchtop pH Meter (Thermo Fisher Scientific, Massachusetts, United States) was used to determine the pH of buffers and mobile phases. Samples were dried down in a Genevac™ miVac DUO centrifugal vacuum concentrator fitted with a miVac SpeedTrap (Ipswich, United Kingdom). A Stuart block heater (Staffordshire, United Kingdom)

was used for incubation of samples. A Nanodrop 2000c spectrophotometer from Thermo Fisher Scientific (Massachusetts, United States) was used to determine venom protein/peptide concentration after precipitation with acetonitrile.

3.1.3 Instrumentation

3.1.3.1 HR-LC-MS/MS

A Thermo Fisher Scientific UltiMate™ 3000 RSLC nano Liquid chromatography system was utilised. The samples were pre-concentrated on a 100 µm x 20 mm C₁₈ trap column (Thermo Fisher Scientific), then loaded onto a CSH 1.7 µm particle size C₁₈, 75 µm x 250 mm analytical column (Waters Corporation, Milford, MA, USA). The instrumentation that was used to perform mass spectrometry was a Thermo Scientific Orbitrap Fusion™ Tribrid™ mass spectrometer equipped with a Nano-spray Flex™ ion source.

3.1.3.2 HPLC

Snake venom from the species *Bitis arietans*, *Bitis atropos* and *Naja nivea* were run on an HPLC system fitted with an Agilent 1260 Infinity binary pump and degasser, Agilent 1100 autosampler and column compartment and a variable wavelength detector (VWD) and OpenLab CDS ChemStation software. Samples were chromatographically separated on a Venusil XBP C18 (4.6 mm x 100 mm, 5µm) column from Agela Technologies (Torrance, United States).

3.1.3.3 SEC

The venom fractions were prepared by partial purification of crude venom by size exclusion chromatography on a G75 – Superdex GL 10/300 column connected to an ÄKTA explorer system. The ÄKTA Explorer 100 was purchased from GE Healthcare Amersham Pharmacia (Uppsala, Sweden). The Superdex 75 10/300 column was purchased from Cytiva (Marlborough, MA, USA) . The freeze-drying equipment that was used was a SP Virtis Benchtop Pro with Omnitronics (SP Industries Inc., St. Louis, Missouri, USA).

3.1.3.4 LC-MS/MS

Method development was done on a Shimadzu 8040 Liquid chromatograph tandem mass spectrometer fitted with LC-20ADXR pumps, a DGU-20A3 degasser, SIL-20AC auto sampler, CTO-20A column oven and electrospray ionisation source (Kyoto, Japan).

3.1.3.5 *In vivo* study

Morphological effects in zebrafish larvae were assessed with a stereo PZMTIII-MI Microscope fitted with a PRO-300 HDS camera from World Precision Instruments (Florida, United States). The zoom range of the microscope is 0.67x to 4.5x with a total magnification of 6.77x – 45x. Larval swimming behavior was tracked with a Noldus DanioVision™ Observation chamber coupled to Ethovision XT video tracking software (Wageningen, the Netherlands).

3.2 Methods

3.2.1 Gel electrophoresis of venom proteins

Native PAGE was used as an initial screen of crude venoms from the snake species, *N. nivea*, *B. atropos* and *B. arietans*. In PAGE an electrical current is applied which causes proteins to separate based on their molecular weight (Laemmli, 1970). In native PAGE no denaturants are used in the preparation of the sample and the protein mixture (venom) is separated without unfolding of the proteins and migration is based on the molecular mass, charge and structure of the protein complexes (Arndt et al., 2012; Walker, 1994). The standard operating procedure (SOP) for PAGE from the Division of Molecular Biology and Human Genetics Laboratory at Stellenbosch University that is based on the protocol by Laemmli (1970) was followed. Multiple venom samples were run on PAGE during the course of the study to establish a basic understanding of native venom composition based on apparent molecular weight distribution of venom components. Further fractionation of venom by PAGE decreased sample complexity for analysis by mass spectrometry.

Venom samples were prepared in deionised water and native page sample buffer was added to a ratio of 4:1. A quantity of 3 µg of the venom in solution was made up to a total volume of 20 µL, after which 5 µL of sample buffer was added. All samples were prepared and kept on ice until loaded onto the gel to avoid degradation. Gels were run at 100 V for 45-60 min at 4°C until the bromophenol blue reached the bottom of the gel and electrophoresis was stopped. The gels were stained with Coomassie brilliant blue for 30-60 min and then, de-stained overnight or until all bands including weaker bands were visible on the gel. The gels were then imaged and analysed.

3.3 Trypsin digestion protocols

Below in Figure 3.2 is a flow diagram showing the general workflow for proteomic sample preparation for mass-spectrometry.



Figure 3.2 Workflow overview of proteomic sample preparation for mass spectrometry

3.3.1 In gel tryptic digestion of proteins

Figure 3.3 below show a diagram for the in-gel protein digestion sample preparation protocol that was followed.

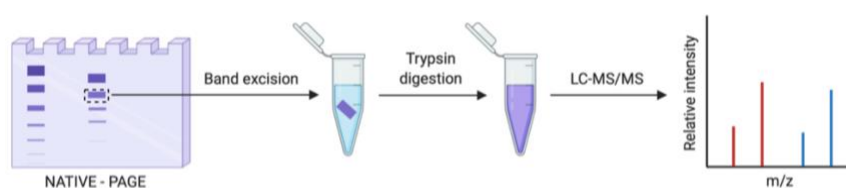


Figure 3.3 In-gel protein digestion for analysis by HR-LC-MS/MS

The protein bands were excised according to apparent molecular weight in sections from the gel, each section further sliced into 1 mm x 1 mm blocks and placed into 1.5 mL microcentrifuge tubes. Coomassie blue stain was eluted from the PAGE gel slices containing the separated native venom proteins with a 200 mM ammonium bicarbonate in 50 % acetonitrile solution for 1 hour. The de-staining solution was removed, and acetonitrile was added to dehydrate the gel blocks. The gel blocks were dried in the miVac vacuum centrifuge for 10 min, with no heat. Samples were reduced for 1-hour by a 5mM TCEP with 100mM ammonium bicarbonate solution. An aliquot of 100 μ L was added to each sample. After reduction, the samples were dehydrated with 250 – 400 μ L acetonitrile, the dehydration agent was removed, and samples were rehydrated for 5 -10 minutes with 250 μ L 100 mM ammonium bicarbonate. Thereafter samples were dehydrated again with acetonitrile and 250 μ L MMTS blocking/ alkylating agent was added. After 30 minutes the samples were washed with 100 mM ammonium bicarbonate, then dehydrated with acetonitrile. Wash and dehydration steps were repeated twice. The dehydrated gel blocks containing venom proteins were dried in the miVac vacuum centrifuge without heat. Thereafter, samples were placed on ice. An aliquot of 20 μ g trypsin was removed from -20 $^{\circ}$ C and resuspended in 1 mL deionized water. A volume of 100 μ L trypsin (20 μ g/mL) was then added to each sample. After 1 hour, the samples were removed from the ice and placed in a 37 $^{\circ}$ C preheated oven and incubated for 18 hours (overnight). After incubation, the trypsin solution containing digested peptides and proteins was removed and placed in new microcentrifuge tubes. The same volume that was removed

was replaced with ~100 μL of water and left for 1 hour. This was repeated twice to produce a total sample volume of $\pm 270 \mu\text{L}$. The samples were then dried down in the miVac vacuum centrifuge with no heat overnight. Dried down samples were resuspended in 30 μL 0.1% formic acid, 2% acetonitrile in water (A), vortexed, placed in the ultrasonic cleaner (United scientific, South Africa) and sonicated for 5 min, then centrifuged at 12 000 g for 10 min. Digested samples were cleaned by binding peptides to the C18 membrane solid phase extraction column with 2% acetonitrile with 0.1% formic acid in water and eluting them with 50% 0.1 % formic acid in acetonitrile (B). The samples were dried in a miVac vacuum centrifuge on [OH⁻] mode for 45 minutes to 1 hour, until dry. Prior to analysis by mass spectrometry the samples were resuspended in 20 μL 2% acetonitrile with 0.1% formic acid (A), vortexed for 30 seconds and sonicated for 1 minute, vortexed again for 30 seconds and centrifuged in the combi-spin mini centrifuge. The samples were transferred to glass sample loading vials and placed in the autosampler of the Thermo 3000 RS nanoLC.

3.3.2 On-bead (HILIC) tryptic digestion of proteins

A 10 mg/mL stock solution of lyophilized venom in 10 mM ammonium acetate buffer was prepared. Then 5 μL venom stock solution was added to 20 μL 50 mM ammonium bicarbonate for a final volume of 25 μL and reduced by incubation with 50 mM TCEP for 60 min at 60 °C in a block heater. After 60 min incubation of the sample, the alkylating agent, MMTS was added and the sample volume adjusted to a minimum of 25 μL , an equal volume of binding buffer (200 mM ammonium acetate, pH 4.5, 30% acetonitrile) was added and thoroughly mixed.

The HILIC magnetic microparticles were prepared according to the manufacturers protocol (https://resynbio.com/wp-content/uploads/2019/12/IFU_HILIC.pdf). Briefly, the microparticles were resuspended in the shipping solution, an aliquot of 25 μL was placed into a new micro centrifuge tube, placed onto a magnetic separator and the shipping solution removed. The beads were washed and equilibrated in an equilibration buffer consisting of 100 mM ammonium acetate (pH 4.5) and 15% acetonitrile. Once the equilibration buffer was removed, the beads were ready for binding proteins. The sample containing an unknown mixture of venom proteins and peptides was added to the magnetic beads, and gently stirred on the orbital shaker at 60 rpm for 30 minutes to allow binding. The microcentrifuge tubes containing protein bound microparticles were placed on the magnetic separator and the supernatant removed. The particles were then resuspended in a wash buffer (95% acetonitrile and 5% water) and gently mixed, placed on a magnetic separator and the supernatant removed. Trypsin (20 $\mu\text{g}/\text{mL}$ trypsin in 50 mM ammonium bicarbonate) was added at a 1:50 protein to substrate ratio. The samples were incubated at 37 °C for 18 hours (overnight).

The following morning the solution was placed in the magnetic separator and the supernatant (containing all the digested peptides) removed. The particles were resuspended in 0.5% TFA to remove any peptides left on the beads and the supernatant removed. The supernatant was dried in the miVac vacuum centrifuge on (OH⁻) for 6 hours with no heat, then reconstituted with 30 µL 0.1% Formic acid in water (A), vortexed and sonicated in the sonicating water bath for 5 min on a soft setting, then centrifuged for 10 min at x 12 000 g. The sample was then loaded onto inhouse manufactured C₁₈ column tips (as previously explained in section 3.3.1) and filtered through to remove any particles that could still be in sample. First the digested sample binds to the solid phase (C₁₈), after which it was washed with 30 µL solvent A and eluted with 30 µL 50% solvent B into glass inserts in a new microcentrifuge tube. The cleaned sample was then dried in the miVac (OH⁻) for 15 min, then reconstituted in solvent A and sonicated 1 minute. The insert was placed into a chromatography sampling vial and loaded into the autosampler of the Thermo 3000 RSLCnano.

3.4 Liquid chromatography

Mobile phases consisted of 2% acetonitrile in water with 0.1% formic acid (A) and acetonitrile with 0.1% formic acid (B). The samples were loaded onto the column at a flow rate of 2 µL/min with the autosampler temperature set to 7 °C. A 5-minute loading time was completed before the sample was loaded onto the analytical column. Chromatography was performed at a flow rate of 0.3 µL/min creating a gradient starting at 2% B for 5 min; 2% - 30% B over 60 min; an increase from 30% - 50% B over 15 min; and 50% - 80% B in 0.1 min; remaining at 80% B for 10 min; 80% - 5% B in 0.1 min and equilibration for 5 min.

3.5 Mass spectrometry

Crude venom samples, fractionated venom samples, as well as plasma spiked with venom samples were analysed using this method. Approximately 1 µg of material was injected. Introduction of the sample was done through a stainless steel nano-bore emitter. Data collection was in positive ion mode with 1.8 kV spray voltage and transfer capillary temperature set to 275 °C. An Orbitrap detector was used to perform MS 1 scans, the detector was set at 120 000 resolution with a scan range of 375-1500. The AGC target was set at 4E5 and the injection time maximum of 50 milliseconds. Data acquisition was in positive profile mode. The MS 2 scans were performed using monoisotopic precursor selection for ion charges +2 to +7, with an error tolerance of ± 10 ppm. The precursor ions were selected for fragmentation using HCD mode, with HCD energy set to 30% with precursor selection in the quadrupole mass

analyser. Detection of the fragment ions were accomplished with the Orbitrap mass analyser set to 30 000 resolution, AGC target set to 5E4 and maximum injection time of 100 milliseconds. Data acquisition was in centroid mode. MS data that were generated by HR-LC-MS/MS were captured in Proteome Discoverer and processed to generate raw data files, then exported in Scaffold format to acquire an integrated overview of identified proteins and peptides or imported into Skyline to identify unique peptides and potential targets.

3.5.1 Scaffold

3.5.1.1 Database searching

Tandem mass spectra were extracted by Thermo Scientific Proteome Discoverer version 1.4.1.14. Charge state deconvolution and deisotoping were not performed. All MS/MS samples were matched to database sequences using Sequest (Thermo Fisher Scientific, San Jose, CA, USA; version 1.4.1.14) and X! Tandem (The GPM, thegpm.org; version CYCLONE (2010.12.01.1)) algorithms. Sequest was set up to search UniProt cobra database (24521 entries) assuming the digestion enzyme trypsin. X! Tandem was set up to search the UniProt cobra database (24888 entries) also assuming trypsin. Sequest and X! Tandem were searched with a fragment ion mass tolerance of 0.020 Da and a parent ion tolerance of 10.0 PPM. Methyl thiolation of cysteine residues was specified in Sequest and X! Tandem as a fixed modification. Deamidation of asparagine and glutamine and oxidation of methionine were specified in Sequest as variable modifications. Glu->pyro-Glu of the n-terminus, ammonia-loss of the n-terminus, gln->pyro-Glu of the n-terminus, deamidation of asparagine and glutamine and oxidation of methionine were specified in X! Tandem as variable modifications.

3.5.1.2 Criteria for protein identification

Scaffold (version Scaffold_5.0.1, Proteome Software Inc., Portland, OR) was used to validate MS/MS based peptide and protein identifications. Peptide identifications were accepted if they could be established at greater than 95.0% probability. Peptide Probabilities from Sequest were assigned by the Scaffold Local FDR algorithm. Peptide Probabilities from X! Tandem were assigned by the Peptide Prophet algorithm (Keller et al., 2002) with Scaffold delta-mass correction. Protein identifications were accepted if they could be established at greater than 99.0% probability and contained at least 2 identified peptides. Protein probabilities were assigned by the Protein Prophet algorithm (Nesvizhskii et al., 2003). Proteins that contained similar peptides and could not be differentiated based on MS/MS analysis alone were grouped to satisfy the principles of parsimony. Proteins sharing significant peptide evidence were grouped into clusters.

3.6 Reversed-phase high performance liquid chromatography (RP-HPLC)

RP-HPLC was used as an initial chromatographic screen of plasma samples that were spiked with venom and high molecular weight proteins depleted with acetonitrile. The objective was to develop a rapid sample preparation protocol to detect snake venom when spiked in plasma without proteolytic digestion prior to chromatographic analysis. This would increase the applicability of the sample preparation protocol to a clinical setting where time is of the essence when dealing with a patient that was envenomated by a snake. The protein precipitation sample preparation and RP-HPLC method development protocols were based on (Katali et al., 2020; Kay et al., 2008) and The Protein Protocols Handbook (Katali et al., 2020; Kay et al., 2008; Stone and Williams, 2009).

3.6.1 Acetonitrile precipitation of high molecular mass venom proteins

Two sets of samples were prepared, these included crude venom in water with 0.1% formic acid (A) and crude venom spiked into human plasma.

The venoms were reconstituted in 80% acetonitrile with 0.1% formic acid to a concentration of 5 µg/µL. A 200 µL sample was prepared for each venom and centrifuged for 10 min at 12 000 x g. The supernatant was carefully aspirated into microcentrifuge tubes and dried in the vacuum centrifuge on OH⁻ mode with no heat. Thereafter each sample was reconstituted in 0.30 mL water with 0.1% formic acid (A) and transferred into 2000 µL HPLC sample vials.

Lyophilized snake venoms were resuspended into a volume of 15 mM (pH 6.4) ammonium acetate buffer to a concentration of 1 mg/10 µL buffer. The venom was spiked into blood plasma at a concentration of 5 mg/100 µL plasma. Equal aliquots were measured out and to each sample a volume/volume ratio of 2, 3 and 4 volumes of acetonitrile were added. The samples were thoroughly mixed by vortex for 1 min and soft sonication in the sonicating water bath for 5 min. The samples were centrifuged for 15 min at 5000 x g (rcf). Thereafter the supernatant was removed by careful aspiration with a pipette, placed into a microcentrifuge tube and dried down in the MiVac vacuum centrifuge with no heat. The samples were reconstituted in water with 0.1 % formic acid (A), placed into HPLC sample vials and loaded into the sample loading tray of the HPLC instrument. Mobile phases were water with 0.1% formic acid (A) and acetonitrile:water (80:20) with 0.1% formic acid (B). Detection of venom compounds was done at a wavelength of 214 nm, and flow rate of 500 µL/min. The injection volume was 0.05 mL. A gradient elution starting at 10% B, increasing to 100% B over 40 min,

remaining at 100 % B for 2 min, and then decreasing B from 100% - 10% over 1 min and equilibrating for 5 min.

3.6.1.1 HR-LC-MS/MS of undigested samples and protein identification

Samples were prepared as described in section 3.6.1. The tandem mass spectra were extracted by Proteome Discoverer (Thermo Fisher Scientific). Charge state deconvolution and deisotoping were not performed and all MS/MS samples were analyzed using Sequest (Thermo Fisher Scientific, San Jose, CA, USA; version 1.4.1.14) and X! Tandem (The GPM, thegpm.org; version CYCLONE) (2010.12.01.1)). Sequest and X! Tandem was set up to search a combined homo sapiens and serpentes database containing 144402 entries assuming the digestion enzyme non-specific. Sequest and X! Tandem were searched with a fragment ion mass tolerance of 0.020 Da and a parent ion tolerance of 10.0 PPM. Deamidation of asparagine and glutamine and oxidation of methionine were specified in Sequest as variable modifications. Glu->pyro-Glu of the n-terminus, ammonia-loss of the n-terminus, gln->pyro-Glu of the n-terminus, deamidated of asparagine and glutamine and oxidation of methionine were specified in X! Tandem as variable modifications.

Scaffold (version Scaffold_5.0.1, Proteome Software Inc., Portland, OR) was used to validate MS/MS based peptide and protein identifications. Peptide identifications were accepted if they could be established at greater than 98.0% probability to achieve an FDR less than 1.0%. Peptide Probabilities from Sequest were assigned by the Scaffold Local FDR algorithm. Peptide Probabilities from X! Tandem were assigned by the Peptide Prophet algorithm (Keller et al., 2002) with Scaffold delta-mass correction. Protein identifications were accepted if they could be established at greater than 5.0% probability to achieve an FDR less than 1.0% and contained at least 2 identified peptides. Protein probabilities were assigned by the Protein Prophet algorithm (Nesvizhskii et al., 2003). Proteins that contained similar peptides and could not be differentiated based on MS/MS analysis alone were grouped to satisfy the principles of parsimony. Proteins sharing significant peptide evidence were grouped into clusters. The criteria for protein identification were a 95 % or higher protein identification probability, with at least two unique peptides.

3.7 Size-exclusion chromatography of *N. nivea* venom

N. nivea venom was injected and fractionated on a fast protein liquid chromatography (FPLC) ÄKTA system as described in section 3.1.3.3. Crude *N. nivea* venom was reconstituted to 50 mg/1000 μ L in running buffer (20 mM ammonium acetate, pH 7.2). A sample volume of 400 μ L was injected onto the system to fractionate 20 mg crude venom at a flow rate of 800 μ L/min over 60 min. The fractions were collected according to elution peaks that were read at a wavelength of 280 nm. After multiple runs the fractions from each major peak were pooled together and lyophilised/ freeze dried overnight and stored at -80 °C. A schematic of the size exclusion chromatography workflow is shown in Figure 3.4 below. This chromatography technique was done to purify the target low molecular weight venom proteins and peptides.

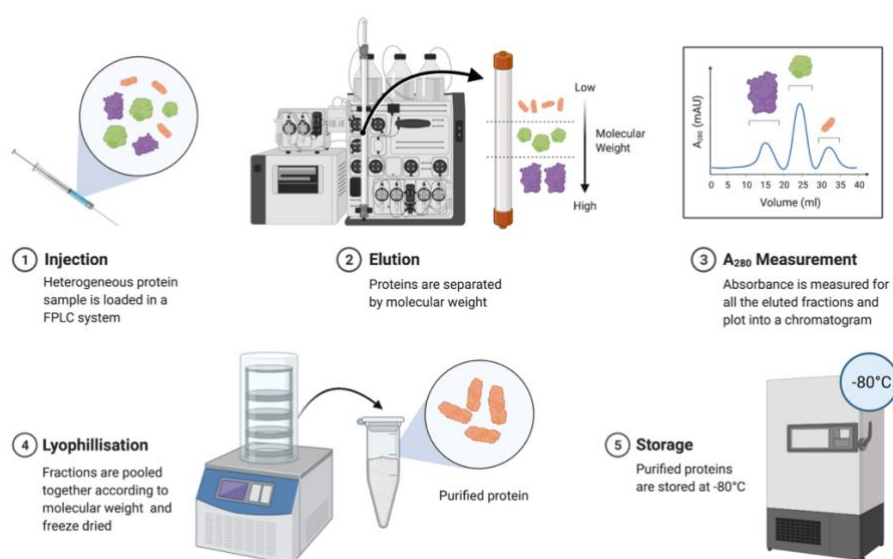


Figure 3.4 *N. nivea* was injected onto a FPLC system and fractionated by size exclusion chromatography. Diagram generated in BioRender.com

3.8 Triple quadrupole LC-MS/MS

3.8.1 Sample preparation

3.8.1.1 iRT peptides

An iRT standard containing eleven synthetic, non-naturally occurring peptides in a pooled mix that has been optimized for stability, sensitivity and retention time spacing over the gradient. The iRT was used as a reference set for quality control and to establish a level of detection on the Shimadzu 8040 LC-MS. The iRT peptides were prepared according to manufacturer's preparation guide and reconstituted with dissolution buffer to a 10-fold iRT Standard solution. The injection volume on the LC-MS/MS instrument was 5 μ L.

3.8.1.2 Venom fractions

N. nivea fraction 5 was used to detect the venom toxin, cytotoxin 1, unique to the species *N. nivea*. The choice was based on the abundance of this toxin within fraction 5, which was established using the HR-LC-MS/MS. For the detection of cytotoxin 1 from human plasma, human plasma was allowed to thaw at room temperature, after which 100 µL plasma was added to 100 µg dried down *N. nivea* venom fraction 5. The samples were precipitated with 200 µL acetonitrile, vortexed for 30 seconds and centrifuged for 5 minutes at 16000 x g at 4°C. The supernatant was transferred to microcentrifuge tubes. The protein concentration within the supernatant was determined by a Nanodrop 2000 spectrophotometer and aliquots of 100 µg were made into new microcentrifuge tubes and dried down in the MiVac drying centrifuge with no heat.

3.8.2 Trypsin digestion protocols of *N. nivea* venom

Three different trypsin digestion protocols were followed for the analysis of plasma spiked with *N. nivea* venom. The traditional 18 h digest and two protocols to manipulate trypsin digestion conditions to accelerated proteolysis and simplify the digestion workflow (Zheng and DeMarco, 2017; Li et al., 2009) were evaluated. For each protocol, a blank un-spiked sample was also prepared.

3.8.2.1 Protocol 1: Traditional trypsin digestion on HILIC beads

A 50 µg aliquot of dried down venom, resuspended in water with 0.1% formic acid that underwent protein precipitation, a 50 µg aliquot of dried down venom spiked into plasma and precipitated, as well as a blank un-spiked precipitated plasma sample was digested with trypsin on MagReSyn® HILIC beads for 18 hours according to the protocol previously described in section 3.3.2. The dried down digest was resuspended in 50 µL 0.1% formic acid in water and sonicated in the sonicating water bath on the soft setting for 1 min and transferred to a sample vial. The injection volume was 10 µL.

3.8.2.2 Protocol 2: Accelerated tryptic digestion protocol

The protocol is based on the method reported by Zheng and DeMarco (2017), with some minor adjustments. An aliquot of 100 µg dried down, spiked and precipitated proteins/peptide in plasma, as well as a blank precipitated plasma sample were reconstituted in 50 µL of 50 mM ammonium bicarbonate. The samples were then vortexed for 30 seconds and placed in a pre-heated heating block at 99 °C for 10 minutes. A 1:50 protease to substrate (1 µg trypsin / 50 µg protein) was added and the samples vortexed for 30 seconds. The samples were incubated for 30 minutes in a 37°C water bath. After incubation, 2.5 µL formic acid, 5% of the total sample

volume, was added to stop the digestion reaction. The samples were vortexed for 30 seconds and centrifuged at 4400 x g (3000 rpm) for 5 min. The injection volume was 10 μ L.

3.8.2.3 Protocol 3: Accelerated tryptic digestion protocol

The protocol is based on that reported by Li *et al.* (2009) with some minor adjustments. An aliquot of 100 μ g dried down spiked and precipitated proteins/peptide in plasma as well as a blank precipitated plasma sample was reconstituted in 50 μ L of 100 mM ammonium bicarbonate. The samples were then vortexed for 30 seconds and a 1:7.4 protease to substrate (13.5 μ g trypsin / 50 μ g protein/peptide) was added and the samples vortexed for 30 seconds after which 100 μ L 50 % methanol was added and the samples vortexed for 30 seconds. The samples were incubated for 30 minutes in a 37°C water bath. After incubation to stop the digestion reaction, 10 μ L LC-MS grade acetic acid was added. The samples were vortexed for 30 seconds and centrifuged at 4400 x g (3000 rpm) for 5 min. The injection volume was 25 μ L.

Figure 3.5 show a schematic diagram of each tryptic digestion protocol that was followed.

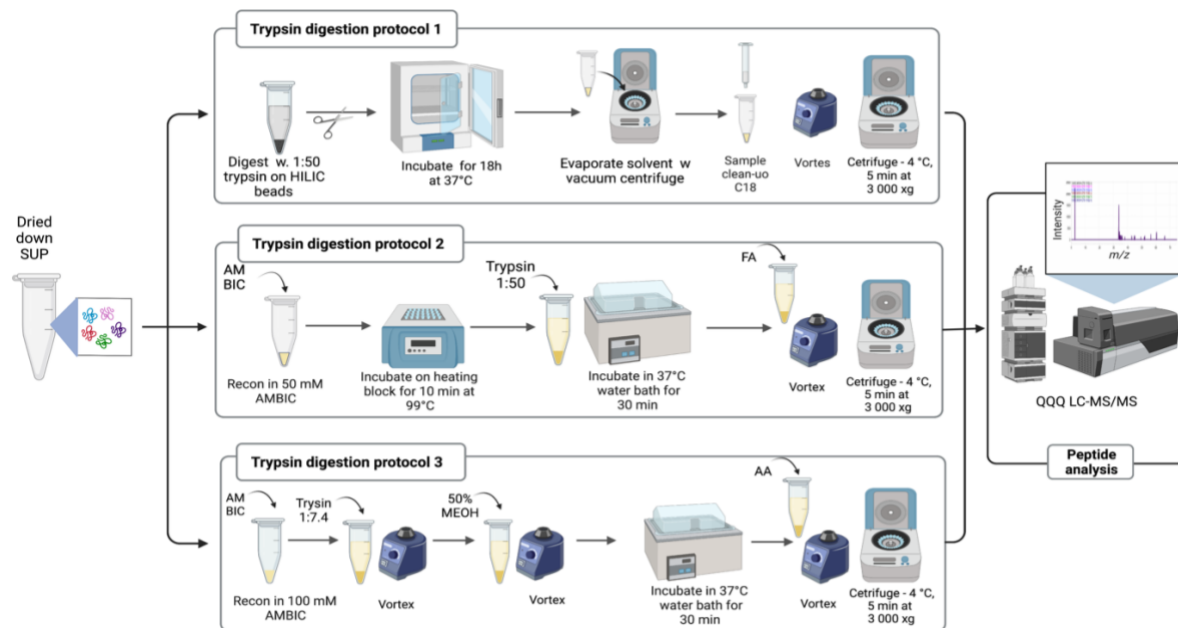


Figure 3.5 Trypsin digestion sample preparation protocols. Aliquots of supernatant containing low molecular weight plasma and venom proteins, obtained following protein precipitation with acetonitrile (ACN) were subjected to three different tryptic digestion protocols prior to peptide analysis by LC-MS/MS. Protocol one followed a traditional in-solution, HILIC assisted tryptic digestion, 20 μ g/mL trypsin was added at a 1:50 enzyme to substrate ratio and incubated overnight in a 37°C oven. Protocol two involves resuspension of supernatant in ammonium bicarbonate (AMBIC), samples were then placed on a 99°C heating block for 10 min, 20 μ g/mL trypsin was added at a 1:50 enzyme to substrate ratio and samples were incubated for 30 min in a 37°C preheated water bath, the digestion process was stopped by the addition of formic acid (FA). The third protocol involves resuspension of the supernatant in ammonium bicarbonate (AMBIC), addition 20 μ g/mL trypsin at a 1:7.4 enzyme to substrate ratio,

samples were thoroughly mixed by vortex and 50% methanol was added, thereafter samples were incubated for 30 min in a 37°C in a preheated water bath. The digestion process was stopped by the addition of acetic acid (AA).

3.8.3 Triple quadrupole LC-MS method development

The Shimadzu application note for the analysis of Trastuzumab was used as a guide for setting up LC-MS parameters during LC-MS method development (Shimadzu Corporation, 2017). Skyline software was used for building the Multiple Reaction Monitoring (MRM) for proteins and peptides of interest for a targeted approach on the Shimadzu LC-MS/MS.

3.8.3.1 Building multiple reaction monitoring peptide transition lists using Skyline

Skyline was used for building a multiple reaction monitoring peptide transition list for the iRT peptides as well as the analysis of data obtained from HR-LC-MS/MS. Skyline is an open-source application (Version 4.1) that was developed by the MacCoss Lab of Biological Mass Spectrometry at the University of Washington, Seattle, WA, USA (MacLean et al., 2010). Skyline proteomics workflow is an analytical tool for the analysis of a variety of mass spectrometry data and is able to display the data in a graphical and interactive fashion to build targeted methods based on prior knowledge of the peptides and proteins of interest. MS data that was generated by HR-LC-MS/MS analysis was imported into Skyline and matched against the UniProt data base, filtered to contain only reviewed, identified and characterised proteins and peptides from the Toxicofera Serpentes (toxin bearing snakes).

The multiple reaction monitoring peptide transition list for the iRT standard was set up by importing the sequences of iRT peptides in FASTA format into Skyline. The FASTA was obtained from <https://biognosys.com/resources/irt-kit-further-user-resources/>. A transition list of the peptides was then exported as a single method after specifying the instrument parameters. The transition table was directly imported into Lab Solutions during method set-up on the Shimadzu LC-MS/MS. A transition list for the unique toxins from *N. nivea* venom was created in a similar way. In Skyline the raw datafile, obtained from analysis of *N. nivea* fraction 5 venom by mass spectrometry, was matched against the UniProt Serpentes database. Peptide settings were set to assume digestion with Trypsin [KR][P], with the maximum of 1 missed cleavages, excluding peptides containing methionine. An MS/MS spectral library was built from Fraction 5 integrated with the reviewed UniProtKB- Serpentes-database FASTA file, and Methylthio (C) selected as structural modification. with the maximum variable mods set to 3 with maximum losses 1. The transition settings were set for

the prediction of monoisotopic mass for both the precursor and product ions. The filter for peptide precursor charges was set to 2, with ion charges of 1 and b and y ion types. The product ion selection was set to include product ions with a m/z larger than the precursor containing up to 3 ions. MS1 filtering was to include counted isotope peaks, up to 3 peaks, a centroided precursor mass analyser and 10 ppm mass accuracy. A targeted acquisition method for MS/MS filtering was selected with centroided product mass analyser with mass accuracy of 10 ppm. Only scans within 5 minutes of the MS/MS IDs were included. The transition list was exported for Shimadzu as one method per protein.

The protein and peptides identified in Skyline under the specified settings were matched to the list of proteins identified in Scaffold for fraction 5 and the toxins with the highest spectral count and unique to *N. nivea* were selected and combined into a single method on the Shimadzu 8040 LC-MS. The method was developed for the identification of the venom toxins, cytotoxin 1 (P01456), cytotoxin 10 (P01453) and cytotoxin 3 (P01459).

3.8.3.2 Liquid chromatography NexeraXR System

A Shimadzu Shim-pack GIST-HP C18 (2.1 x 100 mm, 3 µm) (Kyoto, Japan) was used for chromatographic separation. Column oven temperature was set to 40 °C. The mobile phases that were used were 0.1 % formic acid in water (A) and 0.1 % formic acid in acetonitrile (B). A gradient was created with the LC program starting at 25% (B); 25% to 95% (B) in 60 min; staying at 95% (B) for 5 min; 95% - 25% over 3 min and 7 min equilibration. The total run time was 75 min at a flow rate of 0.4 mL/min.

3.8.3.3 Triple quadrupole mass spectrometry

The Ionization mode was set for positive (ESI +) and the desolvation line (DL) temperature was set at 250°C and heating block at 400°C. The nebulizing gas flow rate was set to 3 L/min, drying gas flow rate 10 L/min and heating gas to a flow rate of 10 L/min.

3.9 *In vivo* zebrafish larval toxicity assay

The aim of this experiment was to evaluate toxicity at non-lethal concentrations of *N. nivea* fractions by implementing phenotypic screening in zebrafish larvae. *N. nivea* fractions 5, 6, 7 and 8, described in section 3.7, were screened for toxicity. These fractions contained mixtures of low molecular mass peptides smaller than 10 kDa, which included α-neurotoxins (long and short neurotoxin), cytotoxins and cardiotoxins (confirmed by HR-LC-MS/MS). During this experiment, we aimed to evaluate cardiovascular and neurobehavioral systems, together with physiological malformations of the zebrafish larvae, cardiac function or damage (thrombosis

or haemorrhage) and attenuated activity levels. The protocols that were followed were based on Álvarez *et al.* (2021), Chan *et al.* (2017) and Zanotty *et al.* (2019) with adjustments to the protocols as described below.

3.9.1 Zebrafish husbandry and breeding

Zebrafish are extremely light, noise and pH sensitive and experiments were conducted under standardized light conditions and noise was minimized. Care was taken after cleaning equipment with bleach to ensure that it was rinsed thoroughly afterwards. Eggs produced by standard husbandry were collected and maintained at 28 °C in E3 medium in petri dishes, with a 14:10 hour light:dark cycle. The eggs were refreshed daily with E3 medium. All the dead/unfertilized eggs were removed and recorded. This process continued until treatment at 3-5 days post fertilization (dpf) (determined by the study design).

3.9.2 Survival/dose response test

To determine the treatment concentration of venom fractions needed to result in significant yet sub-lethal, physiological effects in zebrafish larvae, larvae were exposed to different treatment concentrations and effects were assessed by light microscopy. The larvae were carefully pipetted into a 96-well plate, one larva per well. Directly after capture the larvae were given 30 minutes to calm before exposure to the *N. nivea* venom fractions 5, 6, 7, 8 and fraction C that was collected in-between major peaks 7 and 8 (Figure 4.13). Fraction C was included in the toxicity screen to evaluate whether a unique physiological response was observed in the zebrafish model in the presence of low abundance toxins. The treatment concentrations were 0.5 µg/µL, 0.25 µg/µL and 0.125 µg/µL in E3 solution. Larval heartbeats were confirmed i.e., survival, 10 minutes after exposure on a stereo microscope.

3.9.3 Behavioral Assay – measurement of zebrafish larval locomotion after exposure to venom fractions

Zebrafish larvae were gently pipetted into 96-well plates (1 larvae / well) and acclimatized for 30 minutes. A venom treatment concentration of 0.01 µg/µL of each fraction was added to each larva in the treatment group. The plate was loaded into the DanioVision movement chamber. After 15 minutes incubation with the venom peptides, the swimming behavior of the larvae was recorded for 10 minutes, and total swimming distance for each larva determined using EthoVision software. The sample size was n=12 larvae per treatment group alternating with n=18 larvae control group following every treatment group.

Statistical analysis was done on GraphPad Prism 9.2.0 (283). A D'Agostino and Pearson test were done to test for normal distribution and 2way ANOVA using Turkey's multiple comparisons test.

CHAPTER 4 Results

4.1 Overall venom composition

4.1.1 Native PAGE

An initial screen of the snake venoms was done by subjecting five micrograms (μg) of crude venom to 15% clear native PAGE. A Bio-Rad Precision Plus (10 - 250 kDa) molecular weight marker was used as reference standard. The proteins were visualised by Coomassie Brilliant Blue R-250 stain. Figure 4.1 shows the unique venom protein profiles that were obtained from the different snake species. In a comparison of the species' venom protein profiles, unique differences were seen in the molecular weight range below 20 kDa in *Naja nivea* venom protein profile when compared to the profiles of *Bitis atropos* and *Bitis arietans*. A difference was also observed in band thickness between *Naja nivea* species from different geographical locations in the 15 kDa – 20 kDa range. *Bitis atropos* venom had a unique cluster of protein bands in the 15 – 20 kDa range which is present in *Naja nivea*, however absent in the *Bitis arietans* venom profile. A very dark band was observed in the 25 kDa – 37 kDa range, similar to the band found in *Bitis atropos* venom, with lighter stained bands in 37 kDa – 150 kDa range. The venom from *Bitis arietans* species showed high intensity protein bands in the 25 – 150 kDa range, with the darkest band in the 25 kDa – 37 kDa range.

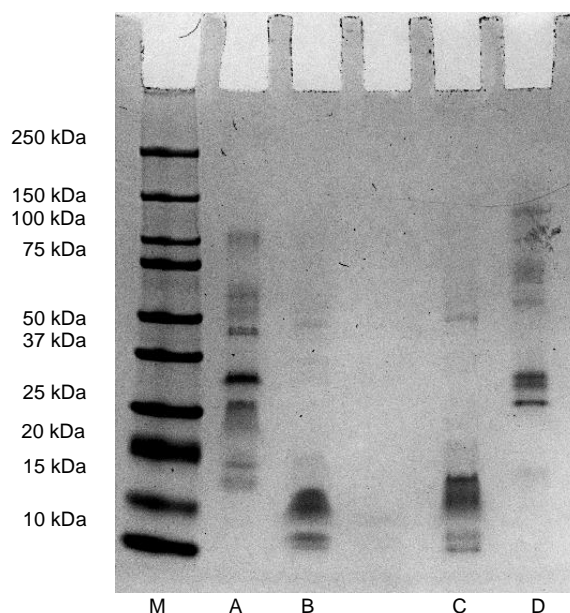


Figure 4.1 Native PAGE protein profiles of crude venom from *B. atropos* (A), *N. nivea* (WC) (B), *N. nivea* (NC) (C) and *B. arietans* (D) (M – molecular weight marker)

The native page of the crude venom from the different snake species revealed a unique protein ladder for each specie. The protein ladder for *Naja nivea* venom contained pronounced protein

bands in the lower molecular weight range, smaller than 20 kDa, whereas the venom protein profile of *Bitis arietans* was more concentrated in the molecular weight range 25 kDa to 150 kDa.

4.1.2 HR-LC-MS/MS analysis of *Naja nivea*, *Bitis arietans* and *Bitis atropos* crude venom

Following HR-LC-MS/MS analysis of in-gel tryptic digestion of crude venoms, 504 proteins were positively identified in the crude venom of *B. atropos*, and 144 and 186 in *N. nivea* and *B. arietans* venoms respectively. A summary of the venom composition of the different species are represented in Figure 4.2. Since the primary focus of this study was to investigate venom toxins, all other cellular and non-toxic proteins were excluded from Figure 4. 2. The complete lists of all the proteins positively identified are in Table 0.1 – 0.3 in the appendix). The three species had 68 proteins in common from 19 protein families. The most abundant snake venom proteins were snake venom serine proteases, snake venom metalloproteinases and L-amino acid oxidases. Compositional variation occurred in the venom proteins that were present in each of the species. Major differences were observed in the venom profiles of *B. arietans* and *N. nivea*, as opposed to the venom profile of *B. atropos* species which had strong similarities to both of these species. Figure 4.3 depicts the compositional relationship of positively identified venom proteins between the three species. The parameters that were employed to determine whether a protein was positively identified, were that the protein must have a 95% or higher protein identification probability and a minimum of two unique peptides. *B. atropos* and *N. nivea* both had a higher abundance of three-finger toxins and cysteine-rich venom proteins compared to *B. arietans*, whereas *B. atropos* and *B. arietans* had a higher abundance of snakelecs compared to *N. nivea* species.

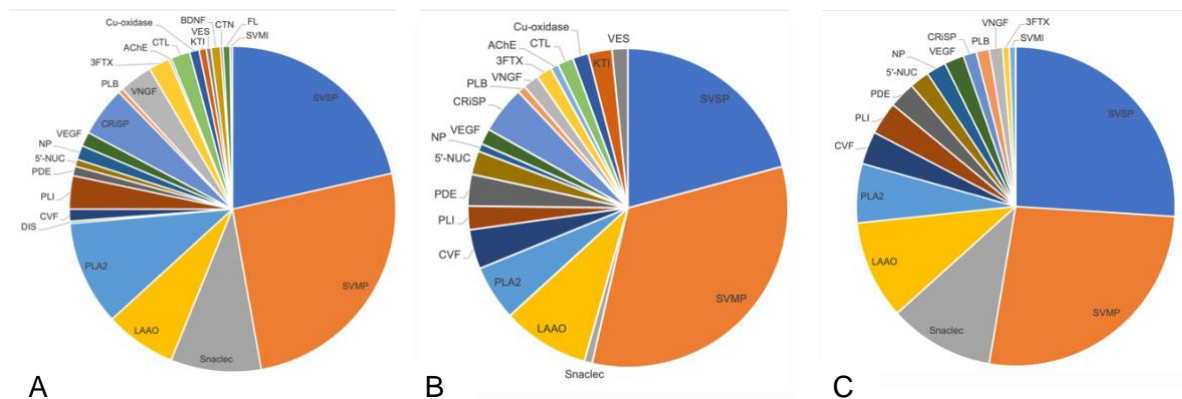


Figure 4.2 A summary of the dominant protein families that were identified in the venom proteomes of the species *B. atropos* (A), *N. nivea* (B) and *B. arietans* venoms (C)

Abbreviations: SVSP, snake venom serine protease; PLA2, phospholipase A2; LAAO, L-amino acid oxidase; SVMP, snake venom metalloproteinase; CRiSP, cysteine-rich venom protein; PLI, phospholipase A2 inhibitor; VNGF, venom nerve growth factor; 3FTX, 3-finger toxin; CTL, C-type lectin; NP, natriuretic peptide; VEGF; Vascular endothelial growth factor; CVF, cobra venom factor; PDE, phosphodiesterase; KTI, Kunitz-type serine protease inhibitor; 5'-NUC, snake venom 5'-nucleotidase, AChE; acetylcholinesterase; FL; ficolin lectin; CTN; cathelicidin; BDNF; Brain-derived neurotrophic factor; VES; vespryn

There were 309 proteins identified that only occurred in *B. atropos* venom, 21 in *N. nivea* venom and 26 in *B. arietans* venom.

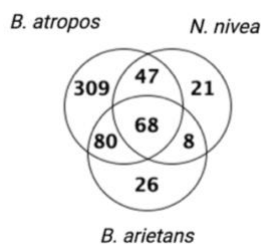


Figure 4.3 Venn diagram showing the qualitative relationship of identified proteins in the venom from *B. atropos*, *N. nivea* and *B. arietans* based on the presence/absence in each venom

4.2 *Naja nivea* venom from the Western Cape and the Northern Cape

The regional variation in venom of *N. nivea* from Western Cape (*N. nivea*-WC) and Northern Cape (*N. nivea*-NC), South Africa were investigated to ensure presence of the target protein candidates in *N. nivea* venom despite regional location of origin. A t-test was used to compare the two regionally different *N. nivea* venoms to determine whether there is a significant difference between venom components. The sample size was n=3 for each group.

Following in-solution tryptic digestion and analysis by mass spectrometry, a total of 56 proteins were identified from the *N. nivea* venom proteome. See Table 4.1 for the complete list of

positively identified proteins, identification probability and percentage of total spectra coverage obtained in the regionally different *N. nivea* venoms.

Three-finger toxins were the most abundant protein family and made up 70% of the venom proteome. Other protein families include cobra venom factor (5%), venom nerve growth factor (18%), snake venom metalloproteinase (3%) and venom phosphodiesterase (2%)(Figure 4.4).

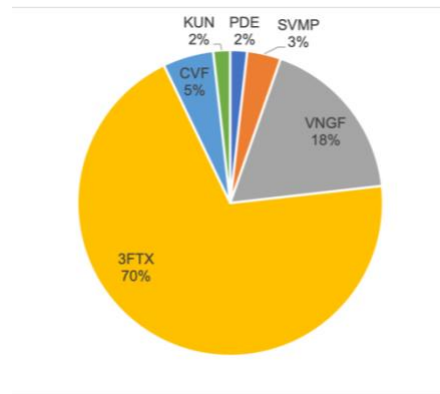


Figure 4.4 Abundant protein families identified in *N. nivea* venom proteome

A high degree of homology in the two venoms of regionally different locations was observed. Figure 4.5 shows a direct qualitative comparison of the abundant protein families identified in two *N. nivea* venoms. Differences were observed in venom nerve growth factor protein family (VNGF), 22% in *N. nivea*-NC and 20% in *N. nivea*-WC venom, venom phosphodiesterase, 2% in *N. nivea*-NC and 0% in *N. nivea*-WC venom and snake venom metalloprotease 5% in *N. nivea*-NC and 4% in *N. nivea*-WC venom. *N. nivea*-WC venom were higher in three finger toxins (3FTX), 67% compared to 62% from the *N. nivea*-NC venom.

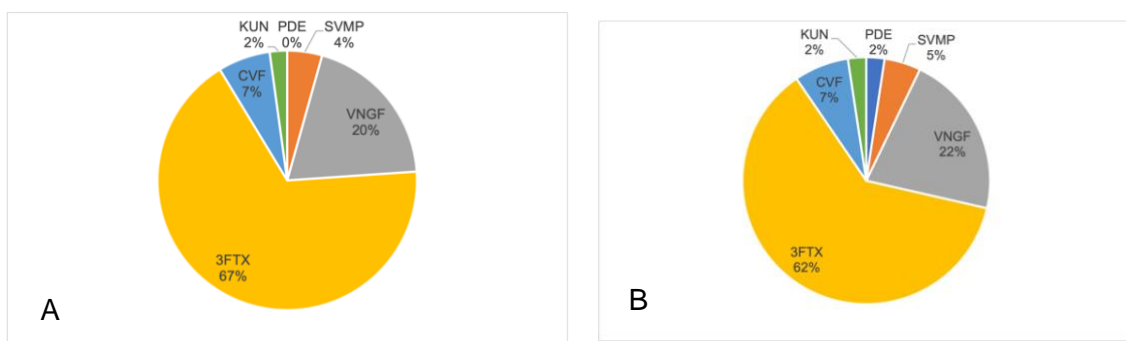


Figure 4.5 Abundant protein families identified from *N. nivea*-WC (A) and *N. nivea*-NC (B) venoms

A total of 56 proteins were identified, 32 proteins were identified in both *N. nivea*-WC and *N. nivea*-NC venoms. Four proteins identified in both venoms were statistically significant ($p < 0.05$) and present at a higher quantity in *N. nivea*-WC venom. Long neurotoxin 1 (3L21_NAJNI) was present at 8.14 fold, short neurotoxin 2 (3S12_NAJNI) at 3.55 fold, zinc metalloproteinase-disintegrin-like atrase-B (VM3B_NAJAT) at 4.26 fold and zinc metalloproteinase-disintegrin-like kaouthiagin-like (VM3KL_NAJAT) at 3.94 fold higher in *N. nivea*-WC than *N. nivea*-NC venom.

Proteins that were only identified in *N. nivea*-WC venom, include nine cytotoxins, cytotoxin 1 (3SA1_NAJME, 3SA1_NAJHA, 3SA1B_NAJAT), cytotoxin 2 (3SA2_NAJMO), cytotoxin 4 (3SA4_NAJAT, 3SA4A_NAJSP), cytotoxin 5 (3SA5_NAJHA), cytotoxin 6 (3SA6_NAJAT), Muscarinic toxin 2 (3SIM2_DENAN) and four neurotoxins, long neurotoxin 2 (3L22_NAJME), long neurotoxin LNTX-2 homolog (3L22H_OPHHA), long neurotoxin OH-55 (3L255_OPHHA), probable weak neurotoxin NNAM3 (3NO23_NAJAT) and venom nerve growth factor 2 (NGFV2_PSEAU). Quantitatively *N. nivea*-WC venom was 27.58 fold higher in the protein long neurotoxin OH-55 (3L255_OPHHA) compared to *N. nivea*-NC venom.

Proteins that were only identified in *N. nivea*-NC venom include cytotoxin 1 (3SA1_NAJMO, 3SA1_NAJNI), cytotoxin 5 (3SA5_NAJHH), mipartoxin-4 (3LK5_BUNMU), kappa-5-bungarotoxin (3SX4_MICMP), probable weak neurotoxin NNAM2 (3NO22_NAJAT), three-finger toxin Mnn I (3S11_MICNI), weak neurotoxin 10 (3NO2A_NAJSP), Venom phosphodiesterase 2 (PDE2_CROAD), venom nerve growth factor 1 (NGFV1_PSEAU). The protein probable weak neurotoxin NNAM2 (3NO22_NAJAT), was present at a 0.11 fold higher in *N. nivea*-NC venom.

Table 4.1 List of proteins positively identified in the two regionally different *N. nivea* WC (n=3) and *N. nivea* NC (n=3) venoms by in-solution tryptic digestion and HR-LC-MS/MS.

Identified Proteins (56)	Protein family	Uniprot Accession Number	Mr (kDa)	P/A	Quantitative Profile	Homology with protein from	Protein Identification Probability						Percentage of Total Spectra					
							<i>Naja nivea</i> -NC			<i>Naja nivea</i> -WC			<i>Naja nivea</i> -NC			<i>Naja nivea</i> -WC		
							1	2	3	1	2	3	1	2	3	1	2	3
Three-finger toxins (3FTX)																		
Cytotoxin 1	CTX	3SA1_NAJME	7	WC	NS	<i>Naja melanoleuca</i>	0	60%	52%	82%	0	95%	0	0.009%	0.0063%	0.011%	0	0.0068%
Cytotoxin 1	CTX	3SA1_NAJMO	7	NC	NS	<i>Naja mossambica</i>	0	96%	67%	80%	84%	62%	0	0.009%	0.0063%	0.021%	0.018%	0.010%
Cytotoxin 1	CTX	3SA1_NAJNI	7	NC	NS	<i>Naja nivea</i>	83%	100%	89%	89%	87%	83%	0.040%	0.036%	0.048%	0.034%	0.031%	0.031%
Cytotoxin 1	CTX	3SA1_NAJHA	7	WC	NS	<i>Naja annulifera</i>	70%	78%	78%	97%	76%	70%	0.037%	0.030%	0.048%	0.034%	0.031%	0.027%
Cytotoxin 1b	CTX	3SA1B_NAJAT	9	WC	NS	<i>Naja atra</i>	0	54%	82%	95%	97%	45%	0	0.009%	0.0063%	0.011%	0.0046%	0.0068%
Cytotoxin 2	CTX	3SA2_NAJNI	7	NC WC	NS	<i>Naja nivea</i>	100%	100%	100%	100%	100%	100%	0.074%	0.066%	0.067%	0.060%	0.057%	0.075%
Cytotoxin 2	CTX	3SA2_NAJMO	7	WC	NS	<i>Naja mossambica</i>	0	56%	50%	68%	97%	32%	0	0.012%	0.016%	0.027%	0.020%	0.014%
Cytotoxin 3	CTX	3SA3_NAJNI	7	NC WC	NS	<i>Naja nivea</i>	100%	100%	100%	100%	100%	100%	0.088%	0.069%	0.035%	0.034%	0.032%	0.048%
Cytotoxin 4	CTX	3SA4_NAJAT	9	WC	NS	<i>Naja atra</i>	0	98%	87%	42%	0	0	0	0.009%	0.0063%	0.011%	0	0
Cytotoxin 4a	CTX	3SA4A_NAJSP	9	WC	NS	<i>Naja sputatrix</i>	0	92%	0	95%	0	74%	0	0.009%	0	0.011%	0	0.0068%
Cytotoxin 5	CTX	3SA5_NAJH	7	NC	NS	<i>Naja haje haje</i>	100%	100%	100%	63%	65%	81%	0.030%	0.024%	0.025%	0.016%	0.020%	0.020%
Cytotoxin 5	CTX	3SA5_NAJMO	7	NC WC	NS	<i>Naja mossambica</i>	97%	0	0	95%	0	0	0.024%	0	0	0.012%	0	0
Cytotoxin 5	CTX	3SA5_NAJHA	7	WC	NS	<i>Naja annulifera</i>	64%	66%	70%	96%	75%	72%	0.074%	0.063%	0.054%	0.044%	0.038%	0.065%
Cytotoxin 6	CTX	3SA6_NAJAT	9	WC	NS	<i>Naja atra</i>	47%	81%	45%	100%	99%	0	0.024%	0.009%	0.0063%	0.011%	0.0046%	0
Cytotoxin 7	CTX	3SA7_NAJHA	7	NC WC	NS	<i>Naja annulifera</i>	100%	100%	100%	100%	100%	100%	0.057%	0.054%	0.048%	0.035%	0.034%	0.061%
Cytotoxin 8	CTX	3SA8_NAJNA	7	NC WC	NS	<i>Naja naja</i>	61%	100%	100%	63%	96%	0	0.020%	0.012%	0.0095%	0.011%	0.0061%	0
Cytotoxin 10	CTX	3SAA_NAJHA	7	NC WC	NS	<i>Naja annulifera</i>	100%	100%	100%	100%	100%	100%	0.047%	0.030%	0.060%	0.027%	0.015%	0.027%
Cytotoxin 10	CTX	3SAA_NAJAT	9	NC WC	NS	<i>Naja atra</i>	0	93%	97%	79%	97%	89%	0	0.009%	0.0063%	0.011%	0.0046%	0.0068%
Cytotoxin homolog 5V	CTX	3SOFV_NAJAT	9	NC WC	NS	<i>Naja atra</i>	95%	98%	95%	97%	98%	9%	0.0067%	0.006%	0.013%	0.0018%	0.015%	0.0034%

Cytotoxin I-like P-15	CTX	3SAPF_NAJAT	9	NC WC	NS	<i>Naja atra</i>	90%	100%	89%	97%	88%	97%	0.024 %	0.033 %	0.022 %	0.018 %	0.017 %	0.014 %
Cytotoxin KJC3	CTX	3SAC3_NAJSP	7	NC WC	NS	<i>Naja sputatrix</i>	0	95%	99%	89%	0	95%	0	0.009 %	0.006 3%	0.011 %	0	0.006 8%
Cytotoxin sagitoxin	CTX	3SAS_NAJSG	7	NC WC	NS	<i>Naja sagittifera</i>	99%	100%	100%	99%	88%	96%	0.024 %	0.012 %	0.009 5%	0.012 %	0.004 6%	0.010 %
Cytotoxin SP13b	CTX	3SADB_NAJAT	7	NC WC	NS	<i>Naja atra</i>	8%	96%	96%	88%	98%	100%	0.020 %	0.009 %	0.006 3%	0.011 %	0.004 6%	0.006 8%
Mipartoxin-4	CTX	3SX4_MICMP	9	NC	NS	<i>Micrurus mipartitus</i>	100%	95%	100%	99%	0	100%	0.006 7%	0.00 %	0.003 2%	0.00 %	0	0.00 %
Muscarinic toxin 2	CTX	3SIM2_DENAN	9	WC	NS	<i>Dendroaspis angusticeps</i>	15%	85%	99%	97%	100%	100%	0.017 %	0.003 %	0.00 %	0.001 8%	0.006 1%	0.010 %
Naniproin	CTX	3SAN_NAJNG	7	NC WC	NS	<i>Naja nigricollis</i>	0	94%	96%	96%	91%	43%	0	0.009 %	0.013 %	0.014 %	0.009 2%	0.006 8%
Kappa-5-bungarotoxin	NTX	3LK5_BUNMU	9	NC	NS	<i>Bungarus multicinctus</i>	97%	92%	85%	75%	0	0	0.006 7%	0.00 %	0.00 %	0.00 %	0	0
Long neurotoxin 1	NTX	3L21_NAJNI	8	NC WC	Northern Cape low, Western Cape high	<i>Naja nivea</i>	100%	100%	100%	100%	100%	100%	0.020 %	0.021 %	0.009 5%	0.057 %	0.064 %	0.078 %
Long neurotoxin 2	NTX	3L22_NAJME	8	WC	NS	<i>Naja melanoleuca</i>	0	72%	55%	10%	100%	84%	0	0.003 %	0.003 2%	0.023 %	0.028 %	0.024 %
Long neurotoxin LNTX-2 homolog	NTX	3L22H_OPHHA	10	WC	NS	<i>Ophiophagus hannah</i>	0	0	20%	95%	0	91%	0	0	0.00 %	0.003 5%	0	0.00 %
Long neurotoxin OH-55	NTX	3L255_OPHHA	10	WC	Northern Cape low, Western Cape high	<i>Ophiophagus hannah</i>	0	49%	64%	53%	96%	60%	0	0.003 %	0.003 2%	0.020 %	0.034 %	0.031 %
Probable weak neurotoxin NNAM2	NTX	3NO22_NAJAT	10	NC	Northern Cape high, Western Cape low	<i>Naja atra</i>	97%	100%	95%	69%	56%	0	0.013 %	0.009 %	0.009 5%	0.001 8%	0.00 %	0
Probable weak neurotoxin NNAM3	NTX	3NO23_NAJAT	10	WC	NS	<i>Naja atra</i>	0	26%	44%	100%	0	0	0	0.003 %	0.003 2%	0.005 3%	0	0
Short neurotoxin 2	NTX	3S12_NAJNI	7	NC WC	Northern Cape low, Western Cape high	<i>Naja nivea</i>	100%	100%	100%	100%	100%	100%	0.034 %	0.033 %	0.035 %	0.059 %	0.046 %	0.075 %
Short neurotoxin 2	NTX	3S12_NAJHA	7	NC WC	NS	<i>Naja atra</i>	92%	94%	91%	99%	100%	93%	0.044 %	0.033 %	0.032 %	0.032 %	0.029 %	0.048 %
Short neurotoxin 3	NTX	3S13_NAJHA	7	NC WC	NS	<i>Naja annulifera</i>	100%	100%	100%	100%	100%	100%	0.013 %	0.018 %	0.019 %	0.011 %	0.018 %	0.020 %
Three-finger toxin Mnn I	NTX	3S11_MICNI	7	NC	NS	<i>Micrurus nigrocinctus</i>	82%	97%	99%	72%	100%	7%	0.027 %	0.015 %	0.019 %	0.007 1%	0.007 7%	0.014 %
Weak neurotoxin 10	NTX	3NO2A_NAJSP	10	NC	NS	<i>Naja sputatrix</i>	100%	65%	59%	85%	0	53%	0.020 %	0.006 %	0.013 %	0.001 8%	0	0.006 8%
Weak toxin CM-11	NTX	3NO2B_NAJHH	8	NC WC	NS	<i>Naja haje haje</i>	100%	100%	100%	100%	100%	100%	0.024 %	0.018 %	0.022 %	0.007 1%	0.007 7%	0.017 %

A. superbus venom factor 1	CVF	VCO31_AUS SU	185	NC WC	NS	<i>Austrelaps superbus</i>	98%	100%	100%	100%	100%	100%	0.013 %	0.012 %	0.013 %	0.018 %	0.004 6%	0.010 %
A. superbus venom factor 2	CVF	VCO32_AUS SU	185	NC WC	NS	<i>Austrelaps superbus</i>	100%	100%	100%	100%	100%	100%	0.010 %	0.027 %	0.009 5%	0.012 %	0.006 1%	0.010 %
Cobra venom factor	CVF	VCO3_NAJK A	185	NC WC	NS	<i>Naja kaouthia</i>	100%	100%	100%	100%	100%	100%	0.017 %	0.012 %	0.019 %	0.025 %	0.006 1%	0.031 %
Kunitz-type serine protease inhibitor 2	KUN	VKT2_NAJN I	6	NC WC	NS	<i>Naja nivea</i>	100%	100%	100%	100%	100%	100%	0.11 %	0.13 %	0.12 %	0.041 %	0.060 %	0.051 %
Venom phosphodi- esterase 2	PDE	PDE2_CRO AD	92	NC	NS	<i>Crotalus adamanteus</i>	99%	100%	100%	100%	100%	100%	0.020 %	0.006 %	0.003 2%	0.001 8%	0.003 1%	0.003 4%
Zinc metalloprotein ase- disintegrin- like atrase-B	SVMP	VM3B_NAJA T	66	NC WC	Northern Cape low, Western Cape high	<i>Naja atra</i>	94%	100%	98%	100%	100%	100%	0.017 %	0.012 %	0.013 %	0.027 %	0.023 %	0.031 %
Zinc metalloprotein ase- disintegrin- like kaouthiagin- like	SVMP	VM3KL_NAJ AT	66	NC WC	Northern Cape low, Western Cape high	<i>Naja atra</i>	93%	100%	100%	100%	99%	99%	0.017 %	0.012 %	0.016 %	0.027 %	0.023 %	0.031 %
Venom nerve growth factor	VNGF	NGFV_PSE PO	27	NC WC	NS	<i>Pseudechis porphyriacus</i>	90%	100%	99%	99%	94%	100%	0.003 4%	0.015 %	0.003 2%	0.003 5%	0.011 %	0.003 4%
Venom nerve growth factor	VNGF	NGFV_NAJK A	13	NC WC	NS	<i>Naja kaouthia</i>	100%	100%	100%	100%	100%	100%	0.027 %	0.036 %	0.029 %	0.025 %	0.011 %	0.020 %
Venom nerve growth factor 1	VNGF	NGFV1_PSE AU	27	NC	NS	<i>Pseudechis australis</i>	99%	68%	6%	79%	0	0	0.010 %	0.012 %	0.003 2%	0.005 3%	0	0
Venom nerve growth factor 2	VNGF	NGFV2_NAJ SP	27	NC WC	NS	<i>Naja sputatrix</i>	100%	100%	100%	100%	100%	100%	0.044 %	0.057 %	0.038 %	0.023 %	0.023 %	0.037 %
Venom nerve growth factor 2	VNGF	NGFV2_NO TSC	28	NC WC	NS	<i>Notechis scutatus scutatus</i>	67%	100%	98%	56%	96%	73%	0.003 4%	0.015 %	0.003 2%	0.003 5%	0.011 %	0.003 4%
Venom nerve growth factor 2	VNGF	NGFV2_PSE AU	27	WC	NS	<i>Pseudechis australis</i>	95%	73%	71%	97%	100%	100%	0.003 4%	0.012 %	0.003 2%	0.003 5%	0.012 %	0.006 8%
Venom nerve growth factor 2	VNGF	NGFV2_PSE TE	27	NC WC	NS	<i>Pseudonaja textilis</i>	11%	96%	100%	99%	84%	98%	0.003 4%	0.012 %	0.003 2%	0.003 5%	0.011 %	0.003 4%
Venom nerve growth factor 2	VNGF	NGFV2_HO PST	28	NC WC	NS	<i>Hoplocephalus stephensii</i>	94%	100%	97%	99%	99%	100%	0.006 7%	0.015 %	0.003 2%	0.003 5%	0.011 %	0.010 %

Venom nerve growth factor 3	VNGF	NGFV3_PSE AU	27	NC WC	NS	<i>Pseudechis australis</i>	6%	95%	100%	97%	89%	67%	0.003 4%	0.012 %	0.009 5%	0.005 3%	0.011 %	0.003 4%
Venom nerve growth factor 5	VNGF	NGFV5_TR OCA	28	NC WC	NS	<i>Tropidechis carinatus</i>	100%	94%	98%	99%	94%	87%	0.010 %	0.012 %	0.003 2%	0.003 5%	0.011 %	0.003 4%

Abbreviations: 3FTX, three finger toxin; CTX, cytotoxin, NTX, neurotoxin; CVF, cobra venom factor; SVMP, snake venom metalloproteinase; PDE, phosphodiesterase; VNGF, Venom nerve growth factor; Mr, molecular weight; kDa, kilodaltons; P/A, presence/absence; NC, Northern Cape; Western Cape; NS, non-significant. Statistical analysis was performed using Scaffold version 5.0.1.

4.3 Depletion of highly abundant proteins from venom and plasma

4.3.1 Reversed phase HPLC

The lyophilized venom samples from the snake species *B. atropos*, *N. nivea* and *B. arietans* were resuspended in with water with 0.1% formic acid and spiked into plasma to make a 200 μL aliquot with a concentration of 5 $\mu\text{g}/\mu\text{L}$. After precipitation with 2, 3 and 4 volumes of acetonitrile, the similarities, and dissimilarities in composition of the samples were assessed based on the RP-HPLC elution profile. This was done to determine the optimum acetonitrile concentration for down the line analysis of target venom peptides. Venom proteins were detected at a wavelength of 215 nm (Walker, 2009).

In Figure 4.6 differences in RP-HPLC chromatograms of different snake venoms (B-D) in 0.1% formic acid in water precipitated with two volumes acetonitrile was observed between venom as well as from blank mobile phase (A). All venoms had a peak at 12-minute retention time, that was absent from the blank sample. *N. nivea* (WC) (C) and *N. nivea* (NC) (D) venoms showed no peak separation with one major peak eluting between from 12 to 16 minutes retention time. *B. atropos* (B) venom showed prominent peaks at retention times 13,15 and 16 minutes. *B. arietans* venom (E) showed four well defined peaks at a retention times 9, 11, 16 and 19 minutes.

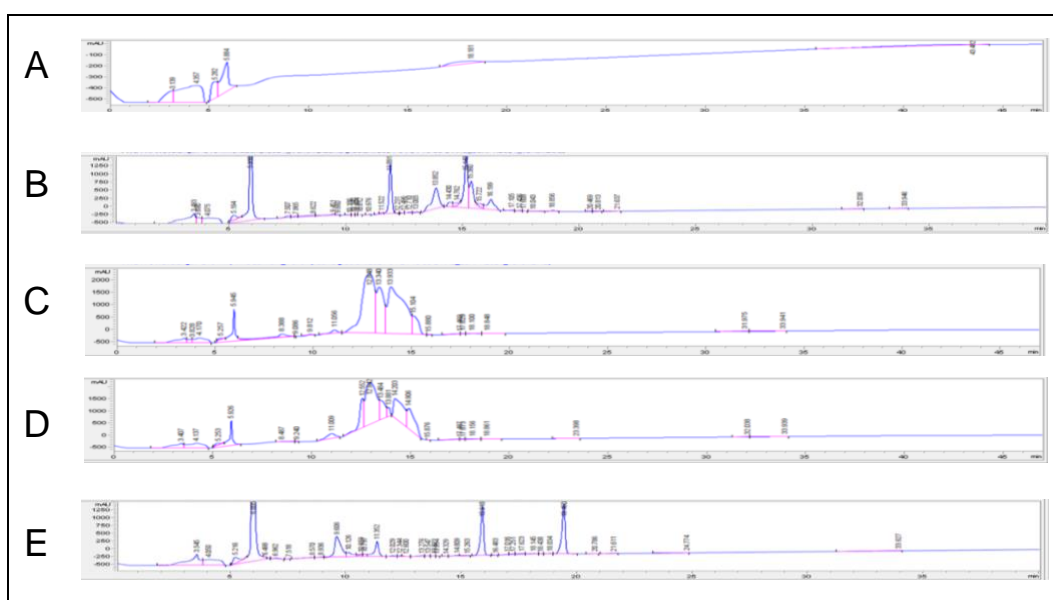


Figure 4.6 RP-HPLC chromatograms of Blank 0.1% formic acid in water (A), *B. atropos* (B), *N. nivea* (WC) (C), *N. nivea* (NC) (D) and *B. arietans* venoms in water with 0.1% formic acid (D) precipitated with two volumes acetonitrile.

Figure 4.7 shows the RP-HPLC chromatograms of blood plasma spiked with venom and precipitated with two volumes acetonitrile. The blank blood plasma (A) had peaks at retention time 10.7 and 13 minutes which were not present in the blank mobile phase Figure 4.6 (A).

Crude *B. atropos* (B), *N. nivea* (WC) (C) and *N. nivea* (NC) (D) and *B. arietans* venoms (E) spiked into plasma and precipitated with two volumes acetonitrile had elution profiles similar to that observed in Figure 4.6, with major peaks at the same retention times.

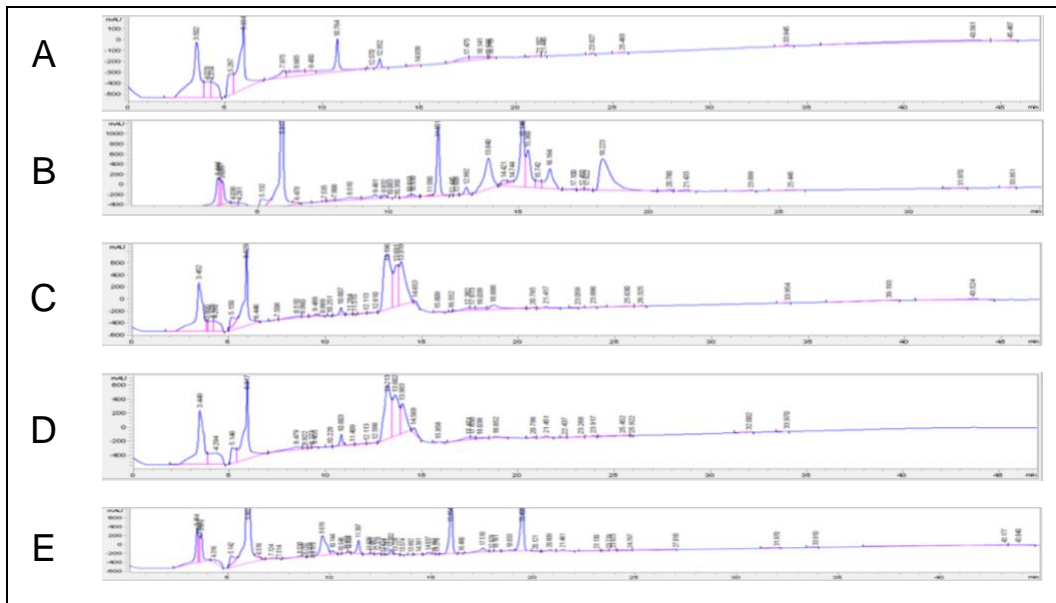


Figure 4.7 RP-HPLC chromatograms obtained from blank blood plasma precipitated with two volumes acetonitrile (A). Crude *B. atropos* (B), *N. nivea* (WC) (C) and *N. nivea* (NC) (D) and *B. arietans* venoms (E) spiked into plasma and precipitated with two volumes acetonitrile.

When the volume of acetonitrile for protein precipitation was increased to 3 volumes (Figure 4.8 and Figure 4.9) and 4 volumes (Figure 4.10 and Figure 4.11), the chromatographic profiles showed depletion of proteins from venom and plasma in comparison to the profiles obtained after precipitation with 2 volumes acetonitrile. A considerable decrease of peak intensity was observed for *N. nivea* venoms.

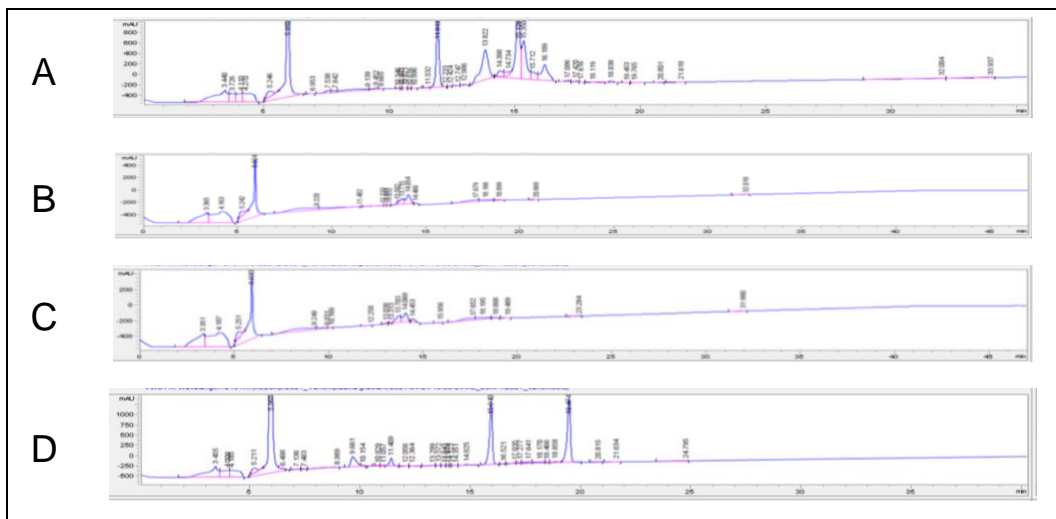


Figure 4.8 Crude venoms from *B. atropos* (A), *N. nivea* (WC) (B), *N. nivea* (NC) (C) and *B. arietans* (D) in 0.1% formic acid in water precipitated with three volumes acetonitrile

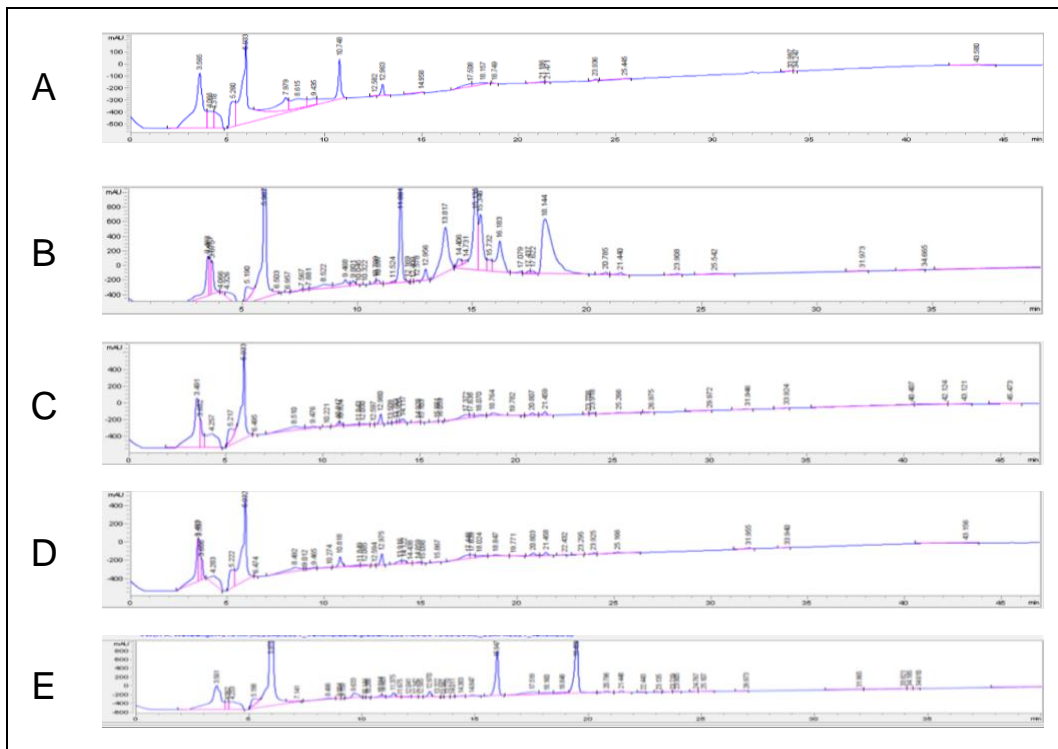


Figure 4.9 RP-HPLC chromatograms of plasma (A) and plasma spiked with crude venom from *B. atropos* (B), *N. nivea* (WC) (C), *N. nivea* (NC) (D) and *B. arietans* (E) precipitated with three volumes acetonitrile

Figure 4.10 and Figure 4.11 are the chromatograms of venom in mobile phase A and in blood plasma that were subjected to protein precipitation with four volumes of acetonitrile. No change or improvement was observed in the elution profile of *B. atropos* and *N. nivea* venoms Figure 4.10 (A-C) and Figure 4.11 (A-D). As before *B. arietans* venom samples had a stable baseline and good separation producing symmetrical peaks at retention times 15.9 and 19.4 minutes (Figure 4.10 (D) and Figure 4.11 (E)).

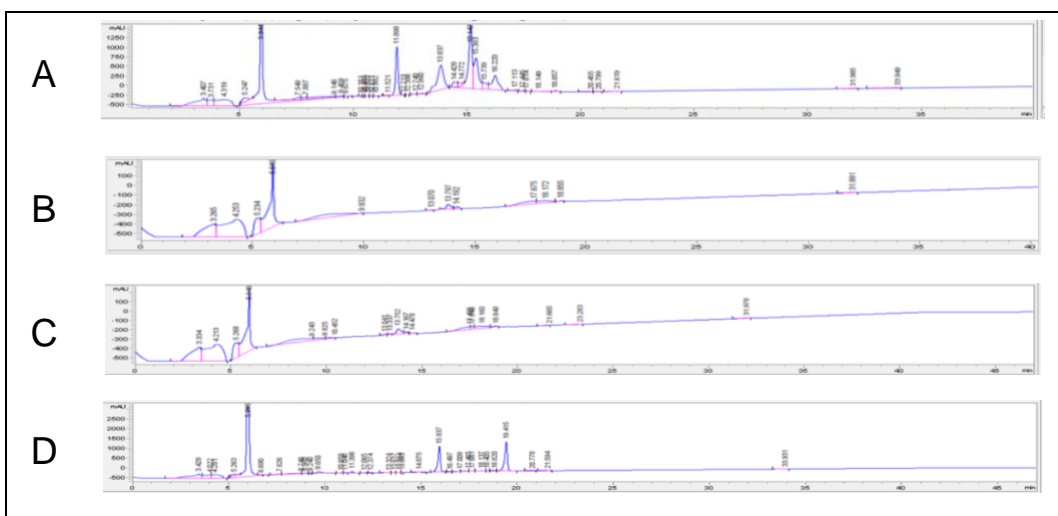


Figure 4.10 RP-HPLC chromatograms of venom from the species *B. atropos* (A), *N. nivea* (WC) (B), *N. nivea* (NC) (C) and *B. arietans* (D) in 0.1% formic acid in water, precipitated with four volumes acetonitrile

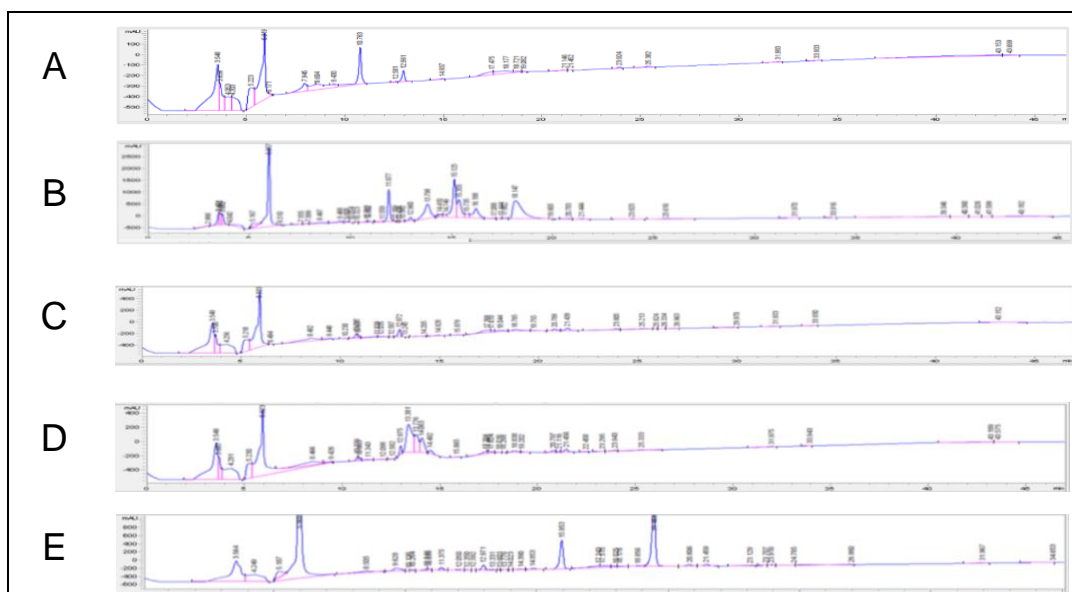


Figure 4.11 RP-HPLC chromatograms of blood plasma precipitated with four volumes acetonitrile (A) and *B. atropos* (B), *N. nivea* (WC) (C), *N. nivea* (NC) (D), *B. arietans* (E) venoms spiked in plasma and precipitated with four volumes acetonitrile

4.3.2 HR-LC-MS/MS analysis plasma spiked with venom of acetonitrile high molecular weight protein depleted venom

After RP-HPLC analysis, precipitation with two volumes of acetonitrile was selected as the preferred protocol, to avoid the loss of low molecular mass venom components that may be unique and in abundance in the venom proteomes of the snake species under investigation. This is also the volume of organic solvent used in sample preparation of serum/plasma for analysis by mass spectrometry (Luque-Garcia and Neubert, 2007). The supernatants were directly injected, and proteins identified by HR-LC-MS/MS. Figure 4.12 shows the total ion chromatograms (TIC) that were generated in Excalibur (Thermo Scientific) during mass spectrometry for *B. arietans* (A) and *N.nivea*-NC (B) venoms spiked into plasma. Visually a difference in the chromatogram between the venom samples can be seen.

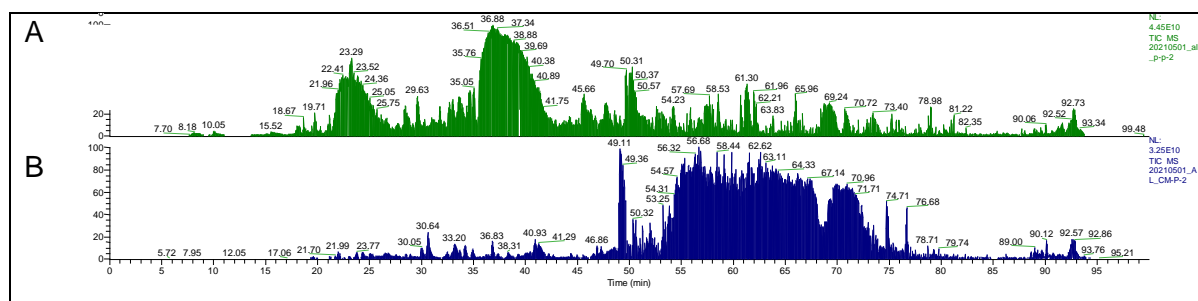


Figure 4.12 Mass spectrometry of crude venom from *B. arietans* (A) and *N. nivea*-NC (B) spiked into plasma with two volumes of acetonitrile and injected onto the HR-LC-MS/MS. TIC generated in Excalibur, Thermo Scientific™ .

In total, 158 proteins were identified, 118 *Homo sapiens* and 40 of Serpentes taxonomic origin. All the snake venom proteins that were positively identified are listed in Table 4.2. Three proteins, protein snake venom 5'-nucleotidase (V5NTD_NAJAT, V5NTD_CROAD) and snake venom metalloproteinase-disintegrin-like mocarhagin protein (VM3M1_NAJMO) were detected in in samples that were spiked with *B. arietans* and *N. nivea* venom.

Complement C3 (VCO3_NAJKA), cytotoxin 1 (3SA1_NAJHA), cobra venom factor (VCO3_NAJKA), zinc metalloproteinase-disintegrin-like atrase-B (VM3B_NAJAT), zinc metalloproteinase-disintegrin-like cobrin (VM3_NAJKA), L-amino-acid oxidase (OXLA_NAJAT), Thaicobrin (VESP_NAJKA) and vespryn (VESP_CROAD) were positively identified from the sample spiked with *N. nivea* venom.

From the samples spiked with *B. arietans* venom, twenty nine unique proteins were positively identified. These proteins belong primarily to snake venom metalloproteinase-disintegrin (n=14) and L-amino-acid oxidase (n=7) protein families. The protein zinc metalloproteinase-disintegrin BA-5A (VM25A_BITAR) was specific to *B. arietans* species. Other proteins that were positively identified in plasma sample spiked with *B. arietans* venom include snake venom 5'-nucleotidase (V5NTD_GLOBR), cystatin (CYT_BITAR), snake venom 5'-nucleotidase (V5NTD_CROAD), snake venom metalloprotease inhibitor 02D01 (SVM1_ECHOC), venom phosphodiesterase 1 (PDE1_CROAD), the snake venom metalloproteinase inhibitors Poly-His-poly-Gly peptide 1 (SVM11_ATHSQ) and Poly-His-poly-Gly peptide 2 (SVM12_ATHNI) and venom nerve growth factor 1 (Fragment)(NGFV1_AZEFE).

Table 4.2 List of venom proteins and peptides identified by HR-LC-MS/MS in supernatants (undigested) from human plasma spiked with crude venom from *B. arietans* and *N. nivea* and precipitated with acetonitrile

UniProt Accession Number	Protein family	Identified Proteins	Homology with protein from	Molecular Weight	Identification probability		Unique peptides	
					<i>N. nivea</i>	<i>B. arietans</i>	<i>N. nivea</i>	<i>B. arietans</i>
V5NTD_CROAD	5'-NUC	Snake venom 5'-nucleotidase	<i>Crotalus adamanteus</i>	65 kDa	100%	100%	41	26
V5NTD_GLOBR	5'-NUC	Snake venom 5'-nucleotidase	<i>Gloydius brevicaudus</i>	64 kDa	90%	100%	39	13
V5NTD_NAJAT	5'-NUC	Snake venom 5'-nucleotidase (Fragment)	<i>Naja atra</i>	58 kDa	100%	100%	91	14
CO3_NAJNA	ANA	Complement C3	<i>Naja naja</i>	185 kDa	100%	0	12	0
3SA1_NAJHA	CTX	Cytotoxin 1	<i>Naja annulifera</i>	7 kDa	100%	0	2	0
VCO3_NAJKA	CVF	Cobra venom factor	<i>Naja kaouthia</i>	185 kDa	100%	0	15	0
CYT_BITAR	CYS	Cystatin	<i>Bitis arietans</i>	13 kDa	0	100%	0	3
VM25A_BITAR	SVMP	Zinc metalloproteinase-disintegrin BA-5A	<i>Bitis arietans</i>	59 kDa	0	100%	0	15
VM2AL_TRIAB	SVMP	Zinc metalloproteinase homolog-disintegrin albolatin	<i>Trimeresurus albolabris</i>	54 kDa	0	100%	0	4
VM2DI_GLOHA	SVMP	Zinc metalloproteinase/disintegrin	<i>Gloydius halys</i>	53 kDa	0	100%	0	10
VM2H1_BOTLA	SVMP	Zinc metalloproteinase-disintegrin BlatH1	<i>Bothriechis lateralis</i>	54 kDa	0	97%	0	8
VM2P1_PROMU	SVMP	Zinc metalloproteinase/disintegrin PMMP-1	<i>Protobothrops mucrosquamatus</i>	53 kDa	0	100%	0	11
VM2V2_CROAT	SVMP	Zinc metalloproteinase-disintegrin VMP-II	<i>Crotalus atrox</i>	55 kDa	0	100%	0	12
VM3_NAJKA	SVMP	Zinc metalloproteinase-disintegrin-like cobrin	<i>Naja kaouthia</i>	68 kDa	100%	64%	0	7
VM3_OPHHA	SVMP	Zinc metalloproteinase-disintegrin-like ohanin	<i>Ophiophagus hannah</i>	69 kDa	89%	100%	0	11
VM33_CROAD	SVMP	Zinc metalloproteinase-disintegrin-like 3a	<i>Crotalus adamanteus</i>	69 kDa	72%	96%	0	6
VM39_DRYCN	SVMP	Zinc metalloproteinase-disintegrin-like MTP9	<i>Drysdalia coronoides</i>	68 kDa	79%	99%	4	8
VM3AH_DEIAC	SVMP	Zinc metalloproteinase-disintegrin-like acurhagin	<i>Deinagkistrodon acutus</i>	69 kDa	0	99%	0	12
VM3B_NAJAT	SVMP	Zinc metalloproteinase-disintegrin-like atrase-B	<i>Naja atra</i>	66 kDa	100%	67%	5	7
VM3B1_BOTJR	SVMP	Zinc metalloproteinase-disintegrin-like BjussuMP-1 (Fragment)	<i>Bothrops jararacussu</i>	62 kDa	0	100%	0	12
VM3M1_NAJMO	SVMP	Snake venom metalloproteinase-disintegrin-like mocarhagin	<i>Naja mossambica</i>	68 kDa	100%	99%	2	7
VM3SB_TRIST	SVMP	Zinc metalloproteinase-disintegrin-like stejnihagin-B	<i>Trimeresurus stejnegeri</i>	68 kDa	0	100%	0	11

VM3TM_TRIST	SVMP	Zinc metalloproteinase-disintegrin-like TSV-DM	<i>Trimeresurus stejnegeri</i>	69 kDa	92%	100%	1	10
VM3VB_MACLB	SVMP	Zinc metalloproteinase-disintegrin-like VLAIP-B	<i>Macrovipera lebetina</i>	69 kDa	0	97%	0	15
OXLA_BOTPC	LAAO	L-amino acid oxidase (Fragment)	<i>Bothrops pictus</i>	56 kDa	0	100%	0	84
OXLA_BOTSC	LAAO	L-amino acid oxidase Bs29 (Fragment)	<i>Bothriechis schlegelii</i>	56 kDa	0	100%	0	64
OXLA_CALRH	LAAO	L-amino-acid oxidase	<i>Calloselasma rhodostoma</i>	58 kDa	0	100%	0	53
OXLA_DABRR	LAAO	L-amino-acid oxidase	<i>Daboia russelii</i>	57 kDa	0	100%	0	121
OXLA_ECHOC	LAAO	L-amino-acid oxidase	<i>Echis ocellatus</i>	57 kDa	0	100%	0	39
OXLA_NAJAT	LAAO	L-amino-acid oxidase (Fragment)	<i>Naja atra</i>	58 kDa	100%	88%	6	3
OXLA_OXYSC	LAAO	L-amino-acid oxidase	<i>Oxyuranus scutellatus scutellatus</i>	59 kDa	0	100%	0	5
OXLA_TRIPP	LAAO	L-amino oxidase (Fragments)	<i>Trimeresurus purpureomaculatus</i>	54 kDa	0	100%	0	13
PDE1_CROAD	PDE	Venom phosphodiesterase 1	<i>Crotalus adamanteus</i>	96 kDa	0	100%	0	4
SVMI_ECHOC	SVMI	Snake venom metalloprotease inhibitor O2D01	<i>Echis ocellatus</i>	33 kDa	0	100%	0	4
SVMI1_ATHSQ	SVMI	Poly-His-poly-Gly peptide 1	<i>Atheris squamigera</i>	2 kDa	0	99%	0	5
SVMI2_ATHNI	SVMI	Poly-His-poly-Gly peptide 2	<i>Atheris nitschei</i>	3 kDa	0	100%	0	7
VM3CX_DABSI	SVMP	Coagulation factor X-activating enzyme heavy chain	<i>Daboia siamensis</i>	70 kDa	50%	97%	0	15
VESP_NAJKA	VES	Thaicobrin	<i>Naja kaouthia</i>	12 kDa	100%	0	25	0
VESP_CROAD	VES	Vespryn	<i>Crotalus adamanteus</i>	25 kDa	100%	0	4	0
NGFV1_AZEFE	VNGF	Venom nerve growth factor 1 (Fragment)	<i>Azemiops feae</i>	25 kDa	0	100%	0	3
Abbreviations: 5' NUC, snake venom 5'-nucleotidase; ANA, anaphylotoxin; CTX, cytotoxin; CVF, cobra venom factor; CYS, cystatin; LAAO, L-amino acid oxidase; PDE, phosphodiesterase; SVMP, snake venom metalloproteinase; SVMI, snake venom metalloproteinase inhibitor; VES, vespryn; VNGF, venom nerve growth factor								

4.4 Size exclusion chromatography

Eight major peaks were consistently obtained on the chromatogram of fractionation of *Naja nivea* venom. The fractionation was detected at wavelengths 215 nm, 250 nm and 280 nm. The 215 nm and 250 nm wavelengths were completely saturated and therefore detection for maximum peak separation was performed at 280 nm (Figure 4.13).

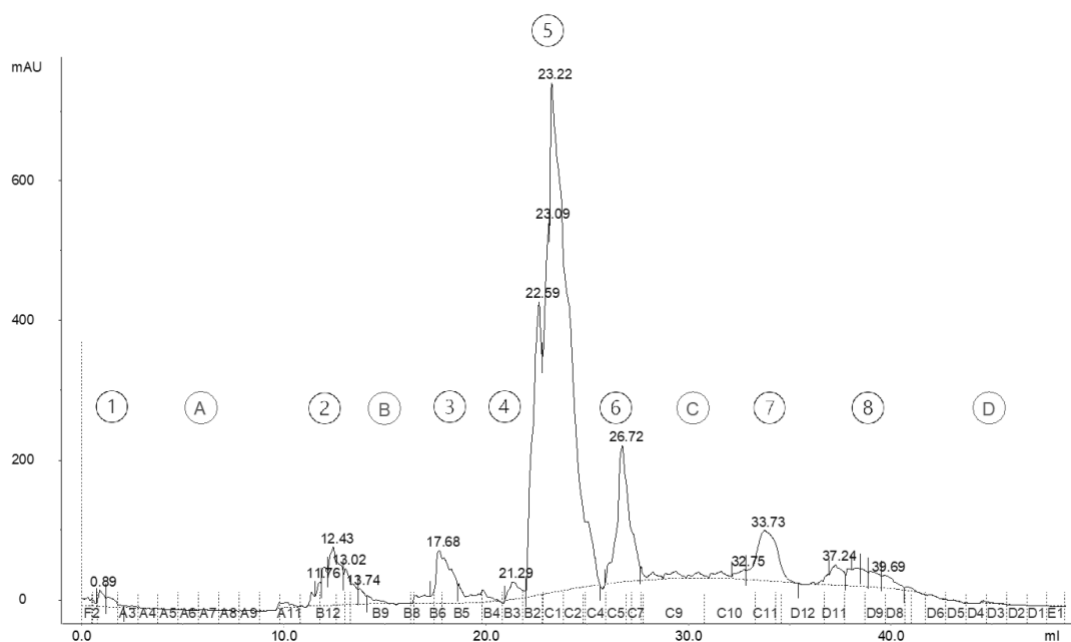


Figure 4.13 Chromatogram obtained during fractionation of *N. nivea* venom on AKTA Explorer, read at 280 nm.

There were 20 major peaks detected, with a total area (mAU*mL) of 1633.92. Fractions that were collected for each of the major peaks were pooled together as well as fractions collected over the areas in-between the major peaks. This produced twelve pooled fractions. The fractions containing peaks were numerically labelled (1 - 8) and the fractions in-between alphabetically (A - D). (Figure 4.13) The peaks are indicative of the molecular weights of the venom proteins/peptides with high molecular weight proteins eluting first and the area under the curve proportional to the protein quantity in that particular weight range. Based on the area under the curve and retention, fractions were selected for further analysis. Table 4.3 shows the 20 major peaks detected, retention in millilitres (mL) and area. The highest area under the curve was 762.7240 mAU*mL at a retention volume of 23.22 mL. Therefore the fractions 5, 6, 7, 8 and C were selected for further analysis as these include the largest fractions and the smallest venom components.

Table 4.3 Major peaks detected during fractionation of *N. nivea* venom by size exclusion chromatography on an AKTA explorer

No	Retention (mL)	Area (mAU*mL)	Height (mAU)
1	0.890	7.72	23.3
2	1.27	7.52	13.7
3	11.8	8.10	34.3
4	12.0	15.0	55.2
5	12.4	51.8	83.5
6	13.0	24.7	52.2
7	13.7	7.28	22.6
8	17.7	64.6	75.8
9	21.3	15.9	25.7
10	22.6	213	421
11	23.1	157	532
12	23.2	763	730
13	26.8	140	196
14	32.8	7.10	13.7
15	33.7	85.4	71.9
16	37.2	18.8	29.5
17	38.4	10.3	26.2
18	38.6	9.56	25.6
19	39.0	13.2	22.8
20	39.7	13.8	18.6

4.4.1 PAGE *Naja nivea* venom fractions

Fractions 5, 6, 7, 8 and C were run on native PAGE to establish an approximate molecular weight of the venom proteins and peptides in each fraction (Figure 4.14). In all the fractions the darkest stained bands were below 9 kDa. It is evident that in fraction 5, the bands 41 kDa and 22 kDa range are not present in any of the other fractions. Fraction 6 and fraction C have one band that migrated separately from the 9 kDa cluster that is not present in the other fractions (indicated red arrows in Figure 4.14).

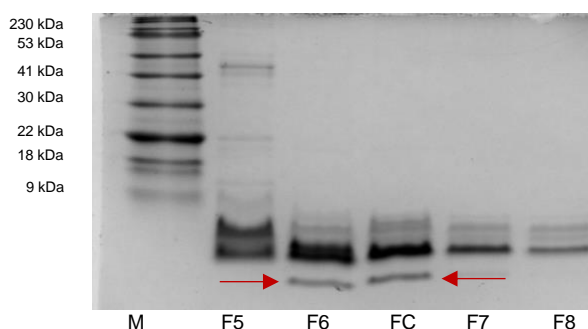


Figure 4.14 Native page protein profile of *N. nivea* venom fractions obtained by size exclusion chromatography

4.4.2 HR-LC-MS/MS of *Naja nivea* venom fractions

Fractions 5, 6, 7, 8 and fraction C were run on HR-LC-MS/MS to identify the proteins and peptides in each fraction. A total of 43 proteins were identified in the partially purified venom fractions. The molecular weight range of the venom proteins were 436 kDa – 7 kDa. Table 4.4 shows all the identified proteins, the fractions in which they occurred (this can be found in the present/absent (P/A) column) and protein identification and percentage of total spectra. For a protein to be positively identified in a fraction, the Scaffold protein identification probability score was above 95% and the protein contained 2 or more unique peptides. The percentage of total spectra was used as an approximate measure of quantification of the protein. Overall, the most abundant toxin family present in the venom fractions were cytotoxins. Less abundant toxin families include snake venom metalloproteinases, cysteine-rich venom proteins, snake venom serine proteases and cobra venom factors.

The species specific toxins from *N. nivea*, cytotoxin 1 (3SA1_NAJNI), cytotoxin 2 (3SA2_NAJNI) and cytotoxin 3 (3SA3_NAJNI) were positively detected in all fractions (5, 6, 7, 8 and C). In fraction 5, 31 proteins were identified, 10 of these were cytotoxins. The toxins, cytotoxin 1 (3SA1_NAJNI), cytotoxin 10 (3SAA_NAJHA) and cytotoxin 2 (3SA2_NAJNI, 3SA2_NAJHA) had the highest percentage of total spectra. The venom toxins unique to this fraction, include cobra venom factor (VCO3_NAJKA), cytotoxin 1 (3SA1_NAJNI), cytotoxin 5 (3SA5_NAJHH), endonuclease domain-containing 1 protein (V8N4Y2_OPHHA), snake venom metalloproteinase-disintegrin-like mocarhagin (VM3M1_NAJMO), zinc metalloproteinase-disintegrin-like atragin (VM3H_NAJAT) and zinc metalloproteinase-disintegrin-like atrase-B (VM3B_NAJAT).

Unique toxins that were only identified from Fraction 6 were cytotoxin 1a (3SA1A_NAJAT) and weak toxin CM-2a (3SOK2_NAJHA). The other proteins identified from this fraction were non-toxic. Cytotoxin 2 (3SA2_NAJHA) was the only unique protein detected in fraction 7. The other proteins identified in fraction included weak toxin S4C113 (NO2B_NAJME), snake venom 5'-nucleotidase (Fragment) (V5NTD_NAJAT), cysteine-rich venom protein natrin-1 (CRVP1_NAJAT, cytotoxin homolog (3SOFH_NAJKA), cytotoxin 1 (3SA1_NAJNI), cytotoxin 10 (3SAA_NAJHA), cytotoxin 2 (3SA2_NAJNI, 3SA2_NAJHA), cytotoxin 3 (3SA3_NAJNI), cobra venom factor (VCO3_NAJKA), Histone H4 (Fragment) (V8PGJ1_OPHHA), Keratin, type II cytoskeletal 1 (Fragment) (V8NYV8_OPHHA), endonuclease domain-containing 1 protein (Fragment) (V8NCE3_OPHHA), Peptidase S1 domain-containing protein (Fragment) (V8N4Y3_OPHHA) and cationic trypsin-3 (Fragment) (V8N4Z1_OPHHA).

No unique proteins were identified in Fraction 8. This fraction consists of cytotoxins 1, 2, 3 and 10, the snake venom serine proteases, peptidase S1 domain-containing protein (Fragment) and Cationic trypsin-3 (Fragment) and the non-toxic protein Keratin, type II cytoskeletal 1 (Fragment) and IF rod domain-containing protein (Fragment). All of these proteins were also identified in fractions 5, 6, 7 and C.

Table 4.4 Proteins identified in *N. nivea* venom fractions 5, 6, 7, 8 and C with protein identification probability and percentage of total spectra

UniProt Accession Number	Protein family	Identified Proteins	Homology with protein from	MW	P/A	Protein identification probability					Percentage of total spectra (%)				
						5	6	7	8	C	5	6	7	8	C
3SOK2_NAJHA	3FTX	Weak toxin CM-2a	<i>Naja annulifera</i>	7 kDa	6	0	100%	0	0	96%	0	0.025	0	0	0.015
3NO2B_NAJME	3FTX	Weak toxin S4C11	<i>Naja melanoleuca</i>	7 kDa	6 7	100%	100%	100%	100%	100%	0.036	0.10	0.15	0.17	0.091
V5NTD_NAJAT	5'-NUC	Snake venom 5'-nucleotidase (Fragment)	<i>Naja atra</i>	58 kDa	5 7 C	100%	100%	100%	0	100%	0.36	0.008 4	0.13	0	0.030
V8NYW9_OPHH A	5'-NUC	5'-nucleotidase (Fragment)	<i>Ophiophagus hannah</i>	28 kDa	5	96%	0	8%	0	0	0.12	0	0.056	0	0
V8N8G6_OPHHA	ACT	Uncharacterized protein (Fragment)	<i>Ophiophagus hannah</i>	40 kDa	6 C	100%	100%	100%	100%	100%	0.012	0.034	0.019	0.035	0.030
V8P2P2_OPHHA	BC	Junction plakoglobin	<i>Ophiophagus hannah</i>	83 kDa	6	59%	100%	0	41%	0	0.00	0.050	0	0.00	0
CRVP2_NAJAT	CRISP	Cysteine-rich venom protein natrin-2	<i>Naja atra</i>	26 kDa	5 6 C	100%	100%	78%	51%	100%	0.097	0.050	0.019	0.035	0.091
CRVP1_NAJAT	CRISP	Cysteine-rich venom protein natrin-1	<i>Naja atra</i>	27 kDa	5 7 C	100%	100%	100%	98%	100%	0.39	0.008 4	0.037	0.035	0.060
C1JZW4_OPHHA	CRISP	Opharin	<i>Ophiophagus hannah</i>	26 kDa	6 C	90%	98%	66%	40%	96%	0.085	0.042	0.019	0.035	0.075
3SA1_NAJPA	CTX	Cytotoxin 1	<i>Naja pallida</i>	7 kDa	5	98%	50%	31%	16%	16%	0.061	0.034	0.019	0.035	0.015
3SA5_NAJHH	CTX	Cytotoxin 5	<i>Naja haje</i>	7 kDa	5	100%	79%	69%	56%	71%	0.13	0.084	0.019	0.035	0.045
3SA4_NAJAT	CTX	Cytotoxin 4	<i>Naja atra</i>	9 kDa	6	99%	98%	0	0	0	0.012	0.017	0	0	0
3SA1A_NAJAT	CTX	Cytotoxin 1a	<i>Naja atra</i>	9 kDa	6	99%	100%	100%	0	100%	0.024	0.034	0.019	0	0.015
3SA5_NAJAT	CTX	Cytotoxin 5	<i>Naja atra</i>	9 kDa	5 6	100%	100%	100%	0	100%	0.17	0.050	0.074	0	0.060
3SOFH_NAJKA	CTX	Cytotoxin homolog	<i>Naja kaouthia</i>	7 kDa	5 6 7	100%	100%	100%	86%	0	0.061	0.042	0.074	0.00	0
3SA1_NAJNI	CTX	Cytotoxin 1	<i>Naja nivea</i>	7 kDa	5 6 7 8 C	100%	100%	100%	100%	100%	2.6	0.75	0.87	1.1	0.80

3SAA_NAJHA	CTX	Cytotoxin 10	<i>Naja annulifera</i>	7 kDa	5 6 7 8 C	100%	100%	100%	99%	99%	2.6	0.74	0.84	1.0	0.79
3SA2_NAJNI	CTX	Cytotoxin 2	<i>Naja nivea</i>	7 kDa	5 6 7 8 C	100%	100%	100%	100%	100%	2.4	2.4	3.3	2.8	2.4
3SA2_NAJHA	CTX	Cytotoxin 2	<i>Naja annulifera</i>	7 kDa	5 6 7 8 C	100%	100%	100%	100%	100%	2.5	2.4	3.3	2.7	2.4
3SA3_NAJNI	CTX	Cytotoxin 3	<i>Naja nivea</i>	7 kDa	5 6 7 8 C	100%	100%	100%	100%	100%	0.74	0.41	0.48	0.31	0.15
3SA4_NAJHA	CTX	Cytotoxin 4	<i>Naja annulifera</i>	7 kDa	5 6 C	100%	100%	25%	41%	100%	0.22	0.11	0.00	0.00	0.060
3SA3_NAJMO	CTX	Cytotoxin 3	<i>Naja mossambica</i>	7 kDa	6 C	0	100%	91%	5%	100%	0	0.025	0.00	0.00	0.030
VCO3_NAJKA	CVF	Cobra venom factor	<i>Naja kaouthia</i>	185 kDa	5 7	100%	96%	100%	0	92%	0.22	0.00	0.056	0	0.00
VM3H_NAJAT	SVMP	Zinc metalloproteinase-disintegrin-like atragin	<i>Naja atra</i>	69 kDa	5	100%	100%	95%	0	0	0.24	0.008	0.019	0	0
VM3M1_NAJMO	SVMP	Snake venom metalloproteinase-disintegrin-like mocarhagin	<i>Naja mossambica</i>	68 kDa	5	100%	93%	0	0	0	0.27	0.008	0	0	0
VM3_NAJKA	SVMP	Zinc metalloproteinase-disintegrin-like cobrin	<i>Naja kaouthia</i>	68 kDa	5	100%	51%	0	0	0	0.17	0.00	0	0	0
VM3B_NAJAT	SVMP	Zinc metalloproteinase-disintegrin-like atrase-B	<i>Naja atra</i>	66 kDa	5	100%	0	0	0	0	0.085	0	0	0	0
V8P395_OPHHA	GPX	Glutathione peroxidase (Fragment)	<i>Ophiophagus hannah</i>	30 kDa	5 6 C	100%	100%	100%	0	100%	0.097	0.042	0.019	0	0.030
V8PB36_OPHHA	GTP	Elongation factor 1-alpha	<i>Ophiophagus hannah</i>	50 kDa	6	100%	100%	93%	98%	100%	0.012	0.017	0.00	0.035	0.015
V8PGJ1_OPHHA	HIS	Histone H4 (Fragment)	<i>Ophiophagus hannah</i>	21 kDa	5 6 7 C	100%	100%	100%	90%	100%	0.024	0.034	0.056	0.00	0.045

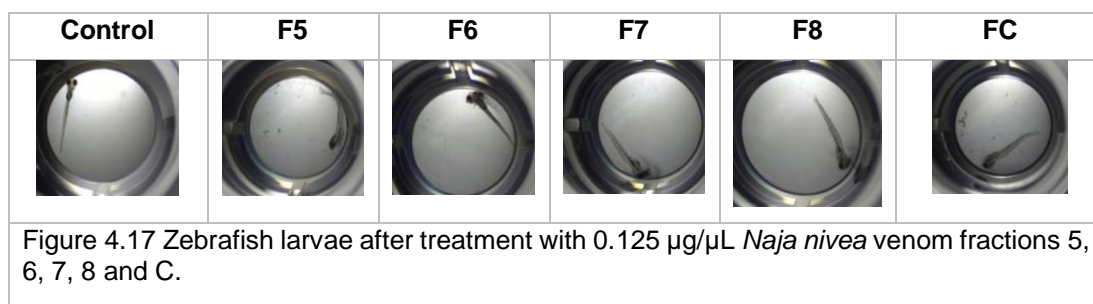
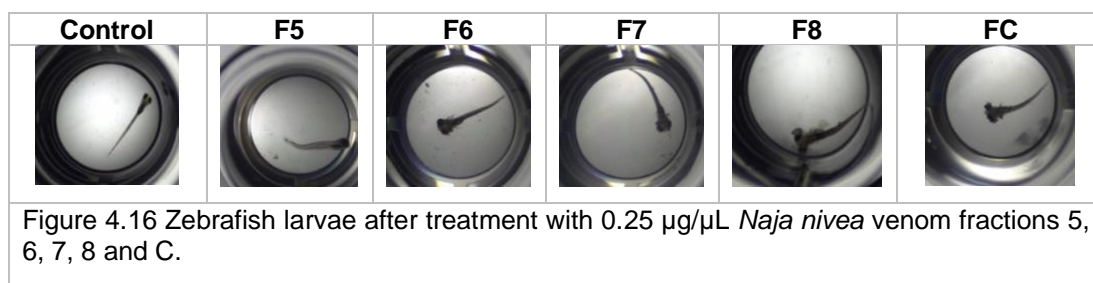
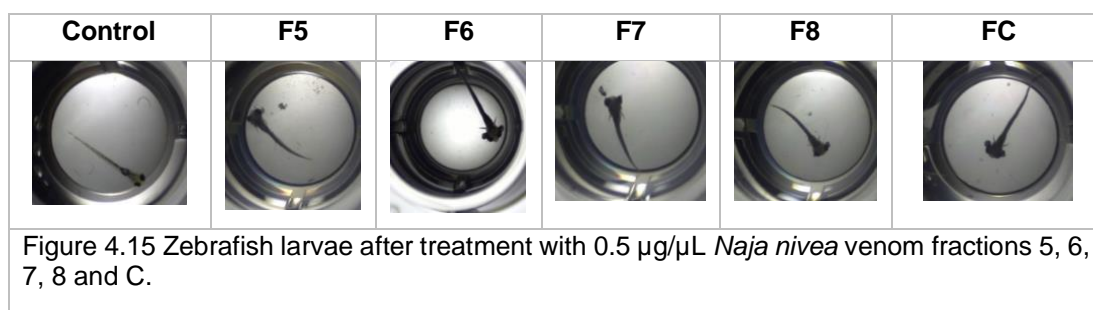
V8P8L1_OPHHA	IF	Keratin, type I cytoskeletal 19 (Fragment)	<i>Ophiophagus hannah</i>	436 kDa	6	100%	100%	44%	67%	0	0.012	0.059	0.00	0.00	0
V8NSX6_OPHHA	IF	Keratin, type I cytoskeletal 14	<i>Ophiophagus hannah</i>	103 kDa	6	12%	98%	0	9%	0	0.00	0.042	0	0.00	0
V8NBM9_OPHHA	IF	Keratin, type II cytoskeletal 5	<i>Ophiophagus hannah</i>	38 kDa	6	0	100%	0	100%	98%	0	0.025	0	0.035	0.015
V8NYV8_OPHHA	IF	Keratin, type II cytoskeletal 1 (Fragment)	<i>Ophiophagus hannah</i>	241 kDa	5 6 7 8 C	100%	100%	100%	100%	100%	0.073	0.10	0.11	0.17	0.075
V8NRX1_OPHHA	IF	IF rod domain-containing protein (Fragment)	<i>Ophiophagus hannah</i>	52 kDa	5 6 8 C	100%	100%	44%	98%	99%	0.049	0.084	0.037	0.070	0.030
V8N4Y2_OPHHA	NUC	Endonuclease domain-containing 1 protein	<i>Ophiophagus hannah</i>	18 kDa	5	100%	0	96%	71%	94%	0.11	0	0.019	0.00	0.015
V8NCE3_OPHHA	NUC	Endonuclease domain-containing 1 protein (Fragment)	<i>Ophiophagus hannah</i>	51 kDa	5 7	100%	0	100%	98%	26%	0.049	0	0.056	0.035	0.015
V8N4Y3_OPHHA	SVSP	Peptidase S1 domain-containing protein (Fragment)	<i>Ophiophagus hannah</i>	9 kDa	5 6 7 8 C	100%	100%	100%	100%	100%	0.16	0.14	0.26	0.21	0.14
V8N4Z1_OPHHA	SVSP	Cationic trypsin-3 (Fragment)	<i>Ophiophagus hannah</i>	34 kDa	5 6 7 8 C	100%	100%	100%	100%	100%	0.049	0.10	0.20	0.14	0.11
A8QL55_OPHHA	CVF	Complement-depleting factor	<i>Ophiophagus hannah</i>	184 kDa	5	100%	0	36%	0	81%	0.073	0	0.037	0	0.00
V8NEU2_OPHHA	VES	B30.2/SPRY domain-containing protein	<i>Ophiophagus hannah</i>	25 kDa	5	100%	93%	84%	0	47%	0.16	0.017	0.037	0	0.015
VESP_NAJKA	VES	Thaicobrin	<i>Naja kaouthia</i>	12 kDa	5 6	98%	100%	76%	0	39%	0.15	0.025	0.037	0	0.015
NGFV2_NAJSP	VNGF	Venom nerve growth factor 2	<i>Naja sputatrix</i>	27 kDa	5 C	100%	60%	100%	0	100%	0.073	0.00	0.019	0	0.030

Abbreviations: P/A, presence / absence; MW, molecular weight; 3FTX, three finger toxin; 5' NUC, snake venom 5'-nucleotidase; ACT, actin; BC, beta-catenin family; CRISP, Cysteine-rich venom protein; CTX, cytotoxin; CVF, cobra venom factor; SVMP, snake venom metalloproteinase; GPX, glutathione peroxidase; GTP, translocation GTPase family; HIS, histone; IF, intermediate filament; NUC, nucleotidase; SVSP, snake venom serine protease; VES, vesprin; VNGF, venom nerve growth factor. UniProt alpha numerical accession number allocated to each identified protein on the UniProt database

4.5 Toxicity assay

4.5.1 Establish treatment concentration

The working concentration of venom fractions was established by exposure of <5 day post fertilisation (dpf) larvae to different concentrations of *Naja nivea* venom. The larvae were treated with fractions 5, 6, 7, 8 and C at concentrations 0.5 µg/µL, 0.25 µg/µL and 0.125µg/µL. Across all concentrations within 1 minute of being treated, no heartbeat was detected in any of the larvae. In Figure 4.15, Figure 4.16 and Figure 4.17 the effects of each venom fraction at three different lethal concentrations can be seen in a larva representative of the treatment group. The degree of body malformation seemed dose-dependent, with the higher concentrations showing more severe C-shaped curvature. However this observation was qualitative only.



The most significant features that were observed were oedematous enlarged eyes, flared gills and flaking of the larval body (Figure 4.18). The same features were observed to varying degrees in all treatment concentrations.

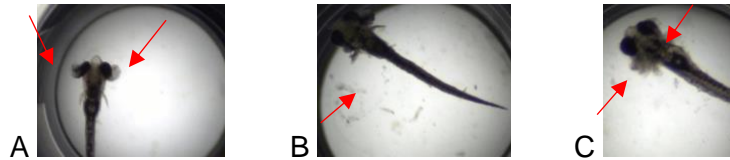
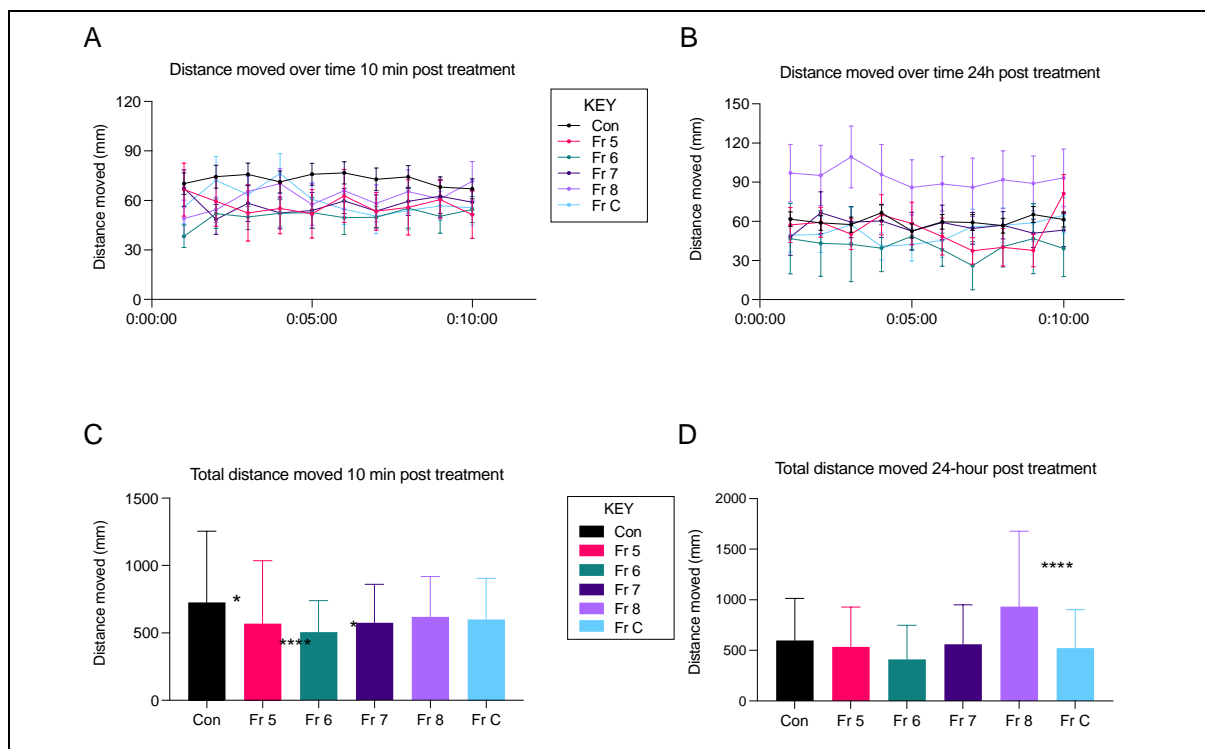


Figure 4.18 Significant toxic effects of *N. nivea* venom fractions observed in zebrafish larva include oedematous enlarged eyes (A), flaking of the skin body (B) and flared gills (C)

4.5.2 Sub-lethal venom treatment acute - 24 hour response

Zebrafish larvae 3 dpf were treated with 0.01 $\mu\text{g}/\mu$ venom fractions. Behavioural tracking was done in the Noldus Daniovision activity tracker after 10 minutes (acute) exposure to venom fractions and 24-hour after exposure. Figure 4.19 shows the locomotor activity of the zebrafish larvae based on the recorded distance moved (expressed as mm/min bins) after treatment with *N. nivea* venom after 10 minutes (A) and measured again after 24-hours (B). Figure 4.19 C and D show the accumulative distance moved per treatment group over the locomotor assay acutely time at 10 minutes (C) and 24-hours (D) after treatment. Activity data were acquired at a rate of 25 frames per second and binned into 1-minute bins for statistical purposes. Figure 4.19 E and F shows the stacked locomotor track visualisation pattern for each treatment group at both assay time points, acute and after 24-hours.



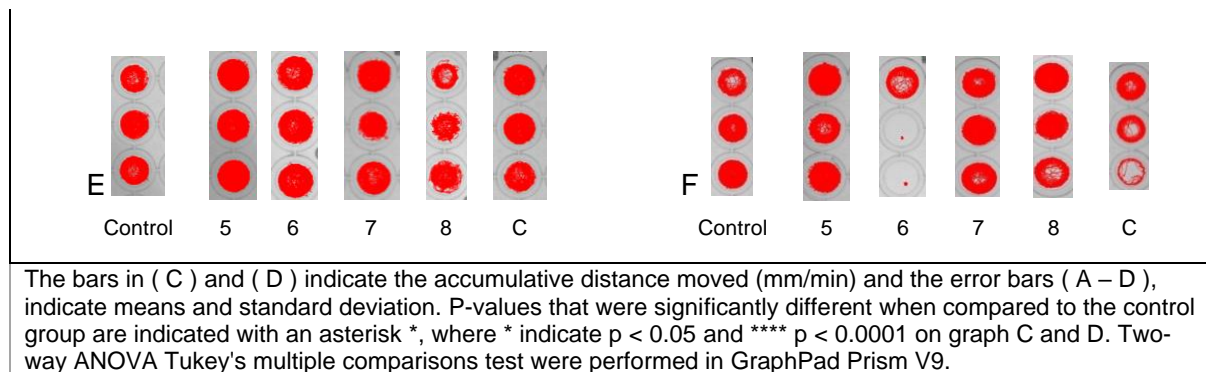
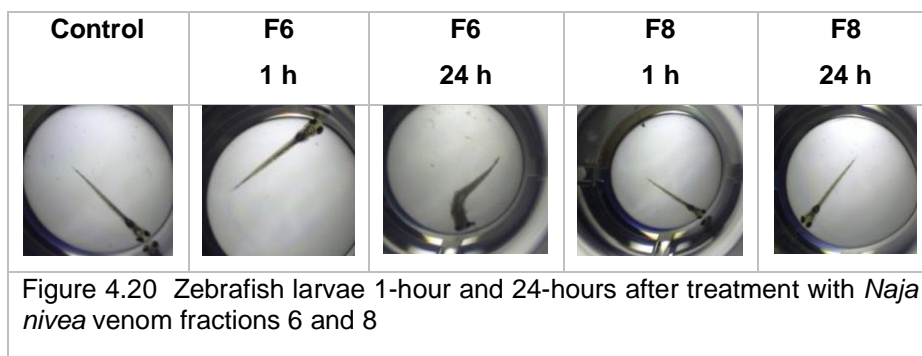


Figure 4.19 Distance moved (mm/min) by zebrafish larvae over a 10-minute observation period, acute after treatment (A) and 24-hours after treatment (B) tracked by Daniovision. Accumulative distance moved per treatment group acute (C) and 24-hours (D) post-treatment. Stacked locomotor track visualisation pattern for each treatment group, acute (E) and 24-hours after treatment (F).

Acutely, the locomotor behaviour of zebrafish larvae treated with fraction 5, 6 and 7 were significantly lower than the control group ($p < 0.05$) Figure 4.19 (A and C). The largest difference in locomotor activity compared to the control group was in the group treated with fraction 6 Figure 4.19 (A and C). No significant difference was observed when comparing the different treatment groups. Daniovision results 24 hours post treatment showed higher locomotor activity in treatment group 8 (purple on Figure 4.19 B and D), compared to the control and other treatment groups.

Figure 4.20 shows light microscopy images captured of the larvae treatment groups that showed statistically significant changes in their locomotor behaviour at 10 minutes and 24-hours after treatment. Although no signs of toxicity based on morphology were observed in the larvae at the acute time point, the larvae treated with fraction 6 showed significant toxicity (body C-shaping) after 24-hours, suggesting that the decrease activity at the immediate time point was already due to envenomation. After 24-hours, 75% of the treatment group had no detectable heartbeat and all the larvae showed a C-shaped curvature in the body. In contrast, a 100% survival rate were observed in the larvae treated with fraction 8, despite their increased activity which also suggested sensitivity to fraction 8. Figure 4.20 shows one larvae representative of each treatment group at time points, 1-hour and 24-hours post treatment.



4.6 LC-MS/MS

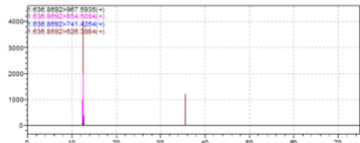
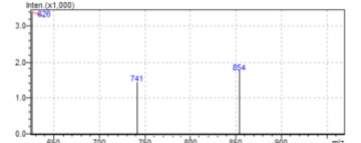
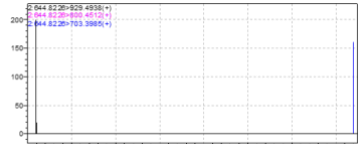
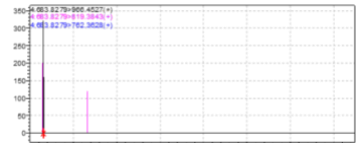
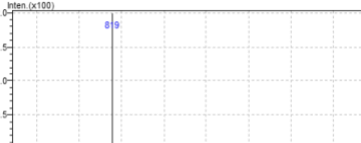

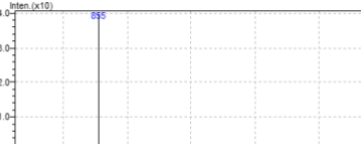
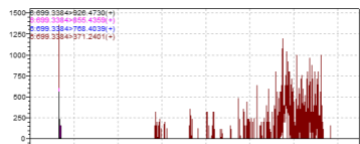
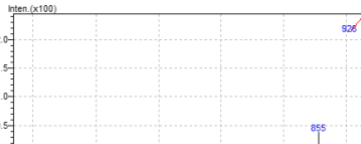
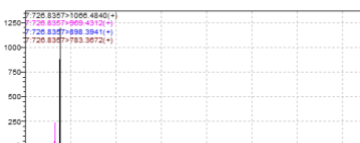
4.6.1 iRT Standard

Detection of the iRT standard peptides provided confirmation for the approach to triple quadrupole LC-MS/MS method development for venom toxins. Table 4.5 shows a summary of the LC-MS/MS results of iRT peptides. There were 8 multiple reaction monitoring transitions generated for the iRT. Peptides 1, 6, 7 and 8 were successfully detected. Peptides 2, 4 and 5 were detected at very low intensities and peptide 3 was undetected.

4.6.2 *N. nivea* venom spiked in human plasma

The multiple reaction monitoring transition list containing the venom toxins cytotoxin 1 (P01456), cytotoxin 10 (P01453) and cytotoxin 3 (P01459) unique to *N. nivea* species contained 42 transitions, generated by Skyline (MacLean et al., 2010) with HR-LC-MS/MS data. A total load of 10 ug of material was injected in 10 µL. Table 4.6 contains the complete multiple reaction monitoring peptide transition list for the detection of the snake venom toxins from human plasma. Transitions 1 - 14 were for *N. nivea* venom toxin cytotoxin 1, transitions 15 – 28 for cytotoxin 3 and transitions 29 – 42 for cytotoxin 10. In Table 4.6 the first column indicate the peptide number and sample. Peptide 1, row V shows the chromatogram and retention time of detection for the toxin when spiked into plasma and prepared by three different tryptic digestion protocols. The toxin was detected at the highest intensity of 11561 counts per second (cps) from the sample prepared by protocol 1, the traditional 18-hour tryptic digestion. The samples prepared by the accelerated digestion protocols detected the peptide at an intensity of 6320 cps using the tryptic digestion protocol 2 that includes a heat treatment step, and a maximum intensity of 960 cps for samples prepared by protocol 3, digestion with a high ratio of trypsin to substrate. The cytotoxins 1 and 10 yielded positive results, cytotoxin 3 transitions were not detected and were indistinguishable from blank plasma. The intensities were too low for positive identification.

Table 4.5 Summary of the iRT standard multiple reaction monitoring transitions

ID#	Peptide Name	Product ion mass (m/z)	Ret. Time	Chromatogram (10x dilution)	Product ion spectrum
1	GTFIIDPAAVIR_light	636.8692>967.5935	15.000		
2	GAGSSEPVTGLDAK_light	644.8226>929.4938	15.000		
3	TPVISGGPYEYR_light	669.8381>1237.6212	2.063	Not detected	
4	VEATFGVDESSNAK_light	683.8279>966.4527	2.165		
5	TPVITGAPYEYR_light	683.8537>1265.6525	19.733		
6	DGLDAASYAPVR_light	699.3384>926.4730	34.233		
7	ADVTPADFSEWSK_light	726.8357>1066.4840	71.429		

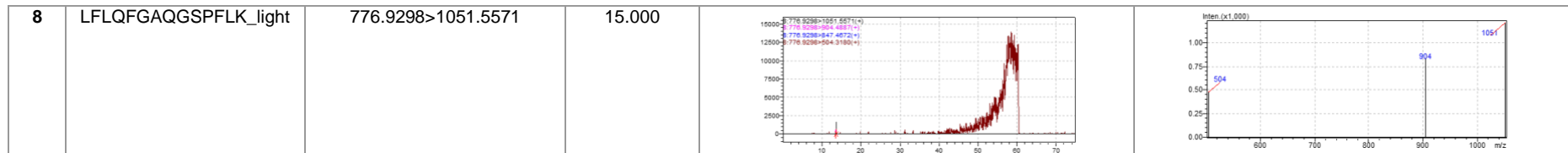
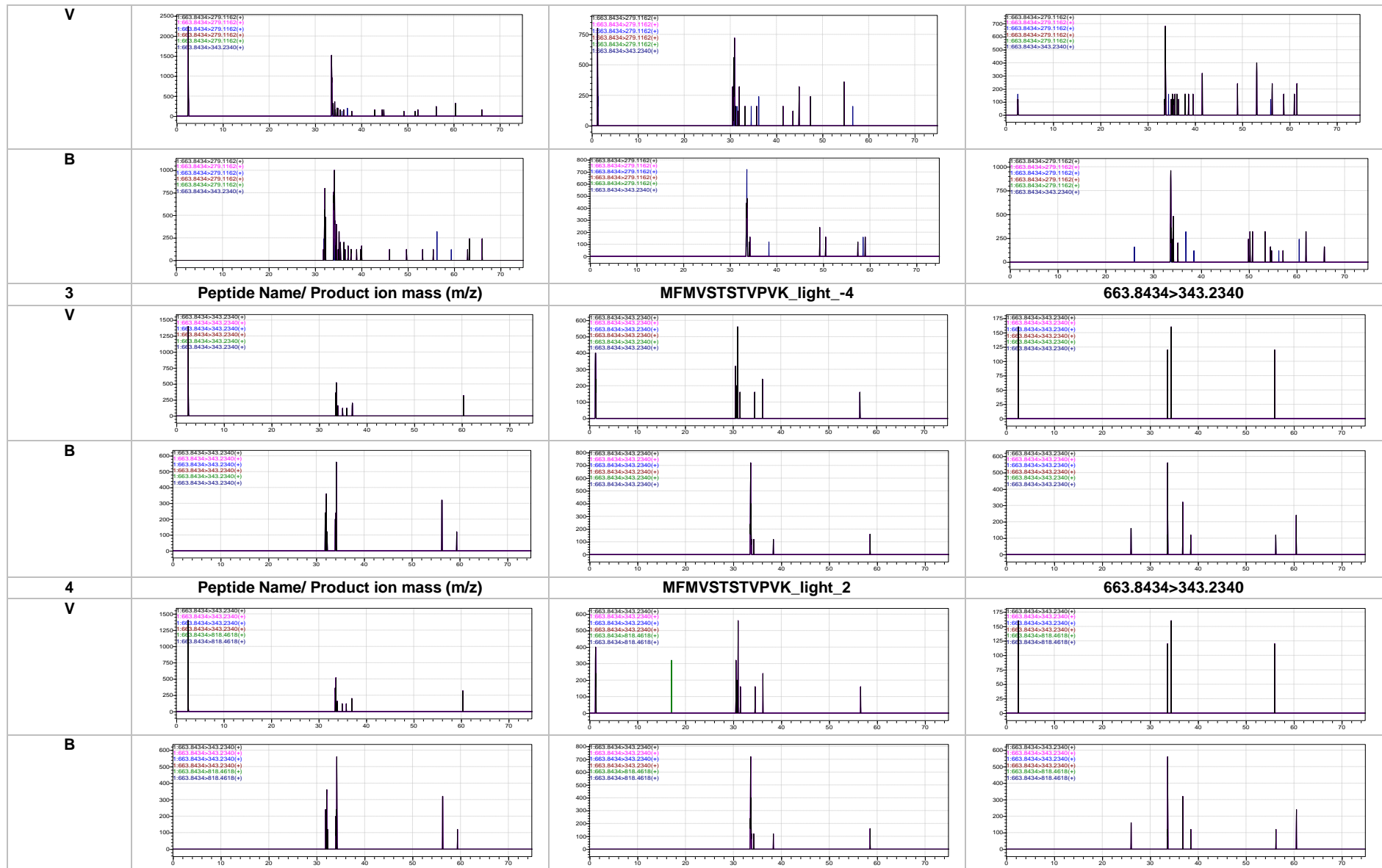
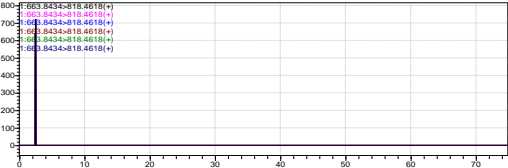
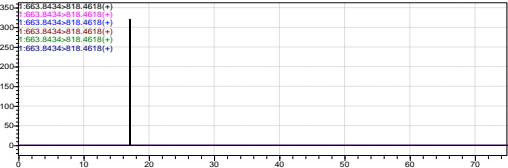
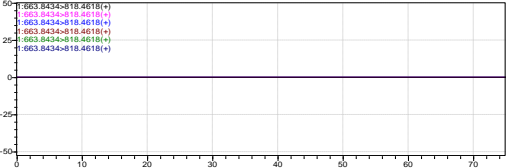
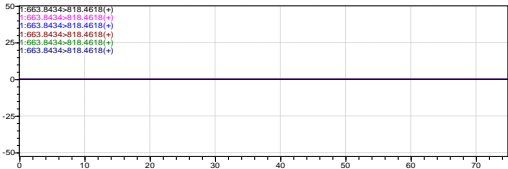
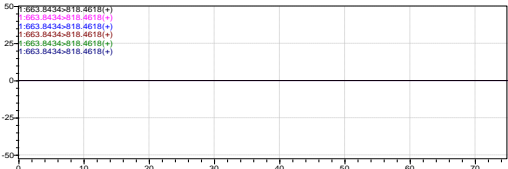
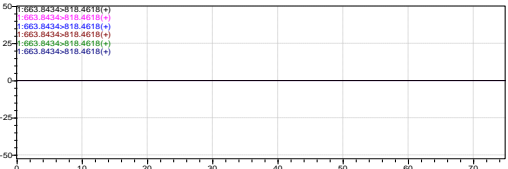
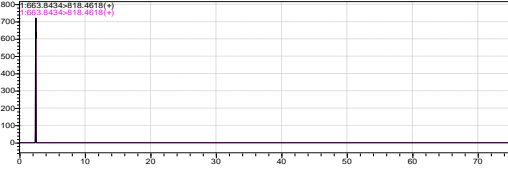
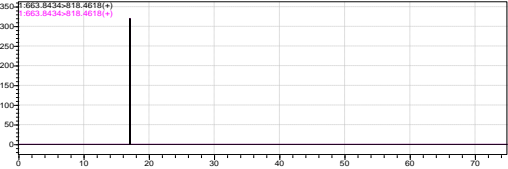
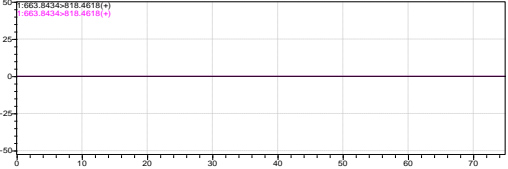
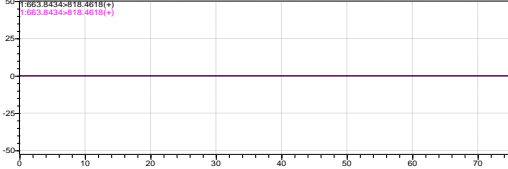
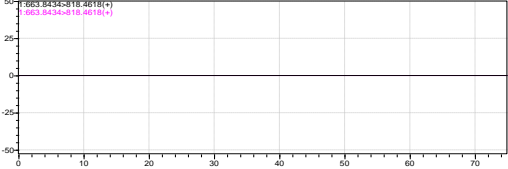
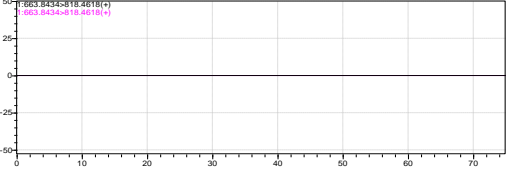
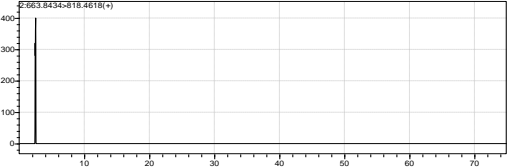
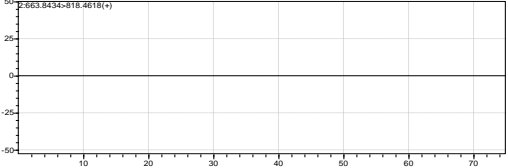
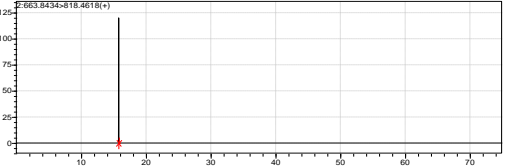


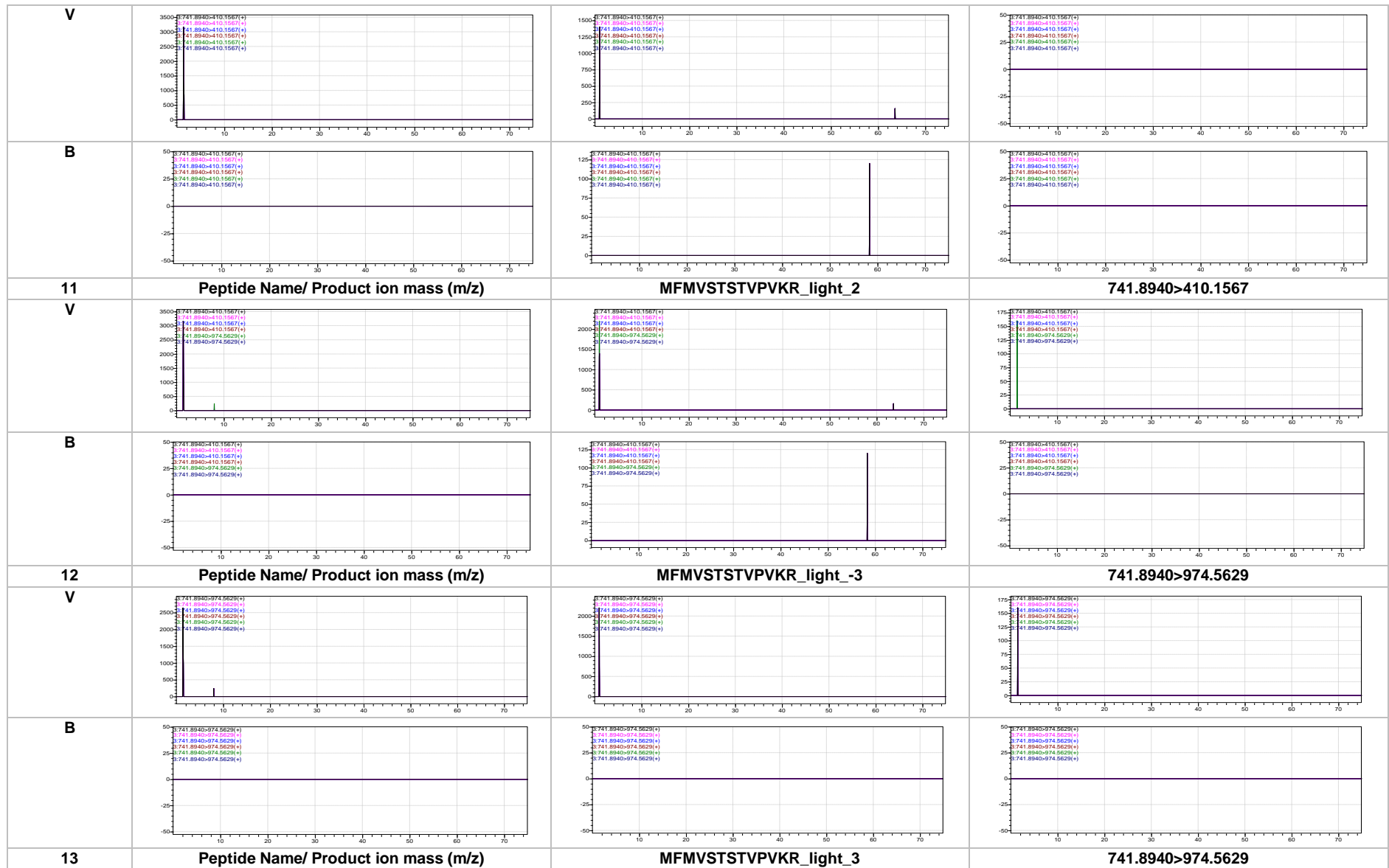
Table 4.6 Multiple reaction monitoring transitions for a shot gun approach of cytotoxin 1, cytotoxin 3 and cytotoxin 10 from human plasma spiked with *N. nivea* venom (V) and unspiked human plasma (B), prepared by three different tryptic digestion protocols (18 h, 50 mm ABC, 100 mm ABC)

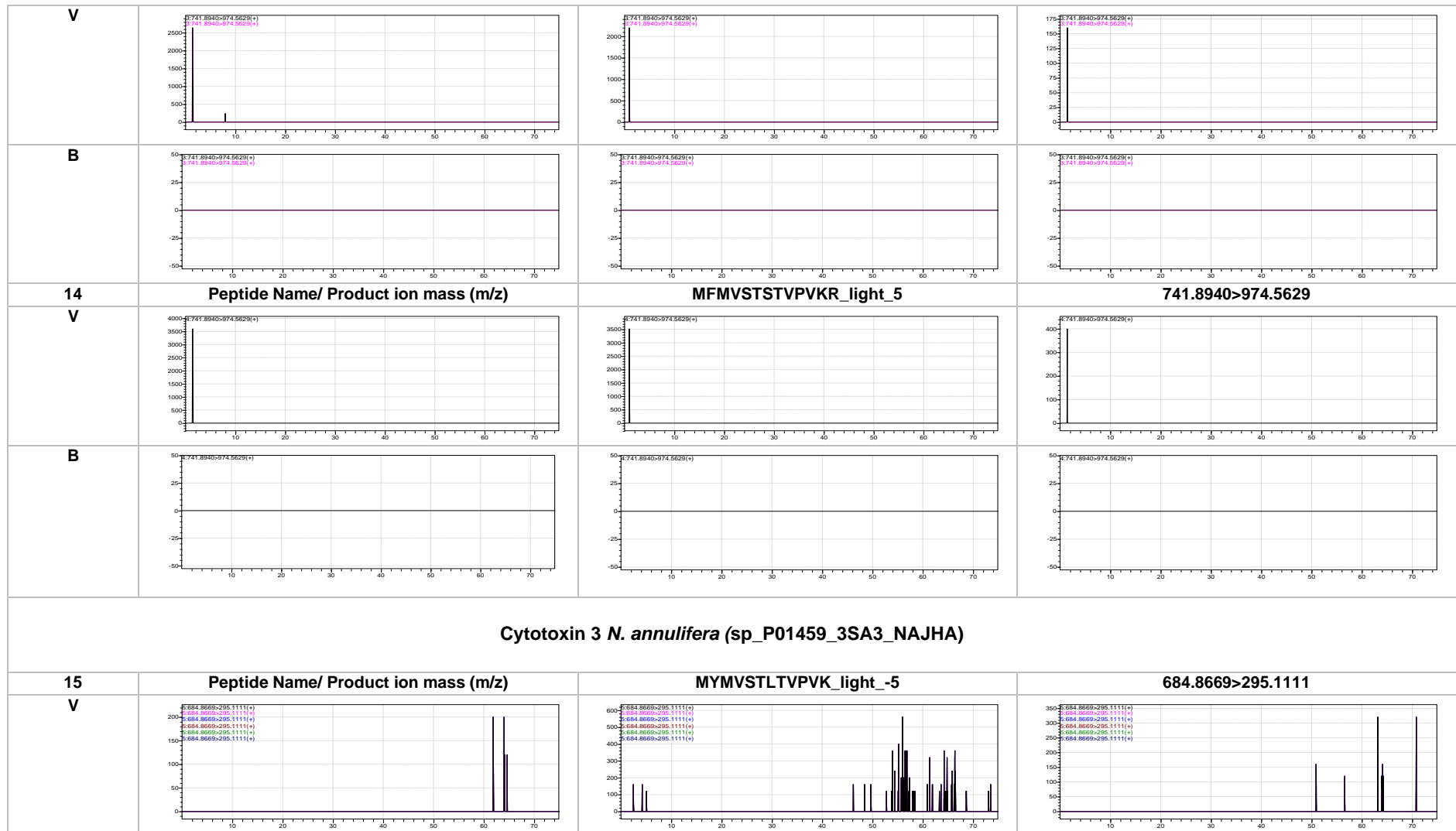
ID#/Sample	Chromatogram (1µg/µL)		
	18h	50 mm ABC	100 mm ABC
Cytotoxin 1 <i>N. nivea</i> (sp_P01456_3SA1_NAJNI)			
1 V	<p style="text-align: center;">Peptide Name/ Product ion mass (m/z) Maximum intensity: 11561</p>	<p style="text-align: center;">MFMVSTSTVPVK_light_-5 Maximum intensity: 6320</p>	<p style="text-align: center;">663.8434>279.1162 Maximum intensity: 960</p>
B	<p style="text-align: center;">Maximum intensity: 2440</p>	<p style="text-align: center;">Maximum intensity: 1200</p>	<p style="text-align: center;">Maximum intensity: 1480</p>
2	<p style="text-align: center;">Peptide Name/ Product ion mass (m/z)</p>	<p style="text-align: center;">MFMVSTSTVPVK_light_1</p>	<p style="text-align: center;">663.8434>279.1162</p>



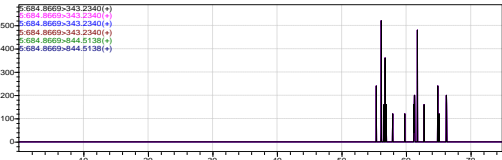
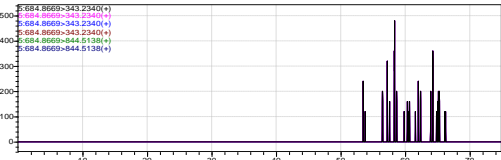
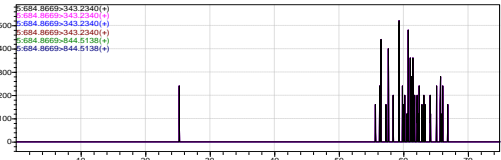
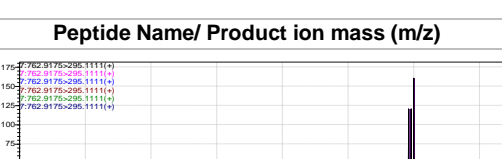

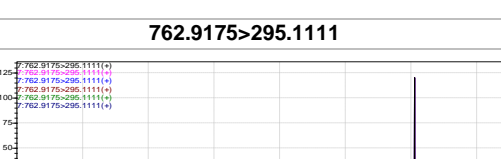
<p>5</p> <p>V</p>	<p>Peptide Name/ Product ion mass (m/z)</p> 	<p>MFMVSTSTVPVK_light_-3</p> 	<p>663.8434>818.4618</p> 
<p>B</p>			
<p>6</p>	<p>Peptide Name/ Product ion mass (m/z)</p>	<p>MFMVSTSTVPVK_light_3</p>	<p>663.8434>818.4618</p>
<p>V</p>			
<p>B</p>			
<p>7</p>	<p>Peptide Name/ Product ion mass (m/z)</p>	<p>MFMVSTSTVPVK_light_5</p>	<p>663.8434>818.4618</p>
<p>V</p>			

B			
8	Peptide Name/ Product ion mass (m/z)	MFMVSTSTVPVKR_light_-5	741.8940>279.1162
V			
B			
9	Peptide Name/ Product ion mass (m/z)	MFMVSTSTVPVKR_light_1	741.8940>279.1162
V			
B			
10	Peptide Name/ Product ion mass (m/z)	MFMVSTSTVPVKR_light_-4	741.8940>410.1567



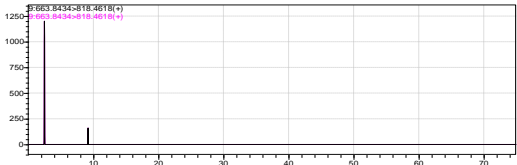
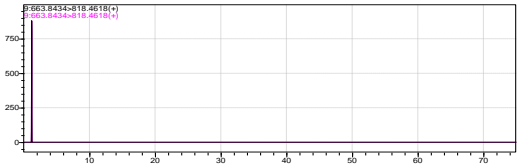
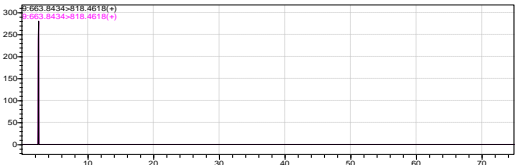
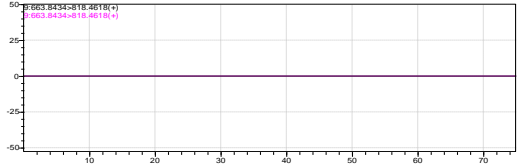
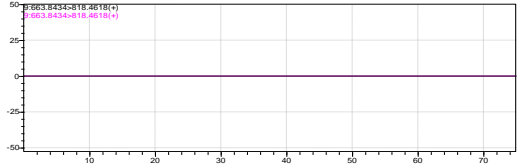
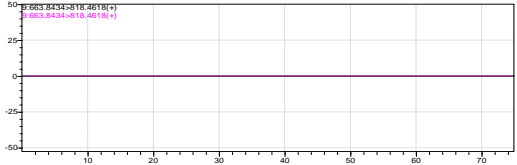
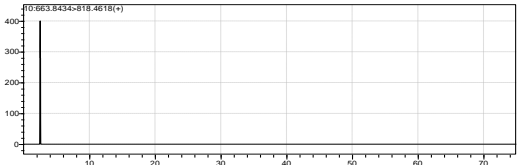
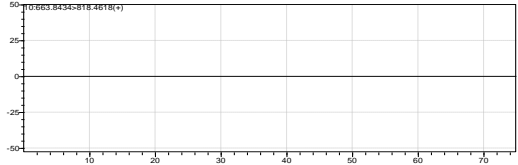
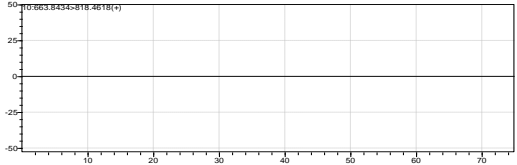
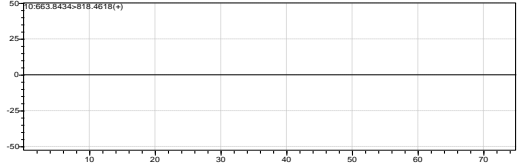
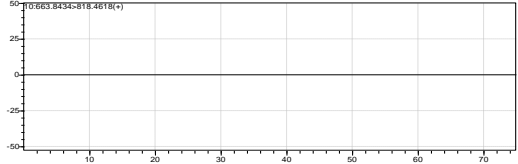
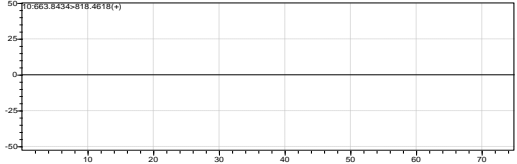
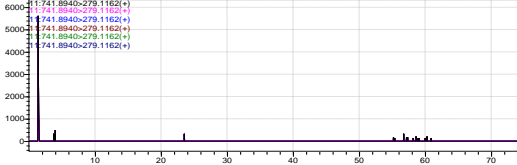
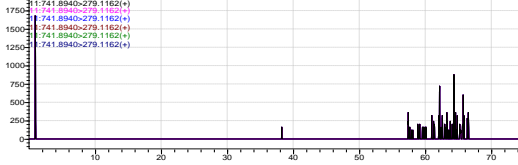
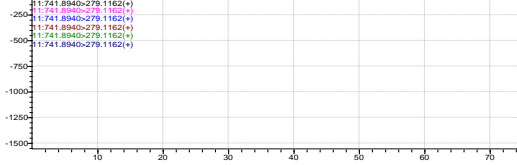
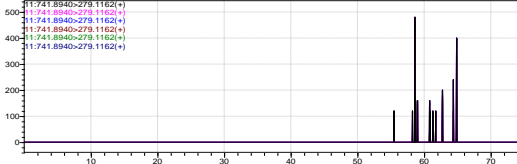
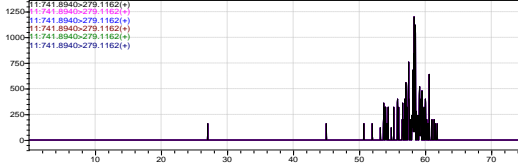
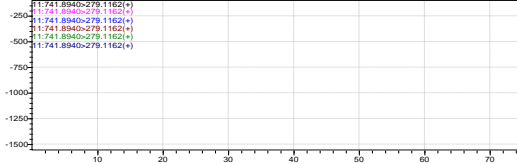




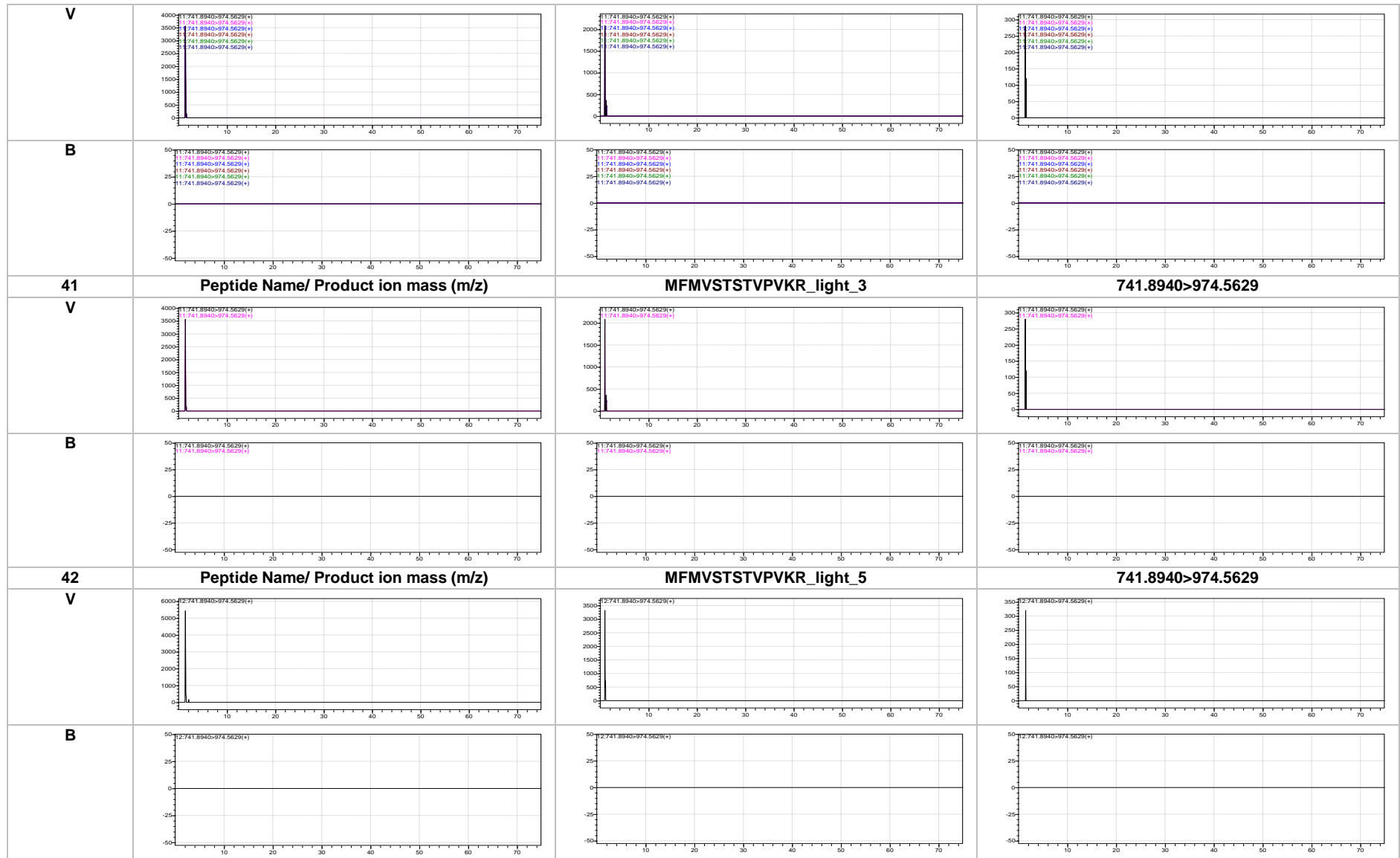
<p>B</p> 	<p>Peptide Name/ Product ion mass (m/z)</p>	 <p>MYMVSTLTPVK_light_-3</p>	 <p>684.8669>844.5138</p>
<p>19</p>		<p>Not detected</p>	
<p>20</p>	<p>Peptide Name/ Product ion mass (m/z)</p>	<p>MYMVSTLTPVK_light_3</p>	<p>684.8669>844.5138</p>
<p>21</p>	<p>Peptide Name/ Product ion mass (m/z)</p>	<p>MYMVSTLTPVK_light_5</p>	<p>684.8669>844.5138</p>
<p>22</p>	<p>Peptide Name/ Product ion mass (m/z)</p>	<p>Not detected</p>	
<p>V</p>	<p>Peptide Name/ Product ion mass (m/z)</p>	<p>MYMVSTLTPVKR_light_-5</p>	<p>762.9175>295.1111</p>
			
<p>B</p>	<p>Peptide Name/ Product ion mass (m/z)</p>	<p>MYMVSTLTPVKR_light_1</p>	<p>762.9175>295.1111</p>
<p>23</p>			
<p>V</p>	<p>Peptide Name/ Product ion mass (m/z)</p>	<p>MYMVSTLTPVKR_light_-4</p>	<p>762.9175>426.1516</p>
<p>B</p>	<p>Peptide Name/ Product ion mass (m/z)</p>	<p>MYMVSTLTPVKR_light_-4</p>	<p>762.9175>426.1516</p>
<p>24</p>			

		Not detected	
25	Peptide Name/ Product ion mass (m/z)	MYMVSTLTPVKR_light_2	762.9175>426.1516
		Not detected	
26	Peptide Name/ Product ion mass (m/z)	MYMVSTLTPVKR_light_-3	762.9175>1000.6150
		Not detected	
27	Peptide Name/ Product ion mass (m/z)	MYMVSTLTPVKR_light_3	762.9175>1000.6150
		Not detected	
28	Peptide Name/ Product ion mass (m/z)	MYMVSTLTPVKR_light_5	762.9175>1000.6150
		Not detected	
Cytotoxin 10 <i>N. annulifera</i> (sp_P01453_3SAA_NAJHA)			
29	Peptide Name/ Product ion mass (m/z)	MFMVSTSTVPVK_light_-5	663.8434>279.1162
V			
B			
30	Peptide Name/ Product ion mass (m/z)	MFMVSTSTVPVK_light_1	663.8434>279.1162
V			
B			
31	Peptide Name/ Product ion mass (m/z)	MFMVSTSTVPVK_light_-4	663.8434>343.2340

V			
B			
32	Peptide Name/ Product ion mass (m/z)	MFMVSTSTVPVK_light_2	663.8434>343.2340
V			
B			
33	Peptide Name/ Product ion mass (m/z)	MFMVSTSTVPVK_light_-3	663.8434>818.4618
V			
B			
34	Peptide Name/ Product ion mass (m/z)	MFMVSTSTVPVK_light_3	663.8434>818.4618

V			
B			
35	Peptide Name/ Product ion mass (m/z)	MFMVSTSTVPVK_light_5	663.8434>818.4618
V			
B			
36	Peptide Name/ Product ion mass (m/z)	MFMVSTSTVPVKR_light_-5	741.8940>279.1162
V			
B			
37	Peptide Name/ Product ion mass (m/z)	MFMVSTSTVPVKR_light_1	741.8940>279.1162





CHAPTER 5 Discussion

5.1 Incidence of snakebite in South Africa

Snakebite envenomation is a global health threat causing devastating outcomes to several million people annually. The magnitude of this issue is gravely underestimated due to limited epidemiological data and under reporting of incidences (Halilu et al., 2019; WHO, 2019; Williams et al., 2019a). The analysis of data recorded by the PIHWC showed that in South Africa 44% of the recorded snakebites were inflicted by an unidentified snake. The incidence of snakebite based on the PIHWC call records was 2.39 per 100 000 population (section 2.3.6), this is in line with the extrapolated incidence of snakebite of 2.34 - 3.3 per 100 000 population for sub-Saharan Africa as a whole (Kasturiratne et al., 2008). However, the incidence of snakebite based on extrapolation of antivenom usage from pharmacy records or the amount of snakebite admissions to the emergency department of public hospitals may indicate a higher incidence ratio. For example in this study the incidence of snakebite for Kwazulu-Natal was 2.7 per 100 000, but based on antivenom usage it was 16 per 100 000 (Wood et al., 2016b) and based on admissions to the emergency department of the district's hospital it was 32 per 100 000 (Wood et al., 2016c).

The most medically significant snakebites were caused by *Bitis arietans* and *Naja nivea* species. The high number of bites from *B. arietans* could be due to various factors such as an abundance of these species in South Africa and their hunting behaviour thereby increasing the likelihood of accidental encounters. *B. arietans* is one of the most wide-spread and abundant venomous snake species in Africa and envenomation is characterised by severe cytotoxicity that presents as haemorrhagic disturbances, blistering, swelling and extensive necrosis, whereas envenomation by *Naja nivea* causes flaccid paralysis and respiratory depression, which could cause death if not closely monitored (Muller et al., 2012b; Wang et al., 2020; Warrell et al., 1975). The case studies in section 2.1.2 show that a delayed or incorrect diagnosis can lead to a treatment delay of days, whereas using a quick LC-MS/MS test could provide results in two hours. This study aimed to partially characterise the venoms of the medically important snakes, *B. arietans*, *N. nivea* and *B. atropos*, then identify unique toxins to each species and develop an LC-MS/MS method to detect the identified toxin when spiked into human plasma as part of a larger study which aims to develop rapid and robust point of care diagnostics for envenomation in South Africa.

5.2 Venom analysis by gel electrophoresis

Following separation of crude snake venom proteins by native PAGE, visually unique protein banding ladders were obtained for the species *B. atropos*, *N. nivea* and *B. arietans*. *B. arietans* showed concentrated protein banding in the 25 kDa – 150 kDa molecular weight range, whereas the *N. nivea* crude venom banding was more in the low molecular weight range below 25 kDa, with one prominent band at 50 kDa (Figure 4.1). This banding profile was expected based on studies performed with other elapid venoms including *N. kaouthia*, *N. naja*, *N. haje* (Deka et al., 2019; Mehrdar et al., 2017; Oukkache et al., 2012). The *B. atropos* venom profile was different from both the other two species and the venom proteins were distributed in the molecular weight range 15 kDa – 100 kDa. The protein ladders were expected since species from the Viperid snake family have an abundance of enzymatic proteins and peptides, whereas species from the Elapid families have more non-enzymatic proteins and peptides. The African *N. nivea* species' protein profile differs from the Indian *N. naja* crude venom protein profile in the molecular weight range above 50 kDa (Choudhury et al., 2017). No significant visual differences were displayed by the crude venom profile of venom of *N. nivea* from the Western Cape and *N. nivea* from the Northern Cape (Figure 4.1).

5.3 Qualitative proteomic analysis of *B. atropos*, *N. nivea* and *B. arietans* venoms

Crude venoms from *N. nivea*, *B. arietans* and *B. atropos* were separated by gel electrophoresis, digested with trypsin, and analysed by HR-LC-MS/MS. This revealed highly complex venom proteomes. A total of 504 proteins, belonging to 52 protein families, were positively identified from *B. atropos* venom, 144 proteins from *N. nivea* venom and 182 proteins from *B. arietans* venom. The considerable number of positively identified proteins from *B. atropos* compared to the number of proteins identified in the other two venoms are due to this species' venom being under studied. This is evident from a search result on the UniProt database, when only 15 unreviewed entries were retrieved for four venom proteins in comparison to 25 proteins for *N. nivea* and 229 proteins for *B. arietans*. The major components identified from *B. atropos* venom were snake venom metalloproteases (26%), snake venom serine proteases (21%), phospholipase A2 (10%), snake venom metalloproteinase (9%), L-amino acid oxidases (7%) and cysteine-rich venom protein (5%). The wide geographical distribution of *B. arietans* species and potent cytotoxicity caused to their victims, has led to numerous studies on the venom proteome. Inter-species variation in venom have been reported (Currier et al., 2010). This study led to the positive identification of 182 proteins. The dominant proteins were snake venom metalloproteinases (27%), snake venom serine proteases (26%), snake venom metalloproteinases (11%), L-amino acid oxidases (10%) and phospholipase A2s (6%). The minor proteins were

phosphodiesterase (3%), snake venom 5'-nucleotidase (3%), cobra venom factors (3%), phospholipase A2 inhibitor (3%), natriuretic peptides (2%), vascular endothelial growth factors (2%), cysteine-rich venom protein (1%), phospholipase B (1%), venom nerve growth factor (1%), three finger toxins (1%) and snake venom metalloprotease inhibitor (1%). This is remarkably similar to the proteomic make-up of the *B. arietans* venom from Nigeria investigated by Dingwoke *et al.* 2021 on similar HR-LC-MS/MS instrumentation that was used during this study (Dingwoke *et al.*, 2021). Snake venom metalloproteinase (33%) and serine protease (21%) were the primary components in *N. nivea* crude venom following in-gel proteomic analysis. Even though three-finger toxins (2%) were positively identified after in-gel digestion from the *N. nivea* venom, the overall composition was unusual compared to the mass spectrometry results following HILIC assisted in-solution tryptic digestion MS results of *N. nivea* venom described sections 4.2 and 4.4.2. This could be due to the proteins not being successfully retrieved from the gel under native conditions or that the proteins and peptides were not retained in the gel. The venom profile of *B. atropos* shared venom protein commonalities with both *N. nivea* and *B. arietans* species. This is different from other viperid species' venom which comprise primarily of enzymatic proteins and peptides. This translates from a protein to a physiological level and could contribute to the understanding of the neuro and cytotoxic effects seen in a patient that was bitten by *B. atropos* described in Case three in section 2.1.2.

5.4 Quantitative proteomic analysis of regionally different *N. nivea* venoms

Previous proteomic and transcriptomic studies have shown that snake venom proteins/peptides belong to only a few protein families and that intra-genus and intra-specie variations in venom composition are due to the relative abundance of toxins from each protein family (Calvete *et al.*, 2007). Geographical variation in snake venoms could affect the clinical presentation in a victim following envenomation, but more importantly the efficacy of the available antivenoms (Wang, 2019; Wong *et al.*, 2016). Consequently, the effectiveness of antivenom against species from different geographical areas has been the subject of various studies (Lingam *et al.*, 2020; Wong *et al.*, 2016). This has not been done in South Africa for *N. nivea* species and future studies into the efficacy of the SAVP polyvalent antivenom could provide insights for the management and treatment strategies of *N. nivea* envenomation in South Africa.

In this study, the variation in venom composition of *N. nivea* species from the Western Cape (*N. nivea*-WC) and Northern Cape (*N. nivea*-NC) were investigated to ensure that the target

proteins from *N. nivea* was present in species from both regional locations in South Africa. Anecdotal evidence suggests that *N. nivea* species from Northern Cape region in South Africa cause more cytotoxic than neurotoxic effects and that the *N. nivea* species from Western Cape region are more potently neurotoxic.

A high degree of homology between the species was observed, however variation in protein abundances and subtypes were observed in the venom of *N. nivea* species from the Western Cape and the Northern Cape regions. Samples were run in triplicate and the results obtained following HR-LC-MS/MS analysis identified 46 and 42 proteins from the *N. nivea*-WC and *N. nivea*-NC venoms. The most evident difference between the two venoms was observed in the three-finger toxin protein family, the major component of *N. nivea* venom, *N. nivea*-WC comprised a higher percentage of these toxins. *N. nivea*-WC venom comprised of three-finger toxins (67%), venom nerve growth factor (20%), cobra venom factor (7%), kunitz-type serine protease inhibitor (2%) and snake venom metalloproteinase (4%). *N. nivea*-NC venom comprised of three-finger toxins (62%), venom nerve growth factor (22%), cobra venom factor (7%), venom phosphodiesterase (2%), kunitz-type serine protease inhibitor (2%) and snake venom metalloproteinase (2%) (Figure 4.5).

Inferential statistics were performed on the spectral counts of the identified venom proteins and a significant difference was observed in six toxins. Five toxins were upregulated in *N. nivea*-WC venom and one in *N. nivea*-NC venom. The neurotoxins, long neurotoxin OH-55 (3L255_OPHHA) was present at a 27.58 fold, long neurotoxin 1 (3L21_NAJNI) at 8.14 fold and short neurotoxin 2 (3S12_NAJNI) at 3.55 fold higher in *N. nivea*-WC venom in comparison to *N. nivea*-NC venom. Two zinc metalloproteinase-disintegrin-like proteins were quantitatively 4.26 fold (VM3B_NAJAT) and 3.94 fold (VM3KL_NAJAT) higher in *N. nivea*-WC venom. Probable weak neurotoxin NNAM2 (3NO22_NAJAT) was upregulated in *N. nivea*-NC venom and present at a 0.11 fold higher than in *N. nivea*-WC venom. The prevalence and higher abundance of three-finger toxins, especially neurotoxins in *N. nivea*-WC venom explain the anecdotal evidence that suggests *N. nivea*-WC venom is more potently neurotoxic and could explain the more severe cytotoxic symptoms that were observed in a victim following envenomation by a *N. nivea* bite in the Northern Cape (PIHWC, personal communication, 2021).

5.5 HPLC of *B. atropos*, *B. arietans* and *N. nivea* crude venom

The acetonitrile precipitation strategy that was implemented for the depletion of abundant and high molecular weight proteins from crude *B. atropos*, *B. arietans* and *N. nivea* venom spiked

into plasma venom was based on the acetonitrile-based extraction method developed by Kay et al. (2008) for the preparation of serum proteins prior to MS analysis. A top-down proteomic approach was used, and the samples were injected directly onto the HPLC instrument without prior tryptic digestion. A similar method was used by Katali et al. (2020) during a comparative study on the venom proteomes of two African spitting cobras *N. mossambica* and *N. n. nigricincta*. Precipitation reactions using different volumes of acetonitrile were evaluated and a considerable depletion was observed in the HPLC chromatographic peaks when the volume of acetonitrile increased from two volumes to three and four volumes. This was the case for *N. nivea* venoms. Two volumes of acetonitrile proved to sufficiently deplete the samples of abundant and high molecular weight proteins (>10). A difference in the HPLC chromatographic profiles of the three different species were observed in acetonitrile precipitated crude venoms in 0.1% formic acid in water (A) (Figure 4.8) and in plasma spiked with venom and precipitated with acetonitrile (Figure 4.10). All venoms had a peak at 12-minute retention time, that was absent from the blank sample. *N. nivea*-WC and *N. nivea*-NC venoms showed no peak separation with one major peak eluting between from 12 to 16 minutes retention time. *B. atropos* venom showed prominent peaks at retention times 13,15 and 16 minutes. *B. arietans* venom showed four well defined peaks at a retention times 9, 11, 16 and 19 minutes.

Following analysis by HPLC, the samples spiked with *B. arietans* and *N. nivea* venoms were analysed by HR-LC-MS/MS to confirm the qualitative differences that was observed in the spiked plasma samples and to identify low molecular weight species-specific venom toxins that remained following acetonitrile precipitation. A total of 158 proteins were positively identified of which 40 proteins were of Serpentes taxonomic origin. Seven proteins, cytotoxin 1 (3SA1_NAJHA), complement C3 (VCO3_NAJKA), cobra venom factor (VCO3_NAJKA), zinc metalloproteinase-disintegrin-like atrase-B (VM3B_NAJAT), zinc metalloproteinase-disintegrin-like cobrin (VM3_NAJKA), L-amino-acid oxidase (OXLA_NAJAT), Thaicobrin (VESP_NAJKA) and vespryn (VESP_CROAD) were positively identified from the sample spiked with *N. nivea* venom. There were 29 proteins positively identified that were only present in the samples spiked with *B. arietans* venom. The majority of these proteins belonged to the snake venom metalloproteinase (48%) and L-amino-acid oxidase (24%) protein families. The proteins zinc metalloproteinase-disintegrin BA-5A (VM25A_BITAR) and cystatin (CYT_BITAR), were specific to *B. arietans* species. Other proteins include snake venom 5'-nucleotidase (V5NTD_GLOBR), snake venom 5'-nucleotidase (V5NTD_CROAD), snake venom metalloprotease inhibitor (SVM1_ECHOC), venom phosphodiesterase 1 (PDE1_CROAD), the snake venom metalloproteinase inhibitors Poly-His-poly-Gly peptide (SVM11_ATHSQ, SVM12_ATHNI) and venom nerve growth factor (NGFV1_AZEFE).

This confirmed that unique species specific venom proteins responsible for envenomation could remain intact *in vivo* following envenomation, allowing for their use in the development of diagnostic tools for envenomation in South Africa.

5.6 Size exclusion chromatography

Naja nivea venom was successfully fractionated by size exclusion chromatography and the fractions were pooled together according to the elution profile. The chromatogram that was generated during size exclusion chromatography (Figure 4.13), showed resemblance to the chromatograms of the *N. nivea* chromatograms obtained by HPLC (Figure 4.8) and shows how the presence of characteristic protein families in the venoms of the different genera of venomous snake species i.e., *Naja species* or *Bitis species* can add predictive value (Tasoulis and Isbister, 2017). Separation was confirmed on 1-dimensional PAGE and proteomic composition of each fraction determined by HR-LC-MS/MS. Scaffold was used to integrate mass spectrometry results and visualise data.

A total of 43 proteins were positively identified. The most abundant protein family was cytotoxins (30%). Fraction 5 had the largest area under the curve and high percentage of total spectrum counts, that made the toxins identified in this fraction viable candidates for LC-MS/MS method development later on. The three toxins, cytotoxin 1 (3SA1_NAJNI), cytotoxin 2 (3SA2_NAJNI) and cytotoxin 3 (3SA3_NAJNI) specific to *N. nivea* species were positively detected in all fractions (5, 6, 7, 8 and C). In fraction 5, 31 proteins were identified, 10 of these were cytotoxins. The toxins, cytotoxin 1 (3SA1_NAJNI), cytotoxin 10 (3SAA_NAJHA) and cytotoxin 2 (3SA2_NAJNI, 3SA2_NAJHA) had the highest percentage of total spectra. Less abundant toxin families include snake venom metalloproteinases, cysteine-rich venom proteins, snake venom serine proteases and cobra venom factors. The toxins cobra venom factor (VCO3_NAJKA), cytotoxin 1 (3SA1_NAJNI), cytotoxin 5 (3SA5_NAJHH), endonuclease domain-containing 1 protein (V8N4Y2_OPHHA), snake venom metalloproteinase-disintegrin-like mocarhagin (VM3M1_NAJMO), zinc metalloproteinase-disintegrin-like atragin (VM3H_NAJAT) and zinc metalloproteinase-disintegrin-like atrase-B (VM3B_NAJAT) were only detected in fraction 5. A cytotoxin 1a (3SA1A_NAJAT) and weak toxin CM-2a (3SOK2_NAJHA) were only detected in fraction 6. The other proteins identified from this fraction were non-toxic. Cytotoxin 2 (3SA2_NAJHA) was the only unique protein detected in fraction 7. Fraction 8 had no unique proteins. All of the proteins identified in this fraction, were also identified in fractions 5, 6, 7 and C. A possible reason for the presence of the same proteins in multiple fractions, is that the smaller proteins formed complexes with the larger proteins and therefore eluted earlier on. One way to minimise this effect is the addition of a

salt, for example sodium chloride, to the buffer. However this was not an option given the downstream application.

Fraction 5 MS data was imported into Skyline to identify unique peptides that could be used as targets. By using a manual integration approach of Skyline and Scaffold, a MRM was built containing cytotoxins 1, 10 and 3. The decision to use cytotoxin 1 as primary target was confirmed by the preceding MS data that was generated.

5.7 Development of an LC-MS/MS method to detect *N. nivea* venom toxins when spiked into plasma

Using peptides identified during HR-LC-MS/MS analysis, a transition list was constructed and converted into a MRM onto the triple quadrupole. A MRM containing 42 transitions for three abundant *N. nivea* toxins cytotoxin 1 (P01456), cytotoxin 10 (P01453) and cytotoxin 3 (P01459) was built and a triple quadrupole LC-MS/MS method was developed using the Shimadzu application note for the LCMS bioanalysis of antibody drugs using Fab-selective Proteolysis nSMOL based on the work by Iwamoto et al. (2016, 2014). This application note shows that it is becoming a well-accepted method of performing lower cost triple quadrupole analysis of proteins. The only difference was the LC column oven temperature, the application note stated a column oven temperature of 50 °C, and in this study the column oven temperature was decreased to 40 °C. The LC gradient of this study was a slow gradient, 70 minutes longer than that of the application note. This was done due to the highly complex nature of the sample to increase the likelihood of detection of the target toxins. Eight transitions for cytotoxin 3 (P01459) were unsuccessful. All transitions for cytotoxin 1 (P01456) and cytotoxin 10 (P01453) were successfully detected. The toxins were detected at various intensities under all three tryptic digestion protocols (section 4.6.2). The HILIC assisted 18 hour tryptic digest showed the highest intensity, however the accelerated tryptic digestion protocol 2, described in section 3.8.2.2 could be a viable option for rapid sample preparation in time sensitive cases. This LC-MS/MS method could now be refined to remove the undetected transitions and improve the loop time to potentially improve the method sensitivity.

Currently, to the knowledge of the author, there has been no other research published using a triple quadrupole LC-MS/MS method for the analysis and detection of snake venom toxins. A triple quadrupole LC-MS/MS method to detect *N. nivea* unique cytotoxin 1 and cytotoxin 10 from human plasma was successfully developed.

5.8 *In vivo* toxicity assay

The use of a zebrafish toxicity model provides a fast, inexpensive and ethical alternative to other mammalian models used for *in vivo* studies on venom toxins. At treatment concentrations 0.125 - 0.5 $\mu\text{g}/\mu\text{L}$ larval heartbeats had stopped after 2 minutes and the survival rate was 0% in all treatment groups. Morphological changes such as curvature of the larval bodies into C- or S-shapes were observed, however it was not the most prominent feature in the larvae treated with venom fractions. Pericardial oedema was not observed in the larvae as is typically seen in toxicity assays (Rubinstein, 2006). The morphological and behavioural changes that were observed after administration of the venom fractions include seizure like movements, flaking of the of the larval body, flared gills and protruding eyes (ocular oedema). This could be due to the effects of *N. nivea* toxins that caused paralysis of the respiratory system thereby inhibiting sufficient oxygen exchange that led to hypoxia or ischaemia and asphyxia as observed in victims of neurotoxic snakebite envenomation (Chacko et al., 2015; Feola et al., 2020; Paniagua et al., 2020) or that hypoxia was caused by the administration of venom at toxic doses. Studies on pathological outcomes observed in patients after envenomation by various Elapidae and Viperidae snake species indicated variability in clinical manifestations, which include neurological disturbances, increased capillary permeability and oedema (Oukkache et al., 2012). In an *in vivo* study, mice envenomated with *N. haje* venom presented with oedema and symptoms of myotoxicity. Snake venom protein families capable of causing oedema include cytotoxins, and they do so by the formation of pores in cell membranes that cause an increase in calcium influx, with oedema as a side effect. Whereas snake venom zinc metalloproteinases have the ability to induce oedema by initiating slow and selective degradation of alpha-chain fibrinogen (Oukkache et al., 2012; Sun and Bao, 2010).

At a treatment concentration of 0.01 $\mu\text{g}/\mu\text{L}$ behavioural changes were observed after locomotor activity tracking with DanioVision in a 24-hour assay. Acutely, the locomotor behaviour of zebrafish larvae treated with fraction 5 and 7 ($p < 0.05$) and fraction 6 ($p < 0.0001$) were significantly different from the control group, of most significance was fraction 6 ($p < 0.0001$) (Figure 4.19 (A)). Larvae that were treated with fraction 8 (purple on Figure 4.19 (B)), showed a significantly different ($p < 0.0001$) locomotor behaviour compared to the other treatment and control groups. Analysis of the venom fractions by SEC showed eight unique proteins that were only identified in fraction 6. These include the toxins weak toxin CM-2a, a three finger toxin, cytotoxin 1a and cytotoxin 4 and four non-toxin proteins, keratin, elongation factor alpha and junction plakoglobin. The neurotoxic effects caused by envenomation by *Naja species* are primarily due to the action of non-enzymatic three-finger toxins, which could explain the low survival rate (25%) that was observed 24 hours after treatment in the group

treated with fraction 6. Interestingly no proteins were identified that only occurred in fraction 8, on the contrary the protein composition consisted of proteins that were identified in all the other fractions. These proteins are cytotoxin 1, 2, 3 and 10, cationic trypsin, peptidase S1 domain containing protein and non-toxin components an intermediate filament rod and keratin. These results are indicative of how the pathophysiological effects of envenomation observed in the zebrafish larvae treated with different venom fractions differ from one another based on either the action of a single toxin or the synergistic action of a combination of venom molecules. The toxicity assay confirmed toxicity of venom fractions.

CHAPTER 6 Conclusion, Limitations and Future work

6.1 Conclusion

Serious medical implications and life altering consequences are caused to the victims of snakebite envenomation (Kasturiratne et al., 2008). Frequently the correct snake responsible for the bite remains unidentified because the snake was not seen, or the anxious victim gave the wrong description. In South Africa, this is the case in approximately 44% of the snakebite calls received by the PIHWC (Section 2.3.1). Therefore, a rapid diagnostic test to determine cause of envenomation could aid the effective and efficient management of snakebite patients.

This study involved the partial proteomic analysis of three medically important snake species, *Naja nivea*, *Bitis arietans* and *Bitis atropos* associated in the pathogenesis of snakebite in South Africa. This was done by using a combination of proteomic techniques that include native PAGE, reverse-phase HPLC, size exclusion chromatography, HR-LC-MS/MS, LC-MS/MS, tryptic digestion, and database searches, as well as an *in vivo* zebrafish model for toxicity assays. Following a shotgun proteomic approach combined with analytical pharmacology protocols, snake venom components were identified and similarities and differences in venom composition were observed. Acetonitrile precipitation of high molecular weight compounds proved to be an effective strategy to decrease sample complexity. The use of an accelerated tryptic digestion protocol (addition of a heat treatment step prior to digestion), provides a viable alternative for sample preparation in time sensitive cases. Method optimization strategies in terms of loop and dwell times could improve this method and reduce the run time. Unique venom toxins from *N. nivea* species were identified and a triple quadrupole LC-MS/MS method on a Shimadzu instrument was developed for the detection of Cytotoxin 1 ([P01456](#)) and Cytotoxin 10 ([P01453](#)). These two toxins have unique peptides found only in *N. nivea* species, whether from the Northern Cape or the Western Cape, therefore having considered regional difference in venom composition. This study shows a proof of concept that that these venom toxins can be detected over and above complex human plasma derived matrix, indicative that this method could be specific.

6.2 Limitations

The incidence study over a 5-year study period of snakebite calls in South Africa is not a true reflection of all the snakebites that occurred over this period, due to the general trend of under reporting of snakebites and the locality of PIHWC based centres in Cape Town causing bias

in the amount of calls that were received from the Western Cape. This study did not report on the management of envenomed patients, whether antivenom was administered and final outcomes. An LC-MS/MS method was only developed for a unique toxin from *N. nivea* species and not for all three snake species as stated in the aim of the study due to time constraints. Shotgun proteomics are database dependent and therefore unique venom components might have been missed. This is especially the case for *B. atropos* venom.

The level of detection of the *N. nivea* venom fraction spiked into plasma was 1 µg/µL. This concentration is higher than what the concentration of this venom component would be in blood plasma of an envenomed patient, which would be on average 0.02 – 0.03 µg/µL. This is based on an average injection of 100 - 150 mg venom (dry weight) per bite and 5 L of circulating blood in the average adult human body (Minton, 1974; Sharma and Sharma, 2022). This also does not account for consecutive bites that a single snake can deliver. Currently this concentration of *N. nivea* venom fraction spiked into plasma is not feasible and appropriate for use in a clinical setting based on the concentration of these toxins that would be present in a human after snakebite. The stability of the toxins cytotoxin 1 and cytotoxin 10 from *N. nivea* venom once in humans are unknown. This would need to be established to determine the window in which diagnosis could be performed.

6.3 Future work

This study was a proof of concept and the developed methodologies and workflow serve as a platform for the development of diagnostic tools for envenomation in South Africa, and use of snake venom toxins as therapeutics. Insights into the complex nature of snake venom toxins from the South African *Naja nivea*, *Bitis arietans* and *Bitis atropos* species have highlighted an arsenal of potential therapeutics for the treatment of various disease states. Future work into the pathophysiological action of venom toxins using *in vivo* zebrafish model combined with pharmacokinetic modelling of the mechanism of action of venom toxins could contribute to the knowledge of pathophysiological envenomation syndromes seen in snakebite victims. The use of snake venom toxins as potential drug candidates and investigation of target specificity of the toxins. The final aim is to build on this platform to develop a sensitive and robust lateral-flow point of care test which can be used at rural healthcare facilities to diagnose envenomation.

CHAPTER 7 References

- African Snakebite Institute, 2021. Everything you need to know about antivenom - African Snakebite Institute [WWW Document]. URL <https://www.africansnakebiteinstitute.com/articles/everything-you-need-to-know-about-antivenom/> (accessed 2.28.21).
- Andrejčáková, Z., Petrilla, V., Sopková, D., Vlčková, R., Bila, S., Krešáková, L., Petrillová, M., 2015. Comparisons of the African Cobras using electrophoretical analysis of venom and their morphology. *International Research Journal of Natural and Applied Sciences*.
- Arndt, C., Koristka, S., Bartsch, H., Bachmann, M., 2012. Native Polyacrylamide Gels. Humana Press, Totowa, NJ, pp. 49–53. https://doi.org/10.1007/978-1-61779-821-4_5
- Baker, B., Utaisincharoen, P., Tu, A.T., 1992. Structure-function relationship of myotoxin a using peptide fragments. *Arch Biochem Biophys* 298, 325–31. [https://doi.org/10.1016/0003-9861\(92\)90418-v](https://doi.org/10.1016/0003-9861(92)90418-v)
- Bjarnason, J.B., Fox, J.W., 1994. Hemorrhagic metalloproteinases from snake venoms. *Pharmacology & Therapeutics* 62, 325–372. [https://doi.org/10.1016/0163-7258\(94\)90049-3](https://doi.org/10.1016/0163-7258(94)90049-3)
- Blaylock, R.S., 2005. The identification and syndromic management of snakebite in South Africa. *South African Family Practice* 47, 48–53. <https://doi.org/10.1080/20786204.2005.10873288>
- Boldrini-França, J., Cologna, C.T., Pucca, M.B., Bordon, K. de C.F., Amorim, F.G., Anjolette, F.A.P., Cordeiro, F.A., Wiezel, G.A., Cerni, F.A., Pinheiro-Junior, E.L., Shibao, P.Y.T., Ferreira, I.G., de Oliveira, I.S., Cardoso, I.A., Arantes, E.C., 2017. Minor snake venom proteins: Structure, function and potential applications. *Biochimica et Biophysica Acta (BBA) - General Subjects* 1861, 824–838. <https://doi.org/10.1016/J.BBAGEN.2016.12.022>
- Bourne, Y., Taylor, P., Marchot, P., 1995. Acetylcholinesterase inhibition by fasciculin: Crystal structure of the complex. *Cell* 83, 503–512. [https://doi.org/10.1016/0092-8674\(95\)90128-0](https://doi.org/10.1016/0092-8674(95)90128-0)
- Burke, J.E., Dennis, E.A., 2009. Phospholipase A2 biochemistry. *Cardiovasc Drugs Ther* 23, 49–59. <https://doi.org/10.1007/s10557-008-6132-9>
- Calderón-Celis, F., Diez-Fernández, S., Costa-Fernández, J.M., Encinar, J.R., Calvete, J.J., Sanz-Medel, A., 2016. Elemental Mass Spectrometry for Absolute Intact Protein Quantification without Protein-Specific Standards: Application to Snake Venomics. *Analytical Chemistry* 88, 9699–9706. <https://doi.org/10.1021/acs.analchem.6b02585>
- Calvete, J.J., 2014. Next-generation snake venomics: protein-locus resolution through venom proteome decomplexation. *Expert Rev Proteomics* 11, 315–29. <https://doi.org/10.1586/14789450.2014.900447>
- Calvete, J.J., Escolano, J., Sanz, L., 2007. Snake venomics of *Bitis* species reveals large intragenus venom toxin composition variation: Application to taxonomy of congeneric taxa. *Journal of Proteome Research* 6, 2732–2745. <https://doi.org/10.1021/pr0701714>
- Calvete, J.J., Marcinkiewicz, C., Monleón, D., Esteve, V., Celda, B., Juárez, P., Sanz, L., 2005. Snake venom disintegrins: evolution of structure and function. *Toxicon* 45, 1063–1074. <https://doi.org/10.1016/J.TOXICON.2005.02.024>

- Chacko, A., Andronikou, S., Ramanjam, V., 2015. Hypoxic brain injury and cortical blindness in a victim of a Mozambican spitting cobra bite. *South African Journal of Surgery* 53, 67. <https://doi.org/10.7196/sajsnew.7851>
- Chahardehi, A.M., Arsad, H., Lim, V., 2020. Zebrafish as a successful animal model for screening toxicity of medicinal plants. *Plants* 9, 1–35. <https://doi.org/10.3390/PLANTS9101345>
- Chan, J.Y.W., Zhou, H., Kwan, Y.W., Chan, S.W., Radis-Baptista, G., Lee, S.M.Y., 2017. Evaluation in zebrafish model of the toxicity of rhodamine B-conjugated crotamine, a peptide potentially useful for diagnostics and therapeutics. *Journal of Biochemical and Molecular Toxicology* 31, 1–7. <https://doi.org/10.1002/jbt.21964>
- Chippaux, J.-P., 2017. Snakebite envenomation turns again into a neglected tropical disease! *Journal of Venomous Animals and Toxins including Tropical Diseases* 23, 38. <https://doi.org/10.1186/s40409-017-0127-6>
- Chippaux, J.-P., 2011. Estimate of the burden of snakebites in sub-Saharan Africa: A meta-analytic approach. *Toxicon* 57, 586–599. <https://doi.org/10.1016/j.toxicon.2010.12.022>
- Chippaux, J.-P., 2008. Estimating the Global Burden of Snakebite Can Help To Improve Management. *PLoS Medicine* 5, e221. <https://doi.org/10.1371/journal.pmed.0050221>
- Choudhury, M., McCleary, R.J.R., Keshewani, M., Kini, R.M., Velmurugan, D., 2017. Comparison of proteomic profiles of the venoms of two of the 'Big Four' snakes of India, the Indian cobra (*Naja naja*) and the common krait (*Bungarus caeruleus*), and analyses of their toxins. *Toxicon* 135, 33–42. <https://doi.org/10.1016/j.toxicon.2017.06.005>
- Chuat, M., Alcoba, G., Eyong, J., Wanda, F., Comte, E., Nkwescheu, A., Chappuis, F., Hudelson, P., 2021. Dealing with snakebite in rural Cameroon: A qualitative investigation among victims and traditional healers. *Toxicon X* 9–10, 100072. <https://doi.org/10.1016/J.TOXCX.2021.100072>
- Cochran, C., Hax, S., Hayes, W.K., 2019. Case reports of envenomation and venom composition differences between two Arizona populations of the Southwestern Speckled Rattlesnake, *Crotalus pyrrhus* (Cope, 1867). *Toxicon* 171, 29–34. <https://doi.org/10.1016/J.TOXICON.2019.09.022>
- Cox, J.C., Moisidis, A. v., Shepherd, J.M., Drane, D.P., Jones, S.L., 1992. A novel format for a rapid sandwich EIA and its application to the identification of snake venoms. *Journal of Immunological Methods* 146, 213–218. [https://doi.org/10.1016/0022-1759\(92\)90230-Q](https://doi.org/10.1016/0022-1759(92)90230-Q)
- Currier, R.B., Harrison, R.A., Rowley, P.D., Laing, G.D., Wagstaff, S.C., 2010. Intra-specific variation in venom of the African Puff Adder (*Bitis arietans*): Differential expression and activity of snake venom metalloproteinases (SVMPs). *Toxicon* 55, 864–873. <https://doi.org/10.1016/j.toxicon.2009.12.009>
- Da, M., Salomão, G., 1994. Activity patterns in the colubrid snake genus *Philodryas* and their relationship to reproduction and snakebite.
- de Silva, H.A., Ryan, N.M., de Silva, H.J., 2016. Adverse reactions to snake antivenom, and their prevention and treatment. *Br J Clin Pharmacol* 81, 446–52. <https://doi.org/10.1111/bcp.12739>
- Debono, J., Dobson, J., Casewell, N.R., Romilio, A., Li, B., Kurniawan, N., Mardon, K., Weisbecker, V., Nouwens, A., Kwok, H.F., Fry, B.G., 2017. Coagulating *Colubrids*: Evolutionary, Pathophysiological and Biodiscovery Implications of Venom Variations between Boomslang

- (*Dispholidus typus*) and Twig Snake (*Thelotornis mossambicanus*). *Toxins (Basel)* 9. <https://doi.org/10.3390/toxins9050171>
- Deka, A., Reza, M.A., Faisal Hoque, K.M., Deka, K., Saha, S., Doley, R., 2019. Comparative analysis of *Naja kaouthia* venom from North-East India and Bangladesh and its cross reactivity with Indian polyvalent antivenoms. *Toxicon* 164, 31–43. <https://doi.org/10.1016/j.toxicon.2019.03.025>
- Department of Statistics South Africa, 2019. Mid-year population estimates. Pretoria.
- Dhananjaya, B.L., D'Souza, C.J.M., 2010. The pharmacological role of nucleotidases in snake venoms. *Cell Biochem Funct* 28, 171–7. <https://doi.org/10.1002/cbf.1637>
- Dias-Lopes, C., Paiva, A.L., Guerra-Duarte, C., Molina, F., Felicori, L., 2018. Venomous Arachnid Diagnostic Assays, Lessons from Past Attempts. *Toxins (Basel)* 10. <https://doi.org/10.3390/toxins10090365>
- Dingwoke, E.J., Adamude, F.A., Mohamed, G., Klein, A., Salihu, A., Abubakar, M.S., Sallau, A.B., 2021. Venom proteomic analysis of medically important Nigerian viper *Echis ocellatus* and *Bitis arietans* snake species. *Biochemistry and Biophysics Reports* 28, 101164. <https://doi.org/10.1016/J.BBREP.2021.101164>
- Dorner, B.G., Zeleny, R., Harju, K., Hennekinne, J.-A., Vanninen, P., Schimmel, H., Rummel, A., 2016. Biological toxins of potential bioterrorism risk: Current status of detection and identification technology. *TrAC Trends in Analytical Chemistry* 85, 89–102. <https://doi.org/10.1016/J.TRAC.2016.05.024>
- Duong-Ly, K.C., Gabelli, S.B., 2014. Salting out of proteins using ammonium sulfate precipitation. *Methods Enzymol* 541, 85–94. <https://doi.org/10.1016/B978-0-12-420119-4.00007-0>
- Duracova, M., Klimentova, J., Fucikova, A., Dresler, J., 2018. Proteomic methods of detection and quantification of protein toxins. *Toxins (Basel)* 10, 1–30. <https://doi.org/10.3390/toxins10030099>
- Dyba, B., Rudolphi-Szydło, E., Barbasz, A., Czyżowska, A., Hus, K.K., Petrilla, V., Petrillová, M., Legáth, J., Bocian, A., 2021. Effects of 3FTx Protein Fraction from *Naja ashei* Venom on the Model and Native Membranes: Recognition and Implications for the Mechanisms of Toxicity. *Molecules* 26, 2164. <https://doi.org/10.3390/molecules26082164>
- El-Aziz, T.M.A., Soares, A.G., Stockand, J.D., 2020. Advances in venomics: Modern separation techniques and mass spectrometry. *Journal of Chromatography B Analytical Technologies in the Biomedical and Life Sciences* 1160, 122352. <https://doi.org/10.1016/j.jchromb.2020.122352>
- El-Aziz, T.M.A., Soares, A.G., Stockand, J.D., 2019. Snake venoms in drug discovery: Valuable therapeutic tools for life saving. *Toxins (Basel)* 11, 1–25. <https://doi.org/10.3390/toxins11100564>
- El-Faramawy, A., Siu, K.W.M., Thomson, B.A., 2005. Efficiency of Nano-Electrospray Ionization. *J Am Soc Mass Spectrom* 16, 1702–1707. <https://doi.org/10.1016/J.JASMS.2005.06.011>
- Epstein, F.H., Levin, E.R., Gardner, D.G., Samson, W.K., 1998. Natriuretic Peptides. *New England Journal of Medicine* 339, 321–328. <https://doi.org/10.1056/nejm199807303390507>
- Fathi H, B., Rowan, E.G., Harvey, A.L., 2001. The facilitatory actions of snake venom phospholipase A(2) neurotoxins at the neuromuscular junction are not mediated through voltage-gated K(+) channels. *Toxicon* 39, 1871–82. [https://doi.org/10.1016/s0041-0101\(01\)00170-2](https://doi.org/10.1016/s0041-0101(01)00170-2)

- Feola, A., Marella, G.L., Carfora, A., della Pietra, B., Zangani, P., Campobasso, C. pietro, 2020. Snakebite Envenoming a Challenging Diagnosis for the Forensic Pathologist: A Systematic Review. *Toxins (Basel)* 12, 699. <https://doi.org/10.3390/toxins12110699>
- Ferguson, R.K., Vlasses, P.H., 1981. Clinical pharmacology and therapeutic applications of the new oral angiotensin converting enzyme inhibitor, captopril. *American Heart Journal* 101, 650–656. [https://doi.org/10.1016/0002-8703\(81\)90233-7](https://doi.org/10.1016/0002-8703(81)90233-7)
- Ferraz, C.R., Arrahman, A., Xie, C., Casewell, N.R., Lewis, R.J., Kool, J., Cardoso, F.C., 2019. Multifunctional toxins in snake venoms and therapeutic implications: From pain to hemorrhage and necrosis. *Frontiers in Ecology and Evolution* 7, 1–19. <https://doi.org/10.3389/fevo.2019.00218>
- Fox, J.W., 2013. A brief review of the scientific history of several lesser-known snake venom proteins: L-amino acid oxidases, hyaluronidases and phosphodiesterases. *Toxicon* 62, 75–82. <https://doi.org/10.1016/j.toxicon.2012.09.009>
- Fox, J.W., Serrano, S.M.T., 2008. Exploring snake venom proteomes: multifaceted analyses for complex toxin mixtures. *PROTEOMICS* 8, 909–920. <https://doi.org/10.1002/pmic.200700777>
- Fox, J.W., Serrano, S.M.T., 2005. Structural considerations of the snake venom metalloproteinases, key members of the M12 reprotolysin family of metalloproteinases. *Toxicon* 45, 969–85. <https://doi.org/10.1016/j.toxicon.2005.02.012>
- Frobert, Y., Créminon, C., Cousin, X., Rémy, M.-H., Chatel, J.-M., Bon, S., Bon, C., Grassi, J., 1997. Acetylcholinesterases from Elapidae snake venoms: biochemical, immunological and enzymatic characterization. *Biochimica et Biophysica Acta (BBA) - Protein Structure and Molecular Enzymology* 1339, 253–267. [https://doi.org/10.1016/s0167-4838\(97\)00009-5](https://doi.org/10.1016/s0167-4838(97)00009-5)
- Fry, B.G., 2005. From genome to “venome”: molecular origin and evolution of the snake venom proteome inferred from phylogenetic analysis of toxin sequences and related body proteins. *Genome Res* 15, 403–20. <https://doi.org/10.1101/gr.3228405>
- Fry, B.G., Casewell, N.R., Wüster, W., Vidal, N., Young, B., Jackson, T.N.W., 2012. The structural and functional diversification of the Toxicofera reptile venom system. *Toxicon* 60, 434–448. <https://doi.org/10.1016/J.TOXICON.2012.02.013>
- Fry, B.G., Scheib, H., van der Weerd, L., Young, B., McNaughtan, J., Ramjan, S.F.R., Vidal, N., Poelmann, R.E., Norman, J.A., 2008. Evolution of an arsenal: structural and functional diversification of the venom system in the advanced snakes (*Caenophidia*). *Mol Cell Proteomics* 7, 215–46. <https://doi.org/10.1074/mcp.M700094-MCP200>
- Garcia, G.R., Noyes, P.D., Tanguay, R.L., 2016. Advancements in zebrafish applications for 21st century toxicology. *Pharmacology and Therapeutics* 161, 11–21. <https://doi.org/10.1016/J.PHARMTHERA.2016.03.009>
- Ghezellou, P., Garikapati, V., Kazemi, S.M., Strupat, K., Ghassempour, A., Spengler, B., 2019. A perspective view of top-down proteomics in snake venom research. *Rapid Communications in Mass Spectrometry* 33, 20–27. <https://doi.org/10.1002/rcm.8255>
- Gomes, M., Alvarez, M.A., Quellis, L.R., Becher, M.L., Castro, J.M. de A., Gameiro, J., Caporrino, M.C., Moura-da-Silva, A.M., de Oliveira Santos, M., 2019. Expression of an scFv antibody fragment in *Nicotiana benthamiana* and in vitro assessment of its neutralizing potential against the snake

- venom metalloproteinase BaP1 from *Bothrops asper*. *Toxicon* 160, 38–46. <https://doi.org/10.1016/J.TOXICON.2019.02.011>
- Gutiérrez, J.M., Calvete, J.J., Habib, A.G., Harrison, R.A., Williams, D.J., Warrell, D.A., 2017. Snakebite envenoming. *Nature Reviews Disease Primers* 3, 17063. <https://doi.org/10.1038/nrdp.2017.63>
- Gutiérrez, J.M., Theakston, R.D.G., Warrell, D.A., 2006. Confronting the Neglected Problem of Snake Bite Envenoming: The Need for a Global Partnership. *PLoS Medicine* 3, e150. <https://doi.org/10.1371/journal.pmed.0030150>
- Habib, A.G., Musa, B.M., Ilyasu, G., Hamza, M., Kuznik, A., Chippaux, J.P., 2020. Challenges and prospects of snake antivenom supply in Sub-Saharan Africa. *PLoS Neglected Tropical Diseases* 14, 1–10. <https://doi.org/10.1371/journal.pntd.0008374>
- Halilu, S., Ilyasu, G., Hamza, M., Chippaux, J.P., Kuznik, A., Habib, A.G., 2019. Snakebite burden in Sub-Saharan Africa: estimates from 41 countries. *Toxicon* 159, 1–4. <https://doi.org/10.1016/j.toxicon.2018.12.002>
- Harvey, A.L., 2001. Twenty years of dendrotoxins. *Toxicon* 39, 15–26. [https://doi.org/10.1016/s0041-0101\(00\)00162-8](https://doi.org/10.1016/s0041-0101(00)00162-8)
- Hider, R.C., Karlsson, E., Namiranian, S., 1991. Separation and purification of toxins from snake venoms, in: Harvey, A.L. (Ed.), *Snake Toxins*. Pergamon, New York, N.Y. :, pp. 1–34.
- Hill, A.J., Teraoka, H., Heideman, W., Peterson, R.E., 2005. Zebrafish as a model vertebrate for investigating chemical toxicity. *Toxicological Sciences* 86, 6–19. <https://doi.org/10.1093/toxsci/kfi110>
- Ho, C.S., Lam, C.W.K., Chan, M.H.M., Cheung, R.C.K., Law, L.K., Lit, L.C.W., Ng, K.F., Suen, M.W.M., Tai, H.L., 2003. Electrospray ionisation mass spectrometry: principles and clinical applications. *Clin Biochem Rev* 24, 3–12.
- Inagaki, H., 2017. Snake Venom Protease Inhibitors: Enhanced Identification, Expanding Biological Function, and Promising Future, in: *Snake Venoms*. Springer Netherlands, Dordrecht, pp. 161–186. https://doi.org/10.1007/978-94-007-6410-1_16
- Isbister, G.K., Maduwage, K., Shahmy, S., Mohamed, F., Abeysinghe, C., Karunathilake, H., Ariaratnam, C.A., Buckley, N.A., 2013. Diagnostic 20-min whole blood clotting test in Russell's viper envenoming delays antivenom administration. *QJM* 106, 925–932. <https://doi.org/10.1093/qjmed/hct102>
- Iwamoto, N., Shimada, T., Umino, Y., Aoki, C., Aoki, Y., Sato, T.-A., Hamada, A., Nakagama, H., 2014. Selective detection of complementarity-determining regions of monoclonal antibody by limiting protease access to the substrate: nano-surface and molecular-orientation limited proteolysis. *Analyst* 139, 576–580. <https://doi.org/10.1039/C3AN02104A>
- Iwamoto, N., Umino, Y., Aoki, C., Yamane, N., Hamada, A., Shimada, T., 2016. Fully validated LCMS bioanalysis of Bevacizumab in human plasma using nano-surface and molecular-orientation limited (nSMOL) proteolysis. *Drug Metabolism and Pharmacokinetics* 31, 46–50. <https://doi.org/10.1016/J.DMPK.2015.11.004>

- Jayawardana, S., Arambepola, C., Chang, T., Gnanathanan, A., 2021. Prevalence, vulnerability and epidemiological characteristics of snakebite in agricultural settings in rural Sri Lanka: A population-based study from South Asia. *PLoS ONE* 15, 1–13. <https://doi.org/10.1371/journal.pone.0243991>
- Kamiguti, A.S., Zuzel, M., Theakston, R.D.G., 1998. Snake venom metalloproteinases and disintegrins: interactions with cells. *Brazilian Journal of Medical and Biological Research* 31, 853–862. <https://doi.org/10.1590/s0100-879x1998000700001>
- Kang, T.S., Georgieva, D., Genov, N., Murakami, M.T., Sinha, M., Kumar, R.P., Kaur, P., Kumar, S., Dey, S., Sharma, S., Vrieland, A., Betzel, C., Takeda, S., Arni, R.K., Singh, T.P., Kini, R.M., 2011. Enzymatic toxins from snake venom: structural characterization and mechanism of catalysis. *FEBS Journal* 278, 4544–4576. <https://doi.org/10.1111/j.1742-4658.2011.08115.x>
- Kasturiratne, A., Wickremasinghe, A., de Silva, N., Gunawardena, N., Pathmeswaran, A., Premaratna, R., Savioli, L., Lallo, Dg., de Silva, H., 2008. The global burden of snakebite: a literature analysis and modelling based on regional estimates of envenoming and deaths. *PLoS Med* 5. <https://doi.org/10.1371/JOURNAL.PMED.0050218>
- Katali, O., Shipingana, L., Nyaragó, P., Pääkkönen, M., Haindongo, E., Rennie, T., James, P., Eriksson, J., Hunter, C.J., 2020. Protein Identification of Venoms of the African Spitting Cobras, *Naja mossambica* and *Naja nigricincta nigricincta*. *Toxins (Basel)* 12, 520. <https://doi.org/10.3390/toxins12080520>
- Kay, R., Barton, C., Ratcliffe, L., Matharoo-Ball, B., Brown, P., Roberts, J., Teale, P., Creaser, C., 2008. Enrichment of low molecular weight serum proteins using acetonitrile precipitation for mass spectrometry based proteomic analysis. *Rapid Communications in Mass Spectrometry* 22, 3255–3260. <https://doi.org/10.1002/rcm.3729>
- Keller, A., Nesvizhskii, A.I., Kolker, E., Aebersold, R., 2002. Empirical statistical model to estimate the accuracy of peptide identifications made by MS/MS and database search. *Anal Chem* 74, 5383–92. <https://doi.org/10.1021/ac025747h>
- Kerkkamp, H.M.I., Casewell, N.R., Vonk, F.J., 2015. Evolution of the snake venom delivery system., in: P. Gopalakrishnakone, A. Malhotra (Eds.), *Evolution of Venomous Animals and Their Toxins*. Springer, Dordrecht, The Netherlands, pp. 1–11.
- Kini, R.M., 2003. Excitement ahead: structure, function and mechanism of snake venom phospholipase A2 enzymes. *Toxicon* 42, 827–840. <https://doi.org/10.1016/J.TOXICON.2003.11.002>
- Kini, R.M., 2002. Molecular moulds with multiple missions: Functional sites in three-finger toxins. *Clinical and Experimental Pharmacology and Physiology* 29, 815–822. <https://doi.org/10.1046/j.1440-1681.2002.03725.x>
- Kini, R.M., Doley, R., 2010. Structure, function and evolution of three-finger toxins: Mini proteins with multiple targets. *Toxicon* 56, 855–867. <https://doi.org/10.1016/j.toxicon.2010.07.010>
- Komori, Y., Nikai, T., 1998. Chemistry and Biochemistry of Kallikrein-Like Enzymes from Snake Venoms. *Journal of Toxicology: Toxin Reviews* 17, 261–277. <https://doi.org/10.3109/15569549809040394>
- Kostiza, T., Meier, J., 1996. Nerve growth factors from snake venoms: Chemical properties, mode of action and biological significance. *Toxicon* 34, 787–806. [https://doi.org/10.1016/0041-0101\(96\)00023-2](https://doi.org/10.1016/0041-0101(96)00023-2)

- Kudo, K., Tu, A.T., 2001. Characterization of hyaluronidase isolated from *Agkistrodon contortrix contortrix* (Southern Copperhead) venom. *Arch Biochem Biophys* 386, 154–62. <https://doi.org/10.1006/abbi.2000.2204>
- Kularatne, S.A.M., Senanayake, N., 2014. Venomous snake bites, scorpions, and spiders. *Handbook of Clinical Neurology* 120, 987–1001. <https://doi.org/10.1016/B978-0-7020-4087-0.00066-8>
- Laemmli, U.K., 1970. Cleavage of structural proteins during the assembly of the head of bacteriophage T4. *Nature* 227, 680–5. <https://doi.org/10.1038/227680A0>
- Lambeau, G., Gelb, M.H., 2008. Biochemistry and physiology of mammalian secreted phospholipases A2. *Annu Rev Biochem* 77, 495–520. <https://doi.org/10.1146/annurev.biochem.76.062405.154007>
- Lin, J.H., Sung, W.C., Liao, J.W., Hung, D.Z., 2020. A Rapid and International Applicable Diagnostic Device for Cobra (Genus *Naja*) Snakebites. *Toxins (Basel)* 12, 1–14. <https://doi.org/10.3390/toxins12090572>
- Lingam, T.M.C., Tan, K.Y., Tan, C.H., 2020. Proteomics and antivenom immunoprofiling of Russell's viper (*Daboia siamensis*) venoms from Thailand and Indonesia. *Journal of Venomous Animals and Toxins Including Tropical Diseases* 26, 1–17. <https://doi.org/10.1590/1678-9199-jvatitd-2019-0048>
- Liu, S., Yang, F., Zhang, Q., Sun, M.-Z., Gao, Y., Shao, S., 2011. “Anatomical” view of the protein composition and protein characteristics for *Gloydius shedaoensis* snake venom via proteomics approach. *Anat Rec (Hoboken)* 294, 273–82. <https://doi.org/10.1002/ar.21322>
- Lobetti, R.G., Joubert, K., 2004. Retrospective study of snake envenomation in 155 dogs from the Onderstepoort area of South Africa. *J S Afr Vet Assoc* 75, 169–172. <https://doi.org/10.4102/jsava.v75i4.477>
- Lomonte, B., Križaj, I., 2021. Snake Venom Phospholipase A2 toxins, in: Stephen P. Mackessy (Ed.), *Handbook of Venoms and Toxins of Reptiles*. CRC Press, Boca Raton, p. 393.
- Lu, Q., Navdaev, A., Clemetson, J.M., Clemetson, K.J., 2005. Snake venom C-type lectins interacting with platelet receptors. Structure–function relationships and effects on haemostasis. *Toxicon* 45, 1089–1098. <https://doi.org/10.1016/J.TOXICON.2005.02.022>
- Luque-Garcia, J.L., Neubert, T.A., 2007. Sample preparation for serum/plasma profiling and biomarker identification by mass spectrometry. *J Chromatogr A* 1153, 259–76. <https://doi.org/10.1016/j.chroma.2006.11.054>
- MacLean, B., Tomazela, D.M., Shulman, N., Chambers, M., Finney, G.L., Frewen, B., Kern, R., Tabb, D.L., Liebler, D.C., MacCoss, M.J., 2010. Skyline: an open source document editor for creating and analyzing targeted proteomics experiments. *Bioinformatics* 26, 966–8. <https://doi.org/10.1093/bioinformatics/btq054>
- Maduwage, K., O’Leary, M.A., Isbister, G.K., 2015. Diagnosis of snake envenomation using a simple phospholipase A2 assay. *Scientific Reports* 4, 4827. <https://doi.org/10.1038/srep04827>
- Marcussi, S., Sant’Ana, C.D., Oliveira, C.Z., Rueda, A.Q., Menaldo, D.L., Belebani, R.O., Stabeli, R.G., Giglio, J.R., Fontes, M.R.M., Soares, A.M., 2007. Snake venom phospholipase A2 inhibitors:

- medicinal chemistry and therapeutic potential. *Curr Top Med Chem* 7, 743–56. <https://doi.org/10.2174/156802607780487614>
- Markland, F.S., 1998. Snake venoms and the hemostatic system. *Toxicon* 36, 1749–800. [https://doi.org/10.1016/s0041-0101\(98\)00126-3](https://doi.org/10.1016/s0041-0101(98)00126-3)
- McCleary, R.J.R., Kini, R.M., 2013. Non-enzymatic proteins from snake venoms: a gold mine of pharmacological tools and drug leads. *Toxicon* 62, 56–74. <https://doi.org/10.1016/j.toxicon.2012.09.008>
- McClellan, K.J., Goa, K.L., 1998. Tirofiban. *Drugs* 56, 1067–1080. <https://doi.org/10.2165/00003495-199856060-00017>
- Mehrdar, M.T., Madani, R., Hajhosseini, R., Bidhendi, S.M., 2017. Antibacterial activity of isolated immunodominant proteins of *Naja Naja* (Oxiana) Venom. *Iranian Journal of Pharmaceutical Research*. <https://doi.org/10.22037/ijpr.2017.1971>
- Meier, J., Stocker, K., 1991. Effects of snake venoms on hemostasis. *Crit Rev Toxicol* 21, 171–82. <https://doi.org/10.3109/10408449109089878>
- Mhaskar, D., Agarwal, A., Bhalla, G., 2014. A study of clinical profile of snake bite at a tertiary care centre. *Toxicology International* 21, 203. <https://doi.org/10.4103/0971-6580.139811>
- Minton, S.A., 1987. Present tests for detection of snake venom: clinical applications. *Ann Emerg Med* 16, 932–7. [https://doi.org/10.1016/s0196-0644\(87\)80736-9](https://doi.org/10.1016/s0196-0644(87)80736-9)
- Minton, S.A., Jr., 1974. Venom diseases. *Venom diseases*.
- Mitra, J., Bhattacharyya, D., 2014. Phosphodiesterase from *Daboia russelli russelli* venom: purification, partial characterization and inhibition of platelet aggregation. *Toxicon* 88, 1–10. <https://doi.org/10.1016/j.toxicon.2014.06.004>
- Morita, T., 2005. Structures and functions of snake venom CLPs (C-type lectin-like proteins) with anticoagulant-, procoagulant-, and platelet-modulating activities. *Toxicon* 45, 1099–114. <https://doi.org/10.1016/j.toxicon.2005.02.021>
- Mtewa, A.G., 2019. From Toxins to Drugs: Chemistry and Pharmacology of Animal Venom and other Secretions. *Online Journal of Complementary & Alternative Medicine* 1. <https://doi.org/10.33552/OJCAM.2019.01.000505>
- Muller, G.J., Modler, H., Wium, C.A., Veale, D.J.H., 2012a. Scorpion sting in southern Africa: diagnosis and management. *Continuing Medical Education* 30, 356–361.
- Muller, G.J., Modler, H., Wium, C.A., Veale, D.J.H., Marks, C.J., 2012b. Snake bite in southern Africa: diagnosis and management. *CME* 30, 362–381.
- Murakami, M., Kudo, I., 2002. Phospholipase A2. *J Biochem* 131, 285–92. <https://doi.org/10.1093/oxfordjournals.jbchem.a003101>
- Nesvizhskii, A.I., Keller, A., Kolker, E., Aebersold, R., 2003. A statistical model for identifying proteins by tandem mass spectrometry. *Anal Chem* 75, 4646–58. <https://doi.org/10.1021/ac0341261>
- Newman, W.J., Moran, N.F., Theakston, R.D.G., Warrell, D.A., Wilkinson, D., 1997. Traditional treatments for snake bite in a rural African community. *Annals of Tropical Medicine & Parasitology* 91, 967–969. <https://doi.org/10.1080/00034983.1997.11813228>

- Nimorakiotakis, V. (Bill), Winkel, K.D., 2016. Prospective assessment of the false positive rate of the Australian snake venom detection kit in healthy human samples. *Toxicon* 111, 143–146. <https://doi.org/10.1016/J.TOXICON.2015.12.002>
- Nirthanan, S., Gwee, M.C.E., 2004. Three-Finger α -Neurotoxins and the Nicotinic Acetylcholine Receptor, Forty Years On. *Journal of Pharmacological Sciences* 94, 1–17. <https://doi.org/10.1254/jphs.94.1>
- Ochola, F.O., Okumu, M.O., Muchemi, G.M., Mbaria, J.M., Gikunju, J.K., 2018. Epidemiology of snake bites in selected areas of Kenya. *Pan African Medical Journal* 29, 1–14. <https://doi.org/10.11604/pamj.2018.29.217.15366>
- OmPraba, G., Chapeaurouge, A., Doley, R., Devi, K.R., Padmanaban, P., Venkatraman, C., Velmurugan, D., Lin, Q., Kini, R.M., 2010. Identification of a Novel Family of Snake Venom Proteins Veficolins from *Cerberus rynchops* Using a Venom Gland Transcriptomics and Proteomics Approach. *Journal of Proteome Research* 9, 1882–1893. <https://doi.org/10.1021/pr901044x>
- Osipov, A. V., Utkin, Y.N., 2015. Snake Venom Toxins Targeted at the Nervous System, in: *Snake Venoms*. Springer Netherlands, Dordrecht, pp. 1–21. https://doi.org/10.1007/978-94-007-6648-8_23-1
- Otero, R., Gutiérrez, J.M., Rojas, G., Núñez, V., Díaz, A., Miranda, E., Uribe, A.F., Silva, J.F., Ospina, J.G., Medina, Y., Toro, M.F., García, M.E., León, G., García, M., Lizano, S., De La Torre, J., Márquez, J., Mena, Y., González, N., Arenas, L.C., Puzón, A., Blanco, N., Sierra, A., Espinal, M.E., Lozano, R., 1999. A randomized blinded clinical trial of two antivenoms, prepared by caprylic acid or ammonium sulphate fractionation of IgG, in *Bothrops* and *Porthidium* snake bites in Colombia: correlation between safety and biochemical characteristics of antivenoms. *Toxicon* 37, 895–908. [https://doi.org/10.1016/s0041-0101\(98\)00220-7](https://doi.org/10.1016/s0041-0101(98)00220-7)
- Oukkache, N., Lalaoui, M., Ghalim, N., 2012. General characterization of venom from the Moroccan snakes *Macrovipera mauritanica* and *Cerastes cerastes*. *Journal of Venomous Animals and Toxins including Tropical Diseases* 18, 411–420. <https://doi.org/10.1590/S1678-91992012000400009>
- Paixão-Cavalcante, D., Kuniyoshi, A.K., Portaro, F.C.V., da Silva, W.D., Tambourgi, D. V., 2015. African Adders: Partial Characterization of Snake Venoms from Three *Bitis* Species of Medical Importance and Their Neutralization by Experimental Equine Antivenoms. *PLoS Neglected Tropical Diseases* 9, 1–18. <https://doi.org/10.1371/journal.pntd.0003419>
- Paniagua, D., Crowns, K., Montonera, M., Wertheimer, A., Alagón, A., Boyer, L., 2020. Postmortem histopathology and detection of venom by ELISA following suicide by cobra (*Naja kaouthia*) envenomation. *Forensic Toxicology* 38, 523–528. <https://doi.org/10.1007/s11419-020-00535-w>
- Persson, H.E., Sjöberg, G.K., Haines, J.A., de Garbino, J.P., 1998. Poisoning Severity Score. Grading of Acute Poisoning. *Journal of Toxicology: Clinical Toxicology* 36, 205–213. <https://doi.org/10.3109/15563659809028940>
- Petras, D., Sanz, L., Segura, Á., Herrera, M., Villalta, M., Solano, D., Vargas, M., León, G., Warrell, D.A., Theakston, R.D.G., Harrison, R.A., Durfa, N., Nasidi, A., Gutiérrez, J.M., Calvete, J.J., 2011.

- Snake Venomics of African Spitting Cobras: Toxin Composition and Assessment of Congeneric Cross-Reactivity of the Pan-African EchiTAB-Plus-ICP Antivenom by Antivenomics and Neutralization Approaches. *Journal of Proteome Research* 10, 1266–1280. <https://doi.org/10.1021/pr101040f>
- Prashanth, J.R., Hasaballah, N., Vetter, I., 2017. Pharmacological screening technologies for venom peptide discovery. *Neuropharmacology* 127, 4–19. <https://doi.org/10.1016/J.NEUROPHARM.2017.03.038>
- Pung, Y.F., Kumar, S.V., Rajagopalan, N., Fry, B.G., Kumar, P.P., Kini, R.M., 2006. Ohanin, a novel protein from king cobra venom: Its cDNA and genomic organization. *Gene* 371, 246–256. <https://doi.org/10.1016/j.gene.2005.12.002>
- Puzari, U., Mukherjee, A.K., 2020. Recent developments in diagnostic tools and bioanalytical methods for analysis of snake venom: A critical review. *Analytica Chimica Acta* 1137, 208–224. <https://doi.org/10.1016/j.aca.2020.07.054>
- Ranawaka, U.K., Lalloo, D.G., de Silva, H.J., 2013. Neurotoxicity in Snakebite—The Limits of Our Knowledge. *PLoS Neglected Tropical Diseases* 7, e2302. <https://doi.org/10.1371/journal.pntd.0002302>
- Reid, H.A., Theakston, R.D., 1983. The management of snake bite. *Bull World Health Organ* 61, 885–95.
- Rigoni, M., Paoli, M., Milanesi, E., Caccin, P., Rasola, A., Bernardi, P., Montecucco, C., 2008. Snake phospholipase A2 neurotoxins enter neurons, bind specifically to mitochondria, and open their transition pores. *J Biol Chem* 283, 34013–20. <https://doi.org/10.1074/jbc.M803243200>
- Rivas-Mercado, E.A., Garza-Ocañas, L., 2017. Disintegrins obtained from snake venom and their pharmacological potential. *Medicina Universitaria* 19, 32–37. <https://doi.org/10.1016/j.rmu.2017.02.004>
- Rosing, J., Tans, G., 1992. Structural and functional properties of snake venom prothrombin activators. *Toxicon* 30, 1515–27. [https://doi.org/10.1016/0041-0101\(92\)90023-x](https://doi.org/10.1016/0041-0101(92)90023-x)
- Rossiter, D., Blockman, M., Barnes, K.I., University of Cape Town, D. of C.P., South African Medical Association (1998-) Health and Medical Publishing Group, 2020. *South African Medicines Formulary / a joint initiative of the Division of Clinical Pharmacology, Faculty of Health Sciences, University of Cape Town and the South African Medical Association, 13th ed.* Health and Medical Publishing Group, Cape Town.
- Rubinstein, A.L., 2006. Zebrafish assays for drug toxicity screening. *Expert Opinion on Drug Metabolism & Toxicology* 2, 231–240. <https://doi.org/10.1517/17425255.2.2.231>
- Sajevic, T., Leonardi, A., Križaj, I., 2014. An overview of hemostatically active components of *Vipera ammodytes* venom. *Toxin Reviews* 33, 33–36. <https://doi.org/10.3109/15569543.2013.835827>
- Sanhajariya, S., Duffull, S.B., Isbister, G.K., 2018. Pharmacokinetics of snake venom. *Toxins (Basel)* 10. <https://doi.org/10.3390/toxins10020073>
- Sano-Martins, I.S., Fan, H.W., Castro, S.C., Tomy, S.C., Franca, F.O., Jorge, M.T., Kamiguti, A.S., Warrell, D.A., Theakston, R.D., 1994. Reliability of the simple 20 minute whole blood clotting test

- (WBCT20) as an indicator of low plasma fibrinogen concentration in patients envenomed by Bothrops snakes. Butantan Institute Antivenom Study Group. *Toxicon* 32, 1045–50. [https://doi.org/10.1016/0041-0101\(94\)90388-3](https://doi.org/10.1016/0041-0101(94)90388-3)
- Sant'Ana Malaque, C.M., Gutiérrez, J.M., 2015. Snakebite Envenomation in Central and South America, in: Brent, J., Burkhart, K., Dargan, P., Hatten, B., Megarbane, B., Palmer, R. (Eds.), *Critical Care Toxicology*. Springer International Publishing, Cham, pp. 1–22. https://doi.org/10.1007/978-3-319-20790-2_146-1
- Serrano, S.M.T., 2013. The long road of research on snake venom serine proteinases. *Toxicon* 62, 19–26. <https://doi.org/10.1016/j.toxicon.2012.09.003>
- Serrano, S.M.T., Shannon, J.D., Wang, D., Camargo, A.C.M., Fox, J.W., 2005. A multifaceted analysis of viperid snake venoms by two-dimensional gel electrophoresis: an approach to understanding venom proteomics. *Proteomics* 5, 501–10. <https://doi.org/10.1002/pmic.200400931>
- Sharma, R., Sharma, S., 2022. *Physiology, Blood Volume, StatPearls*. StatPearls Publishing.
- Shimadzu Corporation, 2017. LCMS Bioanalysis of Antibody Drugs Using Fab-Selective Proteolysis nSMOL-Trastuzumab analysis. <https://doi.org/10.1039/c3an02104a>
- Silva, A., Isbister, G.K., 2020. Current research into snake antivenoms, their mechanisms of action and applications. *Biochem Soc Trans* 48, 537–546.
- Slagboom, J., Kaal, C., Arrahman, A., Vonk, F.J., Somsen, G., Calvete, J.J., Wüster, W., Kool, J., 2022. Analytical strategies in venomics. *Microchemical Journal* 107187. <https://doi.org/10.1016/J.MICROC.2022.107187>
- Soares, M.R., Oliveira-Carvalho, A.L., Wermelinger, L.S., Zingali, R.B., Ho, P.L., Junqueira-de-Azevedo, I. de L.M., Diniz, M.R.V., 2005. Identification of novel bradykinin-potentiating peptides and C-type natriuretic peptide from *Lachesis muta* venom. *Toxicon* 46, 31–38. <https://doi.org/10.1016/J.TOXICON.2005.03.006>
- South African Government, 2021. South Africa's provinces | South African Government [WWW Document]. URL <https://www.gov.za/about-sa/south-africas-provinces>
- Stephen, C., Leyser, S., Roberts, C., Mohamed, F., Balme, K., Curling, L., Marks, C., Wium, C., 2016. 36th International Congress of the European Association of Poisons Centres and Clinical Toxicologists (EAPCCT) 24-27 May, 2016, Madrid, Spain. *Clinical Toxicology* 54, 344–519. <https://doi.org/10.3109/15563650.2016.1165952>
- Steuten, J., Winkel, K., Carroll, T., Williamson, N.A., Ignjatovic, V., Fung, K., Purcell, A.W., Fry, B.G., 2007. The molecular basis of cross-reactivity in the Australian Snake Venom Detection Kit (SVDK). *Toxicon* 50, 1041–52. <https://doi.org/10.1016/j.toxicon.2007.07.023>
- Stone, K.L., Williams, K.R., 2009. Reverse-Phase HPLC Separation of Enzymatic Digests of Proteins. Humana Press, Totowa, NJ, pp. 941–950. https://doi.org/10.1007/978-1-59745-198-7_102
- Sun, Q.-Y., Bao, J., 2010. Purification, cloning and characterization of a metalloproteinase from *Naja atra* venom. *Toxicon* 56, 1459–69. <https://doi.org/10.1016/j.toxicon.2010.08.013>
- Swenson, S., Markland, F.S., 2005. Snake venom fibrin(ogen)olytic enzymes. *Toxicon* 45, 1021–1039. <https://doi.org/10.1016/J.TOXICON.2005.02.027>

- Tadokoro, T., Modahl, C.M., Maenaka, K., Aoki-Shioi, N., 2020. Cysteine-Rich Secretory Proteins (CRISPs) From Venomous Snakes: An Overview of the Functional Diversity in A Large and Underappreciated Superfamily. *Toxins (Basel)* 12. <https://doi.org/10.3390/toxins12030175>
- Tans, G., Rosing, J., 2001. Snake Venom Activators of Factor X: An Overview. *Pathophysiology of Haemostasis and Thrombosis* 31, 225–233. <https://doi.org/10.1159/000048067>
- Tasoulis, T., Isbister, G.K., 2017. A Review and Database of Snake Venom Proteomes. <https://doi.org/10.3390/toxins9090290>
- Theakston, R.D.G., Laing, G.D., 2014. Diagnosis of snakebite and the importance of immunological tests in venom research. *Toxins (Basel)* 6, 1667–1695. <https://doi.org/10.3390/toxins6051667>
- Tu, A.T., 1988. Snake venoms: general background and composition, in: *Venoms: Chemistry and Molecular Biology*. pp. 1–19.
- Uzair, B., Khan, B.A., Sharif, N., Shabbir, F., Mena, F., 2018. Phosphodiesterases (PDEs) from Snake Venoms: Therapeutic Applications. *Protein Pept Lett* 25, 612–618. <https://doi.org/10.2174/0929866525666180628160616>
- Uzawa, S., 1932. Über die phosphomonoesterase und die phosphodiesterase. *Journal of Biochemistry Tokyo* 15, 19–28.
- van der Walt, A.J., Muller, G.J., 2019. Berg adder (*Bitis atropos*) envenoming: an analysis of 14 cases. *Clin Toxicol (Phila)* 57, 131–136. <https://doi.org/10.1080/15563650.2018.1499931>
- Visser, J., Chapman, D.S., 1978. *Snakes and Snakebite*, 1st ed. Purnell, Cape Town.
- Wachel, L.W., Cole, L.J., 1964. Who Expert Committee on Biological Standardization. Seventeenth Report. *World Health Organ Tech Rep Ser* 293, 1–86.
- Walker, J.M., 2009. *The protein protocols handbook*. Humana Press.
- Walker, J.M., 1994. Nondenaturing Polyacrylamide Gel Electrophoresis of Proteins, in: *Basic Protein and Peptide Protocols*. Humana Press, New Jersey, pp. 17–22. <https://doi.org/10.1385/0-89603-268-X:17>
- Wang, C.-D.R., 2019. *Structural Investigation of Snake Venom Proteins by Mass Spectrometry*. University of Adelaide.
- Wang, C.R., Bubner, E.R., Jovcevski, B., Mittal, P., Pukala, T.L., 2020. Interrogating the higher order structures of snake venom proteins using an integrated mass spectrometric approach. *Journal of Proteomics* 216, 103680. <https://doi.org/10.1016/J.JPROT.2020.103680>
- Warrell, D.A., 2010. Snake bite. *The Lancet* 375, 77–88. [https://doi.org/10.1016/S0140-6736\(09\)61754-2](https://doi.org/10.1016/S0140-6736(09)61754-2)
- Warrell, D.A., 1999. WHO/SEARO guidelines for the clinical management of snake bites in Southeast Asian region. *Southeast Asian Journal of Tropical Med Public Health* 30(Suppl.), 1–85.
- Warrell, D.A., Davidson NMCD, Greenwood, B.M., Ormerod, L.D., Pope, H.M., Watkins, B.J., Prentice, C.R., 1977. Poisoning by bites of the saw-scaled or carpet viper (*Echis carinatus*) in Nigeria. *Q J Med* 46, 33–62.
- Warrell, D.A., Ormerod, L.D., Davidson, N.M., 1975. Bites by puff-adder (*Bitis arietans*) in Nigeria, and value of antivenom. *Br Med J* 4, 697–700. <https://doi.org/10.1136/bmj.4.5998.697>

- WHO, 2019. Snakebite envenoming [WWW Document]. WHO Fact Sheets. URL <https://www.who.int/news-room/fact-sheets/detail/snakebite-envenoming>
- Wiesel, G.A., dos Santos, P.K., Cordeiro, F.A., Bordon, K.C.F., Selistre-de-Araújo, H.S., Ueberheide, B., Arantes, E.C., 2015. Identification of hyaluronidase and phospholipase B in *Lachesis muta rhombeata* venom. *Toxicon* 107, 359–368. <https://doi.org/10.1016/j.toxicon.2015.08.029>
- Williams, H.F., Layfield, H.J., Vallance, T., Patel, K., Bicknell, A.B., Trim, S.A., Vaiyapuri, S., 2019a. The Urgent Need to Develop Novel Strategies for the Diagnosis and Treatment of Snakebites. *Toxins (Basel)* 11, 363. <https://doi.org/10.3390/toxins11060363>
- Williams, H.F., Mellows, B.A., Mitchell, R., Sfyri, P., Layfield, H.J., Salamah, M., Vaiyapuri, R., Collins-Hooper, H., Bicknell, A.B., Matsakas, A., Patel, K., Vaiyapuri, S., 2019b. Mechanisms underpinning the permanent muscle damage induced by snake venom metalloprotease. *PLoS Neglected Tropical Diseases* 13, 1–20. <https://doi.org/10.1371/journal.pntd.0007041>
- Wilson, D., Daly, N., 2018. Venomics: A Mini-Review. *High-Throughput* 7, 19. <https://doi.org/10.3390/ht7030019>
- Wium, C.A., Marks, C.J., du Plessis, C.E., Müller, G.J., 2017. Berg adder (*Bitis atropos*): An unusual case of acute poisoning. *South African Medical Journal* 107, 1075–1077. <https://doi.org/10.7196/SAMJ.2017.v107i12.12763>
- Wong, K.Y., Tan, C.H., Tan, K.Y., Quraishi, N.H., Tan, N.H., 2018. Elucidating the biogeographical variation of the venom of *Naja naja* (spectacled cobra) from Pakistan through a venom-decomplexing proteomic study. *Journal of Proteomics* 175, 156–173. <https://doi.org/10.1016/J.JPROT.2017.12.012>
- Wong, K.Y., Tan, C.H., Tan, N.H., 2016. Venom and Purified Toxins of the Spectacled Cobra (*Naja naja*) from Pakistan: Insights into Toxicity and Antivenom Neutralization. *The American Journal of Tropical Medicine and Hygiene* 94, 1392–1399. <https://doi.org/10.4269/ajtmh.15-0871>
- Wood, D., Sartorius, B., Hift, R., 2016a. Classifying snakebite in South Africa: Validating a scoring system. *South African Medical Journal* 107, 46. <https://doi.org/10.7196/SAMJ.2017.v107i1.11361>
- Wood, D., Sartorius, B., Hift, R., 2016b. Estimating the Burden of Snakebite on Public Hospitals in KwaZulu Natal, South Africa. *Wilderness Environ Med* 27, 53–61. <https://doi.org/10.1016/j.wem.2015.11.005>
- Wood, D., Sartorius, B., Hift, R., 2016c. Snakebite in north-eastern South Africa: clinical characteristics and risks for severity. *South African Family Practice* 58, 62–67. <https://doi.org/10.1080/20786190.2015.1120934>
- Yamazaki, Y., Matsunaga, Y., Tokunaga, Y., Obayashi, S., Saito, M., Morita, T., 2009. Snake venom Vascular Endothelial Growth Factors (VEGF-Fs) exclusively vary their structures and functions among species. *J Biol Chem* 284, 9885–91. <https://doi.org/10.1074/jbc.M809071200>
- Yamazaki, Y., Morita, T., 2004. Structure and function of snake venom cysteine-rich secretory proteins. *Toxicon* 44, 227–231. <https://doi.org/10.1016/j.toxicon.2004.05.023>

Appendix

Table 0.1 List of proteins that were identified in the venom from *Bitis atropos* after in-gel trypsin digestion and HR-LC-MS/MS analysis

#	Identified Protein	Protein family	Accession Number	Protein Molecular Weight	Protein Identification Probability	# Unique Peptides
1	Synergistic-type venom protein C9S3, chain 2	NC-3FTX	3SIY4_DENAN	7 kDa	100%	2
2	Mipartoxin-1A	NC-3FTX	3SX1A_MICMP	9 kDa	100%	2
3	Alpha-bungarotoxin N3	NC-3FTX	3L2N3_BUNCA	8 kDa	99%	2
4	Cytotoxin 1d/1e	CTX	3SA1D_NAJAT	9 kDa	100%	2
5	Cytotoxin 2	CTX	3SA2_NAJOX	7 kDa	100%	2
6	Cytotoxin 3	CTX	3SB3_HEMHA	7 kDa	100%	2
7	Cytotoxin	CTX	3SA0_NAJSP	9 kDa	100%	2
8	Toxin Lc a	LNTX	3L2A_LATCO	8 kDa	100%	2
9	Long neurotoxin 77	LNTX	3L277_DRYCN	10 kDa	100%	2
10	Disintegrin lebein-2-alpha	DIS	DID2A_MACLB	14 kDa	100%	2
11	Zinc metalloproteinase-disintegrin-like TSV-DM	SVMP	VM3TM_TRIST	69 kDa	100%	14
12	Zinc metalloproteinase-disintegrin-like HV1	SVMP	VM3H1_PROFL	68 kDa	100%	8
13	Zinc metalloproteinase-disintegrin-like halysase	SVMP	VM3HA_GLOHA	68 kDa	100%	8
14	Zinc metalloproteinase-disintegrin-like crostastatin	SVMP	VM31_CRODU	47 kDa	100%	6
15	Zinc metalloproteinase-disintegrin-like 4a	SVMP	VM34_CROAD	68 kDa	100%	5
16	Zinc metalloproteinase-disintegrin-like lachestatin-2	SVMP	VM32_LACMR	47 kDa	99%	5
17	Zinc metalloproteinase-disintegrin-like brevilysin H6	SVMP	VM3H6_GLOBR	68 kDa	100%	5
18	Zinc metalloproteinase-disintegrin-like	SVMP	VM3_CRODD	68 kDa	100%	8
19	Zinc metalloproteinase-disintegrin-like jararhagin (Fragment)	SVMP	VM3JA_BOTJA	64 kDa	100%	3
20	Zinc metalloproteinase-disintegrin-like bothropasin	SVMP	VM3BP_BOTJA	68 kDa	100%	4

21	Zinc metalloproteinase-disintegrin-like BITM06A	SVMP	VM36A_BOTIN	68 kDa	100%	4
22	Zinc metalloproteinase-disintegrin agkistin	SVMP	VM2AG_GLOHA	55 kDa	100%	4
23	Zinc metalloproteinase/disintegrin	SVMP	VM2J_PROJR	54 kDa	100%	5
24	Zinc metalloproteinase/disintegrin	SVMP	VM2T3_PROMU	54 kDa	100%	4
25	Zinc metalloproteinase/disintegrin	SVMP	VM2H1_GLOHA	54 kDa	100%	2
26	Zinc metalloproteinase/disintegrin	SVMP	VM2MB_GLOBR	56 kDa	100%	5
27	Zinc metalloproteinase/disintegrin	SVMP	VM2DI_GLOHA	53 kDa	100%	4
28	Hemorrhagic metalloproteinase-disintegrin-like kaouthiagin	SVMP	VM3K_NAJKA	44 kDa	100%	3
29	Zinc metalloproteinase-disintegrin-like kaouthiagin-like	SVMP	VM3KL_NAJAT	66 kDa	100%	9
30	Zinc metalloproteinase-disintegrin-like atrase-B	SVMP	VM3B_NAJAT	66 kDa	100%	11
31	Zinc metalloproteinase/disintegrin	SVMP	VM2A2_DEIAC	54 kDa	100%	6
32	Zinc metalloproteinase/disintegrin	SVMP	VM2RH_CALRH	54 kDa	100%	5
33	Zinc metalloproteinase-disintegrin-like batroxstatin-1	SVMP	VM31_BOTAT	46 kDa	100%	2
34	Zinc metalloproteinase/disintegrin	SVMP	VM2IA_BOTIN	53 kDa	100%	3
35	Snake venom metalloproteinase BaP1	SVMP	VM1B1_BOTAS	46 kDa	100%	6
36	Zinc metalloproteinase/disintegrin	SVMP	VM2_BOTAS	54 kDa	99%	5
37	Zinc metalloproteinase barnettlysin-1	SVMP	VM1B1_BOTBA	23 kDa	100%	4
38	Zinc metalloproteinase-disintegrin-like atrase-A	SVMP	VM3A_NAJAT	68 kDa	100%	10
39	Zinc metalloproteinase-disintegrin-like brevilysin H2a	SVMP	VM32A_GLOBR	47 kDa	100%	6
40	Zinc metalloproteinase-disintegrin-like brevilysin H2b	SVMP	VM32B_GLOBR	47 kDa	100%	3
41	Zinc metalloproteinase-disintegrin-like daborhagin-K	SVMP	VM3DK_DABRR	70 kDa	100%	8
42	Zinc metalloproteinase/disintegrin	SVMP	VM2AE_CROAT	54 kDa	100%	8
43	Zinc metalloproteinase-disintegrin-like HF3	SVMP	VM3H3_BOTJA	68 kDa	100%	7
44	Zinc metalloproteinase-disintegrin-like NaMP	SVMP	VM3_NAJAT	69 kDa	100%	4
45	Zinc metalloproteinase-disintegrin-like ACLD	SVMP	VM3AD_AGKCL	70 kDa	100%	6
46	Zinc metalloproteinase-disintegrin-like cobrin	SVMP	VM3_NAJKA	68 kDa	100%	3
47	Zinc metalloproteinase-disintegrin-like atragin	SVMP	VM3H_NAJAT	69 kDa	100%	5

48	Zinc metalloproteinase-disintegrin-like MTP4	SVMP	VM34_DRYCN	68 kDa	100%	6
49	Zinc metalloproteinase-disintegrin-like MTP9	SVMP	VM39_DRYCN	68 kDa	99%	4
50	Zinc metalloproteinase-disintegrin-like MTP8	SVMP	VM38_DRYCN	68 kDa	100%	4
51	Zinc metalloproteinase-disintegrin-like VLAIP-A	SVMP	VM3VA_MACLB	69 kDa	100%	7
52	Zinc metalloproteinase-disintegrin-like 2d	SVMP	VM32D_CROAD	68 kDa	100%	7
53	Zinc metalloproteinase-disintegrin-like 8	SVMP	VM38_CROAD	68 kDa	100%	4
54	Zinc metalloproteinase-disintegrin-like ohanin	SVMP	VM3_OPHHA	69 kDa	100%	6
55	Zinc metalloproteinase/disintegrin	SVMP	VM2FL_PROFL	55 kDa	100%	7
56	Zinc metalloproteinase-disintegrin-like agkihagin	SVMP	VM3AK_DEIAC	68 kDa	100%	5
57	Zinc metalloproteinase-disintegrin-like BmMP	SVMP	VM3_BUNMU	69 kDa	100%	7
58	Zinc metalloproteinase-disintegrin-like Eoc1	SVMP	VM3E1_ECHOC	69 kDa	100%	4
59	Zinc metalloproteinase-disintegrin-like VLAIP-B	SVMP	VM3VB_MACLB	69 kDa	100%	6
60	Zinc metalloproteinase-disintegrin-like atrolysin-A (Fragment)	SVMP	VM3AA_CROAT	47 kDa	100%	6
61	Zinc metalloproteinase-disintegrin BA-5A	SVMP	VM25A_BITAR	59 kDa	100%	6
62	Zinc metalloproteinase/disintegrin	SVMP	VM2MD_GLOBR	53 kDa	100%	5
63	Zinc metalloproteinase/disintegrin	SVMP	VM2MC_GLOBR	53 kDa	100%	4
64	Zinc metalloproteinase/disintegrin	SVMP	VM2SA_GLOSA	54 kDa	100%	5
65	Zinc metalloproteinase-disintegrin BlatH1	SVMP	VM2H1_BOTLA	54 kDa	100%	6
66	Zinc metalloproteinase-disintegrin-like ecarin	SVMP	VM3E_ECHCA	69 kDa	100%	6
67	Zinc metalloproteinase-disintegrin-like 3a	SVMP	VM33_CROAD	69 kDa	100%	9
68	Zinc metalloproteinase/disintegrin	SVMP	VM2L2_MACLB	53 kDa	100%	6
69	Zinc metalloproteinase-disintegrin-like stejnihagin-B	SVMP	VM3SB_TRIST	68 kDa	100%	4
70	Zinc metalloproteinase/disintegrin (Fragment)	SVMP	VM2P3_PROMU	46 kDa	100%	5
71	Zinc metalloproteinase/disintegrin	SVMP	VM2OC_ECHOC	55 kDa	100%	2
72	Snake venom metalloproteinase-disintegrin-like mocarhagin	SVMP	VM3M1_NAJMO	68 kDa	100%	2
73	Zinc metalloproteinase-disintegrin-like HR1b	SVMP	VM3HB_PROFL	69 kDa	100%	2
74	Zinc metalloproteinase-disintegrin-like VMP-III	SVMP	VM3V3_AGKPL	68 kDa	100%	3

75	Zinc metalloproteinase/disintegrin	SVMP	VM2J2_BOTJA	53 kDa	100%	6
76	Zinc metalloproteinase-disintegrin-like BfMP (Fragment)	SVMP	VM3_BUNFA	68 kDa	100%	8
77	Zinc metalloproteinase/disintegrin (Fragment)	SVMP	VM2BI_BITGA	37 kDa	100%	2
78	Zinc metalloproteinase-disintegrin VMP-II	SVMP	VM2_CROAD	55 kDa	100%	6
79	Zinc metalloproteinase-disintegrin 8	SVMP	VM28_CROAD	55 kDa	100%	4
80	Zinc metalloproteinase/disintegrin-like HR1a	SVMP	VM3HA_PROFL	69 kDa	100%	5
81	Zinc metalloproteinase/disintegrin VMP-II	SVMP	VM2V2_AGKPL	54 kDa	100%	3
82	Zinc metalloproteinase/disintegrin PMMP-1	SVMP	VM2P1_PROMU	53 kDa	100%	8
83	Zinc metalloproteinase/disintegrin	SVMP	VM2JN_PROJR	55 kDa	100%	2
84	Zinc metalloproteinase-disintegrin-like EoMP06 (Fragment)	SVMP	VM3E6_ECHOC	58 kDa	100%	8
85	Zinc metalloproteinase-disintegrin stejnitin	SVMP	VM2_TRIST	54 kDa	100%	2
86	Zinc metalloproteinase-disintegrin-like acurhagin	SVMP	VM3AH_DEIAC	69 kDa	100%	2
87	Zinc metalloproteinase/disintegrin PMMP-2	SVMP	VM2P2_PROMU	54 kDa	100%	4
88	Zinc metalloproteinase-disintegrin VMP-II	SVMP	VM2V2_CROAT	55 kDa	100%	9
89	Zinc metalloproteinase/disintegrin	SVMP	VM2TA_TRIGA	53 kDa	100%	2
90	Zinc metalloproteinase leucurolysin-B (Fragment)	SVMP	VM3LB_BOTLC	36 kDa	100%	2
91	Zinc metalloproteinase/disintegrin VMP-II	SVMP	VM2V2_CROVV	54 kDa	100%	2
92	Zinc metalloproteinase-disintegrin-like ammodytagin (Fragments)	SVMP	VM3A_VIPAA	20 kDa	100%	2
93	Zinc metalloproteinase/disintegrin ussurin	SVMP	VM2US_GLOUS	53 kDa	100%	7
94	Zinc metalloproteinase-disintegrin-like alternagin (Fragment)	SVMP	VM3A_BOTAL	22 kDa	100%	2
95	Snake venom metalloproteinase H5 (Fragment)	SVMP	VM1H5_DEIAC	46 kDa	100%	3
96	Snake venom metalloproteinase acutolysin-C	SVMP	VM1AC_DEIAC	47 kDa	100%	2
97	Snake venom metalloproteinase aculysin-1	SVMP	VM11_DEIAC	47 kDa	100%	4
98	Snake venom metalloproteinase kistomin	SVMP	VM1K_CALRH	47 kDa	100%	7
99	Snake venom metalloproteinase acutolysin-A	SVMP	VM1AA_DEIAC	47 kDa	100%	4
100	Snake venom metalloproteinase VMP1	SVMP	VM1V1_AGKPL	47 kDa	100%	13

101	Snake venom metalloproteinase BpirMP (Fragment)	SVMP	VM1_BOTPI	23 kDa	100%	2
102	Snake venom metalloproteinase BjussuMP-2 (Fragment)	SVMP	VM1B2_BOTJR	42 kDa	100%	6
103	Snake venom metalloproteinase BmooMPalpha-I	SVMP	VM1BI_BOTMO	23 kDa	99%	2
104	Snake venom metalloproteinase acutolysin-C	SVMP	VM1A3_DEIAC	21 kDa	100%	7
105	Snake venom metalloproteinase lebetase-4 (Fragment)	SVMP	VM1L4_MACLB	24 kDa	100%	6
106	Snake venom metalloproteinase ACLH	SVMP	VM1AH_AGKCL	46 kDa	100%	3
107	Snake venom metalloproteinase HF-1	SVMP	VM1H1_BOTMA	27 kDa	100%	4
108	Snake venom metalloproteinase BITM02A	SVMP	VM1B_BOTIN	46 kDa	100%	7
109	Snake venom metalloproteinase neuwiedase (Fragment)	SVMP	VM1N_BOTPA	23 kDa	100%	3
110	Snake venom metalloproteinase trimereylisin-2	SVMP	VM1T2_PROFL	23 kDa	100%	3
111	Snake venom metalloproteinase	SVMP	VM1_CROMM	47 kDa	100%	5
112	Snake venom metalloproteinase ACLF	SVMP	VM1A_AGKCL	46 kDa	99%	3
113	Snake venom metalloproteinase atrolysin-B	SVMP	VM1AB_CROAT	47 kDa	100%	6
114	Snake venom metalloproteinase atrolysin-C	SVMP	VM1AC_CROAT	47 kDa	99%	8
115	Snake venom metalloproteinase atroxase	SVMP	VM1AT_CROAT	23 kDa	100%	2
116	Snake venom metalloproteinase HT-2	SVMP	VM1H2_CRORU	23 kDa	100%	5
117	Snake venom metalloproteinase adamalysin-2	SVMP	VM12_CROAD	23 kDa	100%	2
118	Coagulation factor X-activating enzyme heavy chain	SVMP	VM3CX_MACLB	69 kDa	100%	3
119	Coagulation factor X-activating enzyme heavy chain	SVMP	VM3CX_DABSI	70 kDa	100%	3
120	Venom prothrombin activator notecarin-D2	Peptidase S1	FAXD2_NOTSC	51 kDa	100%	9
121	Venom prothrombin activator hopsarin-D	Peptidase S1	FAXD_HOPST	51 kDa	100%	4
122	Venom prothrombin activator trocarin-D	Peptidase S1	FAXD_TROCA	51 kDa	100%	4
123	Venom prothrombin activator omicarin-C catalytic subunit	Peptidase S1	FAXC_OXYMI	52 kDa	100%	3
124	Venom prothrombin activator vestarin-D1	Peptidase S1	FAXD1_DEMVE	53 kDa	100%	6
125	Venom prothrombin activator vestarin-D2	Peptidase S1	FAXD2_DEMVE	53 kDa	100%	6
126	Venom prothrombin activator oscutarin-C catalytic subunit	Peptidase S1	FAXC_OXYSU	52 kDa	100%	5
127	Venom prothrombin activator pseutarin-C catalytic subunit	Peptidase S1	FAXC_PSETE	52 kDa	100%	5

128	Venom prothrombin activator porpharin-D	Peptidase S1	FAXD_PSEPO	51 kDa	100%	4
129	Coagulation factor X isoform 2	Peptidase S1	FA102_PSETE	52 kDa	100%	5
130	Coagulation factor X	Peptidase S1	FA10_TROCA	54 kDa	100%	4
131	Coagulation factor X isoform 1	Peptidase S1	FA101_PSETE	54 kDa	100%	4
132	Venom prothrombin activator omicarin-C non-catalytic subunit	Cu-oxidase	FA5V_OXYMI	166 kDa	100%	27
133	Coagulation factor V	Cu-oxidase	FA5_PSETE	166 kDa	100%	17
134	Venom prothrombin activator oscutarin-C non-catalytic subunit	Cu-oxidase	FA5V_OXYSU	166 kDa	100%	20
135	Venom prothrombin activator pseutarin-C non-catalytic subunit	Cu-oxidase	FA5V_PSETE	166 kDa	100%	15
136	Cysteine-rich venom protein pseudechetoxin	CRiSP	CRVP_PSEAU	26 kDa	100%	2
137	Cysteine-rich venom protein	CRiSP	CRVP_AUSSU	26 kDa	100%	2
138	Cysteine-rich venom protein 2	CRiSP	CRVP2_HYDHA	26 kDa	100%	2
139	Cysteine-rich venom protein pseudechetoxin-like	CRiSP	CRVP_HOPST	26 kDa	100%	2
140	Cysteine-rich venom protein pseudecin	CRiSP	CRVP_PSEPO	26 kDa	100%	2
141	Cysteine-rich venom protein ophanin	CRiSP	CRVP_OPHHA	27 kDa	100%	2
142	Cysteine-rich venom protein kaouthin-1	CRiSP	CRVP1_NAJKA	27 kDa	100%	3
143	Cysteine-rich venom protein 2	CRiSP	CRVP_SISCA	27 kDa	100%	2
144	Cysteine-rich venom protein piscivorin	CRiSP	CRVP_AGKPI	27 kDa	100%	4
145	Cysteine-rich secretory protein	CRiSP	CRVP_CROAD	27 kDa	100%	3
146	Cysteine-rich venom protein	CRiSP	CRVP_PROMU	27 kDa	100%	3
147	Cysteine-rich venom protein (Fragment)	CRiSP	CRVP_VIPBN	25 kDa	100%	3
148	Cysteine-rich venom protein DIS2	CRiSP	CRVP2_DISTY	27 kDa	100%	3
149	Cysteine-rich venom protein DIS3	CRiSP	CRVP3_DISTY	27 kDa	100%	3
150	Cysteine-rich venom protein	CRiSP	CRVP_DEMVE	26 kDa	100%	3
151	Cysteine-rich venom protein (Fragment)	CRiSP	CRVP_TRIST	26 kDa	100%	2
152	Cysteine-rich venom protein	CRiSP	CRVP_CERRY	27 kDa	100%	2
153	Cysteine-rich venom protein ablomin	CRiSP	CRVP_GLOBL	27 kDa	100%	2
154	Cysteine-rich venom protein	CRiSP	CRVP_ECHCO	25 kDa	100%	2

155	Cysteine-rich venom protein TRI1 (Fragment)	CRiSP	CRVP_TRIBI	27 kDa	100%	2
156	Serotriflin	CRiSP	CRIS_PROFL	25 kDa	100%	2
157	Natriuretic peptide Na-NP	NP	VNP_NAJAT	17 kDa	100%	2
158	Bradykinin-potentiating and C-type natriuretic peptides	NP	BNP1_BOTJA	27 kDa	100%	4
159	Bradykinin-potentiating and C-type natriuretic peptides	NP	BNP_LACMU	25 kDa	100%	3
160	Bradykinin-potentiating and C-type natriuretic peptides	NP	BNP_GLOBL	27 kDa	100%	4
161	Bradykinin potentiating and C-type natriuretic peptides	NP	BNP_SISCA	21 kDa	100%	3
162	Natriuretic peptide Coa_NP2	NP	BNPL2_CROOA	3 kDa	100%	2
163	C-type lectin BPL	CTL	LECG_BOTPI	16 kDa	100%	3
164	C-type lectin PAL	CTL	LECG_BITAR	16 kDa	100%	3
165	C-type lectin lectoxin-Lio3	CTL	LECM3_ERYPO	18 kDa	100%	3
166	C-type lectin 1	CTL	LECM1_HYDHA	19 kDa	100%	2
167	C-type lectin	CTL	LECM_CERRY	18 kDa	100%	3
168	C-type lectin BFL-2	CTL	LECM2_BUNFA	18 kDa	100%	4
169	C-type Lectin CRL	CTL	LECG_CRORU	16 kDa	99%	2
170	C-type lectin lectoxin-Thr1	CTL	LECM_THRJA	18 kDa	100%	3
171	C-type lectin 9a	Snaclec	SL9A_CROAD	18 kDa	100%	3
172	Snaclec crotocetin	Snaclec	SL_CRODU	17 kDa	100%	3
173	Snaclec A3 (Fragment)	Snaclec	SLA3_MACLB	18 kDa	100%	3
174	Snaclec 5	Snaclec	SL5_DABSI	17 kDa	100%	3
175	Snaclec A8 (Fragment)	Snaclec	SLA8_MACLB	15 kDa	100%	3
176	Snaclec mamushigin subunit beta	Snaclec	SLB_GLOBL	17 kDa	100%	3
177	Snaclec A16	Snaclec	SLAG_MACLB	18 kDa	100%	3
178	Snaclec rhodocetin subunit alpha	Snaclec	SLEA_CALRH	16 kDa	100%	6
179	Snaclec bitiscetin subunit beta	Snaclec	SLB_BITAR	15 kDa	100%	2
180	Snaclec flavocetin-A subunit alpha	Snaclec	SLAA_PROFL	18 kDa	100%	3
181	Snaclec mucrocetin subunit alpha	Snaclec	SLOA_PROMU	18 kDa	100%	2

182	Snaclec mamushigin subunit alpha	Snaclec	SLA_GLOBL	18 kDa	100%	5
183	Snaclec crotoctin-1	Snaclec	SL1_CRODU	18 kDa	100%	3
184	Snaclec rhodocytin subunit alpha	Snaclec	SLYA_CALRH	16 kDa	100%	3
185	Snaclec stejaggregin-A subunit beta-2	Snaclec	SLAB2_TRIST	17 kDa	100%	2
186	Snaclec stejaggregin-A subunit beta-3	Snaclec	SLAB3_TRIST	17 kDa	99%	2
187	Snaclec alboaggregin-A subunit alpha'	Snaclec	SLA2_TRIAB	16 kDa	100%	3
188	Snaclec trimecetin subunit beta	Snaclec	SLTB_PROMU	17 kDa	100%	2
189	Snaclec rhinocetin subunit alpha	Snaclec	SLRA_BITRH	18 kDa	100%	2
190	Snaclec 2	Snaclec	SL2_BITGA	18 kDa	100%	2
191	Snaclec convulxin subunit beta	Snaclec	SLB_CRODU	17 kDa	100%	2
192	Snaclec agkicetin-C subunit beta	Snaclec	SLCB_DEIAC	17 kDa	100%	2
193	Snaclec alboaggregin-D subunit alpha	Snaclec	SLDA_TRIAB	18 kDa	100%	4
194	Snaclec VP12 subunit B	Snaclec	SLB_DABPA	15 kDa	100%	4
195	Snaclec 1	Snaclec	SL1_BITAR	17 kDa	100%	3
196	Snaclec agglucetin subunit alpha-1	Snaclec	SLA1_DEIAC	17 kDa	100%	2
197	Snaclec echicetin subunit alpha (Fragment)	Snaclec	SLA_ECHCA	16 kDa	100%	3
198	Snaclec trimecetin subunit alpha	Snaclec	SLTA_PROMU	18 kDa	100%	2
199	Snaclec alboaggregin-B subunit beta	Snaclec	SLBB_TRIAB	17 kDa	100%	2
200	Snaclec flavocetin-A subunit beta	Snaclec	SLAB_PROFL	17 kDa	100%	2
201	Snaclec bothrojaracin subunit alpha	Snaclec	SLAA_BOTJA	18 kDa	100%	2
202	Snaclec coagulation factor X-activating enzyme light chain 1	Snaclec	SLLC1_MACLB	17 kDa	100%	2
203	Snaclec coagulation factor IX/factor X-binding protein subunit B	Snaclec	SLB_GLOHA	17 kDa	100%	4
204	Snaclec coagulation factor IX/factor X-binding protein subunit B1	Snaclec	SL9B1_TRIST	17 kDa	100%	2
205	Snaclec subunit A	Snaclec	SLA_PHIOL	18 kDa	100%	2
206	Snaclec rhodocetin subunit gamma (Fragment)	Snaclec	SLEC_CALRH	16 kDa	100%	2
207	Snaclec clone 2100755	Snaclec	SL_DEIAC	18 kDa	100%	2
208	Snaclec alboaggregin-A subunit beta'	Snaclec	SLA4_TRIAB	14 kDa	100%	3

209	Kunitz-type serine protease inhibitor homolog dendrotoxin B	KTI	VKTHB_DENPO	6 kDa	100%	2
210	Kunitz-type serine protease inhibitor mulgin-4	KTI	VKT4_PSEAU	9 kDa	99%	2
211	Kunitz-type serine protease inhibitor blackelin-3	KTI	VKT3_PSEPO	9 kDa	100%	2
212	Cystatin	Cystatin	CYT_BITAR	13 kDa	100%	9
213	Cystatin	Cystatin	CYT_CRYNI	16 kDa	99%	2
214	Cystatin	Cystatin	CYT_MICIK	16 kDa	100%	3
215	Cystatin	Cystatin	CYT_PSETE	16 kDa	99%	2
216	Cystatin (Fragment)	Cystatin	CYT_NAJAT	11 kDa	100%	4
217	Bitiscystatin	Cystatin	CYT_BITGA	16 kDa	100%	2
218	Cystatin	Cystatin	CYT_NAJKA	16 kDa	100%	2
219	<i>A.superbus</i> venom factor 2	CVF	VCO32_AUSSU	185 kDa	100%	15
220	<i>A.superbus</i> venom factor 1	CVF	VCO31_AUSSU	185 kDa	100%	15
221	Cobra venom factor	CVF	VCO3_NAJKA	185 kDa	100%	28
222	Venom factor	CVF	VCO3_CROAD	185 kDa	100%	13
223	Ophiophagus venom factor	CVF	VCO3_OPHHA	184 kDa	100%	34
224	Thrombin-like enzyme cerastocytin	SVSP	VSP0_CERCE	28 kDa	100%	2
225	Snake venom serine protease 2	SVSP	VSP2_PROFL	29 kDa	100%	4
226	Venom serine proteinase-like protein	SVSP	VSP1_PROJR	29 kDa	100%	5
227	Snake venom serine protease homolog KN7	SVSP	VSP07_TRIST	29 kDa	99%	2
228	Snake venom serine protease homolog KN4	SVSP	VSP04_TRIST	29 kDa	100%	4
229	Snake venom serine protease KN13	SVSP	VSP13_TRIST	28 kDa	100%	5
230	Snake venom serine protease NaSP (Fragment)	SVSP	VSP1_NAJAT	31 kDa	100%	8
231	Snake venom serine protease BmSP (Fragment)	SVSP	VSP1_BUNMU	31 kDa	100%	8
232	Snake venom serine proteinase 8	SVSP	VSP8_CROAD	28 kDa	100%	5
233	Snake venom serine protease catroxase-2	SVSP	VSP2_CROAT	28 kDa	100%	4
234	Snake venom serine protease rhinocerase (Fragments)	SVSP	VSPR_BITRH	10 kDa	100%	2
235	Snake venom serine proteinase 12	SVSP	VSPC_CROAD	29 kDa	100%	2

236	Snake venom serine protease Dav-KN	SVSP	VSP3_DEIAC	28 kDa	100%	3
237	Snake venom serine protease homolog	SVSP	VSPH_BOTJR	29 kDa	100%	2
238	Serine protease sp-Eoc49	SVSP	VSP_ECHOC	28 kDa	100%	7
239	Serine protease harobin	SVSP	VSPHA_HYDHA	29 kDa	100%	7
240	Snake venom serine protease KN11	SVSP	VSP11_TRIST	28 kDa	100%	4
241	Snake venom serine protease pallabin	SVSP	VSP1_GLOHA	29 kDa	100%	3
242	Snake venom serine protease salmonase	SVSP	VSPSA_GLOBR	29 kDa	100%	3
243	Snake venom serine protease Dav-PA	SVSP	VSP_DEIAC	28 kDa	100%	5
244	Snake venom serine protease HS114	SVSP	VSP14_BOTJA	28 kDa	100%	4
245	Snake venom serine protease	SVSP	VSP_CRODD	28 kDa	100%	4
246	Snake venom serine protease 2B	SVSP	VSPB_TRIGA	29 kDa	100%	3
247	Snake venom serine protease 3	SVSP	VSP3_TRIGA	28 kDa	100%	3
248	Snake venom serine protease PA	SVSP	VSP_TRIST	28 kDa	100%	6
249	Snake venom serine protease	SVSP	VSP_LACST	28 kDa	100%	3
250	Snake venom serine protease	SVSP	VSP_PHIOL	28 kDa	100%	3
251	Snake venom serine protease KN8	SVSP	VSP08_TRIST	28 kDa	100%	4
252	Snake venom serine protease pictobin (Fragment)	SVSP	VSP_BOTPC	28 kDa	100%	3
253	Snake venom serine protease CL2	SVSP	VSP2_TRIST	28 kDa	100%	4
254	Snake venom serine protease nikobin	SVSP	VSP_VIPBN	28 kDa	100%	6
255	Snake venom serine protease HS112	SVSP	VSP12_BOTJA	28 kDa	100%	3
256	Snake venom serine protease serpentokallikrein-1	SVSP	VSP6_PROMU	29 kDa	100%	3
257	Snake venom serine protease VaSP1 (Fragments)	SVSP	VASP1_VIPAA	22 kDa	100%	5
258	Snake venom serine protease 2	SVSP	VSP2_PROJR	28 kDa	100%	4
259	Snake venom serine protease Haly-2	SVSP	VSPH2_GLOBR	28 kDa	100%	4
260	Venom serine proteinase-like protein 1	SVSP	VSP1_BITGA	29 kDa	100%	4
261	Snake venom serine protease 3	SVSP	VSP3_PROFL	28 kDa	100%	2
262	Snake venom serine protease Dav-X	SVSP	VSP4_DEIAC	29 kDa	100%	2

263	Snake venom serine protease 3	SVSP	VSP3_PROJR	28 kDa	100%	5
264	Snake venom serine protease CL5	SVSP	VSP5_TRIST	29 kDa	100%	2
265	Alpha- and beta-fibrinogenase OhS1	SVSP	VSP1_OPHHA	29 kDa	100%	5
266	Alpha-fibrinogenase-like	SVSP	VSPAF_DABSI	28 kDa	100%	2
267	Beta-fibrinogenase brevinase	SVSP	VSPB_GLOBL	26 kDa	100%	4
268	Beta-fibrinogenase stejnefibrase-2	SVSP	VSPS2_TRIST	28 kDa	100%	6
269	Alpha-fibrinogenase albofibrase	SVSP	VSPAF_TRIAB	28 kDa	100%	2
270	Alpha-fibrinogenase shedaoenase	SVSP	VSPSH_GLOSH	26 kDa	100%	2
271	Factor V activator	SVSP	VSPF5_MACLB	29 kDa	100%	3
272	Factor V activator RVV-V gamma	SVSP	VSPG_DABSI	29 kDa	100%	2
273	Factor V activator RVV-V alpha	SVSP	VSPA_DABSI	26 kDa	100%	3
274	Protein C activator	SVSP	VSPCA_AGKPL	28 kDa	100%	7
275	Protein C activator	SVSP	VSPCA_AGKCO	25 kDa	100%	6
276	Thrombin-like enzyme gyroxin analog	SVSP	VSPF_LACMU	26 kDa	100%	3
277	Thrombin-like enzyme ancrod-2	SVSP	VSPF2_CALRH	29 kDa	100%	3
278	Thrombin-like enzyme gyroxin B1,7	SVSP	VSP17_CRODU	28 kDa	100%	6
279	Thrombin-like enzyme saxthrombin	SVSP	VSPSX_GLOSA	28 kDa	100%	5
280	Thrombin-like enzyme contortrixobin	SVSP	VSP2_AGKCO	25 kDa	100%	2
281	Thrombin-like enzyme KN-BJ 2	SVSP	VSP2_BOTJA	28 kDa	100%	2
282	Thrombin-like enzyme TLBm	SVSP	VSP1_BOTMA	33 kDa	100%	2
283	Thrombin-like enzyme kangshuanmei	SVSP	VSP1_GLOBR	26 kDa	100%	5
284	Thrombin-like enzyme bilineobin	SVSP	VSP2_AGKBI	26 kDa	100%	2
285	Thrombin-like enzyme BjussuSP-1	SVSP	VSP1_BOTJR	25 kDa	100%	5
286	Thrombin-like enzyme asperase	SVSP	VSPL_BOTAS	28 kDa	100%	2
287	Thrombin-like enzyme stejnobin	SVSP	VSPST_TRIST	29 kDa	99%	2
288	Thrombin-like enzyme chitribisin	SVSP	VSPC_TRIAB	28 kDa	100%	2
289	Thrombin-like enzyme 2	SVSP	VSP2_TRIAB	29 kDa	100%	3

290	Thrombin-like enzyme glosedobin	SVSP	VSPGL_GLOSH	29 kDa	100%	3
291	Thrombin-like enzyme elegaxobin-2	SVSP	VSP2_PROEL	26 kDa	100%	2
292	Thrombin-like enzyme gyroxin B2,1	SVSP	VSP21_CRODU	27 kDa	100%	3
293	Thrombin-like enzyme bhalterin	SVSP	VSPBH_BOTAL	28 kDa	100%	3
294	Thrombin-like enzyme acutin (Fragment)	SVSP	VSPA_DEIAC	25 kDa	100%	6
295	Thrombin-like enzyme calobin-1	SVSP	VSP1_GLOUS	29 kDa	100%	6
296	Venom plasminogen activator Haly-PA	SVSP	VSPPA_GLOBR	28 kDa	100%	4
297	Venom plasminogen activator	SVSP	VSPPA_AGKPL	28 kDa	100%	4
298	Venom plasminogen activator LV-PA	SVSP	VSPPA_LACMU	28 kDa	100%	4
299	Venom plasminogen activator TSV-PA	SVSP	VSPPA_TRIST	28 kDa	100%	3
300	Venom plasminogen activator GPV-PA	SVSP	VSPPA_TRIAB	28 kDa	100%	3
301	Chymotrypsin-like protease VLCTLP	SVSP	VSPY_MACLB	28 kDa	100%	4
302	Platelet-aggregating proteinase PA-BJ (Fragment)	SVSP	VSP1_BOTJA	26 kDa	100%	4
303	Phospholipase A2 EC1	PLA2	PA21_ECHCO	16 kDa	100%	3
304	Acidic phospholipase A2 CC-PLA2-1	PLA2	PA2A1_CERCE	15 kDa	99%	2
305	Acidic phospholipase A2 Ts-A6	PLA2	PA2AF_TRIST	16 kDa	100%	3
306	Acidic phospholipase A2 6	PLA2	PA2A6_TRIGA	16 kDa	100%	3
307	Acidic phospholipase A2 S7-48J	PLA2	PA2A4_AUSSU	16 kDa	100%	3
308	Acidic phospholipase A2	PLA2	PA2A_AIPLA	16 kDa	100%	2
309	Acidic phospholipase A2 2	PLA2	PA2A2_MACLB	15 kDa	100%	2
310	Acidic phospholipase A2 1	PLA2	PA2A1_MACLB	16 kDa	100%	3
311	Acidic phospholipase A2 Ts-A1	PLA2	PA2AA_TRIST	16 kDa	100%	2
312	Acidic phospholipase A2 S9-53F	PLA2	PA2A5_AUSSU	16 kDa	100%	2
313	Acidic phospholipase A2 1	PLA2	PA2A1_PROFL	16 kDa	100%	4
314	Acidic phospholipase A2 Cvv-E6f	PLA2	PA2AF_CROVV (+1)	16 kDa	100%	2
315	Acidic phospholipase A2 Tbo-E6	PLA2	PA2A_TRIBO	16 kDa	100%	2

316	Acidic phospholipase A2 BITP01A	PLA2	PA2A_BOTIN	16 kDa	100%	3
317	Acidic phospholipase A2 57	PLA2	PA2A5_HYDHA	17 kDa	100%	2
318	Acidic phospholipase A2 1	PLA2	PA2A1_OPHHA	16 kDa	100%	3
319	Acidic phospholipase A2 ammodytin I1	PLA2	PA2A1_VIPAA	15 kDa	100%	2
320	Acidic phospholipase A2 VP8	PLA2	PA2A8_DABPA	15 kDa	100%	2
321	Acidic phospholipase A2 pgPLA 1b/pgPLA 2b	PLA2	PA2AP_PROFL	16 kDa	100%	2
322	Acidic phospholipase A2	PLA2	PA2A_BITGA	13 kDa	100%	2
323	Acidic phospholipase A2 jerdoxin	PLA2	PA2A_PROJR	16 kDa	100%	2
324	Basic phospholipase A2 Drk-b1	PLA2	PA2B1_DABRR	16 kDa	100%	4
325	Basic phospholipase A2 DsM-b1/DsM-b1'	PLA2	PA2B1_DABSI	16 kDa	100%	5
326	Basic phospholipase A2 1 (Fragment)	PLA2	PA2B1_NAJSG	14 kDa	100%	2
327	Basic phospholipase A2 paradoxin-like alpha chain	PLA2	PA2PA_OXYMI	16 kDa	100%	2
328	Basic phospholipase A2 PC20	PLA2	PA2BK_LATCO	17 kDa	100%	3
329	Basic phospholipase A2 vipoxin B chain	PLA2	PA2B_VIPAE	14 kDa	100%	2
330	Basic phospholipase A2 VRV-PL-V	PLA2	PA2B5_DABRR	14 kDa	100%	2
331	Basic phospholipase A2 homolog textilotoxin B chain	PLA2	PA2BB_PSETE	14 kDa	100%	2
332	Basic phospholipase A2 pseudexin B chain	PLA2	PA2BB_PSEPO	13 kDa	100%	3
333	Basic phospholipase A2 Tgc-K49	PLA2	PA2B_TRIGS	16 kDa	100%	3
334	Basic phospholipase A2 daboxin P	PLA2	PA2BD_DABRR	14 kDa	100%	2
335	Basic phospholipase A2 2	PLA2	PA2B2_LATCO	13 kDa	100%	3
336	Basic phospholipase A2 taipoxin alpha chain	PLA2	PA2TA_OXYSC	14 kDa	100%	2
337	Basic phospholipase A2 nigroxin A	PLA2	PA2BA_MICNI	13 kDa	100%	2
338	Basic phospholipase A2 PC1	PLA2	PA2B1_LATCO	17 kDa	100%	2
339	Inactive basic phospholipase A2 W6D49	PLA2	PA2BD_CALRH	15 kDa	100%	3
340	Neutral phospholipase A2 ammodytin I2	PLA2	PA2N2_VIPAA	15 kDa	100%	2
341	Neutral phospholipase A2 paradoxin-like beta chain	PLA2	PA2PB_OXYMI	16 kDa	100%	2
342	Phospholipase A2 acanmyotoxin-2 (Fragment)	PLA2	PA22_ACASS	3 kDa	100%	3

343	Basic phospholipase A2 beta-bungarotoxin A1 chain	PLA2	PA2B1_BUNCE	16 kDa	100%	2
344	Phospholipase A2 homolog EPL_00195	PLA2	PA2HS_ECHPL	14 kDa	100%	2
345	Phospholipase A2 OS1	PLA2	PA21_OXYSC	17 kDa	100%	2
346	Phospholipase A2 EC3	PLA2	PA23_ECHCO	16 kDa	100%	2
347	Phospholipase-B 81	PLB	PLB_DRYCN	64 kDa	100%	5
348	Phospholipase B	PLB	PLB_CROAD	64 kDa	100%	6
349	L-amino-acid oxidase	LAAO	OXLA_CALRH	58 kDa	100%	7
350	L-amino acid oxidase Bs29 (Fragment)	LAAO	OXLA_BOTSC	56 kDa	100%	8
351	L-amino-acid oxidase	LAAO	OXLA_TRIST	59 kDa	100%	6
352	L-amino acid oxidase Lm29	LAAO	OXLA_LACMT	59 kDa	100%	6
353	L-amino-acid oxidase	LAAO	OXLA_SISCA	59 kDa	100%	5
354	L-amino acid oxidase Cdc18 (Fragment)	LAAO	OXLA_CRODM	57 kDa	100%	6
355	L-amino-acid oxidase	LAAO	OXLA_CROAD	59 kDa	100%	4
356	L-amino acid oxidase bordonein-L	LAAO	OXLA_CRODU	59 kDa	100%	7
357	L-amino-acid oxidase	LAAO	OXLA_OPHHA	56 kDa	100%	5
358	L-amino-acid oxidase	LAAO	OXLA_BUNMU	59 kDa	100%	10
359	L-amino-acid oxidase	LAAO	OXLA_BUNFA	59 kDa	100%	10
360	L-amino-acid oxidase	LAAO	OXLA_NOTSC	59 kDa	100%	10
361	L-amino-acid oxidase	LAAO	OXLA_OXYSC	59 kDa	100%	8
362	L-amino acid oxidase (Fragment)	LAAO	OXLA_BOTPC	56 kDa	100%	5
363	L-amino-acid oxidase (Fragment)	LAAO	OXLA_BOTPA	57 kDa	100%	5
364	L-amino-acid oxidase (Fragment)	LAAO	OXLA_BOTJR	56 kDa	100%	6
365	L-amino acid oxidase	LAAO	OXLA_MICMP	57 kDa	100%	12
366	L-amino-acid oxidase	LAAO	OXLA_PSEAU	59 kDa	100%	6
367	L-amino-acid oxidase	LAAO	OXLA_VIPAA	55 kDa	100%	7
368	L-amino-acid oxidase (Fragments)	LAAO	OXLA_MACLB	12 kDa	100%	2
369	L-amino-acid oxidase	LAAO	OXLA_ECHOC	57 kDa	100%	7

370	L-amino-acid oxidase	LAAO	OXLA_DABRR	57 kDa	100%	12
371	L-amino-acid oxidase (Fragments)	LAAO	OXLA_DABSI	46 kDa	99%	9
372	L-amino-acid oxidase (Fragment)	LAAO	OXLA_NAJAT	58 kDa	100%	8
373	L-amino-acid oxidase	LAAO	OXLA_DEMVE	59 kDa	100%	5
374	L-amino acid oxidase (Fragments)	LAAO	OXLAB_CERCE	20 kDa	100%	6
375	L-amino acid oxidase	LAAO	OXLAA_CERCE	59 kDa	100%	6
376	L-amino oxidase (Fragments)	LAAO	OXLA_TRIPP	54 kDa	100%	5
377	L-amino-acid oxidase (Fragments)	LAAO	OXLA_VIPBB	10 kDa	100%	2
378	L-amino-acid oxidase (Fragment)	LAAO	OXLA_BOTIN	5 kDa	100%	2
379	Snake venom 5'-nucleotidase	5'-NUC	V5NTD_GLOBR	64 kDa	100%	14
380	Snake venom 5'-nucleotidase	5'-NUC	V5NTD_CROAD	65 kDa	100%	13
381	Snake venom 5'-nucleotidase (Fragment)	5'-NUC	V5NTD_NAJAT	58 kDa	100%	11
382	Acetylcholinesterase	AChE	ACES_BUNFA	68 kDa	100%	4
383	Snake venom metalloprotease inhibitor 02D01	SVMI	SVMI_ECHOC	33 kDa	100%	4
384	Phospholipase A2 inhibitor subunit A	PLI	PLIA_GLOBS	16 kDa	100%	3
385	Phospholipase A2 inhibitor clone 09	PLI	PLI9_LACMU	18 kDa	100%	2
386	Phospholipase A2 inhibitor subunit gamma B	PLI	PLIGB_GLOBS	22 kDa	100%	2
387	Phospholipase A2 inhibitor 31 kDa subunit	PLI	PLIB_NAJKA	20 kDa	100%	5
388	Phospholipase A2 inhibitor LNF1	PLI	PLI1_LACMU	22 kDa	100%	3
389	Phospholipase A2 inhibitor anMIP	PLI	PLI_ATRNM	18 kDa	100%	4
390	Phospholipase A2 myotoxin inhibitor protein	PLI	PLIP_BOTMO	18 kDa	100%	6
391	Phospholipase A2 inhibitor subunit B	PLI	PLIB_PROFL	16 kDa	100%	4
392	Phospholipase A2 inhibitor B1	PLI	PLIB1_CRODU	18 kDa	100%	4
393	PLIalpha-like protein	PLI	PLILP_ELAQU	18 kDa	100%	2
394	Phospholipase A2 inhibitor 1	PLI	PLI1_PROFL	22 kDa	100%	2
395	Phospholipase A2 inhibitor subunit gamma A	PLI	PLIGA_GLOBS	22 kDa	100%	4
396	Phospholipase A2 inhibitor	PLI	PLI_BOTJA	18 kDa	100%	4

397	Acidic phospholipase A2 inhibitor vaspin A chain	PLI	PA2H_VIPAZ	15 kDa	100%	2
398	Venom phosphodiesterase	PDE	PDE_MACLB	96 kDa	100%	24
399	Venom phosphodiesterase 2	PDE	PDE2_CROAD	92 kDa	100%	16
400	Venom phosphodiesterase 1	PDE	PDE1_CROAD	96 kDa	100%	17
401	Venom phosphodiesterase	PDE	PDE_NAJAT	95 kDa	100%	13
402	Venom nerve growth factor 2	VNGF	NGFV2_TROCA	28 kDa	100%	2
403	Venom nerve growth factor 5	VNGF	NGFV5_TROCA	28 kDa	99%	2
404	Venom nerve growth factor 2	VNGF	NGFV2_NAJSP	27 kDa	100%	4
405	Venom nerve growth factor	VNGF	NGFV_BOTJR	27 kDa	100%	2
406	Venom nerve growth factor	VNGF	NGFV_CRODU	27 kDa	100%	4
407	Venom nerve growth factor 2	VNGF	NGFV2_PSEAU	27 kDa	100%	2
408	Venom nerve growth factor	VNGF	NGFV_PSEPO	27 kDa	100%	2
409	Venom nerve growth factor 3	VNGF	NGFV3_PSEAU	27 kDa	99%	2
410	Venom nerve growth factor 2	VNGF	NGFV2_HOPST	28 kDa	100%	3
411	Venom nerve growth factor	VNGF	NGFV_BUNMU	28 kDa	100%	2
412	Venom nerve growth factor 3	VNGF	NGFV3_DEMVE	27 kDa	100%	4
413	Venom nerve growth factor 1 (Fragment)	VNGF	NGFV1_AZEFE	25 kDa	100%	6
414	Venom nerve growth factor	VNGF	NGFV_DABRR	13 kDa	100%	3
415	Venom nerve growth factor (Fragment)	VNGF	NGFV_ECHOC	18 kDa	100%	3
416	Vascular endothelial growth factor A	VEGF	VEGFA_AGKPI	23 kDa	100%	3
417	Vascular endothelial growth factor A	VEGF	VEGFA_BITGA	22 kDa	100%	3
418	Snake venom vascular endothelial growth factor toxin	VEGF	TXVE2_PROMU	16 kDa	100%	4
419	Snake venom vascular endothelial growth factor toxin	VEGF	TXVE_PROFL	16 kDa	100%	7
420	Snake venom vascular endothelial growth factor toxin vamin	VEGF	TXVE_VIPAA	16 kDa	100%	2
421	Snake venom vascular endothelial growth factor toxin cratrin	VEGF	TXVE_CROAT	16 kDa	100%	2
422	Hyaluronidase	HYA	HYAL_ECHOC	53 kDa	100%	3
423	Hyaluronidase-2	HYA	HYAL2_BITAR	52 kDa	100%	3

424	Vespryn	VES	VESP_CROAD	25 kDa	100%	4
425	Ohanin-like protein	VES	VESP_LACMU	24 kDa	100%	3
426	Waprin-Rha1	WAP	WAP1_RHATT	8 kDa	100%	2
427	Brain-derived neurotrophic factor (Fragment)	BDNF	BDNF_ASPME	25 kDa	100%	3
428	Brain-derived neurotrophic factor (Fragment)	BDNF	BDNF_RAMSP	25 kDa	100%	3
429	Brain-derived neurotrophic factor (Fragment)	BDNF	BDNF_LICTR	25 kDa	100%	4
430	Brain-derived neurotrophic factor (Fragment)	BDNF	BDNF_ERYJY	25 kDa	100%	2
431	Neurotrophin-3 (Fragment)	NTF	NTF3_MORSI	18 kDa	100%	3
432	Neurotrophin-3 (Fragment)	NTF	NTF3_ERYCN	18 kDa	100%	2
433	Neurotrophin-3 (Fragment)	NTF	NTF3_TROHA	19 kDa	100%	3
434	Neurotrophin-3 (Fragment)	NTF	NTF3_RAMSP	19 kDa	100%	3
435	Neurotrophin-3 (Fragment)	NTF	NTF3_XENUN	19 kDa	100%	3
436	Cytochrome b	CYB	CYB_ERYCC	42 kDa	100%	8
437	Cytochrome b	CYB	CYB_CHISM	42 kDa	100%	3
438	Cytochrome b	CYB	CYB_CHIFO	42 kDa	100%	7
439	Cytochrome b	CYB	CYB_CHISR	42 kDa	100%	3
440	Cytochrome b	CYB	CYB_CANCA	42 kDa	100%	8
441	Cytochrome b	CYB	CYB_ASPSC	42 kDa	100%	3
442	Cytochrome b	CYB	CYB_CANAS	42 kDa	100%	7
443	Cytochrome b	CYB	CYB_NOTAT	42 kDa	100%	2
444	Cytochrome b	CYB	CYB_CHIMS	42 kDa	100%	6
445	Cytochrome b	CYB	CYB_ANISC	42 kDa	100%	3
446	Cytochrome b	CYB	CYB_SANME	42 kDa	100%	6
447	Cytochrome b	CYB	CYB_ELANI	42 kDa	100%	4
448	Cytochrome b	CYB	CYB_BOACO	42 kDa	100%	4
449	Cytochrome b	CYB	CYB_ACRDU	42 kDa	100%	8
450	Cytochrome b	CYB	CYB_ACRMA	42 kDa	100%	8

451	Cytochrome b	CYB	CYB_NAJKA	42 kDa	100%	3
452	Cytochrome b	CYB	CYB_EPICE	42 kDa	100%	4
453	Cytochrome b	CYB	CYB_CASDU	42 kDa	100%	3
454	Cytochrome b	CYB	CYB_CORHE	42 kDa	100%	4
455	Cytochrome b	CYB	CYB_LYCSM	42 kDa	100%	3
456	Cytochrome b	CYB	CYB_CHIAG	42 kDa	100%	5
457	Cytochrome b	CYB	CYB_SINJA	42 kDa	100%	2
458	Cytochrome b	CYB	CYB_EUNMU	42 kDa	100%	7
459	Cytochrome b	CYB	CYB_ERYJA	42 kDa	100%	2
460	Cytochrome b (Fragment)	CYB	CYB_ATRMI	24 kDa	100%	2
461	Cytochrome b	CYB	CYB_HEMHA	42 kDa	100%	2
462	Cytochrome b	CYB	CYB_EUNNO	42 kDa	100%	5
463	Cytochrome b	CYB	CYB_ERYTA	42 kDa	100%	2
464	NADH-ubiquinone oxidoreductase chain 4 (Fragment)	NUO	NU4M_POROP	25 kDa	100%	2
465	NADH-ubiquinone oxidoreductase chain 4 (Fragment)	NUO	NU4M_GLOIT	26 kDa	100%	2
466	NADH-ubiquinone oxidoreductase chain 4 (Fragment)	NUO	NU4M_PROFL	25 kDa	100%	2
467	NADH-ubiquinone oxidoreductase chain 4 (Fragment)	NUO	NU4M_BOTER	25 kDa	100%	2
468	NADH-ubiquinone oxidoreductase chain 4 (Fragment)	NUO	NU4M_CROLE	25 kDa	100%	2
469	NADH-ubiquinone oxidoreductase chain 4 (Fragment)	NUO	NU4M_TRICN	26 kDa	100%	3
470	NADH-ubiquinone oxidoreductase chain 4 (Fragment)	NUO	NU4M_CROAD	25 kDa	100%	2
471	NADH-ubiquinone oxidoreductase chain 5	NUO	NU5M_LYCSM	66 kDa	100%	16
472	NADH-ubiquinone oxidoreductase chain 2	NUO	NU2M_LYCSM	38 kDa	100%	4
473	NADH-ubiquinone oxidoreductase chain 1	NUO	NU1M_LYCSM	36 kDa	100%	7
474	NADH-ubiquinone oxidoreductase chain 4	NUO	NU4M_LYCSM	50 kDa	100%	2
475	L-lactate dehydrogenase A chain	LDHD	LDHA_PYTRG	37 kDa	100%	3
476	TATA-box-binding protein	TBP	TBP_TRIGA	33 kDa	99%	2
477	TATA-box-binding protein	TBP	TBP_PROFL	33 kDa	100%	2

478	Translationally-controlled tumor protein homolog	TCTP	TCTP_MICFL	19 kDa	100%	3
479	Translationally-controlled tumor protein homolog	TCTP	TCTP_CROHD	19 kDa	100%	2
480	Putative lysosomal acid lipase/cholesteryl ester hydrolase	AB hydrolase	LICH_CROAD	46 kDa	100%	3
481	Actin, alpha skeletal muscle	Actin	ACTS_ATRMM	42 kDa	100%	8
482	ATP synthase protein 8	ATPases	ATP8_LYCSM	6 kDa	100%	2
483	Small serum protein 3	SSP	MSMB3_PROFL	9 kDa	100%	2
484	Crotalicidin	CTN	CAMP_CRODU	22 kDa	100%	2
485	Calglandulin	CAL	CALGL_HOPST	18 kDa	100%	3
486	Complement C3	CO3	CO3_NAJNA	185 kDa	100%	13
487	Cytochrome c oxidase subunit 1	COX	COX1_LYCSM	60 kDa	100%	2
488	Cytochrome c oxidase subunit 3	COX	COX3_LYCSM	30 kDa	100%	6
489	Cathelicidin-related antimicrobial peptide Na_CRAMP	CAMP	CAMP_NAJAT	22 kDa	100%	2
490	Cathelicidin-related peptide Oh-Cath	CAMP	CAMP_OPHHA	22 kDa	100%	2
491	Alpha-enolase	ENO	ENOA_PYTRG	48 kDa	100%	10
492	HSF-like protein	FE	FETHP_PROFL	37 kDa	100%	4
493	Antihemorrhagic factor HSF	FE	FETAF_PROFL	39 kDa	100%	4
494	Antihemorrhagic factor cHLP-A	FE	FETCA_GLOBR	37 kDa	100%	3
495	Ryncolin-1	FL	FCNV1_CERRY	38 kDa	99%	3
496	Ryncolin-3	FL	FCNV3_CERRY	38 kDa	100%	2
497	Ryncolin-4	FL	FCNV4_CERRY	38 kDa	100%	3
498	Hemoglobin subunit alpha-A	HB	HBA_DRYME	15 kDa	100%	2
499	Hemoglobin subunit alpha	HB	HBA_VIPAS	15 kDa	100%	2
500	Serine/threonine-protein kinase mos (Fragment)	PK	MOS_ATHNI	21 kDa	100%	2
501	Glutaminy-peptide cyclotransferase	QPCT	QPCT_BOIIR	42 kDa	100%	7
502	Glutaminy-peptide cyclotransferase	QPCT	QPCT_BOTJA	42 kDa	100%	5
503	Reticulocalbin-2	RCN	RCN2V_CROAD	36 kDa	100%	2
504	40S ribosomal protein S3a	RS3A	RS3A_OPHHA	30 kDa	100%	3

Abbreviations: 5'-NUC, snake venom 5'-nucleotidase (Fragment); AChE, acetylcholinesterase; ATPases, ATP synthase protein; BDNF, brain-derived neurotrophic factor; CAL, calglandulin; CAMP, cathelicidin-related antimicrobial peptide; CO3, complement C3; COX, cytochrome c oxidase; CRISP, cysteine-rich venom protein; CTL, C-type lectin; CTN, crotalacidin; CTX, cytotoxin; CVF, cobra venom factor; CYB, cytochrome B; DIS, disintegrin; ENO, enolase; FE, fetuin; FL, ficolin lectin; HB, hemoglobin; HYA, hyaluronidase; KTI, Kunitz-type serine protease inhibitor; LAAO, L-amino-acid oxidase; LDHD, lactate dehydrogenase; LNTX, long-neurotoxin; NC-3FTX, non-common 3-finger toxin; NP, natriuretic peptide; NTF, neurotrophic factor; NUO, NADH-ubiquinone oxidoreductase; PDE, venom phosphodiesterase; PK, protein kinases; PLA2, phospholipase A2; PLB, phospholipase B; PLI, phospholipase A2 inhibitor; QPCT, glutamyl-peptide cyclotransferase; RCN, reticulocalbin-2; RS3A, 40S ribosomal protein S3a; SSP, small serum protein; SVMI, snake venom metalloprotease inhibitor; SVMP, snake venom metalloproteinase; SVSP, snake venom serine protease; TBP, TATA-box-binding protein; TCTP, translationally-controlled tumor protein; VEGF, vascular endothelial growth factor; VES, vespryn; VNGF, venom nerve growth factor; WAP, waprin

Table 0.2 List of proteins that were identified in *N. nivea* venom by in-gel tryptic digestion and HR-LC-MS/MS analysis

#	Identified Proteins	Protein family	Accession Number	Molecular Weight	Identification probability	# Unique peptides
1	Cardiotoxin homolog TA-ctx-like	3FTX	3SO9L_BUNMU	10 kDa	100%	2
2	Toxin F-VIII	3FTX	3SOB8_DENAN	9 kDa	100%	3
3	Snake venom 5'-nucleotidase	5'-NUC	V5NTD_CROAD	65 kDa	100%	8
4	Snake venom 5'-nucleotidase	5'-NUC	V5NTD_GLOBR	64 kDa	100%	10
5	Snake venom 5'-nucleotidase (Fragment)	5'-NUC	V5NTD_NAJAT	58 kDa	100%	13
6	Acetylcholinesterase	AChE	ACES_BUNFA	68 kDa	100%	2
7	Actin, alpha skeletal muscle	Actin	ACTS_ATRMM	42 kDa	100%	3
8	Complement C3	CO3	CO3_NAJNA	185 kDa	100%	8
9	Cytochrome c oxidase subunit 3	COX	COX3_LYCSM	30 kDa	100%	5
10	Cysteine-rich venom protein (Fragment)	CRISP	CRVP_TRIST	26 kDa	100%	3

11	Cysteine-rich venom protein ablomin	CRiSP	CRVP_GLOBL	27 kDa	100%	3
12	Cysteine-rich venom protein DIS3	CRiSP	CRVP3_DISTY	27 kDa	100%	2
13	Cysteine-rich venom protein natrin-1	CRiSP	CRVP1_NAJAT	27 kDa	100%	6
14	Cysteine-rich venom protein natrin-2	CRiSP	CRVP2_NAJAT	26 kDa	100%	2
15	Cysteine-rich venom protein ophanin	CRiSP	CRVP_OPHHA	27 kDa	100%	6
16	C-type lectin 16	CTL	SLG_CROAD	17 kDa	100%	3
17	C-type lectin lectoxin-Lio3	CTL	LECM3_ERYPO	18 kDa	100%	2
18	Venom prothrombin activator omicarin-C non-catalytic subunit	Cu-oxidase	FA5V_OXYMI	166 kDa	100%	3
19	Venom prothrombin activator oscutarin-C non-catalytic subunit	Cu-oxidase	FA5V_OXYSU	166 kDa	100%	5
20	<i>A.superbus</i> venom factor 1	CVF	VCO31_AUSSU	185 kDa	100%	5
21	<i>A.superbus</i> venom factor 2	CVF	VCO32_AUSSU	185 kDa	100%	5
22	Cobra venom factor	CVF	VCO3_NAJKA	185 kDa	100%	21
23	Ophiophagus venom factor	CVF	VCO3_OPHHA	184 kDa	100%	16
24	Venom factor	CVF	VCO3_CROAD	185 kDa	100%	6
25	Cytochrome b	CYB	CYB_CANCA	42 kDa	100%	2
26	Cytochrome b	CYB	CYB_ASPSC	42 kDa	100%	2
27	Cytochrome b	CYB	CYB_CANAS	42 kDa	100%	2
28	Cytochrome b	CYB	CYB_COLCO	42 kDa	100%	2
29	Cytochrome b	CYB	CYB_CORHE	42 kDa	100%	2
30	Cytochrome b OS=Liasis mackloti savuensis	CYB	CYB_LIAMS	42 kDa	100%	3
31	Cytochrome c	CYC	CYC_CROVV	12 kDa	100%	2
32	Cystatin	Cystatin	CYT_BITAR	13 kDa	100%	3
33	Hemorrhagic metalloproteinase-disintegrin-like kaouthiagin	SVMP	VM3K_NAJKA	44 kDa	100%	3
34	Zinc metalloproteinase homolog-disintegrin albolatin	SVMP	VM2AL_TRIAB	54 kDa	100%	2
35	Zinc metalloproteinase-disintegrin BA-5A	SVMP	VM25A_BITAR	59 kDa	100%	3
36	Zinc metalloproteinase-disintegrin VMP-II	SVMP	VM2V2_CROAT	55 kDa	100%	3
37	Zinc metalloproteinase-disintegrin-like	SVMP	VM3_CERRY	69 kDa	100%	2

38	Zinc metalloproteinase-disintegrin-like	SVMP	VM3_CRODD	68 kDa	100%	2
39	Zinc metalloproteinase-disintegrin-like 4a	SVMP	VM34_CROAD	68 kDa	99%	2
40	Zinc metalloproteinase-disintegrin-like agkihagin	SVMP	VM3AK_DEIAC	68 kDa	100%	3
41	Zinc metalloproteinase-disintegrin-like atragin	SVMP	VM3H_NAJAT	69 kDa	100%	7
42	Zinc metalloproteinase-disintegrin-like atrase-A	SVMP	VM3A_NAJAT	68 kDa	100%	6
43	Zinc metalloproteinase-disintegrin-like atrase-B	SVMP	VM3B_NAJAT	66 kDa	100%	5
44	Zinc metalloproteinase-disintegrin-like BfMP (Fragment)	SVMP	VM3_BUNFA	68 kDa	100%	4
45	Zinc metalloproteinase-disintegrin-like BmMP	SVMP	VM3_BUNMU	69 kDa	100%	2
46	Zinc metalloproteinase-disintegrin-like brevilysin H6	SVMP	VM3H6_GLOBR	68 kDa	100%	3
47	Zinc metalloproteinase-disintegrin-like cobrin	SVMP	VM3_NAJKA	68 kDa	100%	5
48	Zinc metalloproteinase-disintegrin-like crotastatin	SVMP	VM31_CRODU	47 kDa	100%	3
49	Zinc metalloproteinase-disintegrin-like ecarin	SVMP	VM3E_ECHCA	69 kDa	100%	2
50	Zinc metalloproteinase-disintegrin-like HF3	SVMP	VM3H3_BOTJA	68 kDa	100%	2
51	Zinc metalloproteinase-disintegrin-like HR1b	SVMP	VM3HB_PROFL	69 kDa	100%	3
52	Zinc metalloproteinase-disintegrin-like HV1	SVMP	VM3H1_PROFL	68 kDa	100%	2
53	Zinc metalloproteinase-disintegrin-like kaouthiagin-like	SVMP	VM3KL_NAJAT	66 kDa	100%	5
54	Zinc metalloproteinase-disintegrin-like MTP4	SVMP	VM34_DRYCN	68 kDa	100%	3
55	Zinc metalloproteinase-disintegrin-like NaMP	SVMP	VM3_NAJAT	69 kDa	100%	2
56	Zinc metalloproteinase-disintegrin-like TSV-DM	SVMP	VM3TM_TRIST	69 kDa	100%	4
57	Zinc metalloproteinase-disintegrin-like VLAIP-B	SVMP	VM3VB_MACLB	69 kDa	100%	2
58	Zinc metalloproteinase-disintegrin-like VMP-III	SVMP	VM3V3_AGKPL	68 kDa	100%	2
59	Zinc metalloproteinase/disintegrin	SVMP	VM2DI_GLOHA	53 kDa	100%	2
60	Zinc metalloproteinase/disintegrin	SVMP	VM2AE_CROAT	54 kDa	100%	3
61	Zinc metalloproteinase/disintegrin	SVMP	VM2J_PROJR	54 kDa	100%	3
62	Zinc metalloproteinase/disintegrin	SVMP	VM2J2_BOTJA	53 kDa	99%	2
63	Zinc metalloproteinase/disintegrin	SVMP	VM2JN_PROJR	55 kDa	100%	2
64	Zinc metalloproteinase/disintegrin	SVMP	VM2MB_GLOBR	56 kDa	100%	2

65	Zinc metalloproteinase/disintegrin	SVMP	VM2T3_PROMU	54 kDa	99%	2
66	Zinc metalloproteinase/disintegrin	SVMP	VM2TA_TRIGA	53 kDa	100%	2
67	Zinc metalloproteinase/disintegrin (Fragment)	SVMP	VM2P3_PROMU	46 kDa	100%	2
68	Zinc metalloproteinase/disintegrin ussurin	SVMP	VM2US_GLOUS	53 kDa	100%	2
69	Alpha-enolase	ENO	ENOA_PYTRG	48 kDa	100%	5
70	Antihemorrhagic factor BJ46a	FE	FTE46_BOTJA	39 kDa	100%	2
71	Antihemorrhagic factor cMSF	FE	FETC_GLOBR	37 kDa	100%	3
72	HSF-like protein	FE	FETHP_PROFL	37 kDa	100%	2
73	Hemoglobin subunit alpha-1	HB	HBA1_NAJNA	15 kDa	100%	2
74	Kunitz-type serine protease inhibitor 3	KTI	VKT3_VIPAA	10 kDa	100%	2
75	Kunitz-type serine protease inhibitor bitisilin-2	KTI	VKT2_BITGA	10 kDa	100%	3
76	Kunitz-type serine protease inhibitor C6	KTI	VKTC6_DABSI	10 kDa	100%	2
77	L-amino acid oxidase	LAAO	OXLAA_CERCE	59 kDa	100%	2
78	L-amino acid oxidase (Fragments)	LAAO	OXLAB_CERCE	20 kDa	99%	2
79	L-amino acid oxidase Bs29 (Fragment)	LAAO	OXLA_BOTSC	56 kDa	100%	2
80	L-amino-acid oxidase	LAAO	OXLA_BUNFA	59 kDa	100%	4
81	L-amino-acid oxidase	LAAO	OXLA_BUNMU	59 kDa	100%	3
82	L-amino-acid oxidase	LAAO	OXLA_DABRR	57 kDa	100%	2
83	L-amino-acid oxidase	LAAO	OXLA_NOTSC	59 kDa	100%	2
84	L-amino-acid oxidase	LAAO	OXLA_OPHHA	56 kDa	100%	2
85	L-amino-acid oxidase	LAAO	OXLA_OXYSC	59 kDa	100%	3
86	L-amino-acid oxidase	LAAO	OXLA_PSEAU	59 kDa	100%	2
87	L-amino-acid oxidase (Fragment)	LAAO	OXLA_NAJAT	58 kDa	100%	5
88	Natriuretic peptide PaNP-d (Fragment)	NP	VNPD_PSEAU	4 kDa	100%	2
89	Neurotrophin-3 (Fragment)	NTF	NTF3_RAMSP	19 kDa	100%	2
90	NADH-ubiquinone oxidoreductase chain 4 (Fragment)	NUO	NU4M_TRICN	26 kDa	100%	2
91	NADH-ubiquinone oxidoreductase chain 5	NUO	NU5M_LYCSM	66 kDa	100%	5

92	Venom phosphodiesterase	PDE	PDE_MACLb	96 kDa	100%	8
93	Venom phosphodiesterase	PDE	PDE_NAJAT	95 kDa	100%	9
94	Venom phosphodiesterase 1	PDE	PDE1_CROAD	96 kDa	99%	6
95	Venom phosphodiesterase 2	PDE	PDE2_CROAD	92 kDa	100%	6
96	Coagulation factor X isoform 2	Peptidase S1	FA102_PSETE	52 kDa	100%	2
97	Venom prothrombin activator notecarin-D2	Peptidase S1	FAXD2_NOTSC	51 kDa	100%	5
98	Venom prothrombin activator vestarin-D1	Peptidase S1	FAXD1_DEMVE	53 kDa	100%	2
99	Venom prothrombin activator vestarin-D2	Peptidase S1	FAXD2_DEMVE	53 kDa	100%	3
100	Acidic phospholipase A2 1	PLA2	PA2A1_PSETE	17 kDa	100%	2
101	Acidic phospholipase A2 2	PLA2	PA2A2_TRIGA	14 kDa	100%	2
102	Acidic phospholipase A2 2 (Fragment)	PLA2	PA2A2_NAJSG	14 kDa	100%	2
103	Acidic phospholipase A2 natratoxin	PLA2	PA2A_NAJAT	13 kDa	100%	2
104	Acidic phospholipase A2 Ts-A1	PLA2	PA2AA_TRIST	16 kDa	100%	2
105	Basic phospholipase A2 homolog bothropstoxin-2	PLA2	PA2B2_BOTJR	16 kDa	100%	2
106	Basic phospholipase A2 RV-4	PLA2	PA2B4_DABSI	16 kDa	100%	2
107	Phospholipase B	PLB	PLB_CROAD	64 kDa	100%	2
108	Phospholipase A2 inhibitor 25 kDa subunit	PLI	PLIA_NAJKA	20 kDa	100%	2
109	Phospholipase A2 inhibitor 31 kDa subunit	PLI	PLIB_NAJKA	20 kDa	100%	2
110	Phospholipase A2 inhibitor anMIP	PLI	PLI_ATRNM	18 kDa	100%	2
111	Snaclec rhodocetin subunit alpha	Snaclec	SLEA_CALRH	16 kDa	100%	2
112	Snake venom metalloproteinase	SVMP	VM1_CROMM	47 kDa	100%	4
113	Snake venom metalloproteinase aculyisin-1	SVMP	VM11_DEIAC	47 kDa	100%	2
114	Snake venom metalloproteinase acutolysin-A	SVMP	VM1AA_DEIAC	47 kDa	100%	2
115	Snake venom metalloproteinase acutolysin-C	SVMP	VM1AC_DEIAC	47 kDa	100%	2
116	Snake venom metalloproteinase atroxase	SVMP	VM1AT_CROAT	23 kDa	100%	2
117	Alpha- and beta-fibrinogenase OhS1	SVSP	VSP1_OPHHA	29 kDa	100%	4

118	Chymotrypsin-like protease VLCTLP OS=Macrovipera lebetina OX=8709 PE=1 SV=1	SVSP	VSPY_MACLB	28 kDa	100%	2
119	Protein C activator	SVSP	VSPCA_AGKPL	28 kDa	100%	3
120	Serine protease sp-Eoc49	SVSP	VSP_ECHOC	28 kDa	100%	5
121	Snake venom serine protease	SVSP	VSP_CRODD	28 kDa	100%	2
122	Snake venom serine protease	SVSP	VSP_PHIOL	28 kDa	100%	2
123	Snake venom serine protease 2	SVSP	VSP2_PROFL	29 kDa	100%	2
124	Snake venom serine protease BmSP (Fragment)	SVSP	VSP1_BUNMU	31 kDa	100%	2
125	Snake venom serine protease BPA	SVSP	VSP3_BOTJA	28 kDa	100%	2
126	Snake venom serine protease catroxase-1	SVSP	VSP1_CROAT	29 kDa	100%	2
127	Snake venom serine protease Haly-2	SVSP	VSPH2_GLOBR	28 kDa	100%	2
128	Snake venom serine protease homolog KN4	SVSP	VSP04_TRIST	29 kDa	99%	3
129	Snake venom serine protease NaSP (Fragment)	SVSP	VSP1_NAJAT	31 kDa	100%	2
130	Snake venom serine protease salmonase	SVSP	VSPSA_GLOBR	29 kDa	100%	2
131	Thrombin-like enzyme acutin (Fragment)	SVSP	VSPA_DEIAC	25 kDa	100%	3
132	Thrombin-like enzyme BjussuSP-1	SVSP	VSP1_BOTJR	25 kDa	100%	2
133	Thrombin-like enzyme cerastocytin	SVSP	VSP_CERCE	28 kDa	100%	3
134	Thrombin-like enzyme contortixobin	SVSP	VSP2_AGKCO	25 kDa	100%	2
135	Thrombin-like enzyme gyroxin analog	SVSP	VSPF_LACMU	26 kDa	100%	2
136	Venom plasminogen activator	SVSP	VSPPA_AGKPL	28 kDa	100%	2
137	Venom plasminogen activator GPV-PA	SVSP	VSPPA_TRIAB	28 kDa	100%	2
138	Venom plasminogen activator TSV-PA	SVSP	VSPPA_TRIST	28 kDa	100%	2
139	Snake venom vascular endothelial growth factor toxin	VEGF	TXVE_BOTIN	16 kDa	100%	2
140	Vascular endothelial growth factor A	VEGF	VEGFA_AGKPI	23 kDa	100%	2
141	Vespryn	VES	VESP_CROAD	25 kDa	99%	2
142	Vespryn-21	VES	VESP_DRYCN	21 kDa	99%	2
143	Venom nerve growth factor 2	VNGF	NGFV2_NAJSP	27 kDa	100%	3

144	Venom nerve growth factor 2	VNGF	NGFV2_PSETE	27 kDa	100%	2
-----	-----------------------------	------	-------------	--------	------	---

Abbreviations: 3FTX, 3-Finger toxin; 5'-NUC, snake venom 5'-nucleotidase; AChE, acetylcholinesterase; CO3, complement C3; COX, cytochrome c oxidase; CRiSP, cysteine-rich venom protein; CTL, C-type lectin; CVF, cobra venom factor; CYB, cytochrome B; CYC, cytochrome c; ENO, enolase; FE, fetuin; HB, hemoglobin; KTI, Kunitz-type serine protease inhibitor; LAAO, L-amino-acid oxidase; NP, natriuretic peptide; NTF, neurotrophic factor; NUO, NADH-ubiquinone oxidoreductase; PDE, venom phosphodiesterase; PLA2, phospholipase A2; PLB, phospholipase B; PLI, phospholipase A2 inhibitor; SVMP, snake venom metalloproteinase; SVSP, snake venom serine protease; VEGF, vascular endothelial growth factor; VES, vespryn; VNGF, venom nerve growth factor

Table 0.3 List of proteins that were identified in *B. arietans* venom by in-gel tryptic digestion and HR-LC-MS/MS analysis

#	Identified Proteins	Protein family	Accession Number	Molecular Weight	Identification probability	#Unique peptides
1	Snake venom 5'-nucleotidase	5'-NUC	V5NTD_CROAD	65 kDa	100%	7
2	Snake venom 5'-nucleotidase	5'-NUC	V5NTD_GLOBR	64 kDa	100%	7
3	Snake venom 5'-nucleotidase (Fragment)	5'-NUC	V5NTD_NAJAT	58 kDa	100%	8
4	Complement C3	CO3	CO3_NAJNA	185 kDa	100%	6
6	Cytochrome c oxidase subunit 3	COX	COX3_LYCSM	30 kDa	100%	6
10	Venom factor	CVF	VCO3_CROAD	185 kDa	100%	6
11	Cobra venom factor	CVF	VCO3_NAJKA	185 kDa	100%	11
12	Ophiophagus venom factor	CVF	VCO3_OPHHA	184 kDa	100%	9
13	A.superbus venom factor 1	CVF	VCO31_AUSSU	185 kDa	100%	4
14	A.superbus venom factor 2	CVF	VCO32_AUSSU	185 kDa	100%	4
16	Cytochrome b	CYB	CYB_CANAS	42 kDa	100%	2
17	Cytochrome b	CYB	CYB_CANCA	42 kDa	100%	2
20	Cytochrome b	CYB	CYB_CORHE	42 kDa	100%	2
32	Cystatin	Cystatin	CYT_BITAR	13 kDa	100%	8

35	Zinc metalloproteinase-disintegrin BA-5A	SVMP	VM25A_BITAR	59 kDa	100%	2
36	Zinc metalloproteinase/disintegrin	SVMP	VM2AE_CROAT	54 kDa	100%	4
41	Zinc metalloproteinase/disintegrin	SVMP	VM2J_PROJR	54 kDa	99%	2
45	Zinc metalloproteinase-disintegrin VMP-II	SVMP	VM2V2_CROAT	55 kDa	100%	2
46	Zinc metalloproteinase-disintegrin-like BfMP (Fragment)	SVMP	VM3_BUNFA	68 kDa	100%	2
47	Zinc metalloproteinase-disintegrin-like BmMP	SVMP	VM3_BUNMU	69 kDa	100%	2
49	Zinc metalloproteinase-disintegrin-like	SVMP	VM3_CRODD	68 kDa	100%	4
50	Zinc metalloproteinase-disintegrin-like NaMP	SVMP	VM3_NAJAT	69 kDa	100%	4
51	Zinc metalloproteinase-disintegrin-like crostastatin	SVMP	VM31_CRODU	47 kDa	100%	3
54	Zinc metalloproteinase-disintegrin-like MTP4	SVMP	VM34_DRYCN	68 kDa	100%	2
58	Zinc metalloproteinase-disintegrin-like HV1	SVMP	VM3H1_PROFL	68 kDa	100%	2
60	Zinc metalloproteinase-disintegrin-like HR1b	SVMP	VM3HB_PROFL	69 kDa	100%	4
61	Hemorrhagic metalloproteinase-disintegrin-like kaouthiagin	SVMP	VM3K_NAJKA	44 kDa	100%	3
63	Zinc metalloproteinase-disintegrin-like TSV-DM	SVMP	VM3TM_TRIST	69 kDa	100%	3
64	Zinc metalloproteinase-disintegrin-like VLAIP-B	SVMP	VM3VB_MACLB	69 kDa	100%	3
65	Alpha-enolase	ENO	ENOA_PYTRG	48 kDa	100%	11
67	HSF-like protein	FE	FETHP_PROFL	37 kDa	100%	5
72	L-amino-acid oxidase	LAAO	OXLA_BUNMU	59 kDa	100%	6
74	L-amino-acid oxidase	LAAO	OXLA_DABRR	57 kDa	100%	10
79	L-amino-acid oxidase (Fragment)	LAAO	OXLA_NAJAT	58 kDa	100%	3
80	L-amino-acid oxidase	LAAO	OXLA_OPHHA	56 kDa	100%	2
81	L-amino-acid oxidase	LAAO	OXLA_OXYSC	59 kDa	100%	7
82	L-amino-acid oxidase	LAAO	OXLA_PSEAU	59 kDa	100%	4
91	NADH-ubiquinone oxidoreductase chain 5	NUO	NU5M_LYCSM	66 kDa	100%	9
92	Venom phosphodiesterase	PDE	PDE_MACLB	96 kDa	100%	9
93	Venom phosphodiesterase	PDE	PDE_NAJAT	95 kDa	100%	4
95	Venom phosphodiesterase 2	PDE	PDE2_CROAD	92 kDa	100%	8

97	Coagulation factor X isoform 2	Peptidase S1	FA102_PSETE	52 kDa	100%	3
99	Venom prothrombin activator omicarin-C non-catalytic subunit	Peptidase S1	FA5V_OXYMI	166 kDa	100%	5
100	Venom prothrombin activator oscutarin-C non-catalytic subunit	Peptidase S1	FA5V_OXYSU	166 kDa	100%	8
104	Venom prothrombin activator vestarin-D1	Peptidase S1	FAXD1_DEMVE	53 kDa	100%	4
105	Venom prothrombin activator vestarin-D2	Peptidase S1	FAXD2_DEMVE	53 kDa	100%	3
106	Venom prothrombin activator notecarin-D2	Peptidase S1	FAXD2_NOTSC	51 kDa	100%	6
116	Phospholipase B	PLB	PLB_CROAD	64 kDa	100%	4
118	Phospholipase A2 inhibitor anMIP	PLI	PLI_ATRNM	18 kDa	100%	3
120	Phospholipase A2 inhibitor 31 kDa subunit	PLI	PLIB_NAJKA	20 kDa	100%	2
140	Snake venom metalloproteinase	SVMP	VM1_CROMM	47 kDa	100%	5
141	Snake venom metalloproteinase aculysin-1	SVMP	VM11_DEIAC	47 kDa	99%	2
144	Snake venom metalloproteinase acutolysin-C	SVMP	VM1AC_DEIAC	47 kDa	99%	2
150	Serine protease sp-Eoc49	SVSP	VSP_ECHOC	28 kDa	100%	4
152	Snake venom serine protease	SVSP	VSP_PHIOL	28 kDa	100%	3
155	Thrombin-like enzyme BjussuSP-1	SVSP	VSP1_BOTJR	25 kDa	100%	3
156	Snake venom serine protease BmSP (Fragment)	SVSP	VSP1_BUNMU	31 kDa	99%	6
159	Alpha- and beta-fibrinogenase OhS1	SVSP	VSP1_OPHHA	29 kDa	100%	3
163	Thrombin-like enzyme acutin (Fragment)	SVSP	VSPA_DEIAC	25 kDa	100%	5
167	Protein C activator	SVSP	VSPCA_AGKPL	28 kDa	100%	3
168	Thrombin-like enzyme gyroxin analog	SVSP	VSPF_LACMU	26 kDa	100%	4
170	Thrombin-like enzyme cerastocytin	SVSP	VSP_CERCE	28 kDa	100%	4
171	Venom plasminogen activator	SVSP	VSPPA_AGKPL	28 kDa	100%	2
173	Venom plasminogen activator TSV-PA	SVSP	VSPPA_TRIST	28 kDa	100%	2
179	Vascular endothelial growth factor A	VEGF	VEGFA_AGKPI	23 kDa	100%	3
182	Venom nerve growth factor 2	VNGF	NGFV2_NAJSP	27 kDa	99%	2
9	Cardiotoxin homolog TA-ctx-like	CTX	3SO9L_BUNMU	10 kDa	100%	2
27	Cytochrome b	CYB	CYB_LIAMS	42 kDa	100%	3

38	Zinc metalloproteinase homolog-disintegrin albolatin	SVMP	VM2AL_TRIAB	54 kDa	100%	2
48	Zinc metalloproteinase-disintegrin-like	SVMP	VM3_CERRY	69 kDa	100%	2
68	Hemoglobin subunit alpha-1	HB	HBA1_NAJNA	15 kDa	100%	2
112	Basic phospholipase A2 homolog bothropstoxin-2	PLA2	PA2B2_BOTJR	16 kDa	100%	2
113	Basic phospholipase A2 RV-4	PLA2	PA2B4_DABSI	16 kDa	100%	2
157	Snake venom serine protease catroxase-1	SVSP	VSP1_CROAT	29 kDa	100%	3
94	Venom phosphodiesterase 1	PDE	PDE1_CROAD	96 kDa	100%	8
153	Snake venom serine protease homolog KN4	SVSP	VSP04_TRIST	29 kDa	100%	5
5	Cytochrome c oxidase subunit 1	COX	COX1_LYCSM	60 kDa	100%	2
7	Cysteine-rich venom protein DIS2	CRiSP	CRVP2_DISTY	27 kDa	100%	2
8	Cysteine-rich venom protein 2	CRiSP	CRVP2_HYDHA	26 kDa	100%	2
18	Cytochrome b	CYB	CYB_CASDU	42 kDa	100%	2
19	Cytochrome b	CYB	CYB_CHISM	42 kDa	100%	3
21	Cytochrome b	CYB	CYB_EPICE	42 kDa	100%	2
22	Cytochrome b	CYB	CYB_ERYCC	42 kDa	100%	3
24	Cytochrome b	CYB	CYB_EUNMU	42 kDa	100%	2
25	Cytochrome b	CYB	CYB_EUNNO	42 kDa	100%	2
30	Cytochrome b	CYB	CYB_SANME	42 kDa	100%	4
31	Cytochrome b	CYB	CYB_SINJA	42 kDa	100%	2
33	Cystatin (Fragment)	Cystatin	CYT_NAJAT	11 kDa	100%	3
34	Zinc metalloproteinase-disintegrin stejnitin	SVMP	VM2_TRIST	54 kDa	100%	2
37	Zinc metalloproteinase-disintegrin agkistin	SVMP	VM2AG_GLOHA	55 kDa	100%	4
39	Zinc metalloproteinase-disintegrin BlatH1	SVMP	VM2H1_BOTLA	54 kDa	100%	3
40	Zinc metalloproteinase/disintegrin	SVMP	VM2IA_BOTIN	53 kDa	100%	2
42	Zinc metalloproteinase/disintegrin PMMP-1	SVMP	VM2P1_PROMU	53 kDa	100%	3
43	Zinc metalloproteinase/disintegrin	SVMP	VM2RH_CALRH	54 kDa	100%	3
44	Zinc metalloproteinase/disintegrin VMP-II	SVMP	VM2V2_AGKPL	54 kDa	100%	2

52	Zinc metalloproteinase-disintegrin-like brevilysin H2b	SVMP	VM32B_GLOBR	47 kDa	100%	3
53	Zinc metalloproteinase-disintegrin-like 3a	SVMP	VM33_CROAD	69 kDa	100%	2
55	Zinc metalloproteinase-disintegrin-like ACLD	SVMP	VM3AD_AGKCL	70 kDa	100%	3
57	Zinc metalloproteinase-disintegrin-like Eoc1	SVMP	VM3E1_ECHOC	69 kDa	100%	2
59	Zinc metalloproteinase-disintegrin-like halysase	SVMP	VM3HA_GLOHA	68 kDa	100%	2
62	Zinc metalloproteinase-disintegrin-like stejnihagin-B	SVMP	VM3SB_TRIST	68 kDa	100%	3
66	Antihemorrhagic factor cHLP-A	FE	FETCA_GLOBR	37 kDa	100%	2
69	Hyaluronidase	HYA	HYAL_ECHOC	53 kDa	100%	2
70	L-amino-acid oxidase (Fragment)	LAAO	OXLA_BOTJR	56 kDa	100%	7
71	L-amino acid oxidase (Fragment)	LAAO	OXLA_BOTPC	56 kDa	100%	6
73	L-amino-acid oxidase	LAAO	OXLA_CALRH	58 kDa	100%	6
75	L-amino-acid oxidase	LAAO	OXLA_DEMVE	59 kDa	100%	3
76	L-amino-acid oxidase	LAAO	OXLA_ECHOC	57 kDa	100%	7
77	L-amino acid oxidase Lm29	LAAO	OXLA_LACMT	59 kDa	100%	5
78	L-amino acid oxidase	LAAO	OXLA_MICMP	57 kDa	100%	3
83	L-amino-acid oxidase	LAAO	OXLA_TRIST	59 kDa	99%	6
84	L-amino-acid oxidase	LAAO	OXLA_VIPAA	55 kDa	100%	7
85	L-lactate dehydrogenase A chain	LDHA	LDHA_PYTRG	37 kDa	100%	4
87	Natriuretic peptide Na-NP	NP	VNP_NAJAT	17 kDa	100%	2
90	NADH-ubiquinone oxidoreductase chain 4 (Fragment)	NUO	NU4M_PROFL	25 kDa	100%	2
96	Coagulation factor X	Peptidase S1	FA10_TROCA	54 kDa	100%	3
98	Coagulation factor V	Peptidase S1	FA5_PSETE	166 kDa	100%	6
101	Venom prothrombin activator pseutarin-C non-catalytic subunit	Peptidase S1	FA5V_PSETE	166 kDa	100%	4
102	Venom prothrombin activator omicarin-C catalytic subunit	Peptidase S1	FAXC_OXYMI	52 kDa	100%	3
103	Venom prothrombin activator oscutarin-C catalytic subunit	Peptidase S1	FAXC_OXYSU	52 kDa	100%	2
107	Acidic phospholipase A2 1	PLA2	PA2A1_OPHHA	16 kDa	100%	3
108	Acidic phospholipase A2 1	PLA2	PA2A1_PROFL	16 kDa	100%	2

111	Basic phospholipase A2 Tgc-K49	PLA2	PA2B_TRIGS	16 kDa	100%	2
115	Basic phospholipase A2 paradoxin-like alpha chain	PLA2	PA2PA_OXYMI	16 kDa	100%	2
117	Phospholipase-B 81	PLB	PLB_DRYCN	64 kDa	100%	4
121	Phospholipase A2 inhibitor subunit gamma B	PLI	PLIGB_GLOBS	22 kDa	100%	2
122	Phospholipase A2 myotoxin inhibitor protein	PLI	PLIP_BOTMO	18 kDa	100%	2
123	Snaclec 2	Snaclec	SL2_BITGA	18 kDa	100%	2
128	Snaclec bitiscetin subunit beta	Snaclec	SLB_BITAR	15 kDa	100%	3
129	Snaclec VP12 subunit B	Snaclec	SLB_DABPA	15 kDa	100%	2
130	Snaclec mamushigin subunit beta	Snaclec	SLB_GLOBL	17 kDa	100%	3
134	Snaclec alboaggregin-B subunit beta	Snaclec	SLBB_TRIAB	17 kDa	100%	2
136	Snaclec alboaggregin-D subunit alpha	Snaclec	SLDA_TRIAB	18 kDa	100%	2
138	Snaclec rhodocytin subunit alpha	Snaclec	SLYA_CALRH	16 kDa	100%	2
139	Snake venom metalloprotease inhibitor 02D01	SVMI	SVMI_ECHOC	33 kDa	100%	2
142	Snake venom metalloproteinase adamalysin-2	SVMP	VM12_CROAD	23 kDa	100%	2
143	Snake venom metalloproteinase atrolysin-B	SVMP	VM1AB_CROAT	47 kDa	100%	3
145	Snake venom metalloproteinase BITM02A	SVMP	VM1B_BOTIN	46 kDa	100%	2
146	Snake venom metalloproteinase HT-2	SVMP	VM1H2_CRORU	23 kDa	100%	2
147	Snake venom metalloproteinase lebetase-4 (Fragment)	SVMP	VM1L4_MACLB	24 kDa	100%	3
148	Snake venom metalloproteinase neuwiedase (Fragment)	SVMP	VM1N_BOTPA	23 kDa	100%	3
149	Snake venom serine protease VaSP1 (Fragments)	SVSP	VASP1_VIPAA	22 kDa	100%	2
151	Snake venom serine protease	SVSP	VSP_LACST	28 kDa	100%	2
154	Platelet-aggregating proteinase PA-BJ (Fragment)	SVSP	VSP1_BOTJA	26 kDa	100%	2
158	Thrombin-like enzyme kangshuanmei	SVSP	VSP1_GLOBR	26 kDa	100%	2
161	Snake venom serine protease 2	SVSP	VSP2_PROJR	28 kDa	100%	4
162	Snake venom serine proteinase 8	SVSP	VSP8_CROAD	28 kDa	100%	3
164	Alpha-fibrinogenase-like	SVSP	VSPAF_DABSI	28 kDa	100%	2
166	Thrombin-like enzyme bhalternin	SVSP	VSPBH_BOTAL	28 kDa	100%	3

169	Serine protease harobin	SVSP	VSPHA_HYDHA	29 kDa	100%	2
172	Venom plasminogen activator Haly-PA	SVSP	VSPPA_GLOBR	28 kDa	100%	3
174	Snake venom serine protease rhinocerase (Fragments)	SVSP	VSPR_BITRH	10 kDa	100%	3
175	Beta-fibrinogenase stejnefibrase-2	SVSP	VSPS2_TRIST	28 kDa	100%	2
177	Translationally-controlled tumor protein homolog	TCTP	TCTP_CROHD	19 kDa	100%	2
178	Snake venom vascular endothelial growth factor toxin	VEGF	TXVE_PROFL	16 kDa	100%	2
181	Venom nerve growth factor	VNGF	NGFV_BOTJR	27 kDa	100%	3
15	Cytochrome b	CYB	CYB_ACRGR	43 kDa	100%	3
23	Cytochrome b	CYB	CYB_ERYMN	42 kDa	100%	2
26	Cytochrome b	CYB	CYB_FARAB	42 kDa	100%	2
28	Cytochrome b	CYB	CYB_MICIK	42 kDa	100%	2
29	Cytochrome b	CYB	CYB_NAJAN	42 kDa	100%	2
56	Zinc metalloproteinase-disintegrin-like berythactivase	DIS	VM3BE_BOTER	69 kDa	100%	2
86	Natriuretic peptide BM026	NP	VNP_BUNMU	22 kDa	100%	2
88	Natriuretic peptide	NP	VNP_RHATT	16 kDa	100%	2
89	NADH-ubiquinone oxidoreductase chain 4 (Fragment)	NUO	NU4M_BOTSC	26 kDa	100%	2
109	Acidic phospholipase A2 Drk-a2	PLA2	PA2A2_DABRR	16 kDa	100%	2
110	Acidic phospholipase A2 Tpu-E6c (Fragments)	PLA2	PA2AC_TRIPE	14 kDa	100%	2
114	Basic phospholipase A2 homolog Tbo-K49	PLA2	PA2HB_TRIBO	16 kDa	100%	2
119	Phospholipase A2 inhibitor	PLI	PLIB_GLOBS	37 kDa	100%	3
124	Snaclec 2	Snaclec	SL2_SISCA	17 kDa	100%	2
125	Snaclec 3	Snaclec	SL3_BITGA	18 kDa	100%	2
126	Snaclec bitiscetin subunit alpha	Snaclec	SLA_BITAR	15 kDa	100%	3
127	Snaclec purpureotin subunit alpha	Snaclec	SLA_TRIPP	16 kDa	100%	2
131	Snaclec B9	Snaclec	SLB9_MACLB	17 kDa	100%	2
132	Snaclec alboaggregin-B subunit alpha	Snaclec	SLBA_TRIAB	18 kDa	100%	2
133	Snaclec stejaggregin-B subunit alpha	Snaclec	SLBA_TRIST	18 kDa	100%	2

135	Snaclec lebecin subunit alpha	Snaclec	SLCIA_MACLB	17 kDa	100%	2
137	Snaclec jerdonuxin subunit alpha	Snaclec	SLJA_PROJR	18 kDa	100%	2
160	Thrombin-like enzyme elegaxobin-1	SVSP	VSP1_PROEL	25 kDa	100%	3
165	Beta-fibrinogenase	SVSP	VSPBF_MACLB	28 kDa	100%	2
176	Snake venom serine protease salmobin	SVSP	VSPSN_GLOHA	29 kDa	100%	2
180	Vascular endothelial growth factor A	VEGF	VEGFA_PROFL	26 kDa	100%	2